Metabolomics in Hypertrophic Cardiomyopathy and other Myocardial Diseases

NIKHIL PAL

Radcliffe Department of Medicine

Division of Cardiovascular Medicine

Corpus Christi College

University of Oxford





Supervisors

Professor Houman Ashrafian

Professor Hugh Watkins

Michaelmas Term 2015

A thesis submitted for the degree of Doctor of Philosophy

Declaration

I hereby certify that this thesis, which I submit for the degree of Doctor of Philosophy, is entirely my own work, except where otherwise stated. I also confirm that no part of it has already been submitted for a degree or diploma in any other University or an institution of higher learning.

Abstract

Despite the clinical importance of hypertrophic cardiomyopathy (HCM) and a recognition that aberrant energetics contributes to its pathogenesis, significant uncertainty remains regarding the determinants of the clinical phenotype. The central hypothesis underlying this thesis is that the clinical manifestations of HCM are causatively influenced by perturbations in cellular metabolism, and that the metabolome in HCM, both at rest and during stress, is distinct from that of healthy hearts and other cardiac diseases manifesting left ventricular hypertrophy (LVH). Aortic stenosis, the most common valvular heart disease in the western world, and often presenting with a prominent phenotype of LVH, was the principal comparator disease state.

The metabolome of coronary sinus effluent from densely phenotyped patients with HCM, aortic stenosis with LVH and controls was systematically studied. These patients were assessed under different physiological states (at rest and during stress induced by pacing). The present work focused on fatty acid, carbohydrate and amino acid metabolism. The metabolomic changes identified were then validated by metabolomic and an orthogonal transcriptomic analysis of genes regulating these metabolic pathways in separately recruited patient cohorts.

Most prominently, this study identified substantial metabolic dysregulation in aortic stenosis, consisting of impaired fatty acid β-oxidation at rest and a trend towards reduced uptake of citric acid cycle intermediates and branched chain amino acids (BCAAs) during chronotropic stress (pacing). Transcriptomic analysis revealed only partial and ineffective upregulation in *PPARA* expression, with a corresponding downregulation of several PPARα target genes regulating fatty acid metabolism. In contrast, there was a seemingly appropriate upregulation of citric acid cycle activity and BCAA metabolism in HCM patients during stress. During discovery and validation stages selected metabolites differentiated the control vs aortic stenosis and HCM vs aortic stenosis cohorts with relatively similar and high area under the curve (AUC) values on receiver operating characteristic **(**ROC) analysis.

This work presented in this thesis represents the first comprehensive analysis of changes in metabolic pathways (transcriptional to metabolome) in aortic stenosis, and its comparison to HCM. The findings represent a significant increase in our understanding of the underlying metabolic derangements accompanying these disorders and provide us with promising avenues into potential therapeutic targets (e.g. PPARα), with strong clinical translation potential.

Acknowledgements

I would like to express my sincere thanks to my supervisor Professor Houman Ashrafian for providing me with the opportunity to undertake this research. He has provided me with invaluable guidance, support and encouragement through the course of this work. I am proud and grateful to have worked under his supervision.

Thanks should also go to my supervisor Prof Hugh Watkins for his continued guidance and support during this period. I would also like to thank my collaborator Dr. Jules Griffin for training me in the technique of mass spectroscopy analysis and data processing. Furthermore, I would like to thank Tim Dent who helped me with collection of samples and numerous friendly & fruitful discussions.

Finally I would like to take this opportunity to thank my parents, wife and brother for their endless, selfless and priceless love, support, strength and everything else, which has been the driving force in my life.

TABLE OF CONTENTS

DECLARATION ..... **I**

ABSTRACT ..... **II**

ACKNOWLEDGEMENTS ..... **III**

ABBREVIATIONS ..... **XI**

1 INTRODUCTION **2**

1.1 HYPERTROPHIC CARDIOMYOPATHY 2

1.1.1 Prevalence *2*

1.1.2 Genetics *3*

1.1.3 Cellular pathology *3*

1.1.4 Natural course *6*

1.1.4.1 Sudden death 6

1.1.4.2 Heart Failure 7

1.1.4.3 Atrial fibrillation 8

1.1.5 Clinical diagnosis *8*

1.1.6 Treatment *10*

1.2 AORTIC STENOSIS 12

1.2.1 Prevalence *12*

1.2.2 Pathogenesis *13*

1.2.3 Progression and Treatment *14*

1.3 MYOCARDIAL METABOLISM 17

1.3.1 Cardiac Muscle structure and function *17*

1.3.2 Myocardial metabolism in the healthy heart *18*

1.3.2.1 Source of fuel for myocardial metabolism 20

1.3.2.2 Transport of free fatty acids into the cytoplasm 20

1.3.2.3 Mitochondrial fatty acid transport 23

1.3.2.4 Fatty acid β-oxidation 24

1.3.2.5 Cardiac Mechanical efficiency 29
1.3.2.6 Randle cycle 32
1.3.2.7 Citric acid cycle 34
1.3.3 Myocardial metabolism in disease states 37
1.3.4 Hypertrophic cardiomyopathy and myocardial energetics 40
1.3.4.1 Hypothesis of contractile dysfunction 40
1.3.4.2 Hypothesis of impaired myocardial energetics 42
1.4 METABOLOMICS 46
1.4.1 Historical perspective 46
1.4.2 Metabolomic techniques 48
1.4.2.1 Study design 49
1.4.2.2 Sample preparation 50
1.4.2.3 Analytical platforms 51
1.4.2.3.1 Nuclear magnetic resonance spectroscopy (NMR) 51
1.4.2.3.2 Mass spectrometry 52
1.4.2.4 Data extraction and analysis 53
1.4.3 Emerging role of metabolomics 54
1.5 HYPOTHESIS 57
1.6 AIMS 57
2 METHODS 60
2.1 STUDY DESIGN 60
2.2 PRIMARY AND SECONDARY ENDPOINTS 63
2.3 STUDY PARTICIPANTS 64
2.3.1 Overall Description of Study Participants 64
2.3.2 Inclusion Criteria 64
2.3.3 Exclusion Criteria 65
2.4 STUDY PROCEDURES 66
2.4.1 Check for eligibility 66
2.4.2 Informed Consent 66

2.4.3 Echocardiography *67*
2.4.4 Cardiopulmonary Exercise Test *68*
2.4.5 Coronary angiography *69*
2.4.6 Sample processing *70*
2.4.7 Interventions *70*
2.4.8 Safety *71*
2.4.9 Participant Confidentiality *72*
2.5 MASS SPECTROSCOPY 72
2.5.1 Sample handling *72*
2.5.2 Chemicals *73*
2.5.3 Analysis of acylcarnitines *73*
2.5.3.1 Sample extraction 73
2.5.3.2 Instrumental parameters 74
2.5.3.3 Processing of acylcarnitine data 76
2.5.4 Analysis of aqueous metabolites *77*
2.5.4.1 Sample extraction 77
2.5.4.2 Instrument parameters 77
2.5.4.3 Processing of aqueous metabolite data 81
2.6 STATISTICAL ANALYSIS 81
2.6.1 Power calculation *81*
2.6.2 Analysis of endpoints using univariate analysis *81*
2.6.3 Multivariate analysis *82*
2.6.3.1 Principal component analysis (PCA) 82
2.6.3.2 Partial least squares discriminant analysis (PLS-DA) 83
2.6.3.3 Orthogonal projections to latent structures discriminant analysis (OPLS-DA) 83
2.6.3.4 Scaling for multivariate methods 84
2.6.3.5 Validation of multivariate models 84
2.6.3.6 Variable importance on projection (VIP) analysis 85
2.6.4 Receiver operating characteristic (ROC) curves *85*

3 METABOLOMIC ANALYSIS STRATEGY 88

3.1 CLINICAL CHARACTERISTICS 88

3.1.1 Demographics 88

3.1.2 Echocardiography results 91

3.1.3 Cardiopulmonary exercise testing in HCM 93

3.2 TRANS-CARDIAC GRADIENT VALIDATION 94

3.2.1 Glutamate & alanine 96

3.2.1.1.1 Conclusions 103

3.2.2 Glucose and lactate 105

3.2.2.1.1 Conclusions 113

3.3 METABOLOMICS IN THE CONTROL COHORT 116

3.3.1 Acylcarnitine profile of the control cohort 118

3.3.1.1 Baseline 118

3.3.1.2 Pacing 121

3.3.1.3 Baseline vs pacing 123

3.3.2 Aqueous metabolite analysis of the control cohort 126

3.3.2.1 Baseline 126

3.3.2.2 Pacing 133

3.3.2.3 Baseline vs pacing 139

3.3.2.3.1 Cardiac metabolism (baseline vs pacing) 142

3.3.3 Lessons learnt: justification of proposed analytic strategy 145

4 METABOLOMIC RESULTS FROM THE DISCOVERY COHORT 148

4.1 METABOLOMICS IN THE HCM COHORT 148

4.1.1 Acylcarnitine profile of the HCM cohort 149

4.1.1.1 Baseline 149

4.1.1.2 Pacing 152

4.1.1.3 Baseline vs pacing 154

4.1.2 Aqueous metabolite analysis of the HCM cohort 157

4.1.2.1 Baseline 157

4.1.2.2 Pacing 164
4.1.2.3 Baseline vs pacing 171
4.1.2.3.1 Cardiac metabolism (baseline vs pacing) 174
4.1.2.4 Overall summary 176
4.2 METABOLOMICS IN THE AORTIC STENOSIS COHORT 179
4.2.1 Acylcarnitine profile of the aortic stenosis cohort 179
4.2.1.1 Baseline 179
4.2.1.2 Pacing 182
4.2.1.3 Baseline vs pacing 185
4.2.2 Aqueous metabolite analysis of the aortic stenosis cohort 188
4.2.2.1 Baseline 188
4.2.2.2 Pacing 194
4.2.2.3 Baseline vs pacing 200
4.2.2.3.1 Cardiac metabolism (baseline vs pacing) 203
4.2.2.4 Summary & Future Analytical strategy 205
5 METABOLOMIC DIFFERENCES BETWEEN COHORTS 208
5.1 METABOLOMIC DIFFERENCES BETWEEN THE CONTROL AND HCM COHORTS 209
5.1.1 Analysis of acylcarnitines between the control and HCM cohorts 209
5.1.2 Analysis of aqueous metabolites between the control and HCM cohorts 214
5.1.3 Cardiac metabolism between the control and HCM cohorts at baseline and during pacing 221
5.1.4 Summary 223
5.2 METABOLOMIC DIFFERENCES BETWEEN THE CONTROL AND AORTIC STENOSIS COHORTS 226
5.2.1 Analysis of acylcarnitines between the control and aortic stenosis cohorts 226
5.2.2 Analysis of aqueous metabolites between the control and aortic stenosis cohorts 232

5.2.3 Cardiac metabolism between the control and aortic stenosis cohorts at baseline and during pacing 239

5.2.4 Summary 242

5.3 METABOLOMIC DIFFERENCES BETWEEN THE HCM AND AORTIC STENOSIS COHORTS 246

5.3.1 Analysis of acylcarnitines between the HCM and aortic stenosis cohorts 246

5.3.2 Analysis of aqueous metabolites between the HCM and aortic stenosis cohorts251

5.3.3 Cardiac metabolism between the HCM and aortic stenosis cohorts at baseline and during pacing 258

5.3.4 Summary 260

6 METABOLOMICS IN VALIDATION COHORT 265

6.1 METHODS 265

6.2 RESULTS 267

6.2.1 Clinical characteristics 267

6.2.2 Validation using selected acylcarnitines 268

6.2.3 Validation using selected aqueous metabolites 271

6.2.4 Validation using selected acylcarnitines and aqueous metabolites 275

6.2.5 Conclusions 279

7 BIOLOGICAL VALIDATION – TRANSCRIPTOMIC ANALYSIS 281

7.1 METHODS 281

7.2 RESULTS 283

7.2.1 Clinical characteristics (aortic stenosis vs controls) 283

7.2.2 Transcriptomic analysis 284

7.2.3 Genes encoding AMPK 284

7.2.4 Genes encoding transcriptomic factors 286

7.2.5 Genes regulating transportation of fatty acids for β-oxidation 286

7.2.6 Genes regulating fatty acid β-oxidation 288

7.2.7 Genes regulating microsomal fatty acid oxidation 291

7.2.8 Genes regulating lipid storage and biosynthesis 292

7.2.9 Genes regulating glucose metabolism 294

7.2.10 Genes regulating amino acid metabolism & urea cycle 295

7.2.11 Genes regulating retinoid metabolism 296

7.2.12 Genes regulating the citric acid cycle 297

7.3 CONCLUSIONS FROM TRANSCRIPTOMIC ANALYSIS 299

7.3.1 AMPK regulation 300

7.3.2 PPARα regulation 303

8 DISCUSSION & FUTURE WORK 310

8.1 ACYLCARNITINES 310

8.2 AQUEOUS METABOLITES 312

8.3 TRANSCRIPTOMIC REGULATION 318

8.4 CONCLUSIONS: AN EMERGING PARADIGM - AORTIC STENOSIS IS CHARACTERIZED BY PPARA/LONG CHAIN FATTY ACID METABOLIC DEFECTS 319

8.5 LIMITATIONS 320

REFERENCES 322

Abbreviations

AAA	amino adipic acid
ACAT	acetyl-coenzyme A acetyltransferase
ACC	acetyl-coenzyme A carboxylase
ADP	adenosine diphosphate
BAIBA	β-aminoisobutyric acid
ANOVA	analysis of variance
AMPK	5' adenosine monophosphate-activated protein kinase
ATP	adenosine triphosphate
AUC	area under curve
BMHC	β-myosin heavy chain
CI	chemical ionisation
C-C	cystine
CoA	coenzyme A
COX	cyclooxygenase
CMV	cytomegalovirus
CPEX	cardiopulmonary exercise stress test
CPT	carnitine palmitoyl transferase
CPT1	carnitine palmitoyl transferase 1
CPT2	carnitine palmitoyl transferase 2
CYP	cytochrome P-450
ECHO	echocardiography
ECG	electrocardiogram
EI	electron impact
ESI	electrospray ionisation
eGFR	estimated glomerular filtration rate

FFA	free fatty acid
FAHD2	reduced flavin adenine dinucleotide
FBC	full blood count
GC	gas chromatography
GTP	guanosine triphosphate
HCM	hypertrophic cardiomyopathy
ICD	implantable cardioverter defibrillator
LFT	liver function tests
LC	liquid chromatography
LDL	low density lipoprotein
LV	left ventricle
LVH	left ventricle hypertrophy
LVOT	left ventricular outflow tract
m/z	mass to charge ratio
MALDI	matrix-assisted laser desorption
MAPK	mitogen activated protein kinase
miRNA	microRNA
MYBPC	myosin binding protein-C
MS	mass spectrometry
NADH	reduced nicotinamide adenine dinucleotide
NMR	nuclear magnetic resonance
NYHA	new york heart association
Par	pareto
PCA	principal component analysis
PCr	phosphor-creatine
PLS-DA	partial least squares discriminant analysis

PPAR	peroxisome proliferator-activate receptor
PPARα	peroxisome proliferator-activate receptor alpha
PPARβ	peroxisome proliferator-activate receptor beta
PPARγ	peroxisome proliferator-activate receptor gamma
PPARβ/δ	peroxisome proliferator-activate receptor beta and delta
PGC-1	proliferator-activated receptor γ coactivator-1
QQQ	triple quadrupole
Q-Trap	quadrupole ion trap hybrid configuration
ROC	receiver operation characteristics
RXR	retinoid X receptor
SAM	S-adenosyl methyonine
SERCA	sarcoplasmic reticulum Ca^{2+} reuptake
TAG	triacylglycerol
TAVR	transcatheter aortic-valve replacement
TCA	tricarboxylic acid
TOF	time of flight
U&E	urea and electrolytes
UV	unit variance
VIP	variable importance on projection
VLDL	very-low-density lipoproteins
Wy-14643	4-chloro-6-(2,3-xylidino)-pyrimidynylthioaceticacid

Chapter 1

Introduction

1 Introduction

1.1 Hypertrophic cardiomyopathy

Hypertrophic cardiomyopathy (HCM) is the most common inherited cardiac disorder, characterised by unexplained cardiac hypertrophy.[1] It was first described nearly 50 years ago and over time significant advancements have been made in understanding its aetiology by gaining insights into underlying genetic, biophysical and physiological mechanisms.[2,3] Despite the delineation of HCM's basic biology, arising from predominantly single sarcomeric gene mutation, yet to be delineated genetic and environmental modifiers result in substantial heterogeneity even within families.[4] Current therapies are empirical with little evidence-base and are not disease modifiying.[5] Accordingly, complementary approaches are necessary to refine our understanding of HCM and enable discovery of improved tools for patient diagnosis, stratification and targeted therapy.

1.1.1 Prevalence

HCM is a global disease with cases reported from all continents and over 50 countries.[6,7] The prevalence of the disease is reported at 1 in 500 (0.2%), therefore estimated to affect nearly 120,000 people in the United Kingdom.[8] Though its initial prevalence was described in studies such as the CARDIA, significant advancement in genetic understanding and diagnostic techniques have suggested a higher prevalence of 1 in 200.[1,9] The disease affects both genders and people of all ethnic and racial origins.[10,11] Patients can be genotype positive but phenotype negative representing a subset of patients which were not described in the initial studies. These patients now form an

important subgroup, who require active management with consideration of the potential for phenotype development and thus the need for risk stratification.

1.1.2 Genetics

HCM is the most common genetic cardiac disorder, which has a Mendelian autosomal dominant pattern of inheritance. It largely caused by heterozygous mutations in 11 or more genes in the thick or thin contractile myofilament protein components of the sarcomere or the adjacent Z-disc.[12-18] 70% of mutations are identified in β-myosin heavy chain (*MYH7*) and myosin binding protein-C (*MYBPC-3*), while Troponin T (*TNNT2*) accounts for less than 5% of cases.[14-18]

Though genetic mutations have been unable to accurately predict clinical outcome in patients, their identification is significant in clinical testing.[16,17,19-21] If a patient with a phenotype of HCM is found to have a genetic mutation, this permits targeted cascade screening of their relatives. Thus family members can be genetically tested and if found negative, be appropriately reassured without the need for ongoing clinical phenotypic assessment. This also enables exclusion of certain other metabolic diseases, with similar phenotypic presentation but a different clinical course such as Fabry disease.

1.1.3 Cellular pathology

At the cellular level HCM is characterised by abnormal architecture, increased interstitial collagen and scarring.[22-25] In the left ventricle the myocardial architecture is disorganised with hypertrophied myocytes of abnormal shapes arranged chaotically at abnormal angles resulting in faulty intracellular

connections (figure 1.1.1). This pattern of cellular disarray is seen more extensively on the autopsy of young individuals who die of HCM.[23,26,27]

Extensive collagen deposition is observed in the intimal and medial layers of the intramural coronary arteries. This results in a narrowed lumen and a reduced coronary vasodilatory reserve due to the stiff vessel wall. This can result in a demand-supply mismatch and small vessel rarefaction, causing myocyte death and replacement with scar tissue.[28-32]

Together the disorganised cellular architecture, microvascular ischaemia and myocardial fibrosis form the substrate for malignant ventricular arrhythmia, which can result in sudden cardiac death.[33-35]

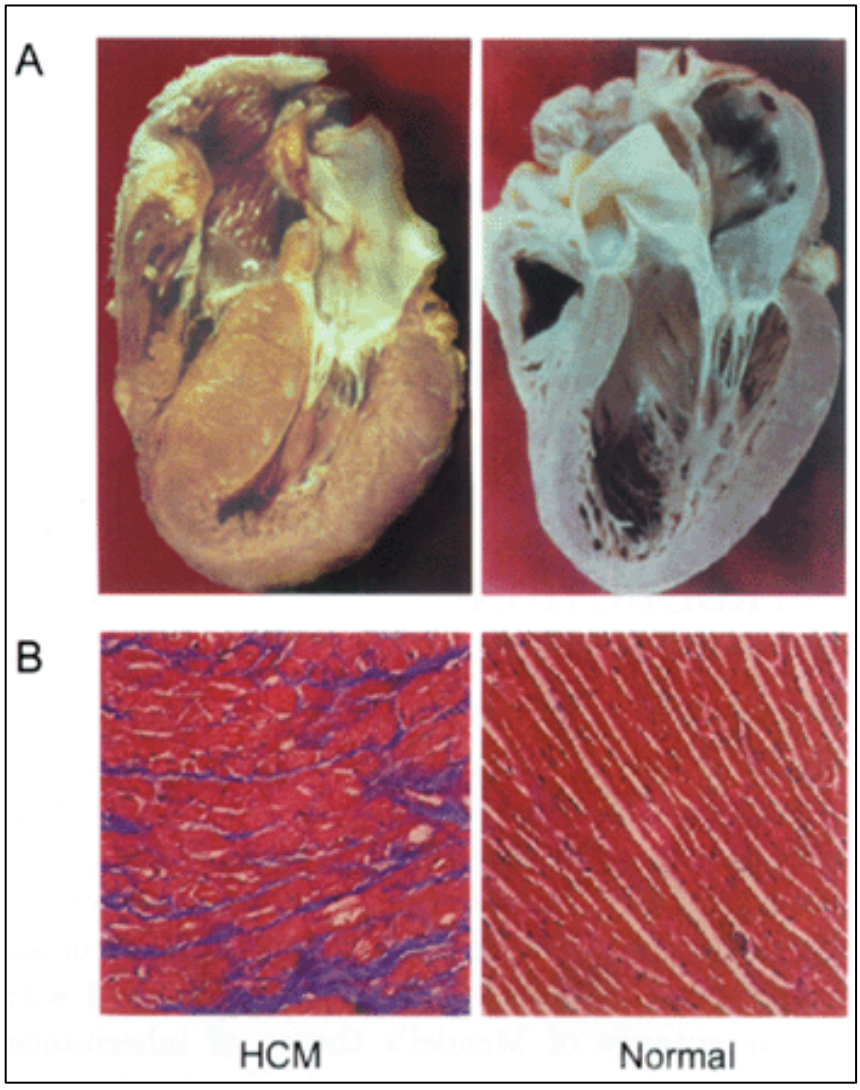

Figure 1.1.1: A) Post-mortem examination of the heart from a patient with HCM (left image) as compared to a normal heart (right image) B). Heart sections from HCM patient stained with Massons trichrome showing myofibre disarray and interstitial fibrosis (left image). Figure reproduced by author with permission from: Chung M-W *et al*. Hypertrophic cardiomyopathy: from gene defect to clinical disease. Cell Res 2003; 13:9-20.[36]

1.1.4 Natural course

HCM can present at any age from infancy to adulthood.[6,11,37-39] The majority of patients have a normal life expectancy with no clinical symptoms or disability.[37,38,40]

Patients who are diagnosed with one of the known disease-causing mutations will usually present with LVH (left ventricular hypertrophy) in early adulthood.[41] During adolescence, accelerated body growth results in LV (left ventricular) remodeling and the appearance of LVH in mutation carriers.[42,43] In some patients hypertrophy appears during mid life, where it's usually modest in size. Notably, the left ventricle can undergo further remodeling during patients lifetime, with hypertrophy increasing or decreasing in extent.[44]

The three most prominent clinical pathways, with which HCM progresses and presents with, are: a) sudden death b) heart failure and c) atrial fibrillation.

1.1.4.1 Sudden death

Sudden death is the most devastating presentation of HCM. The most common cause of sudden death in children and young adults is HCM.[45,46] The mortality was initially thought to be as high as 3-6%, but this data is skewed towards high-risk patients seen in tertiary care centers.[47] More recent estimates of mortality consider this to now be 1%, similar to that of the general population in the United States.[6,48-50] The most frequent cause of sudden death in these circumstances is ventricular fibrillation and ventricular tachycardia.[35,40,51,52] They often occur in patients during moderate to severe exercise, but have been reported to occur during sedentary activities including sleeping. The incidence of sudden death decreases during mid-life, with a significant drop after the age

of sixty.[53] This is because of a drop in the occurrence of life threatening arrhythmias in that age group.

Accordingly, risk stratification is an important part of the clinical management of these patients with HCM. Risk stratification identifies approximately 55% of these patients to have no excess risk, with only 10-20% of individuals identified as high risk. The following risk factors are considered in HCM patients: a) sudden death in the family b) unexplained syncopal episode c) interventricular septum greater than 30 mm in thickness d) evidence of ventricular tachycardia on holter monitoring e) impaired blood response to exercise, identified on upright exercise stress testing. The presence of any 2 or more of these risk factors warrants the use of implantable cardioverter defibrillator (ICD).[54]

ICD therapy is the only treatment known to alter the natural course of the disease.[35,40] Drugs such as amiodarone are thought to be effective in preventing lethal arrhythmias, but cannot be used for prolonged periods in younger patients due to the known organ toxicities. Other commonalty utilised drugs such as β-blockers and verapamil are not effective in mitigating the risk of sudden cardiac death.[55]

1.1.4.2 Heart Failure

HCM patients with heart failure initially present with symptoms of dyspnea, paroxysmal nocturnal dyspnea and orthopnea. These patients initially have normal to supranormal left ventricular function, with diastolic impairment.[56] The later is characterised by increased left ventricular wall stiffness, impaired relaxation and compromised left atrial systolic function. This leads to impaired filling and raised left atrial and left ventricular end-diastolic pressures, resulting

in reduced stroke volume and cardiac output.[56] These patients have decreased exercise capacity and reduced peak oxygen uptake on cardiopulmonary exercise testing.[57-59]

The progression to NYHA (New York Heart Association) class III and IV symptoms occurs gradually in 15-20% of the patients.[60] This is associated with periods of stability in-between the relapse episodes, finally culminating in severe end stage heart failure, where the left ventricular function is severely impaired, also termed the burnt-out phase of HCM.[44,61] The progression to end-stage heart failure is determined by the gradient of left ventricular outflow tract obstruction, atrial fibrillation and diastolic impairment.[56,62-64] However, the degree of LVH does not predict the progression to systolic heart failure in later life.

1.1.4.3 Atrial fibrillation

Atrial fibrillation is the most common sustained arrhythmia affecting 20% of patient with HCM. The incidence of atrial fibrillation is four times higher in patients with HCM compared to the general population. The likelihood of developing atrial fibrillation is higher with increasing age and in those who have a dilated left atrium. Furthermore, the presence of atrial fibrillation acts as an independent risk factor for developing heart failure in patients with HCM, and carries an increased risk of embolic events, which requires adequate anticoagulation.[63,64]

1.1.5 Clinical diagnosis

Patients are usually diagnosed following a clinical examination and routine tests such as an electrocardiogram. The finding of a murmur prompts the routine

tests such as an electrocardiogram, where a commonly a pattern of left ventricular hypertrophy is present. Other abnormal electrocardiographic findings may be seen in patients with different patterns of hypertrophy, for example deep T-wave inversion across the anterolateral leads which is associated with apical HCM.[65]

Echocardiography is the routinely used imaging modality to diagnose HCM.[8] Asymmetrical left ventricular hypertrophy is the most common pattern of hypertrophy identified, with some also featuring apical hypertrophy.[43] Truly symmetrical hypertrophy is rare. The usual wall thickness is 13-15mm, but massive LVH upto 50 mm has been reported. Other notable findings can include systolic anterior motion of the mitral valve, hyperdynamic left ventricular systolic function and dynamic left ventricular outflow tract obstruction.

Cardiac MRI has now emerged as a favoured imaging modality for better characterisation of HCM.[66-68] In particular it has advantages for visualsing:

a) Hypertrophy in specific areas of the left ventricle such as the anterolateral free wall, apex and posterior septum
b) Apical aneurysm
c) Elongated or enlarged mitral valve
d) Accessory or displaced hypertrophied papillary muscle

Cardiac MRI is also useful in the characterisation of patients who are genotype positive but phenotype negative.[69] Specific abnormalities can be identified which are characteristic of HCM such as myocardial fibrosis with a predominantly focal / regional pattern of distribution and blood-filled myocardial crypts.[70-72] Genotype positive but LVH negative patients can also have the presence of electrocardiographic abnormalities, diastolic dysfunction, mitral

leaflet elongation and elevated collagen markers.[69,71,73] There is limited data available regarding the progression of disease and risk of events including sudden death in this cohort of patients. More longitudinal studies are required to better understand this, while in the mean time patients should be managed on a case-by-case basis.

Family screening is an integral part of the management of HCM patients. In case of a documented pathogenic mutation, genotype negative relatives can be reassured and relived of the anxiety of regular screening. However in families where genetic results are negative in the proband, regular screening (with electrocardiogram and echocardiography) is required to detect the potential emergence of a phenotype.

1.1.6 Treatment

The only effective therapy shown to alter the natural course of HCM and prolong life by aborting lethal ventricular arrhythmias, is that provided by an ICD.[35,40] The clinical decision to implant ICD is guided by risk stratification of patients, with high-risk individuals offered the therapy. The decision to implant an ICD is taken on a case-by-case basis, with some high-risk individuals refusing therapy, while others with otherwise low risk but with high familial incidence of sudden death may be offered the therapy. Each patient has to be appropriately counseled before implanting an ICD, where the risks and potential benefits are clearly explained.

Pharmacological therapy with amiodarone is effective in preventing sustained atrial fibrillation and ventricular arrhythmias. But due to the toxic side effects it cannot be used for prolonged periods in young patients. Other pharmacological

therapy is empirical and does not have a strong evidence base in these patients.[55] Therapy with β-blockers and verapamil is routinely used in symptomatic patients with HCM.[74-76] Verapamil is not recommended in patients with resting left ventricular outflow tract obstruction and heart failure.[77] However Disopyramide is an effective alternative in combination with β-Blockers for patients with dynamic left ventricular outflow tract obstruction.[78,79]

Anticoagulation is an important consideration in patients with atrial fibrillation and left atrial dilatation. Although the CHA_2DS_2-VASc score is not validated for use in HCM, use of warfarin is recommended in all patients with paroxysmal, persistent or permanent atrial fibrillation.[54,80]

In patients with heart failure with systolic dysfunction treatment with diuretics, vasodilators and digitalis is recommended. These patients with severe left ventricular systolic dysfunction can also be offered cardiac resynchronization therapy (CRT) or prophylactic ICD implantation if meeting the criteria as per the current guidelines.[54]

Surgical myectomy is the gold standard for treating symptomatic patients with severe left ventricular tract outflow (LVOT) obstruction, who are refractory to pharmacological therapy.[81,82] Patients with a LVOT gradient of more than 30 mm Hg at rest are at high risk of sudden cardiac death. A small mass of the cardiac muscle (nearly 5gm) is excised from the proximal septum to the distal margins of the mitral valve leaflet. Most patients report a subjective improvement in their symptoms 5 years post surgery.[83]

Alcohol septal ablation is an alternative treatment for patients who are unable to undergo surgical myectomy and is the first choice therapy for elderly patients with comorbidities.[84,85] During this procedure absolute alcohol is infused into the

first septal perforator coronary artery branch inducing a septal infarct in that territory. The procedure is associated with risks of coronary artery dissection, large myocardial infarction and high-grade atrioventricular block necessitating permanent pacemaker implantation.

Cardiac transplantation can be offered to eligible symptomatic patients without LVOT obstruction who are refractory to pharmacological therapy. Survival post heart transplantation of these patients is similar to or more favorable than that undertaken for other cardiovascular diseases.[86]

1.2 Aortic stenosis

1.2.1 Prevalence

Aortic stenosis is the most common valve disease in the western world, with a prevalence of 0.2% in adults between the ages of 50-59 years; increasing to 0.9% in adults aged 80-89 years.[87,88] The prevalence has been slowly rising in the aging population and is expected to double in the next 20 years.[89]

The disease is commonly seen as a result of calcification of a normal trileaflet valve, but nearly 40% of the cases over the age of 70 are associated with a bicuspid aortic valve. While familial clustering, sometimes with an autosomal dominant pattern of inheritance, has been observed in patients with bicuspid aortic valve disease, no discrete genetic abnormality has yet been described. For trileaflet aortic valve stenosis familial clustering has also been reported, with a mutation in NOTCH1 documented in certain families with congenital aortic valve abnormalities.[90]

The pathophysiology of aortic stenosis is incompletely understood, with a lack of markers for risk, disease progression and prognosis. Furthermore the treatment of severe asymptomatic aortic stenosis remains valve replacement, either surgically or via the transcatheter route, with no medical therapies proven to be capable of ablating disease progression.

1.2.2 Pathogenesis

The gradual thickening of the aortic valve and development of left ventricular hypertrophy (LV) play a critical role in the pathogenesis of aortic stenosis. Progressive narrowing of the valve results in increased afterload and pressure-overload of the left ventricular inducing cardiomyocyte hypertrophy. While development of LVH is an adaptive response initially in restoring wall stress, ultimately it becomes maladaptive and results in overt heart failure. During the development of calcific aortic stenosis the valve undergoes a number of stages:

1) Mechanical stress and endothelial damage: the first triggering event is a rise in the mechanical stress and reduction in sheer stress, which leads to endothelial damage. This mechanism is similar to that observed in atherosclerosis.[91]
2) Inflammation: endothelial damage allows the penetration of lipids into areas of inflammation.[92] Low-density lipoprotein (LDL) and lipoprotein(a) accumulate in areas of inflammation and allow infiltration of monocytes. These monocytes differentiate into macrophages[93] and T cells, that release proinflammatory cytokines.
3) Neoangiogenesis: the inflammatory process is accompanied by the formation of new vessels in the aortic valve, which act as sites for the entry of inflammatory cells.[94]

4) Fibrosis: the increased inflammatory activity leads to activation of valve interstitial cells, which contain vimentin. They differentiate into myofibroblast that accelerate fibrotic activity in the aortic valve.
5) Calcification: the calcification process starts with the differentiation of myofibroblasts into osteoblasts under the influence of several pathways.[90,95] Osteoblasts lead to local production of osteopontin, osteocalcin, bone sialoprotien and bone morphogenic protein 2. This leads to increased calcification in the aortic valve by a process similar to that of new bone formation.

The development of significant haemodynamic obstruction from aortic stenosis is accompanied by LVH. Other factors such as hypertension and increased arterial stiffness, which increase the pressure afterload, also contribute to the development of LVH. While initially an adaptive response, when failure of the LV to maintain adequate forward flow against the resistance of the stenotic aortic valve occurs, heart failure develops. Histologically this is associated with progressive myocardial apoptosis and fibrosis in the hypertrophied LV.[96]

1.2.3 Progression and Treatment

There is an association between calcific aortic valve disease and diabetes, smoking, hypertension, male sex, increasing age and raised levels of LDL cholesterol and lipoprotein(a). Rapid progression of aortic valve disease from mild to severe over a 2 to 5 year period occurs only in 10-15% of patients.[97,98] In the remainder, there is a significant variability in the presence or onset of symptoms and in the severity of aortic stenosis. Thus while some patients can remain asymptomatic for years with critical aortic stenosis, others decompensate much more rapidly. Individuals with rheumatic aortic stenosis

usually have mixed valve disease, often accompanied by pulmonary arterial hypertension and right heart failure. In several studies it has been shown that the presence of aortic sclerosis was associated with increased cardiovascular risk (Cardiovascular Health Study, Multi-Ethnic study of Atherosclerosis).[97,99]

A detailed assessment of the aortic stenosis patients is required before making an effective management plan. Such an assessment should consider the evaluation of:

a) Clinical symptoms

b) Severity of aortic valve disease

c) LV response to pressure overload

In addition, it is important to exclude concurrent systemic, pulmonary or coronary disease as a contributor to the patient's symptoms.

In patients with typical symptoms (including exertional chest pain or dyspnoea and/or syncope) and a severely calcified aortic valve, the identification of a maximum trans-valvular velocity of more than 4 m/sec by echocardiography confirms the diagnosis of severe aortic stenosis. In patients with low-flow, low-gradient aortic stenosis, the trans-valvular velocity is only moderately elevated, despite the presence of a severely calcified aortic valve. This is most commonly seen in patients with reduced LV ejection fraction (< 50%). Undertaking low-dose dobutamine stress echocardiography can confirm the diagnosis of severe aortic stenosis in these patients by identifying an increase in the trans-valvular velocity to more than 4 m/sec with valve area remaining < 1 cm^2 on stress testing. In patients with low-flow, low-gradient aortic stenosis with normal LV

function, the diagnosis of severe aortic stenosis is established by identification of an:

a) Indexed valve area of 0.6 cm^2 or less

b) Stroke volume index of less than 35ml/m^2

Once a diagnosis of severe symptomatic aortic stenosis is established a multidisciplinary team should make the decision regarding the choice of treatment. These are either surgical aortic valve replacement or transcatheter aortic-valve replacement (TAVR). Surgical aortic valve replacement remains the first choice of therapy, with overall 30-day surgical mortality of less than 3% for isolated aortic valve replacements and 4.5% when accompanied by coronary-artery bypass grafting. TAVR is recommended in the following circumstances:

1) A predicted risk of death or major complication with surgery of greater than 50% at one year.
2) The presence of a medical condition which affects 3 other major organ systems and which is not likely to improve postoperatively.
3) The presence of conditions such as a 'porcelain' aorta, which are a major hindrance to surgery.

Several studies have now shown similar clinical outcomes at one and three years in patients undergoing either TAVR or surgical aortic valve replacement.[100]

1.3 Myocardial metabolism

1.3.1 Cardiac Muscle structure and function

Cardiac muscle is a specialised form of involuntary striated muscle. As with skeletal muscle the primary contractile proteins in the cardiac myocytes are actin and myosin.[101] On electron microscopy, the actin thin filaments in the sarcomere appear as light I bands, whereas the myosin thick filaments appear as A bands. The actin and myosin filaments generate the contractile force of the heart, by forming actomyosin crossbridges as a part of the excitation-contraction coupling mechanism.

Cardiac myocytes are connected to each other by the intercalated discs, which result in the formation of a cardiac syncytium. There is an atrial and a ventricular syncytium, linked to each other via cardiac connection fibres. The very low electrical resistance through the intercalated discs permits ready diffusion of ions, resulting in a rapid transmission of electrical impulses and a co-ordinated contraction of the myocardium. The intercalated discs contain three types of cell-cell junction:

a) Adherens junction: anchor the actin filaments

b) Desmosomes: anchor the intermediate filaments

c) Gap junctions: permit the passage of the action potential between the cardiac myocytes to allow the depolarisation and contraction of the cardiac muscle

The intercalated discs appear as thin dark-staining lines between the myocytes on electron microscopy.

Cardiac muscle differs histologically from skeletal muscle by the presence of larger and wider T-tubules, which are smaller in number. They form the diad, which is located at the sarcomere Z line. A diad is comprised of a single T-tubule paired with the terminal cisterna of the sarcoplasmic reticulum. This plays an important role in the excitation-contraction coupling mechanism, by coupling the electrical wave of depolarisation to the calcium-mediated contraction via the formation of the actomyosin crossbridge.

The contraction of the cardiac myocytes begins with the initiation of the action potential, which requires the entry of sodium ions via the sarcolemma.[102] Unlike skeletal muscle, cardiac muscle requires an inward influx of extracellular calcium ions for contraction to occur and to be sustained for a longer period. The calcium ions enter through voltage gated Ca^{2+} channels (L-type calcium channel). These are required to stimulate calcium release from the sarcoplasmic reticulum via the calcium-induced calcium release mechanism (CICR). The increased Ca^{2+} transient stimulates the troponin complex leading to conformational changes in the thin filament, which result in actomyosin crossbridge formation and thus systolic myocardial contraction. Following the end of the contraction phase, the Ca^{2+} transients are lowered via the reuptake of Ca^{2+} into the sarcoplasmic reticulum using the ATP (adenosine triphosphate) dependent sarcoplasmic reticulum Ca^{2+} reuptake (SERCA-2) pump. This then allows cardiomyocyte relaxation and starts the phase of diastole.

1.3.2 Myocardial metabolism in the healthy heart

The heart is a highly metabolically active organ and requires a large amount of energy to maintain normal function. Energy is required for maintaining contractility, basal metabolic processes and ionic homeostasis. This requires

more ATP per gram of tissue than other organ. The heart consumes approximately ~8–15 ml O_2/min/100 g tissue compared to the brain's ~3 ml O_2/min/100 g tissue. Matching the supply of metabolic substrates to myocardial work to generate ATP, with >70 ml O_2/min/100 g tissue required during exercise, demands profound cellular flexibility over large dynamic and temporal ranges.[103] It is therefore unsurprising that metabolism has been linked to cardiac health and disease.[104]

A healthy heart produces more than 95% of its energy requirements from mitochondrial oxidative phosphorylation, with the remainder from glycolysis and GTP production in the tricarboxylic acid (TCA) cycle. Under varying conditions the heart can use different metabolic substrates for energy production. In normal conditions 50-70 % of energy production is from β-oxidation of free fatty acids, but the heart can also use other carbon substrates such as glucose, lactate, ketones and amino acids for energy production.[105-107] Under normal conditions the heart has to completely turnover its ATP pool every 10 seconds as it has a low ATP content (5 μmol/g wet wt.) and high rate of ATP hydrolysis (30 μmol /g wet wt. min).[106,108]

β-oxidation of fatty acids occurs in the mitochondrial matrix and is under complex control, being dependent upon the following: a) supply of fatty acids to the heart; b) competing energy substrates to fatty acids use, such as glucose, ketones, lactate and amino acids; c) energy demands of the heart; d) cardiac oxygen supply; e) allosteric control of fatty acid uptake into cardiac myocytes, esterification to long chain acyl CoA and transport into the mitochondrial matrix; f) mitochondrial function.[107,109-112]

1.3.2.1 Source of fuel for myocardial metabolism

The major source of free fatty acid to the heart is either the free fatty acid bound to albumin or fatty acid released from triacylglycerol (TAG) contained in chylomicrons or very-low-density lipoproteins (VLDL).[113] During states of sympathetic nervous system activation such as myocardial ischaemia, heart failure and stress, there is a greater release of free fatty acids into the circulation, resulting in increased free fatty acid β-oxidation.[112,114] This occurs due to β-adrenoceptor-mediated stimulation of hormonal lipase activity in adipose tissue.[115]

The majority of circulating free fatty acids are present as triacylglycerol in lipoproteins. Most of the exogenous triacylglycerol is derived from the chylomicrons, while only a small proportion originates from VLDL.[116,117] The hydrolysis of these triacylglycerol's by lipoprotein lipase is an important step in fatty acid uptake and thus β-oxidation. Lipoprotein lipase is initially synthesised as an inactive monomeric proenzyme in the endoplasmic reticulum of the cardiac myocytes.[118] It is then activated and secreted as an active homodimer, which binds to the cardiac myocyte cell surface heparin sulfate proteoglycans (HSPG). Any abnormality in the process of lipoprotein lipase synthesis, secretion, attachment or degradation can alter fatty acid supply and thus impact upon fatty acid β-oxidation.

1.3.2.2 Transport of free fatty acids into the cytoplasm

The transport of free fatty acids across the sarcolemmal membrane occurs via either passive diffusion or protein carrier mediated pathways.[119,120] The protein carriers include the following: fatty acid translocase (FAT)/CD36, fatty acid

binding proteins plasma isoform (FABPpm), and fatty acid transport protein (FATP) (figure 1.3.1).[121] FAT/CD36 can translocate between endosomes and the sarcolemmal membrane. Increased translocation of this protein carrier to the sarcolemmal membrane is stimulated by insulin and increased contractility. This enables greater transport of free fatty acids into the cell and thus increased β-oxidation. A suggested mechanism for the contraction-induced stimulation involves the activation of 5' adenosine monophosphate-activated protein kinase (AMPK).[121] Insulin mediated stimulation occurs via the inhibition of the ubiquination processes in the cell, which downregulates the proteins responsible for degradation of FAT/CD36, resulting in increased levels of FAT/CD36 available for translocation to the sarcolemmal membrane.

In the cytoplasm, free fatty acids are converted to long-chain acyl CoA esters by fatty acyl CoA synthetase (FACS). These long chain fatty acyl CoA esters can then either be transferred into the mitochondrial matrix or be esterified into complex lipids in the cytoplasm. The conversion and accumulation of long chain acyl CoA esters into complex intracellular lipids such as triacylglycerol, diacylglycerol (DAG) and ceramide is associated with insulin resistance, heart failure and cardiac dysfunction.[122-124] Animal models with overexpression of fatty acyl CoA synthetase or fatty acid transport protein, have increased uptake of free fatty acids, greater conversion to long-chain acyl CoA and subsequent accumulation of complex lipids in the myocytes. This results in myofibre disorganization and a phenotype of dilated cardiomyopathy.[125,126]

Carnitine palmitoyltransferase 1 (CPT1) is a mitochondrial enzyme that catalyses the conversion of long-chain acyl CoA esters to long-chain acylcarnitines, which are shuttled across the mitochondrial membrane. Carnitine

palmitoyltransferase 1 is allosterically inhibited by malonyl CoA. Malonyl CoA is synthesized from acetyl CoA catalysed by acetyl CoA carboxylase (ACC) enzyme and is degraded by malonyl CoA decarboxylase (MCD) (Figure 1.3.1).[127] Two isoforms of acetyl CoA carboxylase are: acetyl CoA carboxylase α and acetyl CoA carboxylase β.[128] The acetyl CoA carboxylase β isoform predominates in the heart. AMPK plays an important role in the regulation of acetyl CoA carboxylase activity.[129]

AMPK is a serine/threonine kinase that acts as a fuel sensor of the heart and responds to states of metabolic stress that lead to low ATP, increased adenosine monophosphate (AMP) or increased creatine/phosphocreatine (Cr/PCr) ratio (Figure 1.3.1).[129] It regulates not only fatty acid β-oxidation, but also glucose uptake and glycolysis.[110,130] AMPK is a heterotrimeric protein, which consists of a catalytic α subunit and regulatory β and γ subunits.[129] There is a cardiac expression of both α1 and α2 catalytic subunits, as well as the regulatory β1, β2, γ1 and γ2 subunits. AMPK upregulates β-oxidation during times of increased myocardial energy demand by phosphorylation of acetyl CoA carboxylase α and β isoforms, reducing malonyl CoA mediated inhibition of carnitine palmitoyl transferase 1.

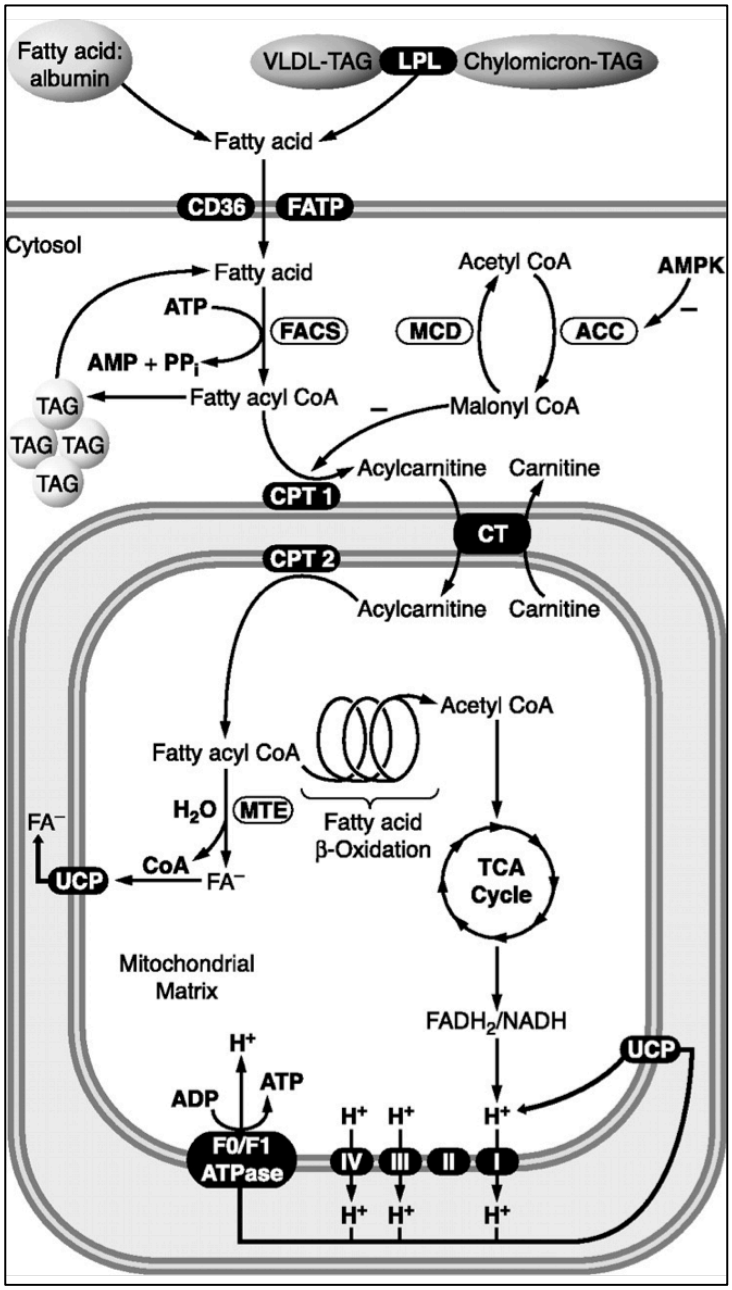

Figure 1.3.1: Overview of fatty acid β-oxidation. Figure reproduced by author with permission from: Lopaschuk *et al*. Myocardial fatty acid metabolism in health and disease. Physiological Reviews 2010;90:207-58.

1.3.2.3 Mitochondrial fatty acid transport

Long chain acylcarnitine is shuttled across the mitochondrial membrane into the matrix by the carnitine:acylcarnitine translocase (CT) (Figure 1.3.1).[131] This process involves the exchange of carnitine for acylcarnitine. Thus

carnitine:acylcarnitne exchange not only plays an important role in the transfer of long-chain acylcarnitine moieties into the mitochondrial matrix for β-oxidation, but also transports free carnitine back into the cytoplasm needed for subsequent carnitine palmitoyl transferase 1 reactions. As a corollary, a deficiency of carnitine:acylcarnitine is linked to development of cardiomyopathies.[132]

In the mitochondrial matrix long-chain acylcarnitine is converted back to long chain acyl CoA and free carnitine by carnitine palmitoyltransferase 2 (CPT2), an enzyme located on the inner mitochondrial membrane (Figure 1.3.1). This enzyme is less sensitive to inhibition by malonyl CoA.[133]

1.3.2.4 Fatty acid β-oxidation

Long-chain acyl CoA is metabolised in the mitochondrial matrix via the process of β-oxidation (figure 1.3.2).[131] In the first step the long-chain acyl CoA is dehydrogenated to 2,3-enoyl CoA, catalysed by the enzyme acyl CoA dehydrogenase generating flavin adenine dinucleotide (FADH2). 2,3-enoyl CoA is hydrated by enoyl CoA hydratase to produce 3-hydroxyacyl CoA. 3-hyodroxyacyl CoA is then dehydrogenated to 3-ketoacyl CoA, by $_{L}$3-hydroxyacyl CoA dehydrogenase generating nicotinamide adenine dinucleotide (NADH). 3-ketoacyl CoA is finally thiolised to acetyl CoA and a fatty acyl chain that is two carbons short, by 3-ketoacyl CoA thiolase. This process repeats itself until all carbons in the fatty acid are converted to acetyl CoA. Every cycle of fatty acid β-oxidation produces acetyl CoA, fatty acyl chain that is 2 carbons short, and a molecule each of $FADH_2$ and NADH. The acetyl CoA enters the citric acid cycle, while the $FADH_2$ and NADH are important coenzymes used in the mitochondrial electron transport chain. The majority of the fatty acids undergoing β-oxidation

are either mono- or polyunsaturated fatty acids. Their metabolism is facilitated by enzymes such as enoyl CoA isomerase and 2,4-dienoyl CoA reductase, which assist in the formation of a *cis* double bound and a trans double bond that allows them to be metabolised by the enzymes of the β-oxidation pathway.[131] When the fatty acid chains are too long their initial β-oxidation occurs in the peroxisomes, until octanoyl-CoA is formed at which point they are transported to the mitochondria.

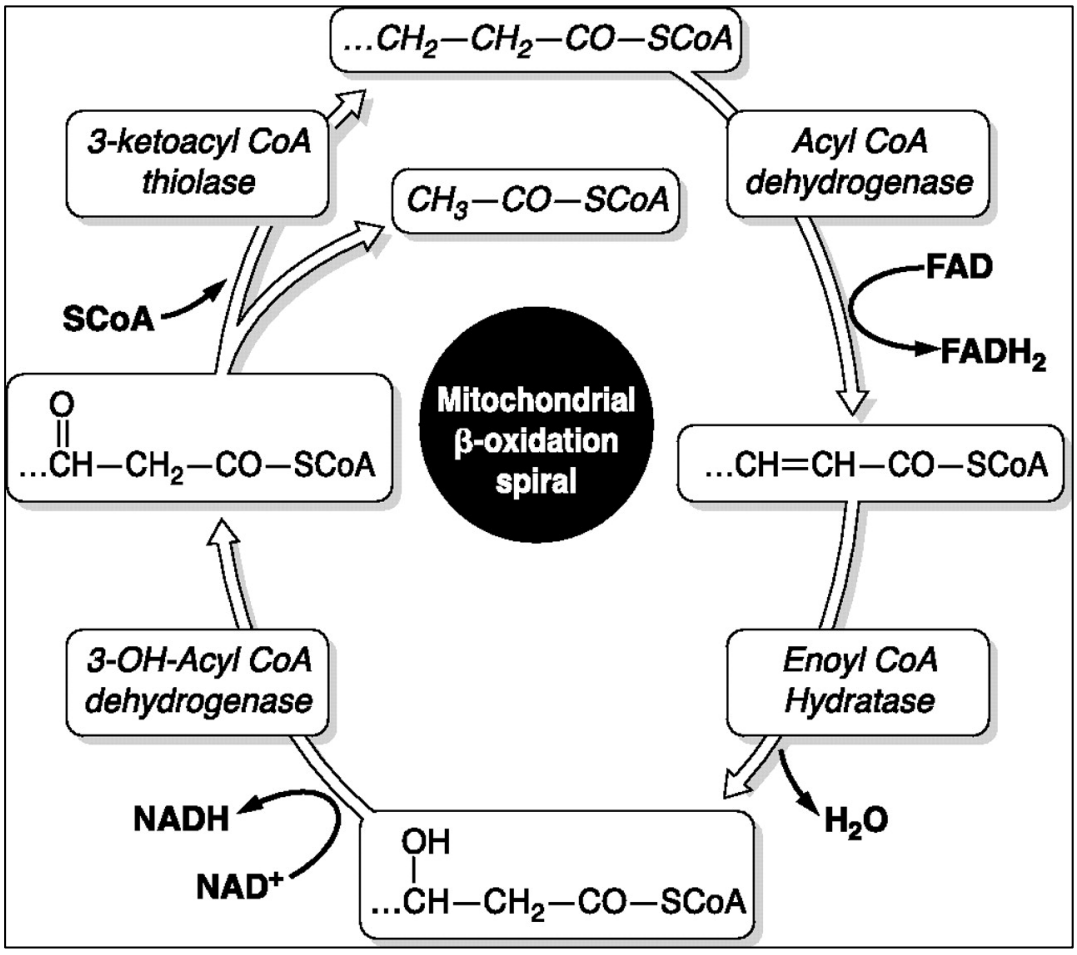

Figure 1.3.2: Fatty acid β-oxidation. Figure reproduced by author with permission from: Lopaschuk *et al*. Myocardial fatty acid metabolism in health and disease. Physiological Reviews 2010;90:207-58.

The four enzymes of the β-oxidation pathway are sensitive to regulation by the various intermediate products of the cycle, $FADH_2$ and NADH (Figure 1.3.2). 3-ketoacyl-CoA is also inhibited by acetyl CoA, the final product of β-oxidation pathway and the pyruvate dehydrogenase complex. Thus during a state of low energy demand, decreased activity of the citric acid cycle results in an accumulation of acetyl CoA and thus inhibition of the β-oxidation pathway.[134]

The enzymes of the β-oxidation cycle are also under transcriptional control regulated by the nuclear receptor transcription factors such as the peroxisomal proliferator activated receptor (PPAR) α and peroxisomal proliferator-activated receptor γ coactivator-1 (PGC-1) α (Figure 1.3.3).[135-137] The PPARs can be activated by various ligands such as fatty acids, eicosanoids and leukotrienes. Post-activation they form heterodimeric complexes with retinoid X receptor (RXR). The PPAR-RXR heterodimeric complex then translocates to the nucleus and binds to the promoter region of various target genes upregulating their expression.

PPARs regulate a wide spectrum of genes encoding proteins involved in the fatty acid metabolism (Figure 1.3.3). This not only includes the enzymes of the β-oxidation pathway but also others involved in fatty acid metabolism such as: fatty acid translocase (FAT)/CD36, fatty acid binding proteins plasma isoform (FABPpm), fatty acid transport protein (FATP), diacylglycerol acyltransferase, malonyl CoA dehydrogenase, carnitine palmitoyltransferase 1, pyruvate dehydrogenase kinase (PDK) 4 and mitochondrial uncoupling proteins (UCP2, UCP3).[137,138]

There are three isoforms of PPAR: α, β/δ and γ. The role of PPARα has now been well studied in animal models, which either over or under-expressed

PPARα in the heart. Overexpression of PPARα, resulting in a gain-of-function, is associated with an increased fatty acid uptake, β-oxidation and lipid accumulation.[139] In contrast deletion of the PPARα gene, a loss of function approach, is associated with a decrease in β-oxidation and increased glucose metabolism.[140]

PPARβ/δ is also abundantly expressed in the heart and like PPARα plays an important role in the transcriptional regulation of fatty acid β-oxidation enzymes. Animal studies utilising loss-of-function or gain-of-function strategies with PPARβ/δ have shown effects opposite to that of PPARα. Overexpression of PPARβ/δ in mice resulted in increased β-oxidation, but no lipid accumulation or cardiac dysfunction.[141] Whereas a deletion of PPARβ/δ has been to shown to reduce β-oxidation, increase lipid accumation and result in cardiomyopathy.[142] A notable difference observed was that PPARβ/δ did not regulate genes encoding proteins involved in fatty acid uptake or esterification.

The third isoform PPARγ is highly expressed in adipose tissue and regulates circulating free fatty acid content. Thus PPARγ overexpression results in a lowering of the quantity of circulating free fatty acids. Thiazolidinediones are PPARγ agonists used as insulin-sensitising agents to treat diabetes, in part by decreasing circulating free fatty acids. Their precise role in the regulation of β-oxidation in the heart is still under study; animal models overexpressing PPARγ developed a phenotype that was similar to that observed with PPARβ/δ overexpression.[143]

Proliferator-activated receptor γ coactivator-1 (PGC-1) has two isoforms 1α and 1β (Figure 1.3.3). Both are highly expressed in the heart and play an important role in regulating mitochondrial biogenesis and fatty acid βoxidation.[144] They act

by interacting with the transcriptional factors attached to the promoter regions of a gene. They co-activate various nuclear receptor superfamily members such as: PPARs, estrogen-related receptors and nuclear respiratory factor-1. PGC-1 is stimulated under various physiological conditions such as exercise and fasting, and pathological states such as diabetes. Its activity is lowered during heart failure and cardiac hypertrophy.

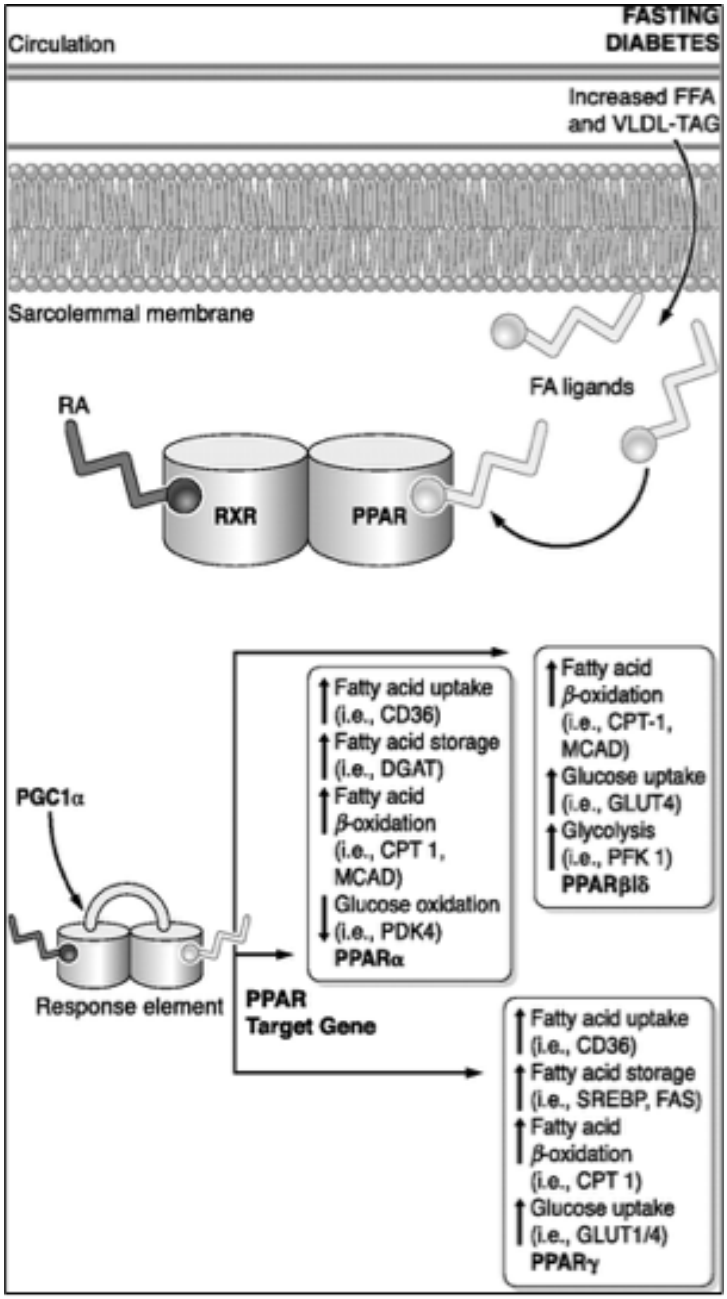

Figure 1.3.3: Peroxisomal proliferator activated receptor (PPAR) family. Figure reproduced by author with permission from: Lopaschuk *et al*. Myocardial fatty acid metabolism in health and disease. Physiological Reviews 2010;90:207-58.

1.3.2.5 Cardiac Mechanical efficiency

Cardiac mechanical efficiency is defined as the ratio of external cardiac power generated relative to the energy expended by the left ventricle.[145] As the majority of resting cardiac metabolism occurs under oxidative conditions, myocardial oxygen consumption (MV_{O2}) can be used to estimate myocardial energy expenditure.

It has been seen that a lower rate of fatty acid βoxidation relative to glucose, yields greater contractile power of the left ventricle for a given MV_{O2}. This has been reported in various studies where stimulation or inhibition of either fatty acid or glucose metabolism results in changes in myocardial energetic efficiency.[146,147] Increasing the plasma free fatty acid concentration in dogs with an infusion of heparin and TAG emulsion results in a 25% increase of MV_{O2} without altering the mechanical power of the left ventricle.[148] Acute elevation of free fatty acid concentration in plasma has been similarly associated with a lowering of cardiac mechanical efficiency in humans, pigs and dogs.[146,147] In contrast inhibition of fatty acid β-oxidation with 4-bromocrotonic acid resulted in increased mechanical power and a lower MV_{O2} in a perfused rat heart.[149] A similar improvement was observed in the left ventricle of pigs when infused with insulin and glucose.[147]

During fatty acid β-oxidation the mechanical power of the left ventricle does not increase proportionately to the increased MV_{O2} consumption with increased workload, thus suggesting use of ATP for non-contractile purposes. This inefficient use of ATP during fatty acid β-oxidation is explained by the following three mechanisms: I) lower phosphate/oxygen ratio (P/O) II) increased uncoupling of mitochondrial oxidative phosphorylation III) increased futile cycling.

I. Phosphate/Oxygen ratio (P/O)

P/O ratio is defined as the number of molecules of ATP produced per atom of oxygen reduced by the mitochondrial electron transport chain using different carbon substrates.[150] This varies depending upon the source of fuel used for energy production. Whereas one molecule of palmitate produces 105 molecules of ATP and consumes 46 molecules of oxygen, one molecule of glucose produces 31 molecules of ATP while consuming only 12 molecules of oxygen. Thus for every molecule of oxygen consumed, glucose produces more ATP than fatty acids and thus has a higher P/O ratio.

Glucose is also a better fuel as the reducing equivalent produced by it pre-citric acid cycle is only NADH, whereas for fatty acids it includes NADH and $FADH_2$. NADH oxidation at complex I of the electron transport chain is indirectly coupled to the production of ATP, while $FADH_2$ bypasses complex I and thus is less efficient for ATP production.

II. Mitochondrial oxidative phosphorylation

The maintenance of an electrochemical proton gradient across the inner mitochondrial membrane is essential for the generation of ATP via oxidative

phosphorylation.[150] In order to maintain this, protons move from the mitochondrial matrix into the intermembrane space via complexes I, III and IV of the electron transport chain.[151] The subsequent reentry of these protons into the mitochondrial matrix via the F0/F1-ATPase results in ATP generation.

Uncoupling proteins (UCP1-UCP5) offer an alternate mechanism for extrusion-reentry of protons, but this is not coupled to ATP synthesis.[152] UCP-3 is an uncoupling protein, highly expressed in the heart, which plays an important role in the translocation of fatty acid anions from the mitochondrial matrix into the intermembrane space and the cytoplasm.[152,153] The fatty acid anions are generated from the hydrolysis of fatty acyl CoA esters by mitochondrial thioesterase (MTE). This process is associated with energy expenditure, but helps in the generation of acyl CoA that is required for various reactions in the matrix.[154] The fatty acid anions transported to the intermembrane space associate with a proton and form a neutral species. This neutral fatty acid species can then reenter the matrix via the so-called 'flip-flop' mechanism and release the proton.[155] While this is not an efficient way of proton transfer as it does not result in production of ATP, the fatty acid anions that are transported to the cytoplasm also result in additional energy expenditure, as they need to be re-esterified before reentering the β-oxidation cycle.

III. Increased futile cycling

The futile use of ATP for purposes other than cardiac contraction occurs via different mechanisms. One of the proposed mechanisms is the cycling of free fatty acids between their acyl moieties and the TAG intracellular pool. While this mechanism prevents the excessive accumulation of free fatty acids in cells, it comes at the expense of extra energy consumption. The free fatty acids cycled

from TAG are either used for energy production after being esterified and converted into their acyl moieties which are channeled into β-oxidation or reconverted back into TAG. Nearly 30% of the intracellular energy is utilised in this process and thus diverted from contractile function.[156]

High intracellular levels of long chain fatty acids also contribute to futile cycling of ATP by stimulating the sarcolemmal calcium channels, which results in an increased transfer of extracellular calcium into the cells.[157] This results in increased energy expenditure required for maintaining calcium homeostasis.

Fatty acids also inhibit adenine nucleotide translocator (ANT), which is required for translocation of the ATP from the mitochondrial matrix into the cytoplasm.[158,159] This results in lack of ATP in the cytosol where it is hydrolysed for left ventricular contractile power generation.

1.3.2.6 Randle cycle

In the healthy heart under normal resting conditions acetyl CoA is the main energy substrate. While 50-70% of acetyl CoA is produced from fatty acid β-oxidation, 30-50% is generated from the oxidation of pyruvate (figure 1.3.4).[111,160,161] Pyruvate is generated from glycolysis and lactate oxidation in equal amounts. Pyruvate is further metabolised in any of three ways: a) converted to lactate b) decarboxylated to acetyl CoA c) carboxylated to oxaloacetate or malate. Decarboxylation of pyruvate to acetyl CoA occurs in the mitochondrial matrix.

In states of increased acetyl CoA production from fatty acid β-oxidation, there is an activation of pyruvate dehydrogenase kinase. Pyruvate dehydrogenase kinase phosphorylates and inhibits pyruvate dehydrogenase, the latter being

the important rate-limiting enzyme converting pyruvate to acetyl CoA. Pyruvate dehydrogenase kinase is also activated by increased ratios of mitochondrial $NADH/NAD^+$. [162]

Increased supply of acetyl CoA via glycolysis inhibits β-oxidation by inhibiting 3-ketoacyl-CoA thiolase. This acetyl CoA can also be translocated back to the cytoplasm via the carnitine:acylcarnitine translocase enzyme which can then be converted to malonyl CoA by malonyl CoA dehydrogenase. Malonyl CoA inhibits carnitine palmitoyl transferase 1 activity and thus limits the fatty acid β-oxidation. Increased supply of acetyl CoA by either β-oxidation or glycolysis-to the citric acid cycle produces a higher amount of citrate, which inhibits phosphofructokinase-1, thereby ultimately limiting the citric acid cycle. This complex interaction of fatty acid and glucose metabolism is known as the Randle cycle, first described by Philip Randle and colleagues.[163]

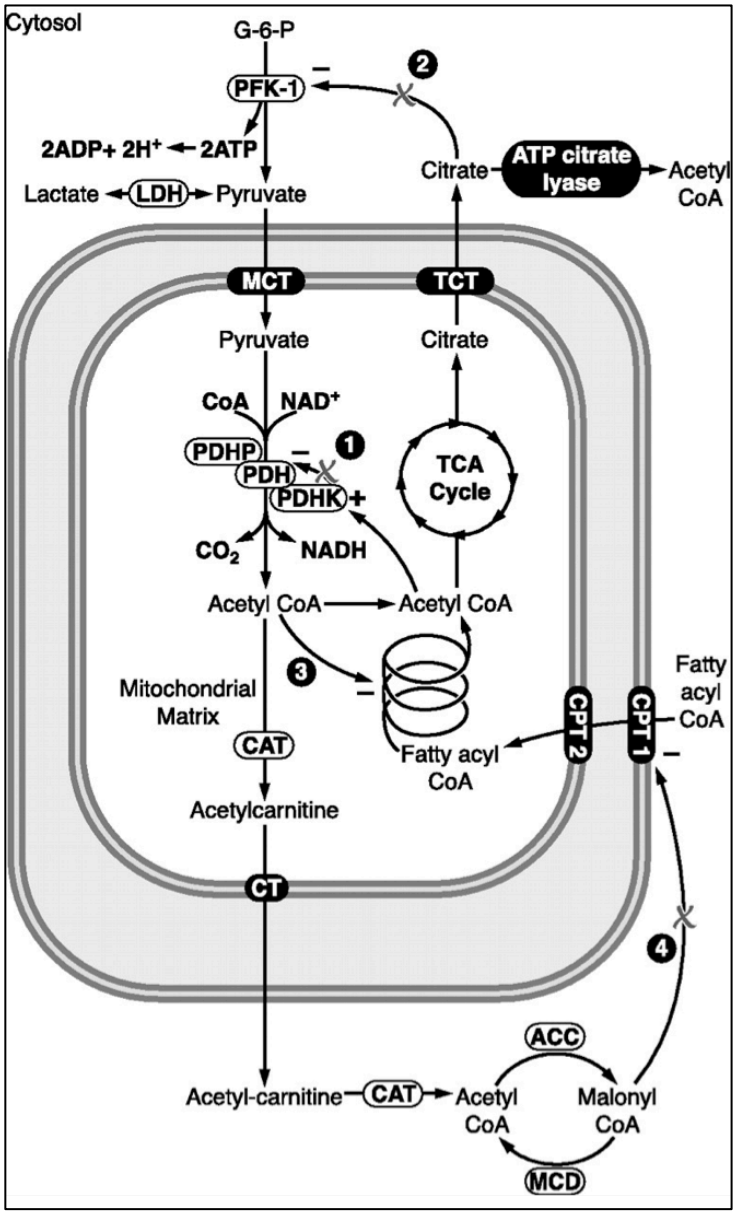

Figure 1.3.4: The Randle cycle. Figure reproduced by author with permission from: Lopaschuk *et al*. Myocardial fatty acid metabolism in health and disease. Physiological Reviews 2010;90:207-58.

1.3.2.7 Citric acid cycle

The citric acid cycle is the main cycle for energy production in aerobic organisms using acetyl CoA as the final common product of carbohydrate, fat and protein catabolism (Figure 1.3.5). It is also known as the tricarboxylic acid (TCA) cycle or the Krebs cycle.[164] The citric acid cycle occurs in the

mitochondrial matrix of eukaryotic organisms and in the cytoplasm of prokaryotic organisms.[165,166]

Using acetyl CoA the citric acid cycle results in the net production of 2 molecules of carbon dioxide, 3 equivalents of NADH, 1 equivalent of $FADH_2$, one equivalent of GTP and precursors for amino acids (Figure 1.3.5). The cycle starts with the transfer of the acetate from acetyl CoA to oxaloacetate forming citrate (catalysed by citrate synthase). Citrate is then dehydrated to cis-aconitate and hydrated to D-isocitrate (catalysed by aconitase). D-isocitrate is then oxidised (generating NADH) and decarboxylated (generating CO_2) to α-ketoglutarate (catalysed by isocitrate dehydrogenase). α-ketoglutarate is then oxidised generating NADH and decarboxylated (generating CO_2) to succinyl-CoA (catalysed by α-ketoglutarate dehydrogenase). Succinyl-CoA is then converted to succinate (generating GTP catalysed by enzyme succinyl-CoA-synthetase). Succinate is in turn oxidised (generating $FADH_2$) to fumarate by succinate dehydrogenase. Fumarate is then hydrated to malate (catalysed by fumarase) and malate is oxadised (generating NADH) back to oxaloacetate (catalysed by malate dehydrogenase) ending the cycle.

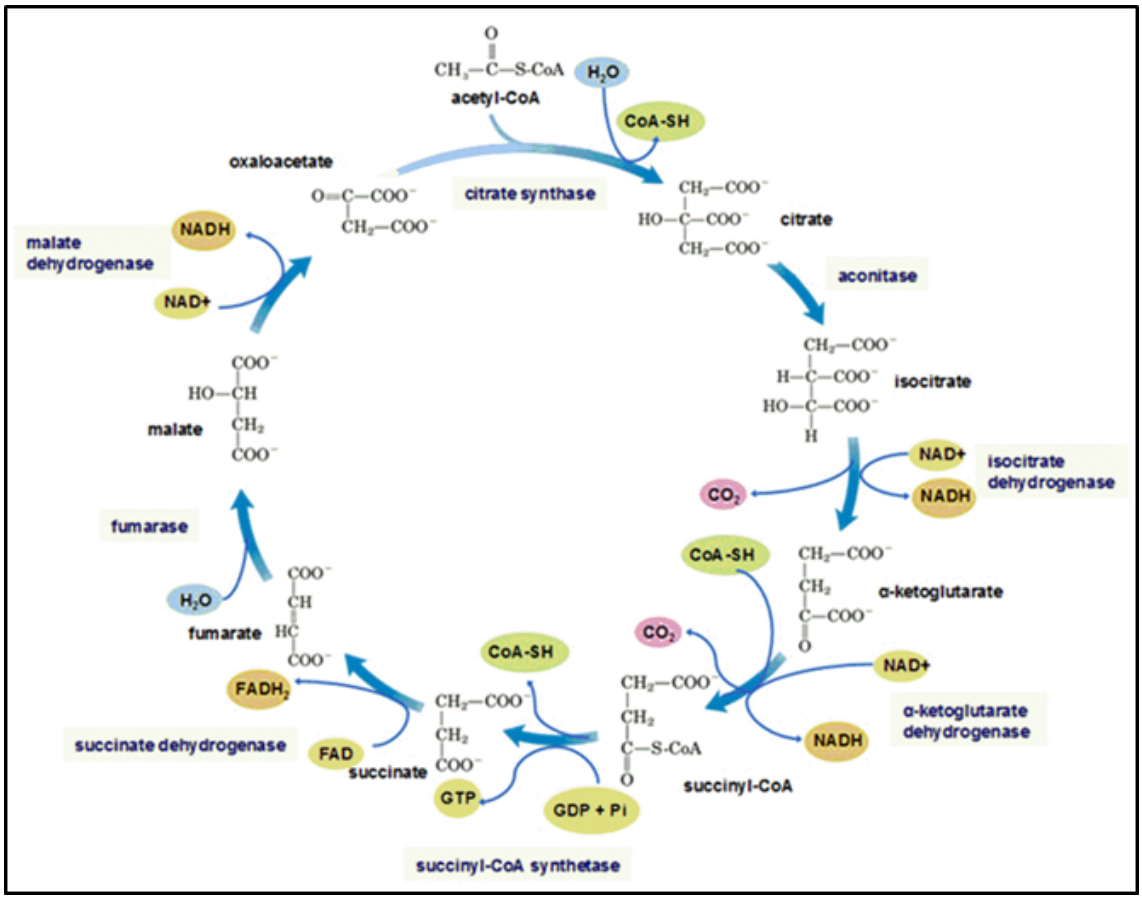

Figure 1.3.5: The citric acid cycle. Figure reproduced by author with permission from: Da Polan, A.T., El-Bacha, T. & Luz, M. R.M.P. (2010) Nutrient Utilization in Humans: Metabolism Pathways. *Nature Education* 3(9):11.

The citric acid cycle is regulated by feedback inhibition from various products of the cycle itself such as: NADH, ATP, citrate and succinyl-CoA. NADH inhibits pyruvate dehydrogenase, isocitrate dehydrogenase, α-ketoglutarate dehydrogenase and citrate synthase. ATP and succinyl CoA inhibit citrate synthase and α-ketoglutarate dehydrogenase. Citrate inhibits phosphofructokinase-1, an important enzyme in glycolysis used in the formation of fructose 1,6-bisphosphate. Calcium also plays an important role in the regulation of citric acid cycle, with increased intracellular calcium levels resulting

in stimulation of pyruvate dehydrogenase phosphatase, isocitrate dehydrogenase and α-ketoglutarate dehydrogenase.[167]

1.3.3 Myocardial metabolism in disease states

Myocardial metabolism undergoes substantial changes during pathological states such as heart failure and ischaemia. Myocardial fatty acid metabolism is directly influenced by substrate availability, such as the levels of circulating free fatty acids and ketone bodies. For example, acute heart failure is accompanied by a catecholamine surge, which results in the activation of lipases, increased concentration of circulating fatty acid and thereby increased β-oxidation.[168,169] A modest increase in the level of ketone bodies has been associated with a decrease in fatty acid uptake and β-oxidation.[168] Thus studies assessing the myocardial fatty acid metabolism should account for the amount of substrate available.

There have been studies measuring myocardial fatty acid metabolism in humans, both by direct invasive and indirect non-invasive methods. The two direct invasive studies had contrasting findings. A study by Paolisso *et al* reported that, compared to controls, heart failure patients had a higher concentration of plasma norepinephrine, insulin and free fatty acids.[169] There was a resulting 40% increase in fatty acid β-oxidation, despite no change in coronary blood flow or energy expenditure. A more recent study by Neglia *et al* reported no change in the levels of plasma free fatty acids, and a lowering of free fatty acid uptake and β-oxidation in patients with heart failure as compared to controls.[170] Indirect non-invasive studies support the latter findings that in the absence of increased levels of circulating free fatty acids, a decrease in fatty acid β-oxidation was observed advanced heart failure patients.[171,172]

Studies from human myocardial samples obtained from heart failure patients undergoing transplantation have shown a decrease in the levels of mRNA and down regulation of proteins regulating the expression of enzymes of β-oxidation.[173] These include enzymes such as long chain acyl CoA dehydrogenase and medium-chain acyl CoA dehydrogenase (MACD). Also noted was a decrease in the activity of CPT1, increased levels of tissue acylcarnitine and decreased levels of free carnitine.[174] In animal models of heart failure a wide spectrum of enzymes involved in fatty acid and carbohydrate metabolism have been identified to be downregulated.[175,176]

It was seen that that this downregulation of various enzymes is mediated by a fall in the activity of PPARα. PPARα, as described above, is a member of the nuclear receptor superfamily which provides transcriptional regulation of genes encoding for proteins controlling the activity of enzymes involved in fatty acid and carbohydrate metabolism. Decreased activity of PPARα has been reported in both in vitro and in vivo animal models of cardiac hypertrophy and heart failure.[177-180] Furthermore, PPARα protein levels were low in myocardial biopsy samples obtained from patients with end stage heart failure undergoing transplant.[181] However, variable results have been reported in pre-clinical studies utilising the PPARα agonist finofibrate. While some studies reported no change or even a decline in the left ventricular function, others reported prevention in the decline of left ventricular function.[179,182,183] Accordingly there is no clear evidence to support the concept that a downregulation of PPARα levels results in the development or progression of heart failure.

Mitochondrial respiration and oxidative phosphorylation are also defective in patients with heart failure. Although there is a normal production of the reducing

equivalents (NADH, $FADH_2$), there is a decrease in the amount of supercomplexes consisting of complex I, III & IV.[184,185] Defects in the fatty acid metabolism of heart failure patients have been used as therapeutic targets with clinical trials using perhexiline, etomoxir, oxfenicine and trimetazidine having shown beneficial effects.[186-190] The exact mechanism underlying these beneficial effects is not known, but is postulated to be due to increased mitochondrial coupling and decreased β-oxidation resulting in higher ATP production.

Myocardial ischaemia results in a state of demand-supply mismatch in the myocardium for essential nutrients and oxygen, resulting in impaired energy production via oxidative phosphorylation. The accompanying catecholamine surge results in increased adipose tissue lipolysis, decreased pancreatic insulin release and peripheral insulin sensitivity.[115] The surge in circulating levels of free fatty acids provides higher substrate delivery to the myocardium and thus influences its metabolism.[191]

During ischaemia it is not only the lack of nutrient supply but also the decreased clearance of by-products of metabolism that influences cardiomyocyte function. Fatty acid β-oxidation remains the primary source of energy production during states of decreased oxygen supply.[192,193] In response to hypoxia there is uncoupling of glycolysis, which promotes conversion of pyruvate to lactate to maintain anaerobic glycolysis.[194,195] The resulting accumulation of lactic acid and H^+ ions further disrupts the ionic homeostasis. This state of increased β-oxidation, anaerobic glycolysis and lactate production persists even during the reperfusion stage and can therefore hamper cardiomyocyte recovery.[196]

At the subcellular level during ischaemia there is activation of AMPK, phosphorylation-induced inhibition of ACC and a resulting increased activity of MCD. This produces lower levels of malonyl CoA, reliving CPT1 inhibition and thus promoting β-oxidation.[197,198] The lack of ATP production also inhibits the Na^+-K^+-ATPase and sarcoplasmic Ca^{2+}-ATPase at the subcellular level. There is a resultant intracellular accumulation of Na^+ and Ca^{2+} ions. The intracellular Ca^{2+} overload inhibits the contractile proteins, stimulates proteases and causes mitochondrial disruption.[199,200] The cellular architecture is also disrupted by intracellular accumulation of unused acyl CoA esters and fatty acylcarnitines, when increased levels of NADH and $FADH_2$ inhibit β-oxidation during ischaemia.[201,202]

1.3.4 Hypertrophic cardiomyopathy and myocardial energetics

1.3.4.1 Hypothesis of contractile dysfunction

Following the discovery of HCM as a monogenic disorder resulting from sarcomeric gene mutations, there was an expectation that the pathogenesis and clinical heterogeneity of the disease could be explained.[203] Though initial studies found several robust and clinically relevant genotype-phenotype correlations, there still remained unexplained heterogeneity in the phenotype and in the natural course of HCM, despite families or patients being carriers of a similar genetic mutation.[14,204]

Initial attempts to explain the pathogenesis of HCM were made based on the postulated impaired contractile function of the mutated sarcomeric protein. This was hypothesised to cause systolic and diastolic impairment of the left ventricle, which will lead to increased wall stress and a decreased cardiac output. The

resulting state of impaired cardiac function and depressed circulatory reserve would lead to the activation of neuroendocrine-mechanoreceptor signalling pathways resulting in cardiac hypertrophy.[205,206]

Though an attractive hypothesis, it could not explain the following characteristics of HCM:

I. While initial studies had suggested that there was a reduced translocation and force generation in myocardial contractile proteins such as the β-MHC (β-myosin heavy chain), subsequent studies had contrary findings and revealed increased motor activity in the β-MHC mutants, increased translocation velocity in troponin T mutants and increased Ca^{2+} sensitivity of force production in troponin I mutants.[207-209]

II. The distribution and magnitude of the hypertrophy could not be explained by the hypothesis. In HCM the usual pattern of enlargement is the asymmetrical hypertrophy of the septum and to a degree greater than the symmetrical hypertrophy seen in compensatory response to pressure overload in conditions such as hypertension.[8,210]

III. The appearance of hypertrophy is most commonly seen during early adolescence when there is accelerated body growth, with completion of the phenotype by adulthood. In rare cases hypertrophy manifests itself during midlife. This is not readily explained by the above hypothesis given that the mutated sarcomeric protein and contractile dysfunction are present from birth.[38,67]

The initial excitement to explain the heterogeneous nature of HCM based on genotype-phenotype correlation was soon subdued. Though some associations between a specific mutation and the risks of the disease were robust, a large

section of this heterogeneity could not be explained by existing genotype-phenotype correlations.[204,211] Accordingly, both within and in-between families with members bearing the same mutation, the heterogeneous nature of the multiple disease features could not be explained: a) onset and severity of symptoms; b) the severity and pattern of hypertrophy; c) incidence of arrhythmia; d) histological pattern of the disease; e) occurrence of heart failure; f) predisposition to sudden cardiac death. This suggested the presence of other downstream and environmental factors contributing to the pathogenesis of HCM.

1.3.4.2 Hypothesis of impaired myocardial energetics

A new hypothesis of impaired myocardial energetics resulting in HCM was proposed. It was suggested that mutated sarcomeric proteins could not utilise the ATP efficiently and thus created an energy demand-supply mismatch. The resultant increased energy requirement at the subcellular level could not be met, resulting in myocardial dysfunction and hypertrophy. This hypothesis is supported by several observations:

I. Different classes of sarcomeric mutations have separate mechanisms resulting in inefficient energy utilisation. For example, mutations in β-MHC alter the cycling rate of myosin heads.[208] The mutated thick filament in these circumstances is comprised of both wild type and mutant myosin heads. The strain produced by active crossbridge formation on the same filament results in an increased rate of detachment. Thus the slower heads are forced to detach before the completion of the power stroke. This premature detachment results in reduced force production despite consuming a similar

amount of energy resulting in an inefficient energy-mechanical force coupling mechanism.

Mutations in other sarcomeric proteins such as troponin T result in increased contractile velocity but reduced force production.[212] This is thought to be secondary to increased crossbridge detachment and shortening of the power stroke, in spite of consuming an adequate amount of ATP. This results in increased energy requirements of the heart as it tries to pump adequate volume of blood against the systemic vascular resistance, using an in-efficient mutated sarcomeric protein.

The increased energy cost of force production in hypercontractile protein mutations originates from increased crossbridge activation for the same level of Ca^{2+}, thus consuming excessive ATP. This hypercontractility does not contribute to an increased stroke volume in spite of excessive energy utilisation however: following the prolonged contractile phase, as the Ca^{2+} transient falls and excessive ATP has been used, it results in impaired relaxation and diastolic dysfunction.

II. A number of phenocopies of HCM exist which have a similar phenotype, but which are caused by non-sarcomeric mutations with energy deficiency as a primary pathogenic mechanism. These include diseases affecting mitochondrial function such as mitochondrial tRNA mutations and Friedriech ataxia which affects expression of an inner mitochondrial membrane protein, frataxin.[213,214] The phenotype of asymmetrical hypertrophy phenotype is also seen in disorders affecting fatty acid uptake (e.g. CD36 deficiency) and defective mitochondrial fatty acid oxidation (e.g. very long chain acyl-CoA dehydrogenase deficiency).[215,216]

III. In rodent knockout models involving genes encoding GLUT-4 glucose transporter and adenine nucleotide translocation-1, a phenotype of asymmetrical septal hypertrophy similar to that of HCM is observed.[217]

IV. Mutations in the gene (PRKAG2) encoding the γ2 regulatory subunit of AMP-activated protein kinase (AMPK) have been described in patients with a phenotype of HCM and ventricular pre-excitation.[218,219] AMPK plays vital role in maintaining cellular energy homeostasis and identification of mutations in energy-sensing subunits of AMPK suggests a final common pathway of energy deficiency shared with the sarcomeric mutations causing HCM.

V. Reduced phospho-creatine (PCr)/ATP ratio, increased carbohydrate utilisation and decreased coronary sinus pH have been identified in patients with HCM.[220] These physiological changes are seen in a setting of normal capillary oxygen pressure, implying a state of increased energy requirement in HCM. Similar findings of decreased PCr/ATP have been seen in patients who are genotype positive but phenotype negative, suggesting that these findings cannot be attributed solely to the presence of hypertrophy.[221] Moreover, more extreme phenotypes with greater degrees of hypertrophy and myocardial dysfunction are observed in patients with both sarcomeric and mitochondrial mutations.[222] This suggests a final common pathway being affected by two different mutations that share a similar pathogenesis. Similar findings have been reported in transgenic rodent models of HCM with myosin mutations.[223,224]

The state of energy deficiency in HCM results in compromise of Ca^{2+} reuptake and removal by the sarcoplasmic reticulum Ca^{2+} re-uptake (SERCA-2) pump.[223]

This results in an increased Ca^{2+} transient which activates various downstream pathways such as: a) Ca^{2+}-calmodulin-dependent protein phosphatase (calcineurin) b) members of the NF-AT family of transcription factors c) Ca^{2+}-calmodulin-dependent protein kinase (CaMK) c) p38 mitogen-activated protein kinase (MAPK).

The development of hypertrophy during adolescence is potentially explained by the accelerated systemic growth phase, which results in increased metabolic demand. This results in a state of energy compromise, myocardial dysfunction and resultant hypertrophy.[225] The development of asymmetric hypertrophy has now been supported by studies where disproportionate energy demand and compromise has been noted in the interventricular septum.[226,227]

Thus energy deficiency, potentially compounded by microvascular ischaemia, appears to be central to HCM pathogenesis.[228] A priori, it is likely that dynamic (i.e. during exercise) alterations in cardiac metabolism contribute to HCM. The identification of perhexiline (a fatty acid oxidation inhibitor) as a treatment for subgroups of HCM, exemplifies the value of this metabolic strategy for diagnostic and therapeutic purposes.[229] Characterising dynamic changes in cardiac metabolism in HCM is thus likely to: (i) contribute to understanding HCM pathophysiology, (ii) guide novel metabolic therapeutic strategies and (iii) partially illuminate the basis of its clinical variability and to delineate disease subgroups by identifying stratifying biomarkers.

1.4 Metabolomics

1.4.1 Historical perspective

Metabolomics is a maturing field, which incorporates analytical methods for the identification, quantification and characterisation of all small molecules in a biological system and also measuring the changes which occur in these metabolites following perturbations.[230] There have been huge advances in the field over the last five decades with improvements in the design of analytical platforms (mass spectrometer and nuclear magnetic resonance spectrometer) and software, enabling improved processing and data interpretation.

Dalgliesh and co-workers published one of the first works in the field in 1966.[231] They had developed derivatisation methodology for gas chromatography (GC) linked to mass spectrometry (MS) to investigate the metabolic products human urine and tissue samples. In 1971 Horning and Horning used GC-MS to profile human urine and drug metabolites.[232] During the same year Pauling studied the human urine vapour and breath by GC-MS to profile 250-280 metabolites.[233] In 1984 using nuclear magnetic resonance spectroscopy (NMR) Nicholson and colleagues studied human plasma, serum and urine from fasting, normal and diabetic patients.[234] In 1986 Fossel and colleagues published findings from a large cohort of patients with cancer compared to controls using NMR.[235]

The expression metabonomics, often used interchangeably with the term metabolomics, was first coined by Nicholson *et al* in 1999.[236] Following this metabolomics' was coined by Fiehn *et al* in 2000 and further supported by Raamsdonk *et al* in 2001.[237,238] The term metabolome was first introduced in 1998 by Oliver *et al*.[239] The metabolome is defined as the total complement of

all small molecule metabolites produced by the organism (endogenous) and those consumed (exogenous). The human metabolome comprises of ~7,900 metabolites, 1,200 drugs and 3,500 food components which act both as markers and determinants of pathophysiology.[230] Accordingly, while a number of strategies have been advocated to delineate HCM's pathogenesis and heterogeneity (e.g. mapping of genetic modifiers), the study of metabolomics is likely to be at least as informative. Considering the flow of biological information (DNA → RNA → protein → metabolite → phenotype), the metabolome is both closely related to the genome, transcriptome and proteome, but importantly resides immediately proximal to the disease phenotype (figure 1.4.1).[240]

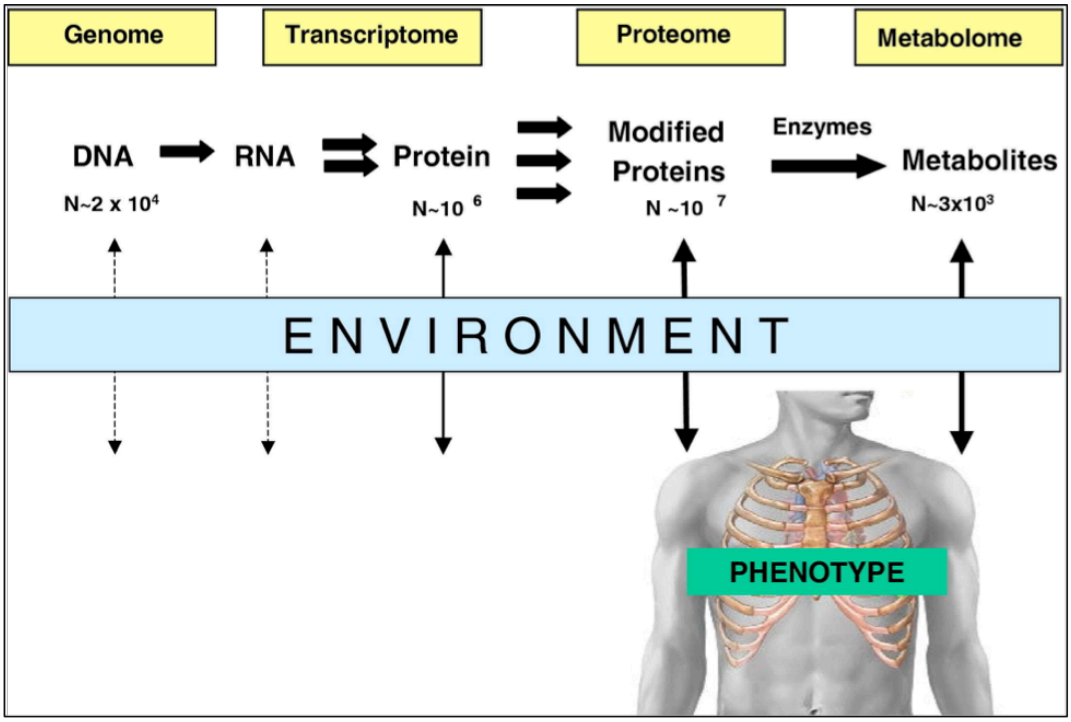

Figure 1.4.1: Illustrating the linkage of metabolomics with other 'Omics' approaches and the phenotype. Figure reproduced by author with permission from: Lewis *et al*. Application of metabolomics to cardiovascular biomarker and pathway discovery. Journal of the American College of Cardiology 2008;52:117-23.[240]

Though the metabolome is closely connected to both the genome and proteome, the degree of alteration in the gene or protein expression does not correlate to the change in metabolome.[241] Firstly a genetic mutation can produce small alterations in the transcriptome and proteome but large changes in the metabolome, exemplified by in-born errors of metabolism. Secondly, environmental factors that alter biological homeostasis in the cell can result in major transcriptomic and proteomic changes, but small alterations in the metabolome.

There are three strategies employed in metabolomic research:[242]

I. Metabolomic fingerprinting: this is the unbiased analysis of metabolites to understand the clinically most relevant differences. It identifies the most significant metabolite pattern or fingerprints which change in response to a disease state, pharmacological intervention or the environment.[243]
II. Metabolic profiling: this is the targeted analysis of a group of preselected compounds aimed to better understand the disease pathways and aid in the discovery of new biomarkers.
III. Metabolic footprinting: this is the measuring and monitoring levels of metabolites, which are secreted or fail to get absorbed by cells.[244]

1.4.2 Metabolomic techniques

The workflow of a well-designed metabolomic project encompasses the following: study design, sample preparation, data acquisition and data extraction & analysis (figure 1.4.2). Each of these components has to be considered carefully for robust and reproducible results.

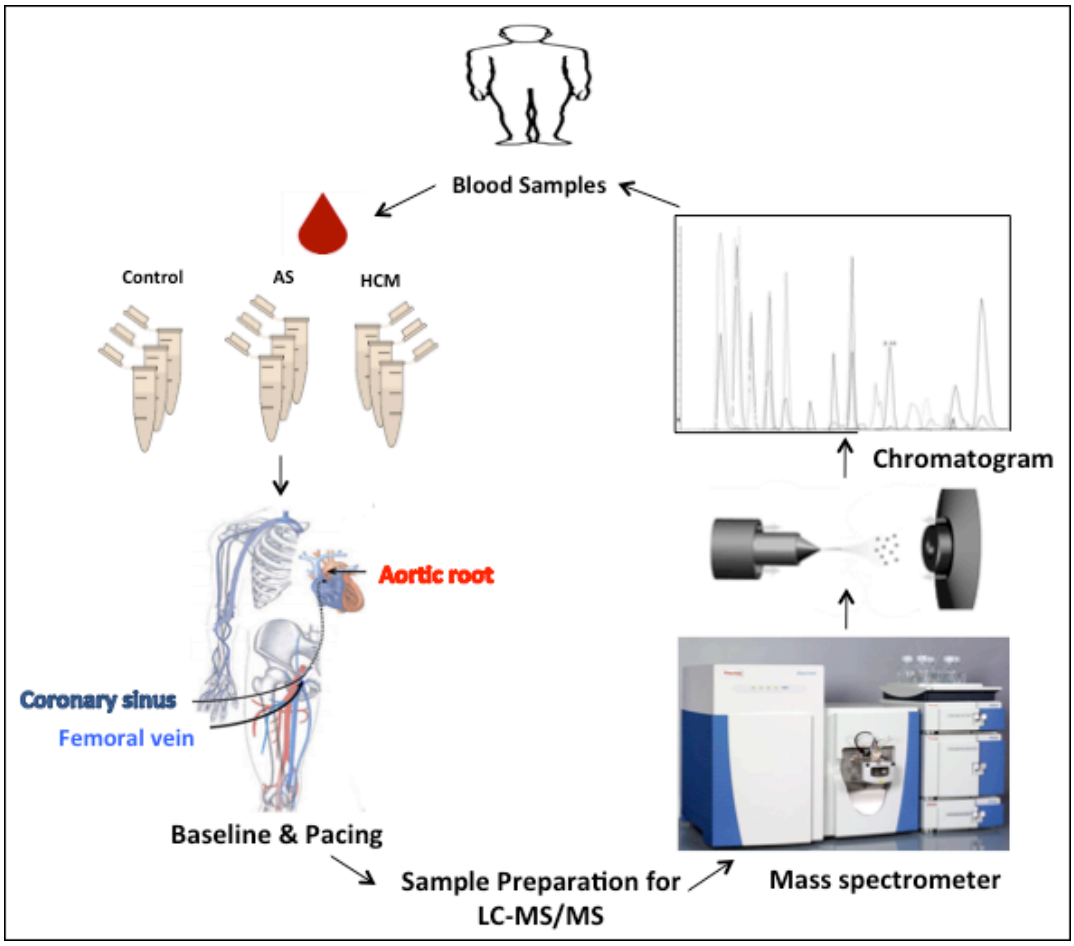

Figure 1.4.2: Overall workflow of a metabolomic study

1.4.2.1 Study design

In designing a human metabolomic project it is important to understand and address the undesired variation that can be produced by various biological and environmental factors affecting participating subjects. Firstly it is important to clearly pre-define the clinical/disease phenotype being studied and equally importantly to select an appropriate control group.[245] Secondly, if possible subjects should be matched for variables such as age, sex and ethnicity. Other variables such as diet, lifestyle and medications should also be controlled if possible.[246,247] This can be achieved by collecting samples from fasting patients, who have not smoked or consumed alcohol for a pre-defined period

and at a given time of the day to minimise the effects of circadian rhythm on metabolism. To reduce the effects of these variables we collected samples from a subject after fasting for six hours, and at baseline and following an intervention (pacing), thus allowing each subject to act as their own control.

The technique of sample collection, processing and storage also needs to be consistent. Samples once collected should be snap frozen at the earliest opportunity; any variability in the time delay between sample collection and freezing can affect the metabolite analysis.

1.4.2.2 Sample preparation

The metabolomic technology can be used to analyse a variety of biological samples, the two most common being plasma and urine. Appropriate sample preparation is a must to minimise the effect of heterogeneity within the metabolome and maximise the ability to detect metabolites present in low concentrations.

Samples are pretreated with solvents such as methanol to maximise protein depletion and increase the extraction of metabolites.[248] Following this the samples may be chemically derivatised to improve their analytical detection. This is especially useful in GC experiments where non-volatile compounds on derivatisation become volatile and thermally stable.[249] It can also be used to introduce isotope labels on metabolites, which allows a quantitative measurement of their flux in a biological system.[250] This technique is sometimes used in liaison with LC, where it increases the ionisation and fragmentation of metabolites, thus improving the overall sensitivity. In our experiment we

derivatised acylcarnitines using butanolic HCL, which produced butyl esters from the carboxylic acid acylcarnitine head group.

1.4.2.3 Analytical platforms

Since metabolites have huge diversity in their chemical structure (polarity and solubility in water & lipids) and size (subnanomolar to millimolar), a comprehensive analysis requires integration from complementary analytical platforms. The two most commonly used platforms are NMR and MS.[251,252] For the purpose of the current work, MS was used for analysis (with specific method is detailed later in Section 2.5).

1.4.2.3.1 Nuclear magnetic resonance spectroscopy (NMR)

NMR is used to analyse compounds that have a NMR nucleus.[253,254] NMR nuclei are those that possess a nuclear spin (nucleus spinning about its own axis) e.g. ^{1}H, ^{13}C, ^{19}F and ^{31}P. ^{1}H is most commonly used as it is abundant in organic compounds. NMR is not effective for those molecules that possess an equal number of protons and neutrons and thus have a resultant zero spin for e.g. ^{12}C and ^{16}O.

NMR identifies metabolites by chemical shift that separates the molecules on the basis of their unique resonance frequency. The resultant spectra plot the molecules in an order of decreasing frequency from left to right. The peaks have characteristics such as resonance frequency, height and width at half-height. The height or area under the curve yields the concentration of a given molecule relative to the internal standard.[255]

The advantages of NMR analysis include little sample preparation, non-destructive technique, absolute quantification of metabolites and provides

information about their structure.[238] The disadvantages of NMR are that it is a less sensitive technique (limit of detection milli to high micromolar) and the resultant spectra is dense making analysis difficult.[256,257]

1.4.2.3.2 Mass spectrometry

Mass spectrometry (MS) has recently been gaining prominence, as it is a more sensitive technique (limit of detection from milli to nanomolar) than NMR, especially when combined with chromatography.[237,258,259] The disadvantages of MS are sample preparation pre-analysis and difficulty in absolute quantification in the absence of proper internal standards.

MS works on the principle of ionisation of molecules and their separation based on the ratio of mass-to-charge (m/z). Molecules adopt different charge based on their physical characteristics and the ionisation mechanism used. The different ionisation techniques include atmospheric pressure chemical ionisation (APCI), MALDI (matrix-assisted laser desorption), NIMS and electrospray ionisation (ESI). [260,261,262] Following the generation of ions they can be measured using different types of mass analysers (quadrupole, ion trap and time of flight (TOF) analyser).

The MS analysis can be combined with different chromatographic techniques allowing better separation of molecules pre-ionisation. The chromatographic techniques differ in the mobile phase being used: gas (GC) and liquid chromatography (LC). GC uses helium or nitrogen as the mobile phase and has it's advantage in being able to measure a wide variety of low molecular weight compounds, but it is not efficient in measuring compounds that are non-volatile.[249,263] LC is a preferred separation technique for compounds that are

non-volatile and soluble in water, methanol, acetonitrile or isopropanol.[264,265] LC techniques such as ultra high performance liquid chromatography are gaining momentum where faster and efficient separation of small particles is performed, by passing them through columns in a ultra high-pressure system.[266]

1.4.2.4 Data extraction and analysis

The extraction of data variables post-MS run is a complicated process involving hundreds of variables in a large number of samples. Thus it is important to ensure that the same compound is compared across all samples. MS data has three dimensions: intensity, mass scale and time. While the first two dimensions are constant, the time domain is variable and difficult to predict. To handle this there are two approaches: i) first is to spread the data over time and compare the resulting mass vectors between samples ii) second to initially identify the metabolites and then align them according to their time of elution for comparison between samples.[257]

Once the data is extracted, various metabolites need to be identified based on their molecular mass. For this various databases can be used: Human metabolome database,[230] ChemDB,[267] METLIN (https://metlin.scripps.edu/), KNApSAcK (kanaya.naist.jp/KNApSAcK/) , SetupX & Binbase (htrp://fiehnlab.ucdavis.edu/db/) and KEGG (http://www.genome.jp/kegg/).

Following this the data needs to scaled or transformed to compensate for any large variations in the data set. This processed data is then analysed using various multivariate statistical methods to determine any inter group differences. The methods routinely utilised are principal component analysis (PCA), partial least square analysis (PLS) discriminant analysis, hierarchical clustering and

correlation networks.[268,269] Some of these methods used in our work, are described in more detail in Section 2.6.3.1.

1.4.3 Emerging role of metabolomics

Metabolomics can play a vital role in the discovery of biomarkers, drug discovery and targeted therapy. The identification of metabolites which undergo a change in their concentration following physiological or pathological changes or following perturbations, can not only help in disease diagnosis but also prognostication and targeting therapy. Thus the newly emerging discipline of pharmacometabonomics is gaining importance, where a specific drug can be used for selected patients depending upon their response to therapy (targeted therapy). An important example of this is the use of Herceptin in patients with breast cancer with overexpression of HER2 (human epidermal growth factor 2).[257]

The discovery of novel pathological pathways will also aid in the discovery of new drugs. Alteration in the activity of an enzyme is a central pathological mechanism of many disorders. Such an alteration changes the flux of downstream molecules such as metabolites, with the corollary that identification of these metabolites and monitoring of their flux can aid identification of novel disease pathways. The potential of this approach is exemplified in the deduction made by Munger and colleagues (2008) who provided ^{13}C-labeled glucose and glutamate to mammalian cells infected with cytomegalovirus (CMV) and demonstrated increased flux thorough the citric acid cycle via the fatty acid consumption pathway. When fatty acid biosynthesis was inhibited by 5-tetradecyloxy-2-furoic acid this resulted in an inhibition of viral replication.[270]

As detailed before, metabolic studies in LVH and heart failure (generally limited to targeted metabolites e.g. glucose) have observed that in the resting state the healthy heart generates ~70% of its ATP from fatty acids.[271] In contrast, failing hearts and those with LVH rely on increased glucose utilisation. Advanced myocardial dysfunction is characterised by myocardial and systemic insulin resistance[272] and mitochondrial dysfunction.[228,273,274] While the degree and merit of these switches remain the subject of vigorous debate, the coupling between metabolic derangements and myocardial dysfunction is highlighted by the correction of both using an LVAD (left ventricular assist device) implantation (through the reduction of myocardial toxic lipids).[275] A more systematic approach, afforded by an analysis of metabolomics that acknowledges the complexity of biological systems, is likely to extend these metabolic insights.

The metabolome includes bioactive amino acid metabolites and free fatty acids (FFA). These entities may be proximal to the pathophysiology of HCM, as alterations in their metabolism reflects the overall changes in myocardial metabolism, which is likely to provide novel insights into the underlying disease mechanisms. Metabolomic examination of such neglected molecules has already yielded biological insights in other conditions (e.g. elucidating the active role of the tryptophan catabolite kynurenine in cancer, immune biology and in post-resuscitation hearts).[276] Similarly, there are early indicators that the systematic profiling of established molecules (e.g. FFA, carbohydrates and TCA intermediates) and novel metabolites (e.g. stachydrine) may identify biologically active entities that could serve to inform both biological understanding and management of cardiomyopathy.[277] Its important to note that some of these

metabolites like β-aminoisobutyric (BAIBA) have low plasma concentrations but still play a vital role in cell signalling and regulatory processes.[278,279]

The study of metabolome in myocardial disease has been limited to date, being confined to myocardial ischaemia, planned myocardial infarction and heart failure.[277,280-285] A number of factors may have contributed to this limited application. Firstly, the challenge of obtaining invasively derived cardiac samples has limited most metabolomic studies to the use of peripheral blood as a metabolic surrogate for the myocardium. The potential for confounding metabolic signals from other organs, especially skeletal muscle, with a decrement in the signal-to-noise ratio is self-evident.[280,286] Accordingly, in the current study it was planned to obtain samples from the coronary sinus to minimise these risks.[281,287,288]

1.5 Hypothesis

The central hypothesis of this work is that the cardiac metabolome in individuals with HCM, both at rest and during stress, is distinct from that of healthy hearts and other forms of pathological cardiac hypertrophy (aortic stenosis). Specifically, it hypothesises that the biology of HCM is determined by changes in cardiac cellular metabolism. Delineation of the metabolic changes will provide novel insights into the biology of HCM and aortic stenosis (e.g. with respect to fatty acid, carbohydrate and amino acid metabolism), with corresponding diagnostic and therapeutic implications.

1.6 Aims

The primary aim of this work was to study the metabolomic profile in coronary sinus effluent by mass spectrometry from patients with (discovery cohort): HCM, aortic stenosis with left ventricular hypertrophy and controls (normal cardiac function with unobstructed coronary arteries). Assessment of Cardiac metabolism was undertaken under different physiological states, both at rest and during myocardial stress induced by pacing. The focus for metabolomic analysis of samples from the discovery cohort was on metabolites and pathways that have previously been associated with other myocardial diseases (specifically fatty acid, carbohydrate and amino acid metabolism), with the aim of obtaining insights into the role of metabolism in the pathophysiology of HCM and aortic stenosis.

The second aim was to validate metabolomic findings and methodology from analysis of the discovery cohort, by replicating the analysis in a separate cohort of patients (validation cohort). To address this, peripheral samples collected

from patients with similar disease characteristics were to be analysed separately to minimise bias.

The third aim was to analyse a transcriptomic dataset from patients with aortic stenosis and controls, to enable correlation of the validated metabolomic findings with changes in the metabolomic transcriptome.

Addressing these aims will yield a robust and reliable account of the cardiac metabolome in left ventricular hypertrophy. By combining insights gained from the transcriptome and the dynamic metabolome, it is anticipated that in contrast to the majority of previous metabolomics studies, the findings of this work may be able to go beyond associations and begin to make causative deductions.

Chapter 2

Methods

2 Methods

I was involved in the conception and design of the study. I obtained ethical approval and managed all operational aspects of the study (including recruitment of all patients, sample collection and phenotypic measurements). I performed the experiments and analysed the entire dataset from the study.

The study was granted ethical approval by National Research Ethics Service (NRES) Committee South Central–C and was monitored by the University of Oxford clinical trials and research governance department.

2.1 Study design

The study design was a prospective single centre observational study to characterise the metabolome from 3 groups of patients: 1) HCM 2) aortic stenosis with left ventricular hypertrophy and 3) controls. The cohort of patients with aortic stenosis was intended as a comparator to aid understanding of the disease process in the HCM cohort, as both share a similar cardiac phenotype of left ventricular hypertrophy (LVH). LVH in patients with HCM develops from an underlying sarcomeric mutation, in patients with aortic stenosis it develops secondary to left ventricular obstruction.

The initial aim was to recruit an equal number (n=35) of participants to each of the three groups, forming a total of 105 participants (the discovery cohort). The results from the discovery cohort were then validated in a set of peripheral samples collected from a separate cohort of patients (the validation cohort). These metabolomic findings were subsequently validated using an orthogonal

technology, by performing transcriptomic analysis of the genes regulating these metabolic pathways, in LV biopsy samples from a separate cohort of patients (controls and patients with aortic stenosis).

The patients were recruited from general cardiology clinics, pre-angiography clinics and angiography waiting list at the John Radcliffe Hospital in Oxford. All patients recruited were undergoing angiography on the basis of prior determined clinical need and underwent study procedures in addition to this. Controls were recruited as patients who presented for routine diagnostic coronary angiography indicated for known or suspected coronary artery disease or valvular heart disease, who had willingly consented to participate in the study and who subsequently had normal results from their investigations. Consented patients then underwent baseline phenotyping and coronary angiography (figure 2.1.1: study flow diagram). I recruited and collected samples for the entire discovery cohort and the control subjects from the validation cohort. Dr Masliza Mahmod and Dr Rina Ariga provided peripheral validation samples for the aortic stenosis and HCM cohorts. Mr Neill Howell collected the LV biopsy samples from controls and aortic stenosis patients.

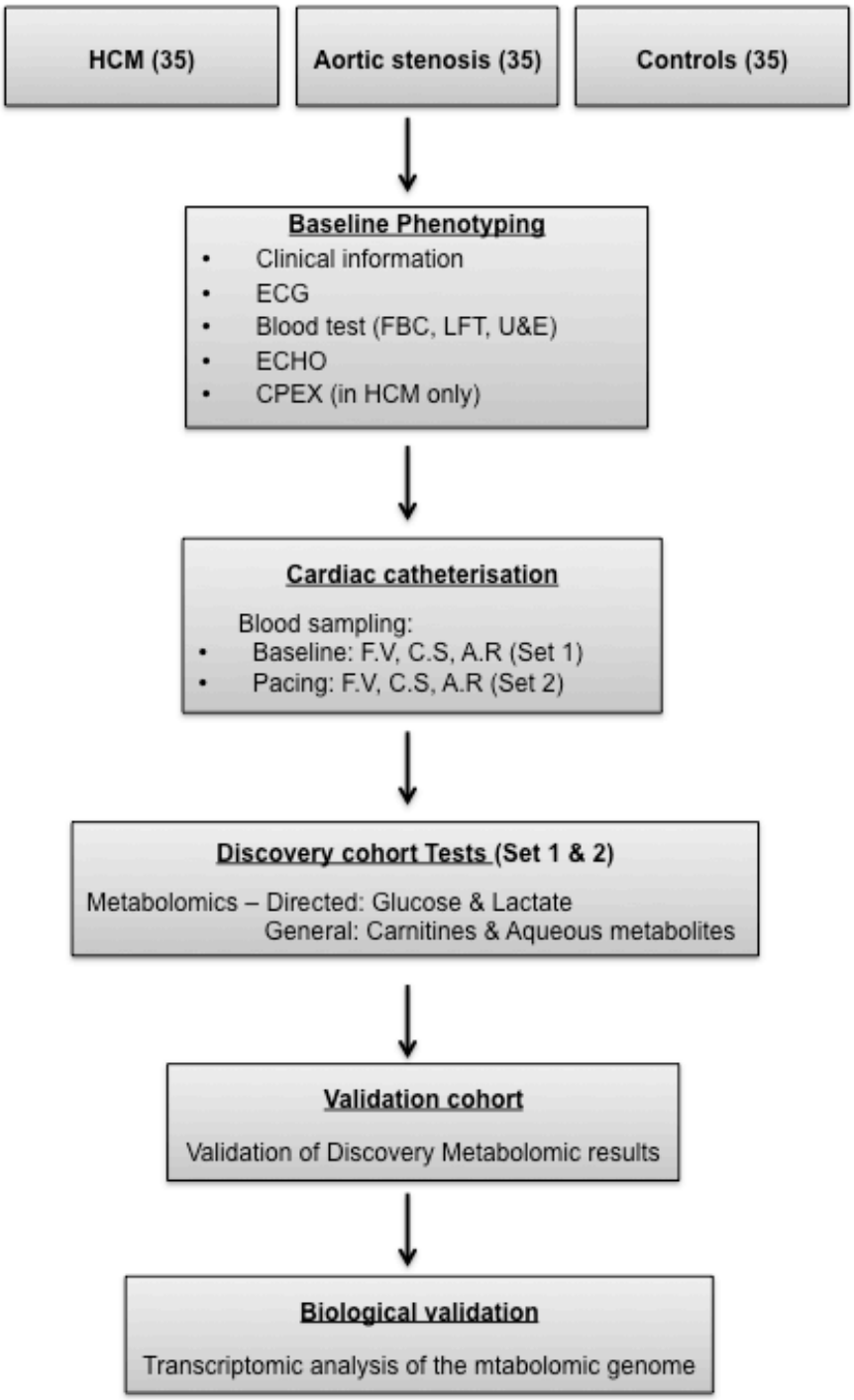

Figure 2.2.1: Flow diagram of the study. AR: aortic root; CS: coronary sinus; FV: femoral vein.

Baseline phenotyping

The following baseline phenotypic measurements were obtained in all consenting patients:

I. Clinical history and examination
II. Routine blood tests (FBC: full blood count, U&E: urea and electrolytes, LFT: liver function tests)
III. ECG (electrocardiogram)
IV. ECHO (transthoracic echocardiography) (optional)
V. CPEX (cardiopulmonary exercise stress test) (performed on HCM patients only)

CPEX was performed on consenting patients with HCM to better understand their exercise cardiovascular physiology and the severity of their disease process.

Cardiac catheterisation

Patients underwent cardiac catheterisation in the coronary angiography suite of the John Radcliffe Hospital, Oxford. I performed the majority of the procedures under the direct supervision of a consultant interventional cardiologist. Samples were collected at baseline and following right ventricular endocardial pacing (if appropriate) from the femoral vein (FV), aortic root (AR) and coronary sinus (CS).

In some patients only a subset of procedures were performed (e.g. blood sampling at baseline) and further interventions were not carried out. This was decided on an individual basis by the supervising consultant, guided by patient compliance / comfort and complexity of the overall procedure.

2.2 Primary and Secondary endpoints

Primary endpoints

a) Identification and quantification of metabolites from specific pathways such as: the citric acid cycle, amino acid metabolism and acylcarnitines.

b) To study complete metabolomic profiles with the aim of novel biomarker discovery to enhance disease diagnosis, prognostication and potentially treatment.

Secondary endpoints

To characterise various metabolites and metabolic pathways (fatty acid, carbohydrate and amino acid metabolism) in HCM to better understand its pathophysiology.

2.3 Study Participants

2.3.1 Overall Description of Study Participants

Participants were aged 18 years or above with a known diagnosis of HCM, including those with either obstructive or non-obstructive disease. Similar numbers of patients with aortic stenosis (with LVH) and controls were also recruited. The control group included the patients who had been routinely referred for coronary angiography and who ultimately had no underlying valvular, coronary artery or heart muscle disease.

2.3.2 Inclusion Criteria

Participants were recruited if they met all of the following criteria:

I. Willing and able to give informed consent for participation in the study
II. Male or female, aged 18 years or above
III. No conduction defects on12-lead ECG

IV. Abstained from caffeine-containing drinks for a minimum of 24 hours, alcohol for 24 hours and from food for at least 4 hours before their coronary angiogram

Participants included in the individual subgroups were as follows:

I. HCM – patients undergoing angiography for clinical indications were recruited. Cardiomyopathy patients with coronary artery disease were either excluded or recruited following an appropriate revascularisation procedure.
II. Aortic stenosis with LVH – these constituted patients who underwent coronary angiography pre-surgical valve replacement. Patients with significant LV dysfunction (ejection fraction < 30%) were excluded.
III. Controls – patients with normal systolic function and unobstructed coronary arteries undergoing coronary angiography for suspected coronary artery disease.

2.3.3 Exclusion Criteria

The participant did not enter the study if any of the following applied:

I. Haemodynamic instability
II. A female participant who was pregnant, lactating or planning pregnancy during the course of the study
III. Severe (ejection fraction < 30%) impairment of left ventricular systolic function
IV. Any other significant disease or disorder which in the opinion of the investigator had the potential to either: a) put the potential participant at risk because of undertaking the study b) influenced the results of the study or c) compromise the participants ability to take part in the study

2.4 Study Procedures

2.4.1 Check for eligibility

In accordance with the predefined inclusion/exclusion criteria, patient eligibility was checked at the time of their attendance to either of the following: cardiology clinics, pre-angiography clinic, angiography procedure waiting list or in-patients awaiting coronary angiography. Patients who then expressed an interest in participation were supplied with a written patient information leaflet (PIL). These patients were then contacted by a phone call, which was made at least a week after they had been provided with a PIL.

For those identified via their referral letter or clinic letter, a letter of invitation and PIL was sent by post. No sooner than a week after the letter was sent, patients were contacted by telephone call to discuss the study further and answer any questions they had. Patients who were already admitted to hospital and awaiting coronary angiography were approached before the procedure and provided with a PIL, with all questions answered satisfactorily prior to the procedure.

2.4.2 Informed Consent

Written and verbal explanation of the study aims and protocol was provided detailing the exact nature of the study, the implications and constraints of the protocol, known potential side effects and any risks involved in taking part. It was clearly stated that all participants were free to withdraw from the study at any time for any reason without prejudice to future care, and with no obligation to give the reason for withdrawal. All participants were recruited by the author and requested to personally sign and date the informed consent form after full

discussion and before any study-specific procedures were performed. A copy of the signed informed consent form was given to all the participants, with the original form retained at the study site. Participants were then considered formally “recruited” and given a study personal identification number (PIN).

This was followed by the following procedures

I. History and physical examination
II. ECG
III. Echocardiography (ECHO) (optional)
IV. Cardiopulmonary exercise testing (CPEX) (optional)
V. Coronary angiography
VI. Processing and analysis of blood samples for routine laboratory tests

2.4.3 Echocardiography

Echocardiographic studies were performed in line with American society of Echocardiography and European Association of Echocardiography recommendations.[289,290] Resting transthoracic echocardiographic images were obtained using the Philips iE33 ultrasound system (Philips medical systems) attached to a X5-1 transducer, with the subject lying in the left lateral decubitus position with continuous ECG monitoring. Images were obtained in the parasternal short- and long-axis and apical 2- and 4-chamber views. Interventricular septal thickness, posterior wall thickness, left ventricular end-diastolic diameter, left ventricular end-systolic diameter, left atrial (LA) size and left ventricular ejection fraction were calculated using standard echocardiographic 2D or M-mode measurements. LV mass was obtained from the 2D echocardiographic measurements using the M-mode formula and

normalized to body surface area.[291] Peak early (E) and late (A) mitral flow velocities and the deceleration time of the early filling velocity (DT) was measured at the tip of the mitral valve leaflets, and the ratio of the early to late peak velocities (E/A) was subsequently derived. Using the 4-chamber apical view, tissue Doppler imaging (TDI) was undertaken at the level of the mitral annulus on the lateral wall of the left ventricle and 2cm above AV junction on the inter-ventricular septum. Early diastolic mitral annular velocity (e') and the late diastolic annular velocity (a') were determined from the average of septal and lateral wall TDI recordings. The mitral E/e' ratio was then calculated.

2.4.4 Cardiopulmonary Exercise Test

Patients with HCM consenting for CPEX performed a symptom-limited erect treadmill or bicycle exercise protocol (according to patient suitability) with simultaneous respiratory gas analysis, as described.[292] All exercise protocols were undertaken on the same platform once selected for an individual patient. Direct measurements of oxygen consumption (VO_2), carbon dioxide production (V_{CO2}) and minute ventilation (V_E) were made. An incremental protocol was utilised whereby speed and inclination (for treadmill exercise) or resistance and speed (for bicycle exercise) were gradually increased every minute during continual blood pressure and ECG measurement. Subjects were encouraged to exercise to exhaustion, with a corresponding adequate respiratory exchange ratio (RER) achieved (RER ≥1) as a requirement for satisfactory effort. Exercise was terminated at subject request due to fatigue or dyspnoea. Peak oxygen consumption ($VO_{2\ peak}$) was determined by averaging VO_2 measures over 30 seconds of peak exercise.

2.4.5 Coronary angiography

As part of their clinical treatment all participants underwent routine coronary angiography. Additional procedures were performed as part of the study, sometimes limited to collection of blood samples at baseline. Further interventions beyond this were only carried out if the consultant in charge deemed that the patient was able to comply with study procedures, and able to tolerate the complexity of the procedure in comfort.

The complete procedure (routine & study) was as follows:

After discussion and the appropriate consent process, percutaneous arterial and venous access was obtained; An arterial sheath was placed under local anaesthesia into the radial or femoral artery to allow access for insertion of a coronary artery or a pigtail catheter. Two femoral venous sheaths were inserted which allowed for insertion of a coronary sinus and a pacing catheter, and also for rapid infusion of fluids or pressor agents should they have been required.

Diagnostic coronary angiography was then performed in a standard manner using appropriate catheters. The coronary sinus was then catheterised using an appropriate endovascular catheter. A pigtail catheter was placed in the aortic root through the arterial sheath. Baseline blood samples were taken from the femoral vein (FV), aortic root (AR) and coronary sinus (CS). A pacing catheter was then placed in the right ventricle and the pacing threshold was checked. Pacing was commenced at 100 beats per minute for 60 sec and then incrementally increased every minute to a maximum of 140 beats per minute. Pacing was undertaken for a total duration of 3 minutes or stopped sooner if patient developed chest pain or ECG changes suggestive of ischaemia.

Towards the end of pacing cycle, blood samples were again collected from FV, AR and CS.

On completion of the cardiac catheterisation procedure the arterial and venous sheaths were removed, and puncture sites (both arterial and venous) closed with an appropriate closure device. The patient then underwent a period of observation and was allowed home, as would normally occur after a routine day case procedure.

2.4.6 Sample processing

Blood samples obtained were centrifuged at 3500 rpm at 4 ºC for 15 minutes. Resulting supernatant was separated and aliquoted into endorphin tubes and was re-centrifuged at 5000 rpm for 5 minutes. The supernatant was then aliquoted and stored at -80 ºC for further evaluation using specific mass spectrometry platforms for unbiased metabolomic analysis (detailed in Section 2.5).

Peripheral blood samples collected from patients as a part of their routine care were sent to the haematology and biochemistry laboratories of the John Radcliffe hospital for FBC, U&E and LFT analysis.

2.4.7 Interventions

A typical patient experienced the following interventions during routine coronary angiography: insertion of radial or femoral arterial sheath and the insertion of a venous sheath. The patients who voluntary underwent the study procedures had the following interventions in addition to their routine angiography: insertion of a coronary sinus and pacing catheter.

2.4.8 Safety

The risk of adverse events during the procedure was considered to be low. Patients referred for cardiac catheterisation underwent this procedure as would routinely be performed. As the study procedure did not add to the risks already present during a routine diagnostic coronary angiography, patients were therefore consented for the standard of care procedure and its associated risks. The blood sampling performed during the procedure was performed through the femoral artery sheath, femoral venous sheath, coronary sinus catheter or pigtail catheter. The femoral artery sheath, pigtail catheter and coronary artery catheter were required for and routinely used in coronary angiography. Some discomfort and possible complications were associated with placement of the femoral arterial sheath, but this was already clinically indicated as a part of the diagnostic coronary angiography.

A femoral venous sheath is not routinely placed for all angiography procedures, but permits placement of catheters into the venous system, and/or introduction of pacing electrodes into the right side of the heart. Potential risks and complications associated with venous sheath placement *per se* are much less than arterial sheath placement, because blood is not at arterial pressure levels and because other potential risks are intrinsically lower in the venous circulation. Placement of a coronary sinus catheter is not routinely used during angiography, but is used routinely during other commonly performed cardiac interventions. The risk of additional complications was felt to be very low, since the catheter was used solely for coronary venous blood sampling, rather than interventions such as placement of catheters or electrodes within the coronary sinus.

CPEX testing involves walking on a treadmill and is regarded as safe in patients with HCM. There is a small risk of developing cardiac arrhythmias (1.6%) during CPEX.[292] Emergency equipment and help was immediately available in case this occurred, to assist in the resuscitation of the patient.

Typical radiation exposure during a routine coronary angiography is 4 mSv, with an additional radiation exposure of .02 mSv estimated for the study procedure and was related to the extra fluoroscopy time required for the positioning of the coronary sinus catheter and pacing wire.

No serious adverse events or serious adverse reactions were identified during the course of the study.

2.4.9 Participant Confidentiality

Maintenance of participants' anonymity was an integral component of the study design. The participants were identified by their unique ID number, which was mentioned on the clinical record form (CRF) and also stored on the electronic database. All documents were stored securely and only accessible by study staff and authorised personnel. The study was fully compliant with the Data Protection Act, which requires data to be anonymised as soon as it is practical to do so.

2.5 Mass spectroscopy

2.5.1 Sample handling

Mass spectrometry work was carried out in collaboration with the group of Dr. Jules Griffin based at the MRC Human Nutrition Research Center in

Cambridge. All the samples once collected by the author were transported to Cambridge. During the course of this work the author went for three sabbatical visits (total duration of 8 weeks) to the laboratory in Cambridge. There under the supervision of Dr. Griffin the author was trained to perform sample preparation, analysis, data processing, statistics analysis and interpretation of the metabolomics data.

2.5.2 Chemicals

HPLC grade solvents were obtained from Sigma Aldrich (Gillingham, Dorset, UK). For aqueous metabolite measurement all standards for optimisation and quantitation were obtained from Sigma Aldrich (Gillingham, Dorset, UK) with the exception of the internal standards, glutamine [U- ^{13}C, ^{15}N], leucine D_{10}, phenylalanine D_8, valine D_8, proline [U-^{13}C, ^{15}N] which were acquired from Cambridge Isotope Laboratories (Andover, MA, USA). All other compounds, chemicals and solutions used are detailed where relevant. For carnitine analysis an internal standard mixture of labelled carnitines (set B, Item # NSK-B-TS-1) was purchased from Cambridge Isotope Laboratories (Andover, MA, USA).

2.5.3 Analysis of acylcarnitines

2.5.3.1 Sample extraction

Acylcarnitines were measured according to the method described by Roberts *et al*. with modifications to accommodate plasma extractions.[293] Briefly, 400 µL internal standard solution mix (1.63 µM [D9] free carnitine, 0.3 µM [D3] acetyl carnitine, 0.06 µM [D3] propionyl-carnitine, 0.06 µM [D3] butyryl-carnitine, 0.06 µM [D9] isovarelyl-carnitine, 0.06 µM [D3] octanoyl-carnitine, 0.06 µM [D9]

myristoyl-carnitine, and 0.12 µM [D3] palmitoyl-carnitine, Cambridge Isotope Laboratories, Andover, MA, USA) in acetonitrile was added to 25 µL of the plasma samples. This step ensures that all proteins are crashed out, while acylcarnitines are extracted. Samples were vortexed, sonicated (10 minutes) and centrifuged (10 minutes at 13,000 rpm). The resulting supernatants were decanted into clean tubes and dried under nitrogen. Dried extracts were derivatised with 100 µL of 3 M butanolic-HCl (Sigma-Aldrich, Louis, Missouri, USA). Samples were evaporated under nitrogen, and finally re-constituted and sonicated using 80:20 acetonitrile: water with 0.1% formic acid, before transferring them to autosampler vials.

2.5.3.2 Instrumental parameters

Samples were analysed using an AB Sciex 5500 QTRAP mass spectrometer (AB Sciex UK Limited, Warrington, Cheshire) coupled to an Acquity UPLC system. Mobile phase A consisted of 0.1 % formic acid in water, while mobile phase B was acetonitrile. Two microliters of each sample was injected onto a Synergi Polar RP phenyl ether column (100 mm × 2.1 mm, 2.5 µm) supplied by Phenomenex (Macclesfield, Cheshire, UK). The analytical gradient started at 30 % B, followed by a linear increase to 100 % B over 3 min. The gradient was then held at 100 % B for 5 min, after which it was returned to the re-equilibration level of 30 % B for 2 min. A flow rate of 0.5 mL/min was used throughout. A list of parent mass to charge ratios of detected compounds is detailed in table 2.5.1.

Table 2.5.1: Parent masses for protonated molecular ions measured in the carnitine assay. All compounds yielded the common fragment of +85.0 Da.

Analysis was performed in positive ion mode with collision energy of 25 eV and a cone voltage of 35 V for each compound.

Compound	Parent Mass/ *m/z*	Compound	Parent Mass/ m/z
Free carnitine butyl ester	218.2	C12 carnitine butyl ester	400.3
d9 carnitine butyl ester	227.2	C6 dicarboxyl carnitine dibutyl ester	402.3
C2 carnitine butyl ester	260.2	C14:2 carnitine butyl ester	424.3
d3 C2 carnitine butyl ester	263.2	C14:1 carnitine butyl ester	426.4
C3 carnitine butyl ester	274.2	C14 carnitine butyl ester	428.4
d3 C3 carnitine butyl ester	277.2	C8 dicarboxyl carnitine dibutyl ester	430.4
C4 carnitine butyl ester	288.2	d9 C14 carnitine butyl ester	437.4
d3 C4 carnitine butyl ester	291.2	C14-OH carnitine butyl ester	444.4
C5:1 carnitine butyl ester	300.2	C16:2 carnitine butyl ester	452.4
C5 carnitine butyl ester	302.3	C16:1 carnitine butyl ester	454.4
d9 C5 carnitine butyl ester	311.3	C16 carnitine butyl ester	456.4
C6 carnitine butyl ester	316.3	d3 C16 carnitine butyl ester	459.4
C5-OH carnitine butyl ester	318.2	C16:1-OH carnitine butyl ester	470.4
C8:1 carnitine butyl ester	342.3	C16-OH carnitine butyl ester	472.4
C8 carnitine butyl ester	344.3	C18:2 carnitine butyl ester	480.4
d3 C8 carnitine butyl ester	347.3	C18:1 carnitine butyl ester	482.4
C8-OH carnitine butyl ester	361.3	C18 carnitine butyl ester	484.4
C10:2 carnitine butyl ester	368.3	C18:2-OH carnitine butyl ester	496.4
C10:1 carnitine butyl ester	370.3	C18:1-OH carnitine butyl ester	498.4
C10 carnitine butyl ester	372.3	C18-OH carnitine butyl ester	500.4
C4 dicarboxyl carnitine dibutyl ester	374.3	C20:2 carnitine butyl ester	508.4
C5 dicarboxyl carnitine dibutyl ester	388.3	C20:1 carnitine butyl ester	510.4
C12:1 carnitine butyl ester	398.3	C20 carnitine butyl ester	512.4

2.5.3.3 Processing of acylcarnitine data

Data were analysed using the Quantitation Wizard within Analyst™ version 1.6 by AB Sciex Ltd. (Warrington, Cheshire, UK) and normalised against the intensity of the internal standard. The concentration of analytes was presented as area ratio after normalisation to the internal standard. The nomenclature for various acylcarnitines measured is described in table 2.5.2.

Table 2.5.2: Nomenclature for the analysed carnitines.

Carnitine nomenclature			
Carnitine	Free carnitine	C6-DC	3-Methylglutarylcarnitine
C2	Acetylcarnitine	C14:2	Tetradecadienoylcarnitine
C3	Propionylcarnitine	C14:1	Tetradecenoylcarnitine
C4	Iso-/Butyrylcarnitine	C14	Tetradecanoylcarnitine
C5:1	Tiglylcarnitine	C8-DC	Octanedioylcarnitine
C5	Isovalerylcarn	C14-OH	3-OH-tetradecanoylcarnitine
C6	Hexanoylcarnitine	C16:2	Hexadecadienoyl carnitine
C5-OH	3-OH-isovalerylcarnitine	C16:1	Hexadecenoylcarnitine
C8:1	Octenoylcarnitine	C16	Hexadecanoylcarnitine
C8	Octanoylcarnitine	C16:1-OH	3-OH-hexadecenoylcarnitine
C8-OH	3-Hydroxyoctanoylcarnitine	C16-OH	3-OH-hexadecanoylcarnitine
C10:2	Decadienoylcarnitine	C18:2	Octadecadienoylcarnitine
C10:1	Decenoylcarnitine	C18:1	Octadecenoylcarnitine
C10	Decanoylcarnitine	C18	Octadecanoylcarnitine
C4-DC	Methylmalonylcarnitine	C18:2-OH	3-OH-octadecadienoylcarn
C5-DC	Glutarylcarnitine	C18:1-OH	3-OH-octadecenoylcarnitine
C12:1	Dodecenoylcarnitine	C18-OH	3-OH-octadecanoylcarnitine
C12	Dodecanoylcarnitine	C20:1	Octadecenedioylcarnitine

C20	Arachidoylcarnitine

2.5.4 Analysis of aqueous metabolites

2.5.4.1 Sample extraction

Samples were aliquoted (25 µL) to 96 well plates and proteins were crashed using 400 µL MeOH containing a mixture of five internal standards at 2.5 µM (described in Section 2.5.2). The crashed samples were placed on a plate shaker for 5 min at 1000 rpm and, using a liquid handling robot (Viaflo 96, Integra Biosciences, Nottingham, UK) transferred onto 96 well 0.66 mm glass fiber polystyrene filter plates (Corning Inc., NY, USA). Samples were filtered using a positive pressure 96 processor (Waters Ltd., Elstree, Hertfordshire, UK.) collected into a 1 mL polypropylene deep-well plate (Thermo Scientific, Hemel Hempstead, Hertfordshire, UK) and dried using an EZ-2 Evaporation system (Genevac Ltd., Ipswich, Suffolk, UK). Samples were re-constituted using 100 µL of water containing 10 mM NH_4OAc, transferred to clean glass coated 200 µL 96-well plates, sealed using pre-slit foils and placed on the auto sampler. From each sample well, 2 µL sample was injected.

2.5.4.2 Instrument parameters

Chromatographic analyses were performed using a Thermo Scientific Dionex UltiMate 3000 system (Thermo Scientific, Hemel Hempstead, Hertfordshire, UK), with an ACE C18-PFP 3 µm column (2.1 x 150 mm) (Advanced Chromatography Technologies Ltd., Aberdeen, UK) coupled to a TSQ Quantiva Triple Quadrupole Mass Spectrometer (Thermo Scientific, Hemel Hempstead,

Hertfordshire, UK). The mobile phase gradient was run at 0.5 mL/min using water (mobile phase A) and acetonitrile (mobile phase B). The gradient started at 100% A, and increased to 60% B from 1.6 to 4.5 minutes, followed by re-equilibration for 2 minutes. The total runtime was 6.5 minutes. Data were acquired in both positive and negative ionisation modes using capillary spray voltages of 3.5 kV and 2.5 kV, respectively. The ion transfer tube was set to operate at 350 °C whilst the vaporizer temperature was set to 400 °C. Sheath, auxiliary and sweep gases were set to 50, 15 and 2 arbitrary units respectively. All other parameters were compound dependent and are detailed in table 2.5.3.

Table 2.5.3: List of aqueous metabolites, precursor and product ions and mass spectrometry parameters.

Abbreviation	Compound	Polarity	Precursor (m/z)	Product (m/z)	Collision Energy (V)	RF Lens (V)	RT (min)
Gly	Glycine	Positive	76.1	48.2	6	30	0.71
Ala	Alanine	Positive	90.1	44.275	11	30	0.73
BAIBA	β-aminoisobutyric	Positive	104.05	85.975	5	36	0.91
Ch	Choline	Positive	104.1	60.1	15	60	0.81
Ser	Serine	Positive	106.075	60.2	10	39	0.71
Cyt	Cytosine	Positive	112	95.104	18	84	3.41
Crn	Createnine	Positive	114.1	86.141	11	49	0.92
Pro	Proline	Positive	115.975	70.175	15	36	0.85
Bet	Betane	Positive	118.1	58.225	26	67	0.81

Val	Valine	Positive	118.1	72.2	10	67	1.12
Thr	Threonine	Positive	120.1	74.125	9	66	0.75
ProIS	Proline internal standard	Positive	121.15	74.188	17	46	0.85
Taur	Taurine	Positive	126.1	44.1	14	93	0.71
Vald8	Valine internal standard	Positive	126.1	80.2	10	41	1.11
MeCyt	Methyl-Cytosine	Positive	126.1	109.164	19	78	2.5
Leu	Leucine	Positive	132.025	86.2	8	35	2.49
Ile	Isoleucine	Positive	132.025	86.2	8	35	2.2
PrOH	Hydroxy-Proline	Positive	132.025	86.2	8	35	0.74
Orn	Ornitine	Positive	133.2	70.168	16	44	0.64
Asn_1	Asparagine	Positive	133.2	74.12	16	44	0.71
Leud10	Leucine internal standard	Positive	142.025	96.2	8	35	2.49
Lys	Lysine	Positive	147.1	84.169	16	48	0.64
Gln	Glutamine	Positive	147.1	84.169	16	48	0.73
Glu	Glutamate	Positive	148	84.15	16	46	0.76
Met	Methionine	Positive	150.05	61.16	23	36	1.4
Glu13C515NP	Glutamine internal standard	Positive	154.1	89.094	15	47	0.76
His	Histidine	Positive	156.1	110.15	13	45	0.7
AAA	Amino adipid acid	Positive	162.125	116.15	11	57	0.89
Phe	Phenylalanine	Positive	166.1	120.15	13	41	3.44
Me-His	Methyl-Histidine	Positive	170.2	95.16	30	59	0.7
Phed5	Phenylalanine internal standard	Positive	171.1	125.15	13	41	3.44
Arg	Arginine	Positive	175.15	70.2	23	52	0.7
Citl	Citruline	Positive	176.15	159.086	8	59	0.78
Tyr	Tyrosine	Positive	182.075	136.125	12	46	3.06
Trp	Tryptophan	Positive	205.2	188.093	11	58	3.79

Carn	Carnosine	Positive	227.25	110.2	21	60	0.71
C-C	Cystine	Positive	241.05	74.152	26	65	0.7
Cyd	Cytidine	Positive	244.1	112.125	14	39	1.54
Urd	Uridine	Positive	245.1	112.917	12	46	2.63
AMP	Adenosine mono phosphate	Positive	348.1	136.123	20	82	1.56
SAM	S-Adenosly Methyonine	Positive	399.1	250.147	16	79	0.85
2OHBA	2-hyroxy butyric acid	Negative	103.025	57.169	12	44	2.32
3OHBA	3-hydroxy butyric acid	Negative	103.025	73.143	10	40	2.29
Fum	Fumarate	Negative	115	71.172	7	50	1.6
KValNF	Keto-Valine not fragmented	Negative	115.1	115.1	0	41	3.01
Suc	Succinate	Negative	117	73	15	60	2.19
KLeu	Keto-Leucine	Negative	129.1	129.1	0	40	4.07
KIleNF	Keto-Isoleucine	Negative	129.1	129.1	0	40	3.86
Oxal	Oxaloacetate	Negative	131	87.084	10	33	0.62
Pyr+formic	Pyruvate	Negative	133	87	5	30	0.99
Mal	Malate	Negative	133	115.081	12	51	1.06
Glu13C515NN	Glutamine internal standard	Negative	152.1	134.102	13	55	0.76
KVal+formic	Keto-Valine +formic	Negative	161.05	115.02	5	30	3.01
Aco	Aconitate	Negative	173.05	85.129	15	39	2.25
KLeu+formic	Keto-Leucine +formic	Negative	175.075	129.04	6	30	4.07
KIle+formic	Keto-Isoleucine + formic	Negative	175.075	129.04	6	30	3.86
Cit	Citrate	Negative	191	111	15	53	1.8
Icit	Isocitrate	Negative	191	111	15	53	1.1

2.5.4.3 Processing of aqueous metabolite data

Peaks were integrated using Xcalibur (version 3.0, Thermo Scientific, Hemel Hempstead, Hertfordshire, UK) and each analyte was normalised to the intensity of the internal standard closest to its retention time. The concentration of analytes was presented as area ratio after normalisation to the internal standard.

2.6 Statistical analysis

2.6.1 Power calculation

A formal power calculation based on metabolomics endpoints was challenging, as the effect sizes were largely unknown prior to this study. Thus a preliminary data analysis was undertaken, which noted a difference between the amino acid, citric acid cycle and acylcarnitine analytes in different patient groups. Based on this a number of 35 participants per group was expected to provide adequate power to observe the differences in various patient groups. Similar or smaller numbers have been able to discriminate ischaemic from non-ischaemic patients (including in the context of HCM).[294] Moreover, theoretical sample size considerations supported this number of patients with an FDR set at 5%.[295] Patients acting as their own control between provocations also enabled increase in statistical power.

2.6.2 Analysis of endpoints using univariate analysis

For univariate statistical analysis Microsoft Excel 2010 (Microsoft UK, Reading) and Graph Pad Prism 5 (La Jolla, California, US) software packages were used.

All participants were included in the final analysis. All variables were tested for normal distribution by using Kolmogorov-Smirnov test. Normally distributed variables were expressed as mean±SD, while non-normally distributed variables were expressed as median with quartiles 1 to 3.

Categorical variables were compared using Chi-square test. Normally distributed variables or those not-normally distributed after transformation were compared between groups by using either the two-tailed Student's t-test or the Mann-Whitney U-test respectively. Differences in the concentration of metabolites between paired samples from two-collection sites within a disease cohort were analysed using either the two-tailed Student's t-test or the Wilcoxon Signed-Rank test. Changes of variables within each group and between groups were tested by using two-way ANOVA for repeated measures, with a suitable post-test (Bonferroni's / Dunns) used for multiple comparisons. Correlations between variables were tested using bivariate analysis and by calculating Pearson's correlations coefficient.

2.6.3 Multivariate analysis

2.6.3.1 Principal component analysis (PCA)

PCA is an unsupervised multivariate analytical method, where no class is assigned to the components before analysis.[296] Here sets of original variables in a large complex dataset are grouped into a smaller number of variables called principal components. The principal components are thus linear combinations of the original variable. These principal components are then projected onto one of the axes and generate a new variable, which maximizes

the description of variance in the given data set. Thus a large dataset is converted into one of lower dimension, facilitating more meaningful analysis.

2.6.3.2 Partial least squares discriminant analysis (PLS-DA)

While the PCA analysis allows an unbiased reduction in the dimensions of a dataset, it is effective only if the variation within a group is less than the variation between the groups. In the later circumstances PLS-DA analysis is effective, which is a multivariate analysis where samples are analysed in a supervised framework.[297] Class membership is given to an observation pre-analysis and this data is then projected creating a separating hyperplane such that the inter-group distance is maximal, while the intra-group variation is minimal. The PLS-DA analysis generates the following variables which help in determining the goodness of a model: a) R^2X: is the coefficient which describes how the variation in a model is related to the difference between groups b) R^2Y: describes how well the model fits the data c) Q^2: is the parameter which estimates the predictability of a model.

2.6.3.3 Orthogonal projections to latent structures discriminant analysis (OPLS-DA)

The use of PLS-DA allows better separation of data following assignment of class membership, however its scores still contain variation not directly correlated to Y. This is over come in OPLS-DA analysis by use of orthogonal signal correction (OSC) filter, which separates Y-predictive variation from the uncorrelated variation in X.

2.6.3.4 Scaling for multivariate methods

The data generated from different spectrometric analysis has huge variances in intensities even for variables with identical units. This leads to the focus of multivariate analysis on small sets of variables with high intensities. This is overcome by autoscaling the mean to zero, allowing better analysis of the data. There are several scaling techniques such as centering, UV, range, pareto and vast.

2.6.3.5 Validation of multivariate models

The models generated by multivariate analysis are validated using random permutations. This involves generating models by assigning class membership randomly to a large number of permutations. A model is validated if the original R^2 and Q^2 values on the right are higher than the permuted values on the left (figure 2.6.2).

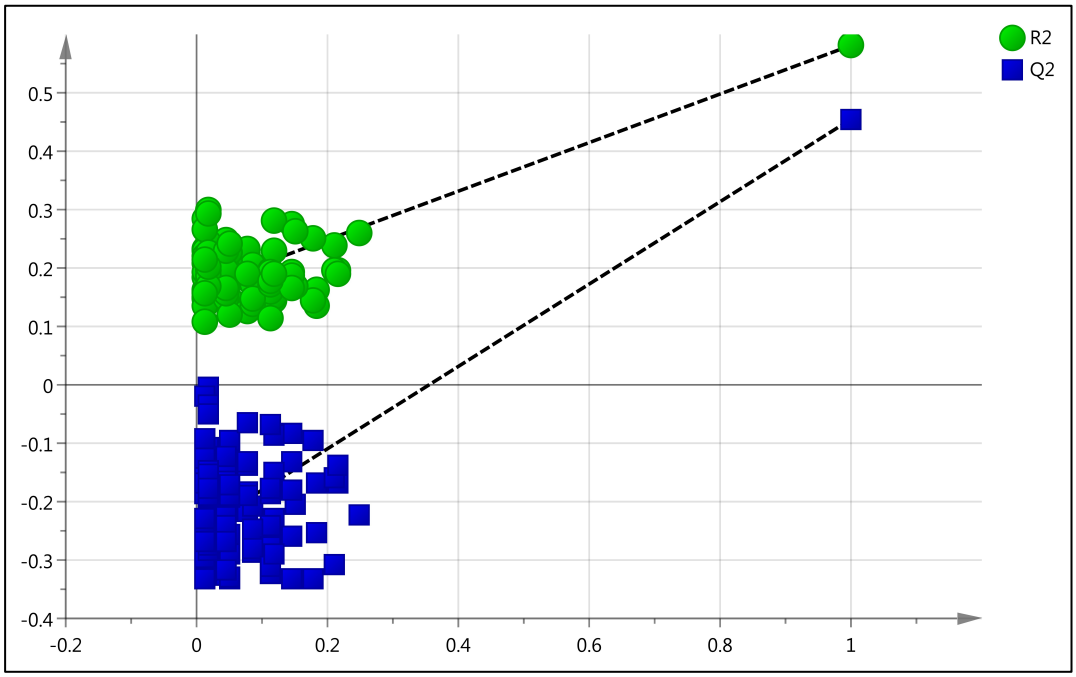

Figure 2.6.2: The figure shows the validation plot for the PLS-DA analysis of aqueous metabolites, performed on aortic root samples between control and aortic stenosis cohorts. The analysis was performed in SIMCA 13 (Umetrics AB, Malmö, Sweden). The R^2 (goodness of fit) and Q^2 (predictive ability) for the original model (far right) and the permuted models (far left) are shown above. This plot indicates a valid original model as the original R^2 and Q^2 values on the right are higher than the permuted values on the left.

2.6.3.6 Variable importance on projection (VIP) analysis

A VIP plot is a type of coefficients plot, which summarizes the relationship between the X and Y variables. This plot summarises the observations from score and loading plots, and describes which X variables characterise the X-matrix well, and also correlate with Y. A high VIP score (≥1) was considered to be significant and subjected to further analysis.

2.6.4 Receiver operating characteristic (ROC) curves

The receiver operating characteristic (ROC) curve is an important analytical technique used to compare similar variables in different conditions. This was first used in World War II to differentiate the enemy aircrafts from a flock of birds.[298] It works by plotting the sensitivity versus 1-specificity, generating a ROC curve. The area under the curve (AUC) gives an estimate of the variables ability to differentiate the given condition (figure 2.6.3). The analysis was performed using the ROC curve analysis tool, ROCCET (ROC curve explorer & tester available at (http://www.roccet.ca).

Both univariate and multivariate ROC test analysis can be performed. Multivariate ROC test analysis is performed using a subset of features

simultaneously.[299] It is well-recognised that a group of results combined can provide superior diagnostic performance when compared to individual tests. Thus, as with univariate ROC test analysis, the area under the curve can be used to assess whether a particular parameter performs better than chance alone.

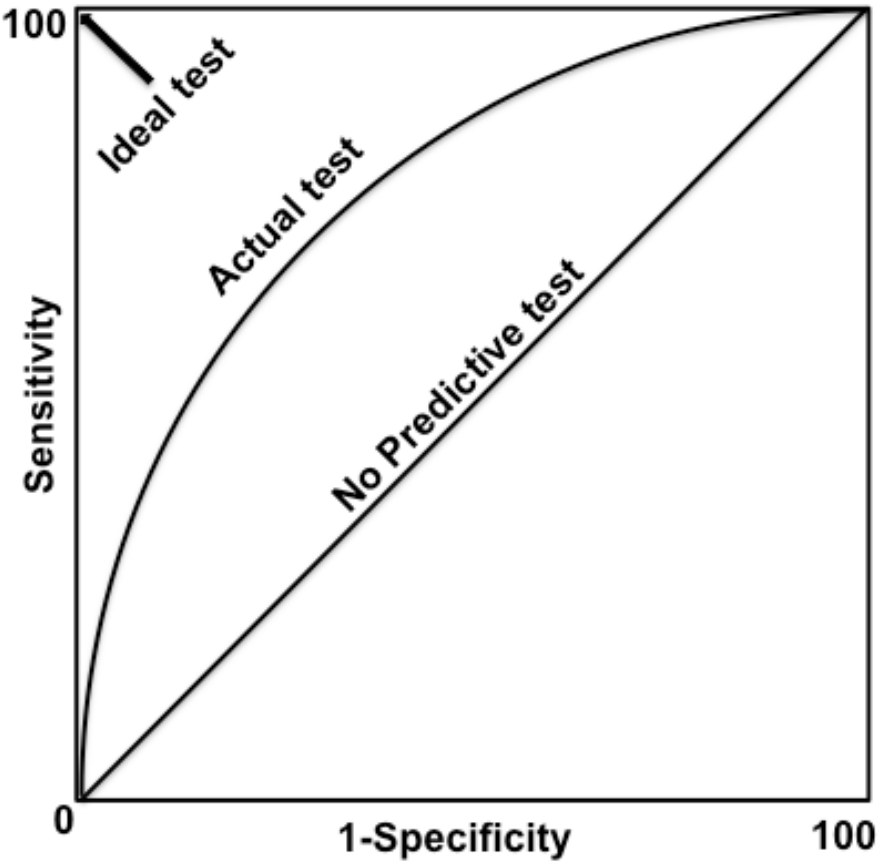

Figure 2.6.3: A graphical representation of a receiver operating characteristic (ROC) curve, generated by plotting the sensitivity (y-axis) vs. 1-specificity (x-axis). The area under the ROC curve is a good measure of the predictive ability of a marker. A marker with a 100% diagnostic ability would have an area of 1, while a marker with no predictive ability will have an area of 0.5 or less.

Results

3 METABOLOMIC ANALYSIS STRATEGY

Recruitment for the study commenced in July 2013 after obtaining the necessary ethical approvals. A total of 109 patients from the three cohorts were included in the final analysis, this included: control (38), aortic stenosis (36) & HCM (35) cohorts. The recruitment was completed ahead of schedule as seen in figure 3.1.

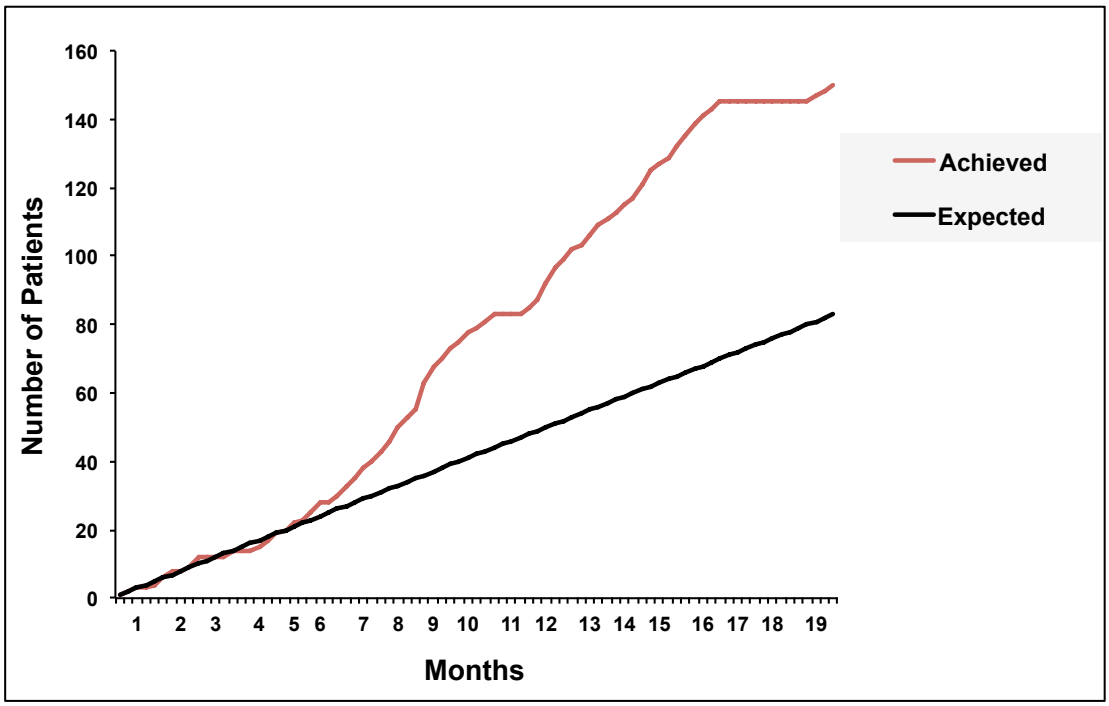

Figure 3.1: The figure above depicts expected (black line) vs achieved (orange line) recruitment over a 19-month period.

3.1 Clinical characteristics

3.1.1 Demographics

Baseline clinical and demographic characteristics of the patients are shown in table 3.1.1. The patients in the control and HCM cohorts were similar in age but

significantly younger than patients in the aortic stenosis cohort. There were more men in the control (79%) and HCM (71%) cohorts as compared to aortic stenosis cohort (53%). All patients had a similar body mass index. While the majority of patients in the control and HCM cohorts were either NYHA (New York heart association) class I or II, there were a higher number of patients in NYHA class III & IV in the aortic stenosis cohort. In the aortic stenosis cohort there were more patients with past medical history of hypertension and dyslipidemia (75% each). Cardiovascular drug therapy was similar between the cohorts, except for significantly higher use of ACE-I/ARB-II (75%) and diuretics (72%) in patients with aortic stenosis.

Table 3.1.1: Clinical and demographic characteristics of the controls, aortic stenosis and HCM cohorts. Differences between the groups statistically analysed using ANOVA with Bonferroni's post-test for multiple comparisons. Statistical significance was defined as a p-value<0.05.

	Controls (n = 38)	Aortic stenosis (n = 36)	HCM (n = 35)	p value
Age (years)	63 ± 10	80 ± 7	62 ± 10	<0.0001
Men, n (%)	79	53	71	0.04
BMI (kg/m^2)	26.1 (23.7 - 28.5)	28.1 (27.2 - 30.8)	27.5 (25.9 - 31.7)	0.06
NYHA I	14 (36%)	3 (8%)	6 (17%)	0.008
NYHA II	18 (47%)	19 (53%)	26 (74%)	0.05
NYHA III	6 (16%)	11 (31%)	3 (9%)	0.05
NYHA IV	0	3 (8%)	0	

PMH, n (%)				
Hypertension	50	75	40	0.009
Diabetes	16	25	11	0.3
Dyslipidemia	53	75	54	0.09
IHD	37	25	3	0.009
COPD / Asthma	13	14	14	0.9
Family History	61	44	69	0.1
Medications, n (%)				
Aspirin	68	42	57	0.07
Clopidogrel	16	3	17	0.1
ACE-I/ARB-II	47	75	14	<0.0001
Beta-blockers	40	47	49	0.7
Statin	66	61	46	0.2
Calcium blockers	24	28	40	0.3
Diuretics	16	72	11	<0.0001
OHA	8	19	9	0.2
Insulin	11	3	0	0.08

Values are mean ± SD, percentages or median (quartiles 1 to 3). BMI = Body mass index; PMH = past medical history; ACE = angiotensin-converting enzyme-inhibitors; IHD = ischemic heart disease; ARB = angiotensin-receptor antagonist-II. OHA = Oral hypoglycemic agent.

As shown in table 3.1.2 on a baseline biochemical analysis there were no difference in hemoglobin, total cholesterol and bilirubin between the 3 cohorts. The patients with aortic stenosis had a significantly lower eGFR (estimated glomerular filtration rate) and higher concentration of creatinine (89.8 µmol/L).

Table 3.1.2: Biochemical characteristics of the controls, aortic stenosis and HCM cohorts. Differences between the groups statistically analysed using ANOVA with Bonferroni's post-test for multiple comparisons. Statistical significance was defined as a p-value<0.05.

	Controls (n = 38)	Aortic stenosis (n = 36)	HCM (n = 35)	p value
Hemoglobin, g/dL	13.6 ± 1.8	13.3 ± 1.5	13.9 ± 1.4	0.15
Creatinine, µmol/L	71.5 ± 13.3	89.8 ± 31.8	84.6 ± 25.4	0.008
eGFR, ml/min/1.73m^2	100.8 ± 22.6	72.2 ± 23.5	86.0 ± 23.0	<0.0001
Cholesterol, mmol/L	4.3 ± 1.3	4.2 ± 1.5	4.3 ± 1.1	0.6
Bilirubin, µmol/L	10 (8 - 13)	10 (8 - 18)	11 (8 - 16)	0.6
ALT, IU/L	25 (18 - 35)	18 (13 - 21)	21 (14 - 31)	0.005
ALP, IU/L	165 (133 - 187)	149 (131 - 225)	166 (127 - 230)	0.9
Albumin, g/L	44 (41 - 47)	43 (41 - 45)	44 (42 - 45)	0.2

Values are mean ± SD or median (quartiles 1 to 3). ALT = alanine transaminase. ALT = alanine transaminase; ALP = alkaline phosphatase; Cholesterol = total cholesterol.

3.1.2 Echocardiography results

Patients in all three cohorts had similar baseline heart rate and systolic blood pressure measurements (table 3.1.3). Echocardiography showed that although the LV (left ventricular) ejection fraction was normal in all the patients, it was significantly higher in patients with HCM when compared with aortic stenosis

(p=0.005). Septal hypertrophy was most marked in patients with HCM (1.8 ± 0.4 cm), having an eccentric hypertrophy pattern as compared to patients with aortic stenosis who had concentric hypertrophy and the highest LV mass index. Diastolic function was impaired in patients with aortic stenosis with a low e' (6.5 cm/s) and a raised E/e' (14.7) ratio. These patients had severe aortic stenosis with a mean AS jet velocity of 419 cm/s (meters per second), aortic valve area of 0.7 cm^2 and an indexed valve area of 0.4 cm^2/m^2.

Table 3.1.3: Baseline hemodynamic and echocardiographic characteristics of the controls, aortic stenosis and HCM cohorts. Differences between the groups statistically analysed using ANOVA with Bonferroni's post-test for multiple comparisons. Statistical significance was defined as a p-value<0.05.

	Controls (n = 22)	Aortic stenosis (n = 34)	HCM (n = 31)	p value
Heart rate, beats/min	68 (60 - 79)	63 (57 - 74)	64 (58 - 70)	0.09
Systolic BP, mmHg	128 ± 21	134 ± 30	129 ± 22	0.6
Diastolic BP, mmHg	70 ± 12	63 ± 9	78 ± 14	<0.0001
LVEF (%)	61 ± 10	56 ±12	66 ± 11	0.005
LVIDd, mm	4.6 ± 0.5	4.8 ± 0.9	4.3 ± 0.7	0.04
IVSd, mm	1.2 ± 0.2	1.4 ± 0.2	1.8 ± 0.4	<0.0001
PWd, mm	1.1 ± 0.2	1.4 ± 0.2	1.2 ± 0.3	0.0001
LVIDs, mm	2.9 ± 0.5	3.2 ± 1.0	2.6 ± 0.6	0.01
LV mass index, g/m^2	96 ± 20	149 ± 50	132 ± 35	<0.0001
E/A ratio	0.8 (0.7 - 1.1)	0.8 (0.7 - 1.8)	0.9 (0.7 - 1.4)	0.6

DT, m/s	224 ± 53	230 ± 87	209 ± 61	0.7
e', cm/s	8.1 ± 2.1	6.5 ± 1.5	6.2 ± 1.7	0.009
E/e' ratio	8.2 ± 1.9	14.7 ± 6.6	10.8 ± 3.6	0.01
AS jet velocity, cm/s	127 (122 - 154)	419 (382 - 485)	136 (123 - 197)	<0.0001
AVA, cm^2		0.7 ± 0.2		
Indexed AVA, cm^2/m^2		0.4 ± 0.1		

Values are mean ± SD, percentages or median (quartiles 1 to 3). LV = left ventricular; LA = left atrial; LVEF = left ventricular ejection fraction; LVIDd = left ventricular internal diameter at end-diastole; IVSd = interventricular septum diameter (cm); PWd = posterior wall diameter; LVIDs = left ventricular internal diameter at end-systole; E = peak early diastolic mitral flow velocity; A = late diastolic mitral flow velocity; DT = E wave deceleration time; e' = peak early diastolic mitral annular velocity (mean of septal and lateral); AS = aortic stenosis; AVA = aortic valve area.

3.1.3 Cardiopulmonary exercise testing in HCM

Patients in the HCM cohort also underwent cardiopulmonary exercise testing to evaluate their baseline cardiovascular physiology. All patients exercised adequately, achieving a RER of more than 1, while exercising for an average of 8 minutes (table 3.1.4). The VO_2 peak was reduced and was much lower than the predicted VO_2 peak (67% [62%-86%]). They had a raised V_E/V_{CO2}, reduced AT (anaerobic threshold) and a normal breathing reserve, suggestive of a cardiac limitation in exercise capacity.

Table 3.1.4: Hemodynamic and exercise parameters in the HCM cohort as measured during cardiopulmonary exercise testing.

	HCM (n=17)
Heart rate, beats/min (rest)	64 ± 9
Heart rate, beats/min (exercise)	122 ± 20
Duration (minutes)	8.0 (5.6 - 8.2)
Percentage of maximum predicted heart rate achieved (%)	78 ± 14
METS	6.3 ± 2.4
RER	1.1 (1.0 - 1.2)
VO_2 peak (L/min)	1.5 ± 0.5
Percentage of predicted VO_2 peak (%)	67 (62 - 86)
V_E/V_{CO2}	35 (33 - 37)
Anaerobic threshold (% of predicted VO2 peak)	46 (35 - 59)
Percentage of breathing reserve (at peak exercise)	41 ± 16.5

Values are mean ± SD, percentages or median (quartiles 1 to 3). METS = Metabolic equivalent of task; VE/VCO2 = minute ventilation-carbon dioxide production ratio; RER = respiratory exchange ratio.

3.2 Trans-cardiac gradient validation

The initial metabolic analysis performed was to measure the trans-cardiac gradient of some specific metabolites (amino acids: glutamate & alanine, glucose & lactate), which have previously been reported to play a key role in

cardiac metabolism at rest and during stress (pacing / ischemia-reperfusion).[285,300,301] The presence of a trans-cardiac gradient of these metabolites would represent a validation of our methodology and would likely provide further insights into cardiac metabolism.

Trans-cardiac gradient is measured as the net difference between the aortic root and coronary sinus concentration of a metabolite (aortic root concentration – coronary sinus concentration). It was measured for each individual patient, with the median values of the entire cohort reported as the final result. A positive value indicated net extraction, while a negative value indicated net elution of the respective metabolite.

We predicate our assumptions of extraction or elution on the concentration of metabolites, while the underlying net substrate flux during cardiac metabolism is calculated as a product of extraction and elution times the coronary sinus blood flow (net flux = aorto-coronary sinus difference × coronary sinus blood flow). The lack of coronary sinus blood flow measurement in our study is a limitation in assessing the net flux of metabolites and will be considered when interpreting the relevant results.

The analysis was divided into 2 parts:

a) Samples from all-three cohorts were combined for assessment and

b) Individual cohorts assessed separately for:

i. Differences in concentration between the aortic root and coronary sinus
ii. Trans-cardiac gradient at baseline and during pacing

3.2.1 Glutamate & alanine

The trans-cardiac gradient of glutamate and alanine was measured for all the patients. Both baseline and pacing samples were analysed to understand the difference in metabolism during the two physiological states: rest and stress induced by pacing. A total of 63 patients were included in the final pair-wise analysis; this included patients who had both aortic root and coronary sinus samples collected, both at baseline and during pacing: controls (20), aortic stenosis (20) & HCM (23).

a) Samples from all-three cohorts combined

i. Aortic root vs coronary sinus

Table 3.2.1 describes the net concentration of glutamate and alanine in the aortic root and coronary sinus for all three patient cohorts combined. There was a significantly lower concentration of glutamate in the coronary sinus both during baseline and pacing, thus implying a net extraction of glutamate by the heart. There was no significant difference in the concentration of alanine between the aortic root and coronary sinus, both during baseline and pacing states (figure 3.2.1).

Table 3.2.1: Glutamate and alanine concentrations in the aortic root and coronary sinus during baseline and pacing, in all patients cohorts combined together. Differences between the groups statistically analysed using either two-tailed Student's t-test or Wilcoxon Signed-Rank test. Statistical significance was defined as a p-value<0.05.

	Aortic root	Coronary sinus	p value
Glutamate, baseline	2.53 (1.91 - 2.93)	1.50 (1.18 - 1.95)	<0.0001
Glutamate, pacing	2.73 (2.21 - 3.32)	2.06 (1.66 - 2.64)	<0.0001
Alanine, baseline	0.73 (0.62 - 0.99)	0.77 (0.62 - 0.99)	0.89
Alanine, pacing	0.71 (0.59 - 0.86)	0.70 (0.60 - 0.86)	0.71

Values shown are median (quartiles 1 to 3) concentrations of the respective metabolites. Glutamate and alanine concentration is presented as area ratio.

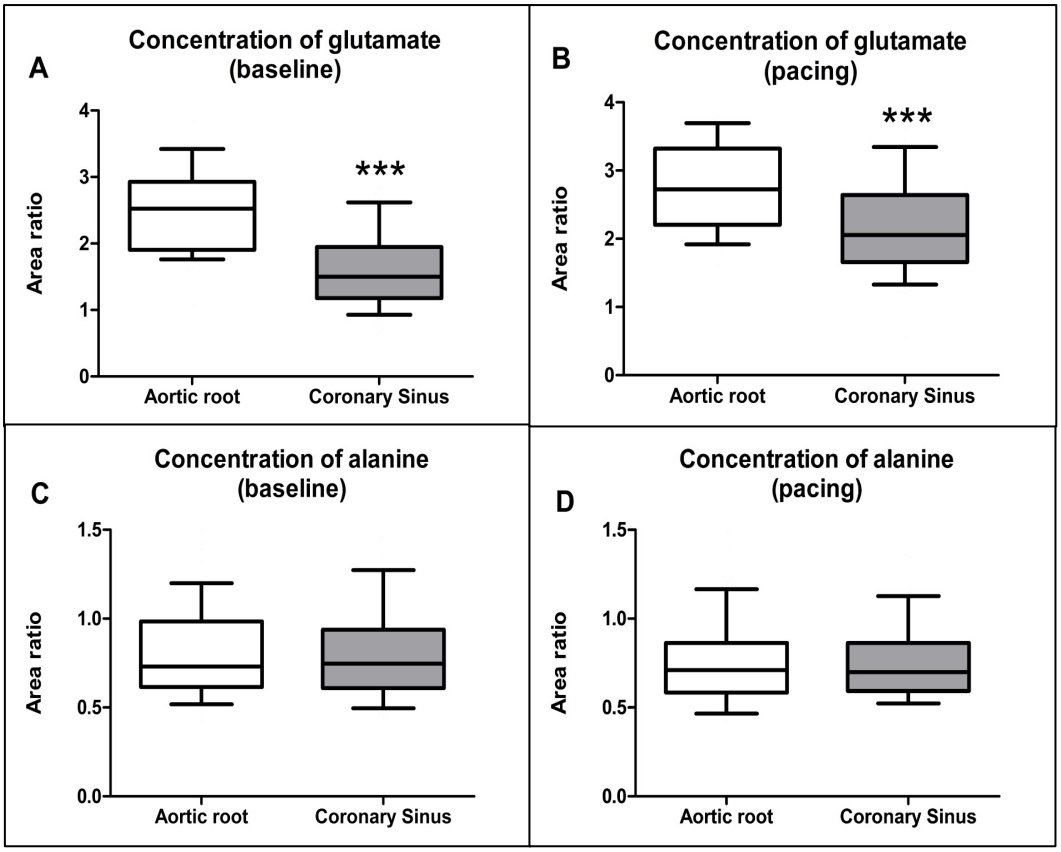

Figure 3.2.1: The figure above depicts the glutamate (A & B) and alanine (C & D) concentrations in the aortic root and coronary sinus as measured in all patient groups combined together, thus showing the gradient across the heart. The concentrations are shown as box plots, with the box

representing quartiles 1 to 3 and the whiskers representing 10 to 90 percentile.

ii. Trans-cardiac gradient

Although there was a net extraction of glutamate in the two physiological states, extraction was significantly lower during pacing (table 3.2.2 & figure 3.2.2). There was no significant trans-cardiac gradient of alanine either during baseline or pacing (Table 3.2.2).

Table 3.2.2: Trans-cardiac gradient (aortic root – coronary sinus) of glutamate and alanine within each patient, in all patients groups combined together. Differences between the groups statistically analysed using either two-tailed Student's t-test or Wilcoxon Signed-Rank test. P value of <0.05 was considered significant.

	Glutamate (Area ratio)	**Alanine** (Area ratio)
Baseline	0.86 (0.57 - 1.20)	−0.03 (−0.08 - 0.07)
Pacing	0.63 (0.35 - 0.91)	−0.001 (−0.10 - 0.07)
p value	0.0005	0.95

Values shown are median (quartiles 1 to 3) concentrations of the respective metabolites. Glutamate and alanine concentration is presented as area ratio.

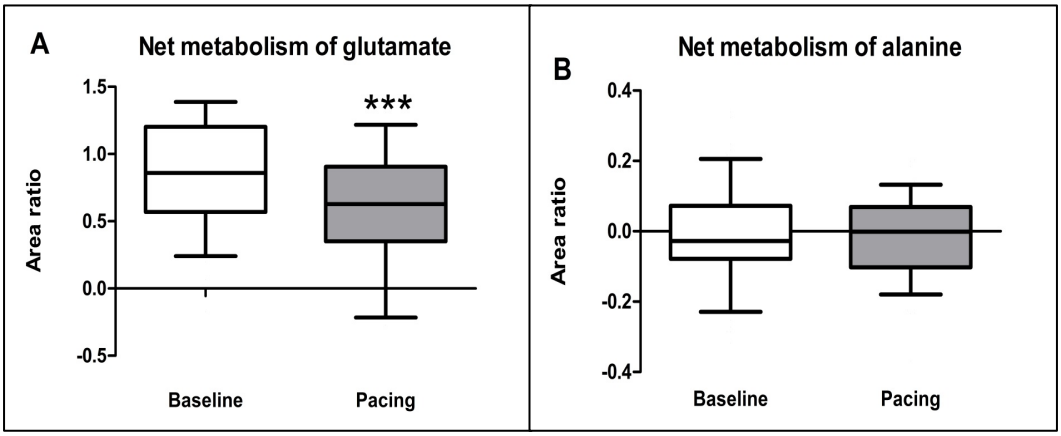

Figure 3.2.2: The figure above depicts the net cardiac metabolism (extraction / elution) of glutamate (A) and alanine (B) during baseline and pacing, as measured in all patient groups combined together. The concentrations are shown as box plots, with the box representing quartiles 1 to 3 and the whiskers representing 10 to 90 percentile.

b) Individual cohorts assessed separately

i. Aortic root vs coronary sinus

The glutamate and alanine concentrations were then measured in the individual patient cohorts (table 3.2.3). There was a significantly higher concentration of glutamate in the aortic root as compared to the coronary sinus in all-patient groups, both during baseline and pacing. This was suggestive of a net extraction of glutamate during baseline and pacing in all patient groups. There was no significant difference in the concentration of alanine between the aortic root and coronary sinus in any of the patient groups.

Table 3.2.3: Glutamate and alanine concentrations in the aortic root and coronary sinus in individual patient groups: controls, aortic stenosis and hypertrophic cardiomyopathy (HCM), during baseline and pacing. This is a paired analysis for the individual patient groups. Differences between the

groups statistically analysed using either two-tailed Student's t-test or Wilcoxon Signed-Rank test. Statistical significance was defined as a p-value<0.05.

	Aortic root	Coronary sinus	p value
Controls, glutamate baseline	2.55 (2.00 - 3.02)	1.50 (1.04 - 1.80)	<0.0001
Controls, glutamate pacing	2.74 (2.27 - 3.41)	2.11 (1.80 - 2.62)	0.02
Controls, alanine baseline	0.71 (0.61 - 1.00)	0.73 (0.56 - 0.95)	0.99
Controls, alanine pacing	0.69 (0.55 - 0.86)	0.69 (0.59 - 0.85)	0.73
Aortic stenosis, glutamate baseline	2.61 (2.11 - 3.00)	1.87 (1.37 - 2.50)	<0.0001
Aortic stenosis, glutamate pacing	2.71 (2.24 - 3.27)	2.24 (1.69 - 3.12)	0.002
Aortic stenosis, alanine baseline	0.94 (0.69 - 1.21)	0.86 (0.62 - 1.28)	0.43
Aortic stenosis, alanine pacing	0.86 (0.64 - 1.13)	0.90 (0.68 - 1.16)	0.09
HCM, glutamate baseline	2.35 (1.82 - 2.79)	1.36 (1.02 - 1.86)	0.0005
HCM, glutamate pacing	2.77 (2.12 - 3.12)	1.91 (1.50 - 2.35)	0.0006
HCM, alanine baseline	0.65 (0.58 - 0.81)	0.71 (0.62 - 0.80)	0.31
HCM, alanine pacing	0.65 (0.50 - 0.82)	0.66 (0.58 - 0.81)	0.32

Values shown are median (quartiles 1 to 3) concentrations of the respective metabolites. HCM = hypertrophic cardiomyopathy. Glutamate and alanine concentration is presented as area ratio.

ii. Trans-cardiac gradient

The extraction of glutamate was significantly lower during pacing as compared to baseline, in controls and in patients with aortic stenosis (table 3.2.4 & figure

3.2.3). In patients with HCM glutamate was extracted during baseline and pacing, but there was no significant difference observed between the net levels of extraction during the two states. There was no significant trans-cardiac gradient of alanine in any of the patient groups, both during baseline and pacing.

Table 3.2.4: Trans-cardiac gradient (aortic root – coronary sinus) of glutamate and alanine in individual patient cohorts during baseline and pacing. This is a paired analysis for the individual patient groups, measuring the gradient within each patient. Differences between the groups statistically analysed using either two-tailed Student's t-test or Wilcoxon Signed-Rank test. Statistical significance was defined as a p-value<0.05.

	Baseline	Pacing	p value
Controls, glutamate	1.15 (0.61 - 1.39)	0.87 (0.39 - 1.09)	0.046
Controls, alanine	−0.02 (−0.06 - 0.09)	0.05 (−0.11 - 0.10)	0.78
Aortic stenosis, glutamate	0.78 (0.54 - 0.86)	0.45 (0.20 - 0.70)	0.005
Aortic stenosis, alanine	−0.01 (−0.07 - 0.08)	−0.03 (−0.17 - 0.05)	0.57
HCM, glutamate	0.89 (0.65 - 1.15)	0.67 (0.35 - 0.80)	0.12
HCM, alanine	−0.04 (−0.12 - 0.04)	−0.02 (−0.09 - 0.05)	0.99

Values shown are median (quartiles 1 to 3) concentrations of the respective metabolites. HCM = hypertrophic cardiomyopathy. Glutamate and alanine concentration is presented as area ratio.

Further analysis was performed to analyse the difference in the net metabolism of glutamate and alanine between the three patient groups during baseline and pacing. Kruskal-Walis test (nonparametric ANOVA) was used to determine the statistical significance across the patient groups. There was a significant difference in the net extraction of glutamate at baseline ($p=0.03$), with highest extraction in the control group. There was no difference in the metabolism of glutamate during pacing or alanine during baseline or pacing between the three patient groups.

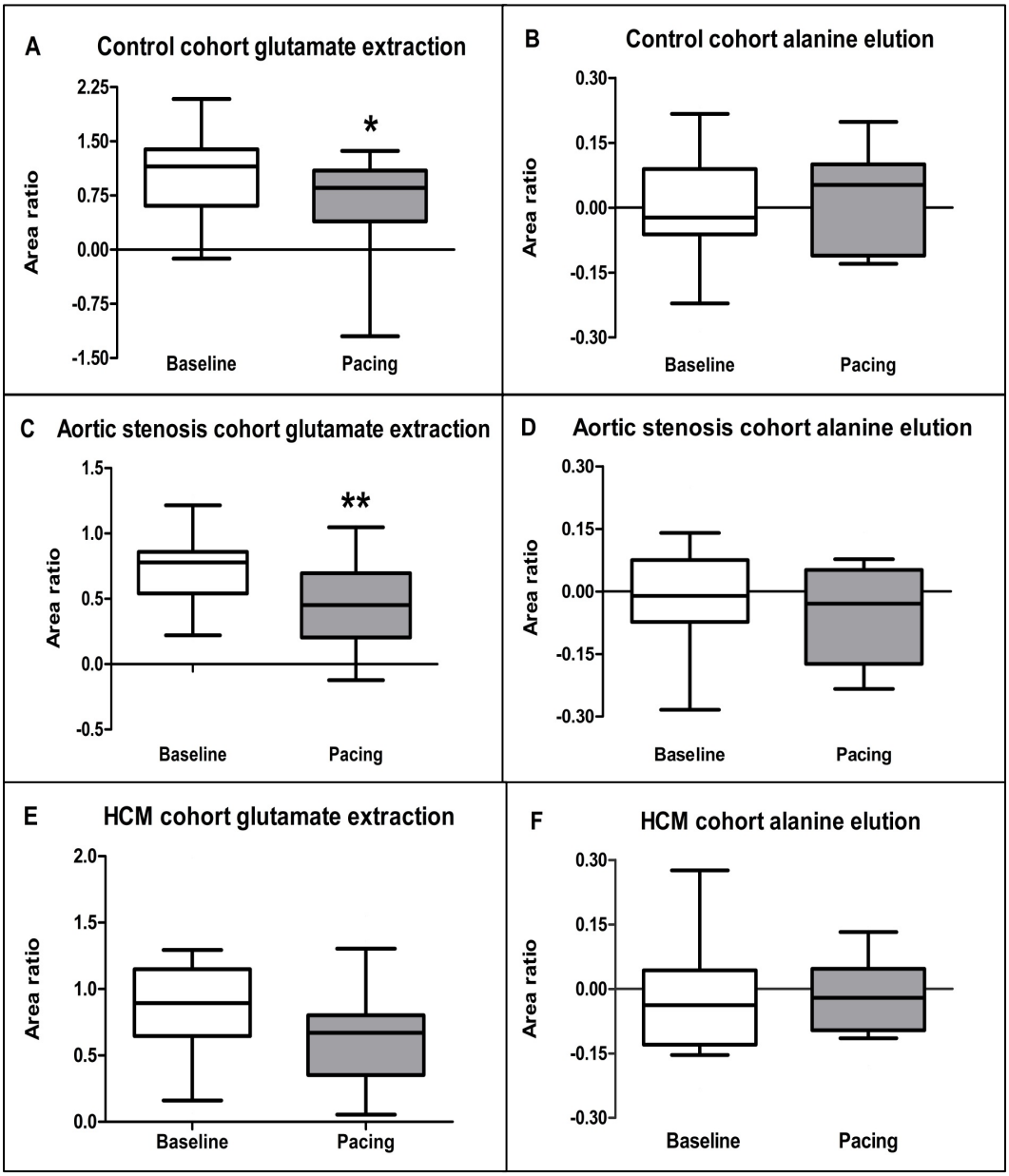

Figure 3.2.3: The figure above depicts the net cardiac metabolism (extraction / elution) of glutamate (A, C & E) and alanine (B, D & F) during baseline and pacing as measured in individual patient groups: controls (A & B), aortic stenosis (C & D) and HCM (E & F). The concentrations are shown as box plots, with the box representing quartiles 1 to 3 and the whiskers representing 10 to 90 percentile.

3.2.1.1.1 Conclusions

The conclusions that can be drawn from the above analysis are (table 3.2.5):

a) Glutamate:

- There was a net extraction of glutamate in all-patient groups both during baseline and pacing.
- Net extraction of glutamate significantly decreased during pacing in the control and aortic stenosis cohorts.
- Highest extraction of glutamate was present in the controls at baseline.

b) Alanine:

- There was no significant trans-cardiac gradient of alanine in any of the patient groups, both during baseline and pacing.

The significance of these metabolic changes in the respective cohorts has been discussed in the following chapters.

Table 3.2.5: Summary of glutamate and alanine analysis in individual patient cohorts during baseline and pacing. This is a paired analysis for the individual patient groups, measuring the gradient within each patient. Differences between the groups statistically analysed using either two-tailed Student's t-test or Wilcoxon Signed-Rank test. Statistical significance was defined as a p-value<0.05.

	Baseline	Pacing	p value
Glutamate			
Controls, glutamate	1.15 (0.61 - 1.39)	0.87 (0.39 - 1.09)	0.046
Aortic stenosis, glutamate	0.78 (0.54 - 0.86)	0.45 (0.20 - 0.70)	0.005
HCM, glutamate	0.89 (0.65 - 1.15)	0.67 (0.35 - 0.80)	0.12

Alanine			
Controls, alanine	−0.02 (−0.06 - 0.09)	0.05 (−0.11 - 0.10)	0.78
Aortic stenosis, alanine	−0.01 (−0.07 - 0.08)	−0.03 (−0.17 - 0.05)	0.57
HCM, alanine	−0.04 (−0.12 - 0.04)	−0.02 (−0.09 - 0.05)	0.99

Values shown are median (quartiles 1 to 3) concentrations of the respective metabolites. HCM = hypertrophic cardiomyopathy. Glutamate and alanine concentration is presented as area ratio.

3.2.2 Glucose and lactate

The trans-cardiac gradient of glucose and lactate was measured for the first consecutive 61 patients. Samples collected both at baseline and pacing were assessed to study the differences in the metabolism of glucose and lactate during the two physiological states.

Some patient samples were not included in the analysis due to unavailability of the samples; 2 patients in baseline and 9 patients in pacing analysis were excluded.

a) Samples from all-three cohorts combined

i) Aortic root vs coronary sinus

As shown in table 3.2.6 at baseline there was a significantly lower concentration of glucose (p=0.0004) and lactate (p=<0.0001) in the coronary sinus, indicative of a possible trans-cardiac extraction. This difference was not observed during pacing due to the rise in the concentration of glucose and lactate in the

coronary sinus. While the concentration of glucose in the coronary sinus increased during pacing, it still remained lower as compared to the aortic root. This indicated a net extraction of glucose, which was lower as compared to baseline. The concentration of lactate was higher in the coronary sinus as compared to the aortic root during pacing; this was opposite to baseline and indicated a possible elution (figure 3.2.4).

Table 3.2.6: Glucose and lactate concentration in the aortic root and coronary sinus during baseline and pacing. Differences between the groups statistically analysed using either two-tailed Student's t-test or Wilcoxon Signed-Rank test. Statistical significance was defined as a p-value<0.05.

	Aortic root	Coronary sinus	p value
Glucose, baseline (n=59)	5390 (4850 - 6160)	5140 (4730 - 5980)	0.0004
Glucose, pacing (n=52)	5405 (4770 - 6175)	5370 (4710 - 6135)	0.31
Lactate, baseline (n=59)	830 (690 - 1110)	760 (620 - 950)	<0.0001
Lactate, pacing (n=52)	800 (703 - 995)	870 (650 - 1068)	0.61

Values shown are median (quartiles 1 to 3) concentrations of the respective metabolites. HCM = hypertrophic cardiomyopathy. Glucose and lactate concentration is presented as µmol/L.

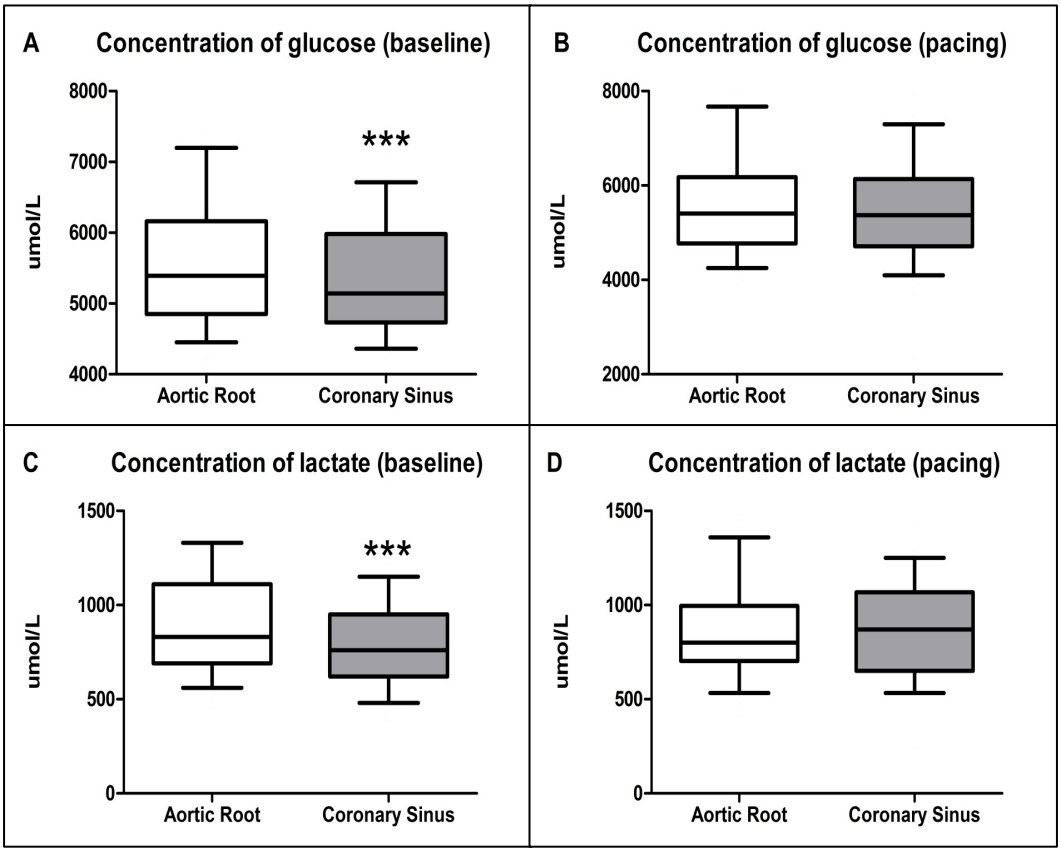

Figure 3.2.4: The figure above depicts the glucose (A & B) and lactate (C & D) concentrations in the aortic root and coronary sinus as measured in all patient groups combined together, thus showing the gradient across the heart. The concentrations are shown as box plots, with the box representing quartiles 1 to 3 and the whiskers representing 10 to 90 percentile.

ii) Trans-cardiac gradient

Table 3.2.7 describes the net trans-cardiac gradient (net metabolism: extraction/elution) of glucose and lactate during baseline and pacing. There was a net extraction of glucose during baseline and pacing, with extraction decreasing during pacing (Table 3.2.6). Lactate was extracted at baseline, which decreased significantly during pacing (p=0.0004) (figure 3.2.5). The

influence of increased coronary blood flow on the trans-cardiac gradient of metabolites has been discussed in the conclusion section.

Table 3.2.7: Trans-cardiac gradient (aortic root – coronary sinus) of glucose and lactate within each patient, in all studied patients combined together during baseline and pacing. Differences between the groups statistically analysed using either two-tailed Student's t-test or Wilcoxon Signed-Rank test. Statistical significance was defined as a p-value<0.05.

	Glucose (µmol/L)	**Lactate** (µmol/L)
Baseline (n=50)	145 (18 - 280)	60 (−10 - 140)
Pacing (n=50)	25 (−65 - 215)	15 (−135 - 140)
p value	0.09	0.0004

Values shown are median (quartiles 1 to 3) concentrations of the respective metabolites.

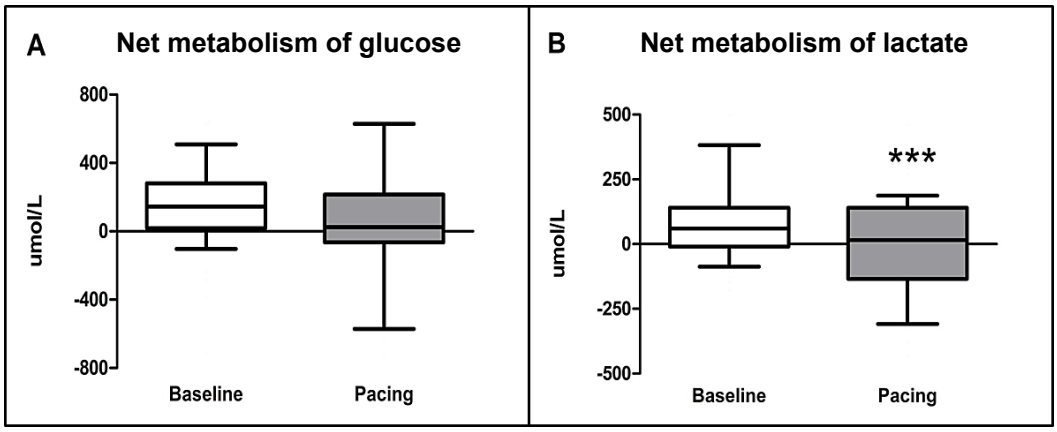

Figure 3.2.5: The figure above depicts the net cardiac metabolism (extraction / elution) of glucose (A) and lactate (B) during baseline and pacing, as measured across all patient groups. The concentrations are shown as box plots, with the box representing quartiles 1 to 3 and the whiskers representing 10 to 90 percentile.

a) Individual cohorts assessed separately

i) Aortic root vs coronary sinus

Analysis of glucose and lactate metabolism in the individual patient cohorts was then performed. Concentration of glucose and lactate in the aortic root and coronary sinus for the individual disease cohorts is described in table 3.2.8.

In all three cohorts the lactate levels were significantly lower in the coronary sinus as compared to the aortic root at baseline, but during pacing this difference was not observed. During pacing a higher concentration of lactate was observed in the coronary sinus of all-patient cohorts, though this difference was not significant. This suggested a net extraction of lactate at baseline in all three cohorts, but a trend towards elution during pacing in the aortic stenosis and HCM cohorts.

There was a lower concentration of glucose in the coronary sinus of all three cohorts at baseline. The difference was significantly lower in the HCM and control cohorts and was suggestive of net extraction. During pacing the glucose levels were lower in the coronary sinus as compared to the aortic root in all patient cohorts, but the difference was not significant. This implied a possible decrease in the net extraction of glucose during pacing in all the three cohorts.

Table 3.2.8: Glucose and lactate concentration in the aortic root and coronary sinus in individual patient groups: controls, aortic stenosis and hypertrophic cardiomyopathy, during baseline and pacing. This is a paired analysis for the individual patient groups. Differences between the groups statistically analysed using either two-tailed Student's t-test or Wilcoxon Signed-Rank test. Statistical significance was defined as a p-value<0.05.

	Aortic root	Coronary sinus	p value
Controls, glucose baseline (n=27)	5410 (5000 - 6200)	5280 (4770 - 6170)	0.0052
Controls, glucose pacing (n=25)	5530 (5055 - 6505)	5520 (4850 - 6385)	0.50
Controls, lactate baseline (n=27)	900 (710 - 1110)	870 (610 - 1000)	0.007
Controls, lactate pacing (n=25)	800 (705 - 1010)	820 (610 - 1045)	0.51
Aortic stenosis, glucose baseline (n=15)	5570 (4940 - 6320)	5180 (4800 - 6310)	0.34
Aortic stenosis, glucose pacing (n=11)	5570 (4700 - 6190)	5400 (4640 - 6020)	0.46
Aortic stenosis, lactate baseline (n=15)	930 (740 - 1150)	840 (620 - 1090)	0.01
Aortic stenosis, lactate pacing (n=11)	860 (540 - 1000)	880 (680 - 1020)	0.74
HCM, glucose baseline (n=17)	4960 (4695 - 5635)	4910 (4615 - 5275)	0.05
HCM, glucose pacing (n=16)	4955 (4700 - 5798)	4930 (4500 - 5673)	0.39
HCM, lactate baseline (n=17)	760 (645 - 895)	730 (605 - 805)	0.009
HCM, lactate pacing (n=16)	790 (688 - 888)	955 (705 - 1100)	0.09

Values shown are median (quartiles 1 to 3) concentrations of the respective metabolites. HCM = hypertrophic cardiomyopathy. Glucose and lactate concentration is presented as µmol/L.

ii) Trans-cardiac gradient

On further pair wise analysis of the individual disease cohorts the net extraction or elution of glucose and lactate was compared between baseline and pacing (table 3.2.9). In the control and aortic stenosis cohorts there was a net extraction of both glucose and lactate at baseline, which decreased though not significantly during pacing. In patients with HCM though there was a net extraction of glucose and lactate at baseline, during pacing a net elution of lactate was observed (p=0.0006)

Table 3.2.9: Trans-cardiac gradient (aortic root – coronary sinus) of glucose and lactate in individual patient cohorts during baseline and pacing. This is a paired analysis for the individual patient groups, measuring the gradient within each patient. Differences between the groups statistically analysed using either two-tailed Student's t-test or Wilcoxon Signed-Rank test. Statistical significance was defined as a p-value<0.05.

	Baseline	Pacing	p value
Controls, glucose (n=24)	160 (20 -245)	35 (−45 - 203)	0.09
Controls, lactate (n=24)	50 (−10 - 138)	45 (−90 - 150)	0.16
Aortic stenosis, glucose (n=10)	120 (33 - 535)	60 (−195 - 638)	0.97
Aortic stenosis, lactate (n=10)	105 (5 - 165)	55 (−53 - 115)	0.15
HCM, glucose (n=16)	138 ± 208	75 ± 342	0.53
HCM, lactate (n=16)	70 (−3 - 170)	−85 (−325 - 50)	0.0006

Values shown are mean ± SD or median (quartiles 1 to 3) concentrations of the respective metabolites. HCM = hypertrophic cardiomyopathy. Glucose and lactate concentration is presented as µmol/L.

As shown in figure 3.2.6, when compared across all three patient cohorts, there was no difference in the metabolism of either glucose or lactate during baseline. However during pacing lactate metabolism was significantly different with elution in HCM as compared to decreased extraction in controls and aortic stenosis (p=0.04, in a nonparametric ANOVA across three patient groups).

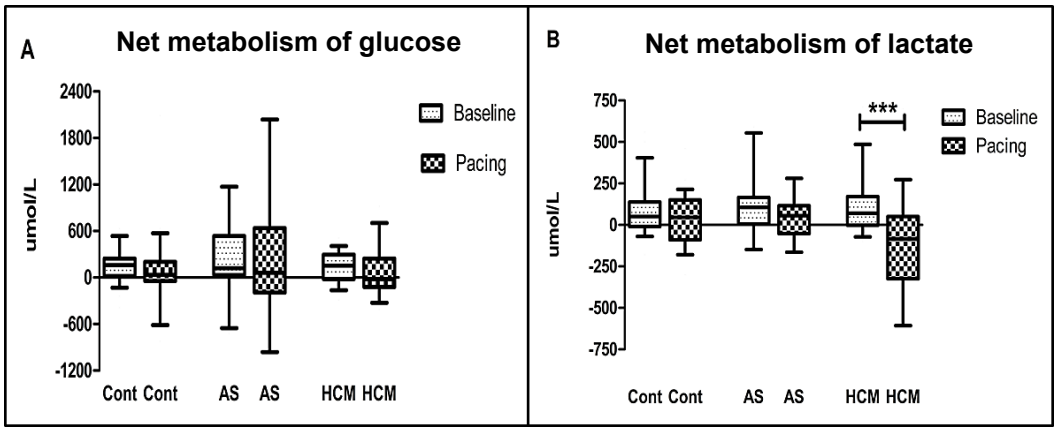

Figure 3.2.6: The figure above depicts the net cardiac metabolism (extraction / elution) of glucose (A) and lactate (B) during baseline and pacing, as measured in individual patient groups. Kruskal-Walis test (nonparametric ANOVA) was used to determine the statistical significance across the patient groups. The concentrations are shown as box plots, with the box representing quartiles 1 to 3 and the whiskers representing 10 to 90 percentile.

3.2.2.1.1 Conclusions

The following conclusions were drawn from the analysis of glucose and lactate in all three patient cohorts (table 3.2.10):

a) Glucose:

- There was a net extraction of glucose in all three patient cohorts during baseline and pacing, with a trend towards decrease in extraction during pacing.

b) Lactate:

- There was a net extraction of lactate in all three patient cohorts at baseline.
- During pacing there was a net elution of lactate in the HCM cohort.

Table 3.2.10: Summary of glucose and lactate analysis in individual patient cohorts during baseline and pacing. This is a paired analysis for the individual patient groups, measuring the gradient within each patient. Differences between the groups statistically analysed using either two-tailed Student's t-test or Wilcoxon Signed-Rank test. Statistical significance was defined as a p-value<0.05.

	Baseline	Pacing	p value
Glucose			
Controls, glucose (n=24)	160 (20 -245)	35 (−45 - 203)	0.09
Aortic stenosis, glucose (n=10)	120 (33 - 535)	60 (−195 - 638)	0.97
HCM, glucose (n=16)	138 ± 208	75 ± 342	0.53

Lactate			
Controls, lactate (n=24)	50 (−10 - 138)	45 (−90 - 150)	0.16
Aortic stenosis, lactate (n=10)	105 (5 - 165)	55 (−53 - 115)	0.15
HCM, lactate (n=16)	70 (−3 - 170)	−85 (−325 - 50)	0.0006

Values shown are mean ± SD or median (quartiles 1 to 3) concentrations of the respective metabolites. HCM = hypertrophic cardiomyopathy. Glucose and lactate concentration is presented as µmol/L.

Thus in summary, in agreement with previous reports, we observed net extraction of glutamate, glucose and lactate at baseline.[285,300,301] Furthermore, during pacing there was a fall in the extraction of glutamate in the control and aortic stenosis cohorts, and an elution of lactate in the HCM cohort.

It is important to highlight that the trans-cardiac gradient of metabolites measured during pacing could be influenced by the increased coronary sinus blood flow. Thomassen e*t al* reported similar observations of a fall in the trans-cardiac gradient of glutamate during pacing. They postulated that the fall in glutamate extraction measured as the aorto-coronary sinus concentration difference may be reflective of an unchanged underlying net flux, which was maintained by the compensatory increase in coronary sinus blood flow during pacing. But on further analysis they found that despite the increased coronary sinus blood flow, the overall net flux of glutamate was significantly lower during pacing and recovery in the coronary disease group.[301]

Similarly one should interpret the higher net elution of lactate during pacing in the HCM cohort with similar considerations. The increased net elution of lactate despite increased coronary sinus blood flow indicates a possible increase in the underlying net flux with a trend towards elution.

3.3 Metabolomics in the control cohort

Control cohort was the first group of patients on which a detailed metabolomic analysis was performed, the results from which are presented in this Chapter. Analysis was performed to understand the metabolism of the control cohort and to develop an analytical strategy, which would be used for the analysis of other cohorts.

A total of 38 control patients were studied in the final analysis. The data was analysed for samples collected at baseline and during pacing from the three-collection sites: femoral vein, aortic root and coronary sinus. A total of 38 acylcarnitine species and 49 aqueous metabolites were measured.

The acylcarnitines and aqueous metabolites were chosen as they are biologically important metabolites and can be measured accurately using the advanced mass spectrometry platforms. It was also important to assess the changes in acylcarnitines as they reflect the underlying alterations in fatty acid metabolism, which is a key source of myocardial energy. Acylcarnitines are likely to be long-lived species, and we thus hypothesized that their concentration would not alter significantly with the brief pacing protocol. The experiment was also conducted, as there was no published literature on changes in acylacrnitine metabolism post cardiac pacing. As acylcarnitines are excreted in the urine, a subsequent analysis of the most significant acylcarnitines was performed after normalisation to the eGFR of respective patients.

The aqueous metabolites were measured to gain insights into amino acid metabolism, glucose metabolism and citric acid cycle activity. We expected

changes to occur following pacing in the metabolism of amino acids and citric acid cycle intermediates, which play a vital role in the energy homeostasis and have been studied before in humans with different cardiac diseases.[285,294,301]

Analytical strategy comprising analysis of both acylcarnitines and aqueous metabolites was devised, and consisted of two sections:

1) Section 1: baseline & pacing samples analysed separately

Acylcarnitines and aqueous metabolites were initially analysed separately during the baseline and pacing states. This was performed between the three-collection sites in a combined and pair wise fashion, and is described bellow:

a) All three-collection sites combined

The initial analysis was performed to provide an overview of any differences between the collection sites by combining them together.

b) Aortic root vs coronary sinus (cardiac metabolism)

Differences between the aortic root & coronary sinus concentration of metabolites were assessed, and they could possibly result from their net-extraction or -elution during cardiac metabolism.

c) Aortic root vs femoral vein (peripheral metabolism)

Differences in the concentration of metabolites between the aortic root and femoral vein were assessed, and these could be indicative of their net-extraction or -elution during peripheral metabolism.

d) Femoral vein vs coronary sinus

Differences in concentration of metabolites between the femoral vein and coronary sinus were assessed, and these could be indicative of changes in metabolite concentration post cardiac and peripheral metabolism.

2) Section 2: baseline vs pacing

Second part of the analysis was done to assess for differences between the baseline and pacing states. The differences in concentration of metabolites were assessed in a given collection site between the two states, this included the following:

a) Femoral vein (baseline vs pacing)

b) Coronary sinus (baseline vs pacing)

c) Aortic root (baseline vs pacing)

d) All three-collection sites combined (baseline vs paving)

3.3.1 Acylcarnitine profile of the control cohort

The acylcarnitines were first to be analysed based on the **analytical strategy** described above:

1) Baseline & pacing samples analysed separately

2) Baseline vs pacing.

3.3.1.1 Baseline

The first subgroup analysis was done to understand the acylcarnitine metabolism at baseline. This included the following:

a) All three-collection sites combined

To gain an unbiased overview of the acylcarnitine distribution between the three-collection sites, unsupervised multivariate analysis using the PCA method was performed. This showed no separation between the three-collection sites as seen on its scores plot in figure 3.3.1 (plot A). On further supervised

multivariate testing using the PLS-DA method no model could be built. Thus the samples from the three-collection sites collected at baseline could not be discriminated using the acylcarnitines.

b) Aortic root vs coronary sinus

PCA analysis of acylcarnitines between the aortic root and coronary sinus samples showed no separation (figure 3.3.1, plot B). This was validated by supervised multivariate testing using the PLS-DA method. No model could be built using this analytical approach either and thus the samples collected from the aortic root and coronary sinus sites at baseline could not be discriminated using the acylcarnitines.

c) Aortic root vs femoral vein

PCA analysis of acylcarnitines between the aortic root and femoral vein collection sites exhibited no separation as seen on its scores plot in figure 3.3.1 (plot C); this was confirmed using the supervised multivariate analysis (PLS-DA) where no model could be built. Thus the aortic root and femoral vein samples collected at baseline could not be discriminated using the acylcarnitines.

d) Femoral vein vs coronary sinus

PCA analysis of acylcarnitines between the femoral vein and coronary sinus samples showed no separation as seen on its scores plot in figure 3.3.1 (plot D). No model could be built either using the supervised multivariate analytical approach (PLS-DA). Thus the samples collected from the femoral vein and coronary sinus at baseline could not be discriminated using the acylcarnitines.

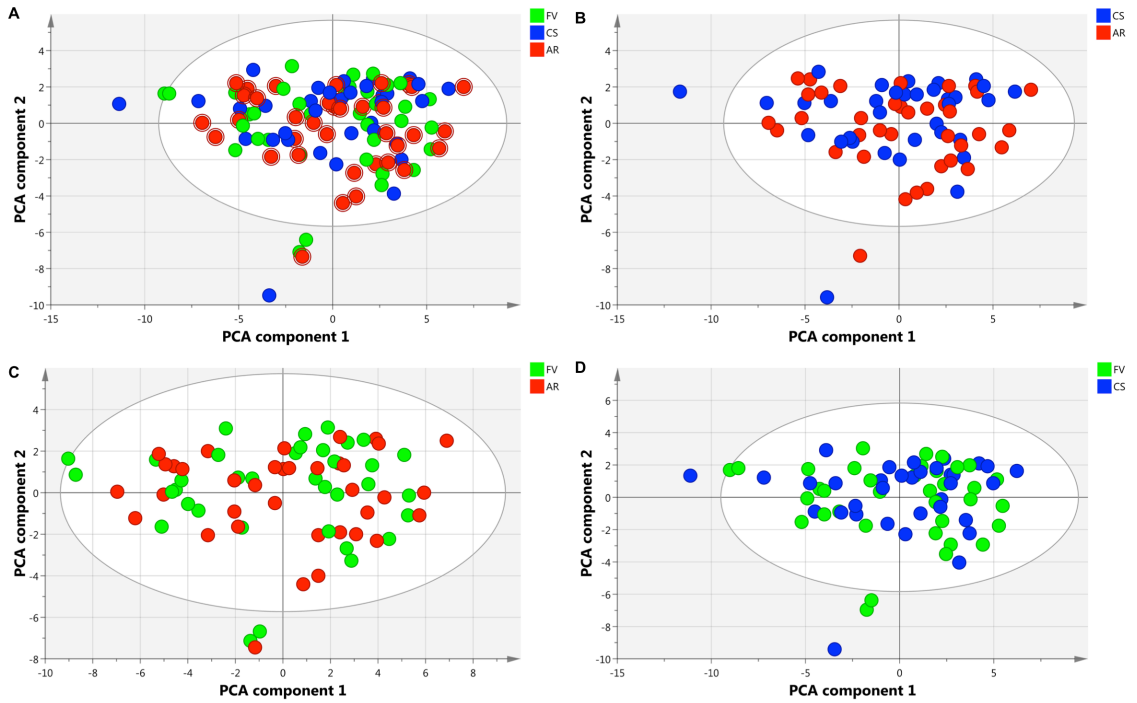

Figure 3.3.1: Principal component analysis (PCA) scores plot of acylcarnitines between all the collection sites combined together (A), AR vs CS (B), AR vs FV (C) and FV vs CS (D); analysis performed in the control cohort at baseline. AR: aortic root (red circle); CS: coronary sinus (blue circle); FV: femoral vein (green circle).

Conclusions from the analysis of acylcarnitines at baseline

By using multivariate analysis it was demonstrated that acylcarnitines could not discriminate between the baseline samples from three-collection sites, and thus it was suggestive of no significant difference in their concentration between the three sites. Turer *et el* reported similar findings for acylcarnitines in patients undergoing cardiac surgery for underlying coronary artery or valvular heart disease. They found no difference in concentrations between the aortic root and coronary sinus during resting conditons.[285] This could be explained, as acylcarnitines are long-lived species that are not rapidly absorbed and

metabolized. Thus no difference is seen in their concentration between samples collected from different sites in the body within a short space of time.

3.3.1.2 Pacing

Acylcarnitine metabolism was then assessed during the pacing state following the analytical strategy:

a) All three-collection sites combined

The samples from all three sites were initially analysed using unsupervised multivariate analysis (PCA). This showed no separation between the three-collection sites as seen on the PCA scores plot in figure 3.3.2 (plot A). On further supervised multivariate testing (PLS-DA) no model could be built, and thus the samples collected from the three sites during pacing could not be discriminated using acylcarnitines.

b) Aortic root vs coronary sinus

PCA analysis of acylcarnitines between the aortic root and coronary sinus samples was performed to assess for any differences between them. This showed no separation between the two-collection sites as seen on its scores plot in figure 3.3.2 (plot B). These samples were further assessed by supervised multivariate analytical approach using the PLS-DA method, where no model could be built either. Thus the samples collected from the aortic root and coronary sinus during pacing could not be discriminated using acylcarnitines.

c) Aortic root vs femoral vein

PCA analysis of acylcarnitines between the aortic root and femoral vein samples demonstrated no separation as visualised on its scores plot in figure

3.3.2 (plot C). On further supervised multivariate testing using the PLS-DA method no model could be built either. Thus the samples collected from the two-collection sites during pacing could not be discriminated using acylcarnitines.

d) Femoral vein vs coronary sinus

Unsupervised multivariate analysis of acylcarnitines between the femoral vein and coronary sinus samples was performed using the PCA approach. This demonstrated no separation between the two-collection sites as seen on the scores plot in figure 3.3.2 (plot D). Supervised multivariate testing was then performed using the PLS-DA method. No model could be built which could discriminate the samples from the two-collection sites.

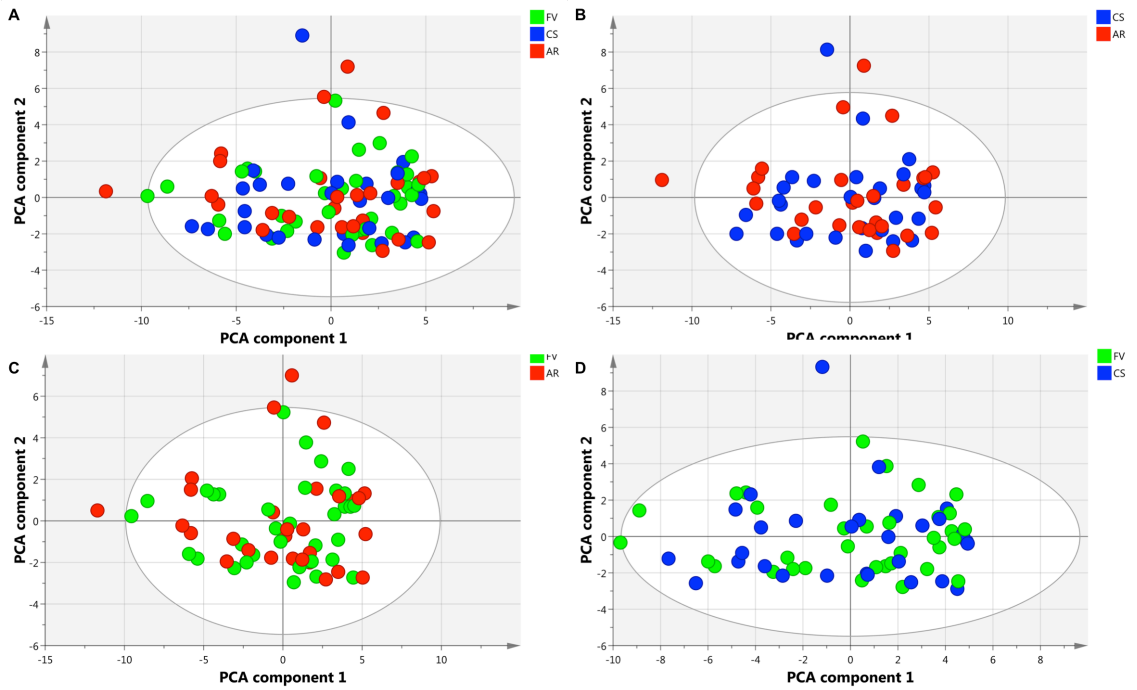

Figure 3.3.2: Principal component analysis (PCA) scores plot of acylcarnitines between all the collection sites combined together (A), AR vs CS (B), AR vs FV (C) and FV vs CS (D); analysis performed in the

control cohort during pacing. AR: aortic root (red circle); CS: coronary sinus (blue circle); FV: femoral vein (green circle).

Conclusions from the analysis of acylcarnitines during pacing

As observed through the analysis of samples collected at baseline (Section 3.3.1.1), the acylcarnitines could not discriminate between the samples collected from the three sites during pacing. This was suggestive of no significant difference in the concentration of acylcarnitines between the three-collection sites; this is possibly explained, as acylcarnitines are long-lived species and has been discussed in Section 3.3.1.1.

3.3.1.3 Baseline vs pacing

As per the analytical strategy described above the acylcarnitines were then analysed for differences between the baseline and pacing states in the individual collection sites and in combination together.

a) Femoral vein

Femoral vein samples were analysed to assess for any differences in acylcarnitines between the baseline and pacing states. PCA analysis was performed to obtain a general overview of the acylcarnitine distribution between the two states. This exhibited no separation between the two states as seen on the PCA scores plot in figure 3.3.3 (plot A). Similarly no model could be built using the supervised multivariate analysis (PLS-DA). Thus femoral vein samples collected at baseline and during pacing could not be discriminated using the acylcarnitines.

b) Coronary sinus

Unsupervised-multivariate analysis (PCA analysis) of acylcarnitines in the coronary sinus samples exhibited no separation between the baseline and pacing states (figure 3.3.3, plot B). Further no model could be built using the supervised multivariate analytical methods (PLS-DA). Thus the baseline and pacing samples collected from the coronary sinus could not be differentiated using the acylcarnitines.

c) Aortic root

The aortic root samples were analysed using the PCA method to provide an unbiased overview of any differences in acylcarnitine distribution between the baseline and pacing states. There was no separation exhibited as seen on the PCA scores plot in figure 3.3.3 (plot C). Further supervised multivariate testing using the PLS-DA analytical method was performed, and no model could be built using this approach either. Thus in summary samples collected from the aortic root during the baseline and pacing states could not be discriminated using the acylcarnitines.

d) All three-collection sites combined

Using the PCA approach the combined samples from all three-collection sites were analysed to assess for any differences in the acylcarnitine distribution between the baseline and pacing states. This unsupervised analysis showed no separation between the two states as seen on the PCA scores plot in figure 3.3.3 (plot D). On further supervised multivariate testing a weak PLS-DA model was built (R^2X=0.46, R^2Y=0.05, Q^2=-0.006), which did not exhibit a separation between the two states. The validity and goodness of fit of the original model were assessed using a 100 random permutations, where the majority of

permuted R^2 and Q^2 values on the left were found to be higher or equal than the original values on the right (intercepts: R^2=[0.0,0.07], Q^2=[0.0,−0.05]). Thus the original model could not be validated and no further analysis was performed.

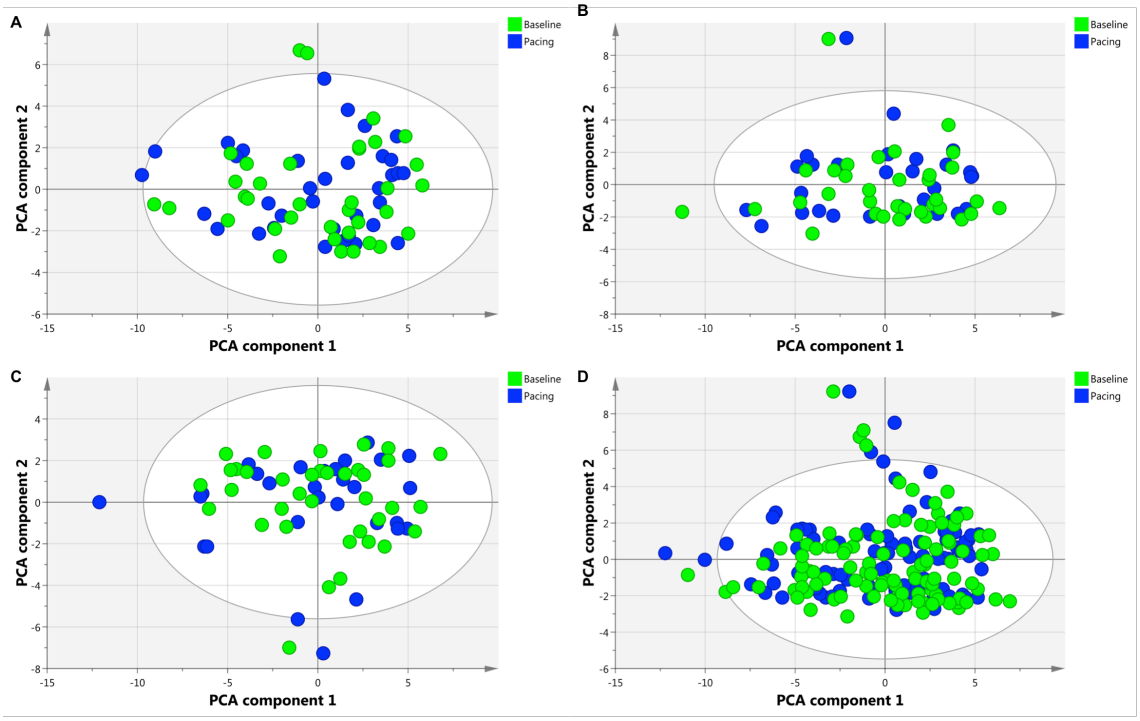

Figure 3.3.3: Principal component analysis (PCA) scores plot of acylcarnitines between baseline (green circles) and pacing (blue circles) states, in the femoral vein (A), coronary sinus (B), aortic root (C) and in all the collection sites combined together (D); analysis performed in the control cohort.

Conclusions from the analysis of acylcarnitines between baseline and pacing states

The analysis of samples from all three-collection sites demonstrated that the baseline and pacing states could not be discriminated using the acylcarnitines. This was suggestive of no significant difference in the concentration of acylcarnitines between the two states (resting & increased heart rate). In a

previous studies on patients undergoing coronary artery bypass surgery, significant net elution of acetyl-carnitine and β-hydroxybutyryl-carnitine was reported post ischaemia reperfusion (I/R).[285] The lack of such observation in our study is possibly explained by the low intensity of myocardial stress induced by pacing as compared to I/R, which could significantly alter the metabolism of acylcarnitines.

3.3.2 Aqueous metabolite analysis of the control cohort

The aqueous metabolites were then assessed using the analytical strategy described in Section 3.3.

3.3.2.1 Baseline

a) All three-collection sites combined

The samples from all three sites collected at baseline were analysed in an unbiased manner using the PCA approach to obtain a general overview of the aqueous metabolite distribution. This demonstrated some separation between the three-collection sites. To obtain a more reliable statistical conformation of the PCA model, PLS-DA analysis was performed. This generated a model separating the samples from the three-collection sites as seen on its scores plot in figure 3.3.4 (plot A) (R^2X=0.57, R^2Y=0.55, Q^2=0.28). Model validity and the degree of over fit were assessed and confirmed by using 100 random permutations (intercepts: R^2=[0.0,0.18], Q^2=[(0.0,−0.45]).

The metabolites which were most discriminating during multivariate analysis (VIP score ≥1) were further independently assessed using univariate analysis. They were analysed using ANOVA, with a post-test correction (Bonferroni's)

used for multiple comparisons. Analysis demonstrated that the concentration of glutamate and KVal was significantly higher, while that of succinate was significantly lower in the aortic root (table 3.3.1).

b) Aortic root vs coronary sinus

Unsupervised multivariate analysis of aqueous metabolites between the aortic root and coronary sinus samples using the PCA approach exhibited a clear separation between the two-collection sites. This was further verified by PLS-DA analysis, where the scores plot of the model built demonstrated distinct clusters (figure 3.3.4, plot B) (R^2X=0.18, R^2Y=0.62, Q^2=0.20). The validity and goodness of fit of the original model were confirmed by using 100 random permutations (intercepts: R^2=[0.0,0.30], Q^2=[0.0,−0.22]).

The metabolites found to be most discriminating on PLS-DA analysis (VIP score ≥1) were further assessed using either the two-tailed Student's t-test or the Mann-Whitney U-test. This revealed a significant difference in the concentration of glutamate, KIle (Keto-Isoleucine), KLeu (Keto-Leucine / 2-Ketoisocaproate), KVal (Keto-Valine / 2-Ketoisovalerate), pyruvate and succinate between the aortic root and coronary sinus. The observations were suggestive of a trans-cardiac extraction of glutamate KIle, KLeu, KVal and pyruvate (concentration was lower in the coronary sinus), and elution of succinate (concentration was higher in the coronary sinus) (table 3.3.2).

c) Aortic root vs femoral vein

Unsupervised multivariate analysis of aqueous metabolites between the aortic root and femoral vein samples using the PCA approach showed a clear separation. Supervised multivariate analysis using the PLS-DA approach verified this by generating a robust model, where a clear separation was seen

on its scores plot (figure 3.3.4, plot C) (R^2X=0.49, R^2Y=0.80, Q^2=0.68). The validity and goodness of fit of the original model were confirmed by using 100 random permutations (intercepts: R^2=[0.0,0.24], Q^2=[0.0,−0.31]).

Further independent univariate analysis of the most discriminating metabolites (VIP score ≥1) was performed using either the two-tailed Student's t-test or the Mann-Whitney U-test. This demonstrated a significantly higher concentration of glutamate in the aortic root, while the opposite was true for alanine, arginine, citrulline, lysine and succinate. These findings were suggestive of glutamate extraction, and elution of alanine, arginine, citrulline, lysine and succinate in the peripheral metabolism (table 3.3.2).

d) Femoral vein vs coronary sinus

An unbiased overview of the aqueous metabolites between the femoral vein and coronary sinus samples using the PCA approach exhibited a separation between the two sites. PLS-DA analysis was then performed, where a robust model was generated and a clear separation was seen between the two-collection sites on its scores plot (figure 3.3.4, plot D) (R^2X=0.51, R^2Y=0.58, Q^2=0.33). The validity and goodness of fit of the original model were confirmed by using 100 random permutations (intercepts: R^2=[0.0,0.29], Q^2=[0.0,−0.27]).

Further univariate analysis of the most significant metabolites (with a VIP score ≥1) revealed a significantly higher concentration of glutamate and a significantly lower concentration of arginine, KVal, pyruvate and tyrosine in the coronary sinus (table 3.3.2).

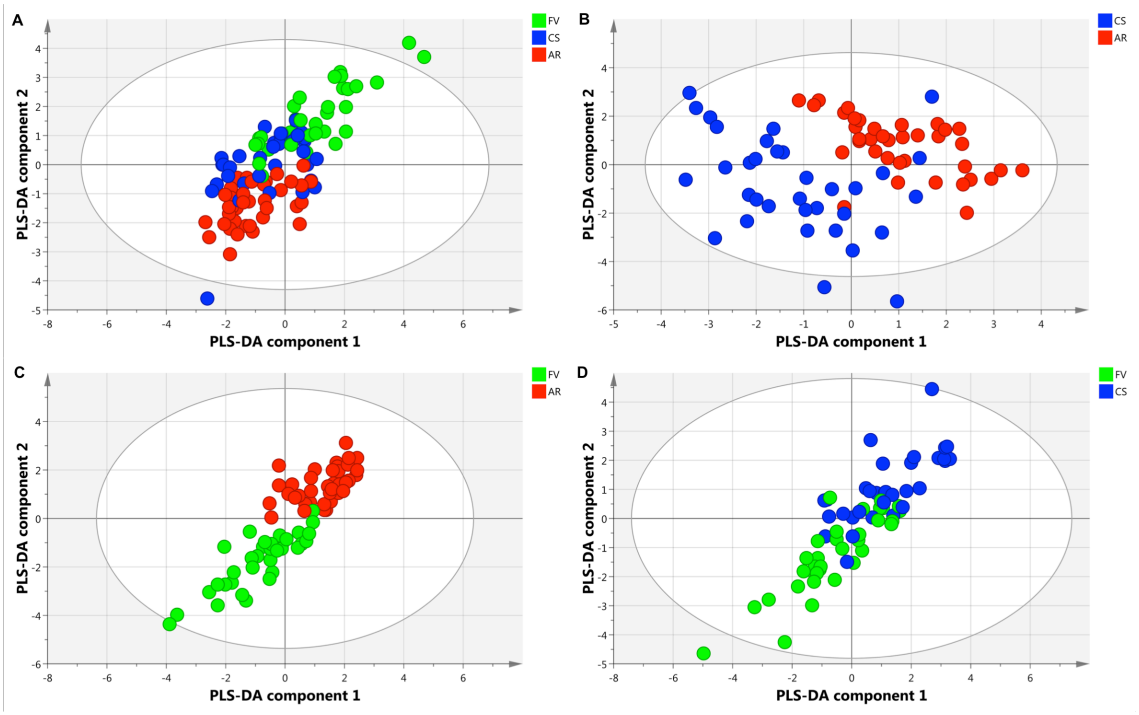

Figure 3.3.4: Partial least squares- discriminant analysis (PLS-DA) scores plot of aqueous metabolites between all the collection sites combined together (A), AR vs CS (B), AR vs FV (C) and FV vs CS (D); analysis performed in the control cohort at baseline. AR: aortic root (red circle); CS: coronary sinus (blue circle); FV: femoral vein (green circle).

Table 3.3.1: Concentration of aqueous metabolites which were significantly different on analysis between the femoral vein, coronary sinus and aortic root samples, in the control cohort at baseline. Differences between the groups statistically analysed using ANOVA with Bonferroni's post-test for multiple comparisons. In comparing aortic root with coronary sinus: * represents p<0.05, ** p<0.01, *** p<0.001 and **** p<0.0001. In comparing aortic root vs femoral vein: $^{\#}$ represents p<0.05, $^{\#\#}$ p<0.01, $^{\#\#\#}$ p<0.001 and $^{\#\#\#\#}$ p<0.0001. In comparing femoral vein vs coronary sinus: ^ represents p<0.05, ^^ p<0.01, ^^^ p<0.001 and ^^^^ p<0.0001. Metabolites listed in alphabetical order.

Metabolite	Femoral vein	Coronary sinus	Aortic root
Glutamate	1.10 (0.86 -1.42)^^^	1.52 (1.29 - 1.89)	2.58 (2.08 - 2.97)***####
KVal	2.34 (1.78 - 2.95)^	1.92 (1.44 - 2.62)	2.70 (2.19 - 3.26)****
Succinate	0.63 (0.53 - 0.89)	0.77 (0.54 - 0.90)	0.55 (0.43 - 0.64)****###

Values shown are median (quartiles 1 to 3) concentrations of the respective metabolites. Concentrations are presented as area ratio after normalisation to the internal standards.

Table 3.3.2: Concentration of aqueous metabolites which were significantly different on a pair wise analysis between the aortic root and coronary sinus, aortic root and femoral vein, and femoral vein and coronary sinus, in the control cohort at baseline. Differences between the groups statistically analysed using either two-tailed Student's t-test or Mann-Whitney U-test. Statistical significance was defined as a p-value<0.05. Metabolites listed in alphabetical order.

Metabolite	Aortic root	Coronary sinus	p value
Glutamate	2.58 (2.08 - 2.97)	1.52 (1.29 - 1.89)	<0.001
KIle	6.59 (5.86 - 7.91)	5.46 (4.07 - 6.99)	0.004
KLeu	10.77 (8.77 - 13.21)	8.92 (6.33 - 11.03)	0.02
KVal	2.70 (2.19 - 3.26)	1.92 (1.44 - 2.62)	<0.0001
Pyruvate	0.31 (0.24 - 0.40)	0.25 (0.16 - 0.33)	0.02
Succinate	0.55 (0.43 - 0.64)	0.77 (0.54 - 0.90)	<0.0001

Metabolite	Aortic root	Femoral vein	p value
Alanine	0.72 (0.62 - 1.03)	0.93 (0.80 - 1.24)	0.0005
Arginine	2.33 (2.06 - 2.83)	2.70 (2.30 - 3.26)	0.005
Citrulline	46.24 (33.99 - 60.36)	58.49 (41.12 - 74.24)	0.04
Glutamate	2.58 (2.08 - 2.97)	1.10 (0.86 - 1.42)	<0.0001
Lysine	0.27 (0.23 - 0.31)	0.30 (0.25 - 0.33)	0.04
Succinate	0.55 (0.43 - 0.64)	0.63 (0.53 - 0.89)	0.0007

Metabolite	Femoral vein	Coronary sinus	p value
Arginine	2.70 (2.30 - 3.26)	2.29 (1.89 - 2.86)	0.007
Glutamate	1.10 (0.86 - 1.42)	1.52 (1.29 - 1.89)	0.0002
KVal	2.34 (1.78 - 2.95)	1.92 (1.44 - 2.62)	0.01
Pyruvate	0.31 (0.22 - 0.41)	0.25 (0.16 - 0.33)	0.02
Tyrosine	0.56 (0.48 - 0.65)	0.49 (0.45 - 0.59)	0.0008

Values shown are median (quartiles 1 to 3) concentrations of the respective metabolites. Concentrations are presented as area ratio after normalisation to the internal standards.

Conclusions from the analysis of aqueous metabolites at baseline

The analysis of aqueous metabolites at baseline provided the following information regarding the differences between cardiac & peripheral metabolism:

1) Glutamate: it was extracted both during cardiac and peripheral metabolism, with a higher extraction peripherally. This is possibly explained, as the lower limbs that have a significantly higher muscle mass than the cardiac muscle, would also have a much larger metabolic requirement. This result is similar to findings in previous human studies where glutamate extraction has been reported during cardiac and peripheral metabolism.[285,301,302] Glutamate plays a vital role in the cahill cycle, where its transamination generates α-ketoglutarate, an anaplerotic substrate of the citric acid cycle.
2) Alanine: there was a significant elution of alanine during peripheral metabolism, which was not observed during cardiac metabolism. Elution of alanine by human skeletal muscle has been reported before by London *et al*.[302] Alanine is generated by the transamination of pyruvate, a reaction catalysed by alanine aminotransferase.
3) Succinate: it was eluted in both cardiac and peripheral metabolism, with no difference between the two. Succinate is an important byproduct of the citric acid cycle and the changes in citric acid cycle activity in different patient cohorts is discussed further in Chapter 8.[164]
4) KVal, KLeu & KIle: these branched chain amino acids (BCAAs) were extracted during cardiac metabolism, with a significantly lower concentration present in the coronary sinus. The role of BCAAs during cardiac metabolism is discussed in detail in Chapter 8.
5) Pyruvate: it was extracted during cardiac metabolism.
6) Citrulline, arginine and lysine: they were eluted during peripheral metabolism.

3.3.2.2 Pacing

a) All three-collection sites combined

The aqueous metabolites were then analysed for any differences between the pacing samples from the three-collection sites. This was performed by using the PCA approach for an unbiased overview of the samples, which did not exhibit a clear separation between the three-collection sites. This was followed by the PLS-DA analysis where a model was built, and some separation was demonstrated between the three-collection sites as seen on its scores plot in figure 3.3.5 (plot A) (R^2X=0.33, R^2Y=0.33, Q^2=0.26). The validity and goodness of fit of the original model were confirmed by using 100 random permutations (intercepts: R^2=[0.0,0.07], Q^2=[0.0,−0.13]).

The most discriminating metabolites (VIP score ≥1) were then assessed using ANOVA, with a post-test correction (Bonferroni's) used for multiple comparisons. This demonstrated a significantly higher concentration of alanine, citrulline and methionine, and a significantly lower concentration of glutamate in the femoral vein (table 3.3.3).

b) Aortic root vs coronary sinus

Unsupervised multivariate analysis of aqueous metabolites between aortic root and coronary sinus samples using the PCA approach showed a clear separation. This was further verified by performing the PLS-DA analysis where a weak model was generated and clear separation was seen between the two-collection sites as seen on its scores plot in figure 3.3.5 (plot B) (R^2X=0.35, R^2Y=0.42, Q^2=0.04). The validity and tightness of fit of the original model were assessed by using 100 random permutations. The majority of the permuted R^2 and Q^2 values on the left were lower than the original values on the right

(intercepts: R^2=[0.0,0.23], Q^2=[0.0,−0.15]), which was indicative of a valid original model.

Further univariate analysis of the most discriminating metabolites (VIP score ≥1) was performed using either the two-tailed Student's t-test or the Mann-Whitney U-test. This demonstrated the following: the concentration of glutamate, KVal and pyruvate was significantly higher in the aortic root, while the concentration of succinate was significantly lower (table 3.3.4). These observations suggested a possible trans-cardiac extraction of glutamate, KVal and pyruvate, and an elution of succinate.

c) Aortic root vs femoral vein

Multivariate analysis of aqueous metabolites between the aortic root and femoral vein samples found several discriminating metabolites, which generated a robust PLS-DA model exhibiting a clear separation on its scores plot (figure 3.3.5, plot C) (R^2X=0.54, R^2Y=0.88, Q^2=0.67). The validity and goodness of fit of the original model was assessed and confirmed by using 100 random permutations (intercepts: R^2=[0.0,0.34], Q^2=[0.0,−0.46]).

The significance of the most discriminating metabolites (VIP score ≥1) was assessed using either the two-tailed Student's t-test or the Mann-Whitney U-test. This demonstrated a significantly lower concentration of fumarate and glutamate in the femoral vein, and a significantly higher concentration of alanine, citrulline, methionine, threonine and succinate (table 3.3.4). These measurements were indicative of a possible extraction of glutamate and fumarate, and elution of alanine, citrulline, methionine, threonine and succinate in the peripheral metabolism.

d) Femoral vein vs coronary sinus

The multivariate and univariate analysis of aqueous metabolites between the femoral vein and coronary sinus collection sites found alanine, arginine, citrulline, glutamate, histidine, KVal, methionine, phenylalanine, pyruvate and threonine to be most differentiating (table 3.3.8). Except for glutamate all the other metabolites were found to be present in a significantly higher concentration in the femoral vein. A robust PLS-DA model was built from these discriminating metabolites (R^2X=0.21, R^2Y=0.80, Q^2=0.59), whose validity and goodness of fit were confirmed by using 100 random permutations (intercepts: R^2=[0.0,0.31], Q^2=[0.0,−0.25]).

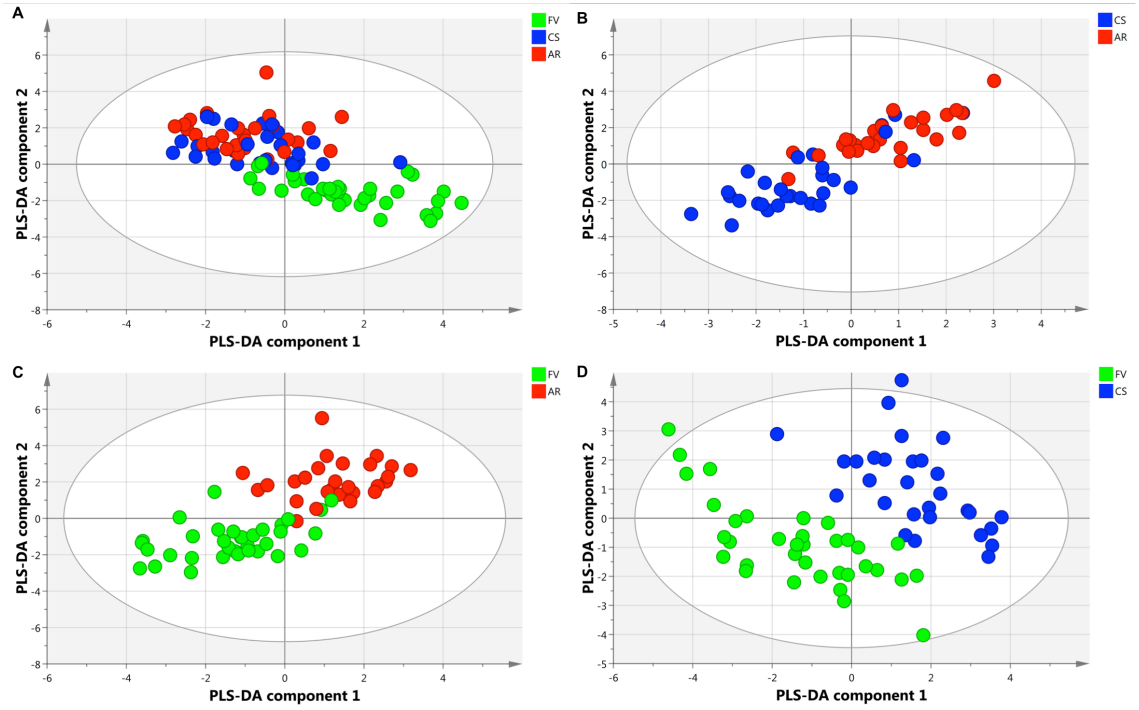

Figure 3.3.5: Partial least squares- discriminant analysis (PLS-DA) scores plot of aqueous metabolites between all the collection sites combined together (A), AR vs CS (B), AR vs FV (C) and FV vs CS (D); analysis performed in the control cohort during pacing. AR: aortic root (red circle); CS: coronary sinus (blue circle); FV: femoral vein (green circle).

Table 3.3.3: Concentration of aqueous metabolites which were significantly different on analysis between the femoral vein, coronary sinus and aortic root samples, in the control cohort during pacing. Differences between the groups statistically analysed using ANOVA with Bonferroni's post-test for multiple comparisons. In comparing aortic root with coronary sinus: * represents p<0.05, ** p<0.01, *** p<0.001 and **** p<0.0001. In comparing aortic root vs femoral vein: # represents p<0.05, ## p<0.01, ### p<0.001 and #### p<0.0001. In comparing femoral vein vs coronary sinus: ^ represents p<0.05, ^^ p<0.01, ^^^ p<0.001 and ^^^^ p<0.0001. Metabolites listed in alphabetical order.

Metabolite	Femoral vein	Coronary sinus	Aortic root
Alanine	0.98 (0.78 - 1.23)^^^	0.72 (0.59 - 1.03)	0.72 (0.58 - 0.85)####
Citrulline	61.47 (47.75 - 74.81)^^	45.78 (37.15 - 61.60)	45.70 (35.05 - 59.77)##
Glutamate	1.14 (0.85 - 1.32)^^^^	2.13 (1.81 - 2.68)	2.73 (2.23 - 3.34)****####
Methionine	67.40 (59.18 - 85.3)^^	58.70 (48.60 - 67.78)	61.47 (51.07 - 71.63)#

Values shown are median (quartiles 1 to 3) concentrations of the respective metabolites. Concentrations are presented as area ratio after normalisation to the internal standards.

Table 3.3.4: Concentration of aqueous metabolites which were significantly different on a pair wise analysis between the aortic root and coronary sinus, aortic root and femoral vein, and femoral vein and coronary sinus, in the control cohort during pacing. Differences between

the groups statistically analysed using either two-tailed Student's t-test or Mann-Whitney U-test. Statistical significance was defined as a p-value<0.05. Metabolites listed in alphabetical order.

Metabolite	Aortic root	Coronary sinus	p value
Glutamate	2.73 (2.23 - 3.34)	2.13 (1.81 - 2.68)	<0.0001
KVal	2.73 (2.27 - 1.41)	2.04 (1.41 - 2.37)	0.0001
Pyruvate	0.29 (0.26 - 0.38)	0.24 (0.17 - 0.31)	0.02
Succinate	0.55 (0.43 - 0.63)	0.72 (0.53 - 0.87)	0.02

Metabolite	Aortic root	Femoral vein	p value
Alanine	0.72 (0.58 - 0.85)	0.98 (0.78 - 1.23)	<0.0001
Citrulline	45.70 (35.05 - 59.77)	61.47 (47.75 - 74.81)	0.002
Fumarate	0.09 (0.05 - 0.16)	0.06 (0.05 - 0.09)	0.03
Glutamate	2.73 (2.23 - 3.34)	1.14 (0.85 - 1.32)	<0.0001
Methionine	61.47 (51.07 - 71.63)	67.40 (59.18 - 85.30)	0.01
Succinate	0.55 (0.43 - 0.64)	0.68 (0.52 - 0.77)	0.03
Threonine	0.29 (0.27 - 0.35)	0.35 (0.29 - 0.39)	0.01

Metabolite	Femoral vein	Coronary sinus	p value
Alanine	0.98 (0.78 - 1.23)	0.72 (0.59 - 1.03)	0.0005
Arginine	2.83 (2.44 - 3.12)	2.42 (1.93 - 3.01)	0.03

Citrulline	61.47 (47.75 - 74.81)	45.78 (37.15 - 61.60)	0.003
Glutamate	1.14 (0.85 - 1.32)	2.13 (1.81 - 2.68)	<0.0001
Histidine	1.67 (1.49 - 1.83)	1.47 (1.14 - 1.74)	0.02
KVal	2.44 (1.89 - 2.98)	2.04 (1.41 - 2.37)	0.009
Methionine	67.40 (59.18 - 85.30)	58.70 (48.60 - 67.78)	0.001
Phenylalanine	1.76 (1.65 - 1.89)	1.64 (1.52 - 1.77)	0.02
Pyruvate	0.32 (0.23 - 0.42)	0.24 (0.17 - 0.31)	0.002
Threonine	0.35 (0.30 - 0.39)	0.30 (0.27 - 0.35)	0.01

Values shown are median (quartiles 1 to 3) concentrations of the respective metabolites. Concentrations are presented as area ratio after normalisation to the internal standards.

Conclusions from the analysis of aqueous metabolites during pacing

On interpretation of the data detailed above the following conclusions were drawn regarding the cardiac and peripheral metabolism in the control cohort during pacing:

1) Glutamate: it was extracted both during cardiac and peripheral metabolism, with a higher extraction peripherally. This has previously been discussed in the Section 3.3.2.1. Mudge *et al* and Thomassen *et al* have previously reported similar findings of glutamate extraction by a normal myocardium during pacing.[300,301]
2) Alanine: it was eluted during peripheral metabolism. Alanine and glutamate play a crucial role in linking the amino acid and carbohydrate metabolism (cahill/alanine cycle) and alanine elution during peripheral metabolism has previously been reported.[300-302]

3) Succinate: it was eluted both during cardiac and peripheral metabolism.
4) KVal: it was extracted during cardiac metabolism, which was not observed during peripheral metabolism.
5) Citrulline, methionine and threonine: they were all eluted during peripheral metabolism.

3.3.2.3 Baseline vs pacing

The aqueous metabolites were then analysed for any differences between the baseline and pacing states in each individual collection site and in combination together.

a) Femoral vein

The aqueous metabolites in the femoral vein samples were analysed to assess for differences between the baseline and pacing states using the PCA analytical approach. Using this unsupervised approach no separation was seen between the baseline and pacing states as seen on the PCA scores plot in figure 3.3.6 (plot A). To verify these findings supervised multivariate analysis was performed using the PLS-DA method, where no model could be built either. Thus the baseline and pacing samples collected from the femoral vein could not be discriminated using the aqueous metabolites.

b) Coronary sinus

Figure 3.3.6 (plot B) shows the PCA scores plot from the analysis of aqueous metabolites between baseline and pacing states in the coronary sinus samples. As seen, no separation was demonstrated between the two states and this was further verified by supervised multivariate testing where no models could be

built either. Thus the baseline and pacing samples collected from the coronary sinus could not be discriminated using the aqueous metabolites.

c) Aortic root

The multivariate analysis of the aortic root samples collected at baseline and during pacing, showed similar results as the femoral vein and coronary sinus samples. Thus the samples collected during the two sates could not be discriminated as seen on the PCA scores plot in figure 3.3.6 (plot C).

d) All three-collection sites combined

Multivariate analysis was then performed after combining samples from all three sites; this was done initially using the PCA approach. There was no separation seen between the baseline and pacing states as demonstrated on the PCA scores plot in figure 3.3.6 (plot D). Further analysis using the PLS-DA approach confirmed these findings as no model could be built. Thus the samples collected during the baseline and pacing states from all three-collection sites combined together could not be discriminated using the aqueous metabolites.

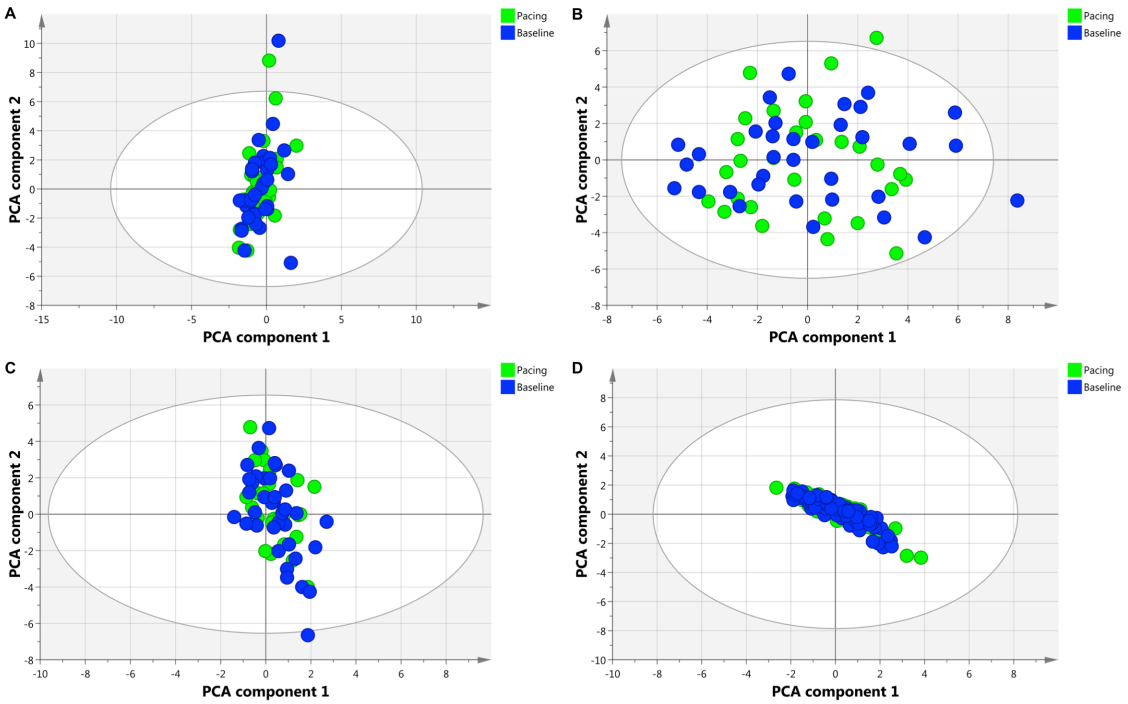

Figure 3.3.6: Principal component analysis (PCA) scores plot of aqueous metabolites between baseline (green circles) and pacing (blue circles) states, in the femoral vein (A), coronary sinus (B), aortic root (C) and in all the collection sites combined together (D); analysis performed in the control cohort.

Conclusions from the analysis of aqueous metabolites between baseline and pacing states

The samples collected during the baseline and pacing states from the three-collection sites could not be discriminated using the aqueous metabolites. This suggested that the concentration of aqueous metabolites did not change significantly between the baseline and pacing states when measured in each individual collection site or when all were combined. Thus the short duration of pacing did not significantly alter the concentration of aqueous metabolites when measured in an individual collection site.

But as reported there was a noticeable difference in the concentration of metabolites between the individual collection sites, which varied between the baseline and pacing states. This possibly resulted from either extraction or elution of metabolites during cardiac and peripheral metabolism. Changes in the cardiac metabolism between the baseline and pacing states are described in the next section.

3.3.2.3.1 Cardiac metabolism (baseline vs pacing)

Table 3.3.5 details the difference in the cardiac metabolism of various aqueous metabolites between baseline and pacing. The analysis was performed on the extraction and elution measured from the paired arterial and coronary sinus samples collected at baseline and during pacing. The most significant results were as follows:

1) Glutamate: it was extracted both during baseline and pacing, with a significant decrease in extraction during pacing.

   Mudge *et al* have previously reported similar findings of decreased glutamate extraction following pacing in the normal human myocardium. They also reported a higher net extraction of glutamate at baseline in the coronary disease group as compared to controls, with a significantly lesser drop in their glutamate extraction during pacing. It was postulated that the higher utilization of glutamate in the coronary disease group was to produce alanine via transamination of pyruvate, rather than conversion of pyruvate to lactate. This difference in amino acid metabolism in the coronary disease group was described to be an adaptive response to increased myocardial

stress during ischaemia.[300] Similarly findings of decreased glutamate extraction following pacing have also been reported by Thomassen *et al.*[301]

Glutamate play a critical role in several biochemical reactions including the cahill cycle, which links the amino acid and glucose metabolism. The changes in glutamate metabolism during pacing in the normal myocardium can possibly be explained by the concurrent changes in lactate. As reported in Section 3.2.2 there was a build up of lactate during pacing in the control cohort. Thus as more of pyruvate is converted into lactate during pacing, it is channeled away from its transamination, which produces alanine; during this reaction glutamate acts the nitrogen donor, and as the flux through this reaction falls, lower amount of glutamate is extracted.

2) Succinate: it was eluted both during baseline and pacing, with no significant difference between the two.

3) KLeu and KVal: these branch chain amino acids (BCAAs) were extracted both during baseline and pacing, with a non-significant increase in their extraction during pacing.

The limitation in assessing the net substrate flux of metabolites in the absence of coronary sinus blood flow measurements should be considered. As discussed before in Section 3.2.2.1.1, the fall in trans-cardiac extraction of glutamate during pacing may occur while the underlying net substrate flux remains unchanged, maintained by the increased coronary sinus blood flow. But as reported by Thomassen *et al* in the coronary disease group, Mudge *et al* reported similar findings in their normal group where significantly decreased glutamate extraction was accompanied with a significant decrease in the net flux too, despite the increased coronary sinus blood flow during pacing.[300,301]

Similar considerations are applied when interpreting the elution of succinate, which remains unchanged during pacing. Thus despite the increased coronary sinus blood flow during pacing, the unchanged aorto-coronary sinus concentration of succinate is possibly indicative of an increase in the underlying net flux of succinate.

Table 3.3.5: Trans-cardiac gradient (aortic root – coronary sinus) of selected aqueous metabolites measured within individual patients in the control cohort, and compared between baseline and pacing. Differences between the groups statistically analysed using either two-tailed Student's t-test or Wilcoxon Signed-Rank test. Statistical significance was defined as a p-value<0.05. Metabolites listed in alphabetical order.

Metabolite	Baseline	Pacing	p value
Alanine	−0.02 (-0.07 - 0.06)	0.05 (−0.11 - 0.09)	0.78
BAIBA	0.0 (−0.0005 - 0.0)	0.0 (−0.0006 - 0.0)	0.38
Citrulline	0.13 (−10.04 - 9.22)	5.79 (−4.13 - 15.35)	0.24
Glutamate	1.15 (0.61 - 1.39)	0.86 (0.39 - 1.09)	0.046
Isocitrate	0.25 (−0.71 - 1.66)	0.33 (−0.57 - 2.45)	0.25
KLeu	2.47 (−0.06 - 3.72)	3.00 (0.57 - 4.35)	0.44
KVal	0.70 (0.34 - 1.13)	0.93 (0.07 - 1.85)	0.59
Malate	−0.04 (−0.26 - 0.21)	0.21 (−0.39 - 0.45)	0.39
Pyruvate	0.07 (−0.02 - 0.18)	0.06 (−0.01 - 0.23)	0.79
Succinate	−0.14 (−0.28 - −0.03)	−0.11 (−0.34 - 0.02)	0.77

Values shown are median (quartiles 1 to 3) concentrations of the respective metabolites. Concentrations are presented as area ratio after normalisation to the internal standards. BAIBA = β–aminoisobutyric acid.

3.3.3 Lessons learnt: justification of proposed analytic strategy

The metabolism of the control cohort was analysed in detail using the proposed analytical strategy. Analysis not only allowed better understanding of the metabolism in the control cohort, but important lessons were also learnt from it, which could be implemented in the analysis of the HCM and aortic stenosis cohorts.

Summary of the findings from the analysis (table 3.3.6):

a) Acylcarnitines: no difference was observed in the concentration of acylcarnitines between the individual collection sites at baseline or during pacing. Thus as hypothesized, this may reflect the fact that acylcarnitines are long-lived species, with no net extraction or elution occurring either in the cardiac or peripheral metabolism during the two states.

b) Aqueous metabolites: on a pair wise analysis of the collection sites there was a significant difference in the concentration of aqueous metabolites both at baseline and during pacing. This difference in concentration between the collection sites was possibly a result of either net extraction or elution occurring during cardiac or peripheral metabolism. Also the trans-cardiac gradient of certain metabolites was found to change as a result of myocardial stress induced by pacing.

   As with acylcarnitines, there was no significant difference found in the concentration of aqueous metabolites between the baseline and pacing samples from an individual collection site. Thus in summary though the

short duration of pacing was not enough to produce a significant change in the concentration of aqueous metabolites within a given collection site, but it did alter their net extraction or elution.

Thus in conclusion, if required the baseline and pacing samples from an individual collection site could be combined when performing an analysis using the acylcarnitines or the aqueous metabolites from the control cohort.

Table 3.3.6: Summary of the most significant results from the metabolomic analysis of the control cohort during baseline and pacing. Differences between the groups statistically analysed using either two-tailed Student's t-test, Mann-Whitney U-test or Wilcoxon Signed-Rank test. Statistical significance was defined as a p-value<0.05.

Control cohort			
Trans-Cardiac gradient (Cardiac metabolism)			
	Aortic root	**Coronary sinus**	**p value**
Baseline			
Glutamate	2.58 (2.08 - 2.97)	1.52 (1.29 - 1.89)	<0.001
KIle	6.59 (5.86 - 7.91)	5.46 (4.07 - 6.99)	0.004
KLeu	10.77 (8.77 -	8.92 (6.33 - 11.03)	0.02
KVal	2.70 (2.19 - 3.26)	1.92 (1.44 - 2.62)	<0.0001
Pyruvate	0.31 (0.24 - 0.40)	0.25 (0.16 - 0.33)	0.02
Succinate	0.55 (0.43 - 0.64)	0.77 (0.54 - 0.90)	<0.0001
Pacing			
Glutamate	2.73 (2.23 - 3.34)	2.13 (1.81 - 2.68)	<0.0001
KVal	2.73 (2.27 - 1.41)	2.04 (1.41 - 2.37)	0.0001

Pyruvate	0.29 (0.26 - 0.38)	0.24 (0.17 - 0.31)	0.02
Succinate	0.55 (0.43 - 0.63)	0.72 (0.53 - 0.87)	0.02

Aorto-Femoral gradient (Peripheral metabolism)

	Aortic root	**Femoral vein**	
Baseline			
Alanine	0.72 (0.62 - 1.03)	0.93 (0.80 - 1.24)	0.0005
Arginine	2.33 (2.06 - 2.83)	2.70 (2.30 - 3.26)	0.005
Citrulline	46.24 (33.99 -	58.49 (41.12 - 74.24)	0.04
Glutamate	2.58 (2.08 - 2.97)	1.10 (0.86 - 1.42)	<0.0001
Lysine	0.27 (0.23 - 0.31)	0.30 (0.25 - 0.33)	0.04
Succinate	0.55 (0.43 - 0.64)	0.63 (0.53 - 0.89)	0.0007
Pacing			
Alanine	0.72 (0.58 - 0.85)	0.98 (0.78 - 1.23)	<0.0001
Citrulline	45.70 (35.05 -	61.47 (47.75 - 74.81)	0.002
Fumarate	0.09 (0.05 - 0.16)	0.06 (0.05 - 0.09)	0.03
Glutamate	2.73 (2.23 - 3.34)	1.14 (0.85 - 1.32)	<0.0001
Methionine	61.47 (51.07 -	67.40 (59.18 - 85.30)	0.01
Succinate	0.55 (0.43 - 0.64)	0.68 (0.52 - 0.77)	0.03
Threonine	0.29 (0.27 - 0.35)	0.35 (0.29 - 0.39)	0.01

Trans-Cardiac gradient (Baseline vs Pacing)

	Baseline	**Pacing**	
Glutamate	1.15 (0.61 - 1.39)	0.86 (0.39 - 1.09)	0.046

Values shown are median (quartiles 1 to 3) concentrations of the respective metabolites. Concentrations are presented as area ratio after normalisation to the internal standards.

4 METABOLOMIC RESULTS FROM THE DISCOVERY COHORT

This chapter details the metabolomic analysis performed for HCM and aortic stenosis patients from the discovery cohort. The detailed demographic and clinical characteristics of these patients are provided in Chapter 3. A total of 35 HCM and 36 aortic stenosis patients from the discovery cohort were included in the final metabolomic analysis. This was done using the analytical strategy devised from the analysis of the control cohort as described in Section 3.3. The strategy focused on a detailed analysis of acylcarnitines and aqueous metabolites during the baseline and pacing states and then to assess for differences in the cardiac metabolism between the two states. The analysis of the HCM cohort is described first and is detailed in the following section.

4.1 Metabolomics in the HCM cohort

The metabolome of the HCM cohort was assessed using the analytical strategy described in Section 3.3 and was divided into two main sections: acylcarnitines and aqueous metabolites. These metabolites were analysed in the following manner:

a) To assess for differences separately at baseline and during pacing between two individual collection sites.
b) To assess for differences between the baseline and pacing states in individual collection sites

c) To assess for differences in the cardiac metabolism between the baseline and pacing states.

4.1.1 Acylcarnitine profile of the HCM cohort

4.1.1.1 Baseline

a) All three-collection sites combined

Samples from all three-collection sites were analysed in combination using the unsupervised multivariate approach (PCA analysis). This was to assess if acylcarnitines could discriminate between the collection sites. As seen in figure 4.1.1 (plot A) no separation was exhibited between the three-collection sites on the PCA scores plot. This was followed by the PLS-DA analysis, using which no model could be built either. Thus samples collected from the three-collection sites could not be discriminated using the acylcarnitines.

b) Aortic root vs coronary sinus

The acylcarnitines were assessed in an unbiased manner in baseline samples collected from the aortic root and coronary sinus. This was performed using the PCA approach, which demonstrated no separation between the two-collection sites as seen on the scores plot in figure 4.1.1 (plot B). On supervised multivariate testing using the PLS-DA approach, no model could be built either. Thus acylcarnitines were unable to discriminate between the aortic root and coronary sinus samples collected from HCM patients at baseline.

c) Aortic root vs femoral vein

The acylcarnitine profile between the aortic root and femoral vein samples was assessed using the PCA approach, which showed no separation between the two-collection sites (figure 4.1.1, plot C). This was further evaluated using the PLS-DA approach, using which no model could be built either. Thus the aortic root and femoral vein samples collected at baseline could not be discriminated using the acylcarnitines.

d) Femoral vein vs coronary sinus

A general overview of the acylcarnitine distribution between the femoral vein and coronary sinus samples was obtained using the PCA analysis. This showed no separation between the two sites (figure 4.1.1, plot D) and was confirmed using the PLS-DA approach where no model could be built either. Thus the baseline femoral vein and coronary sinus samples from the HCM cohort could not be discriminated using acylcarnitines.

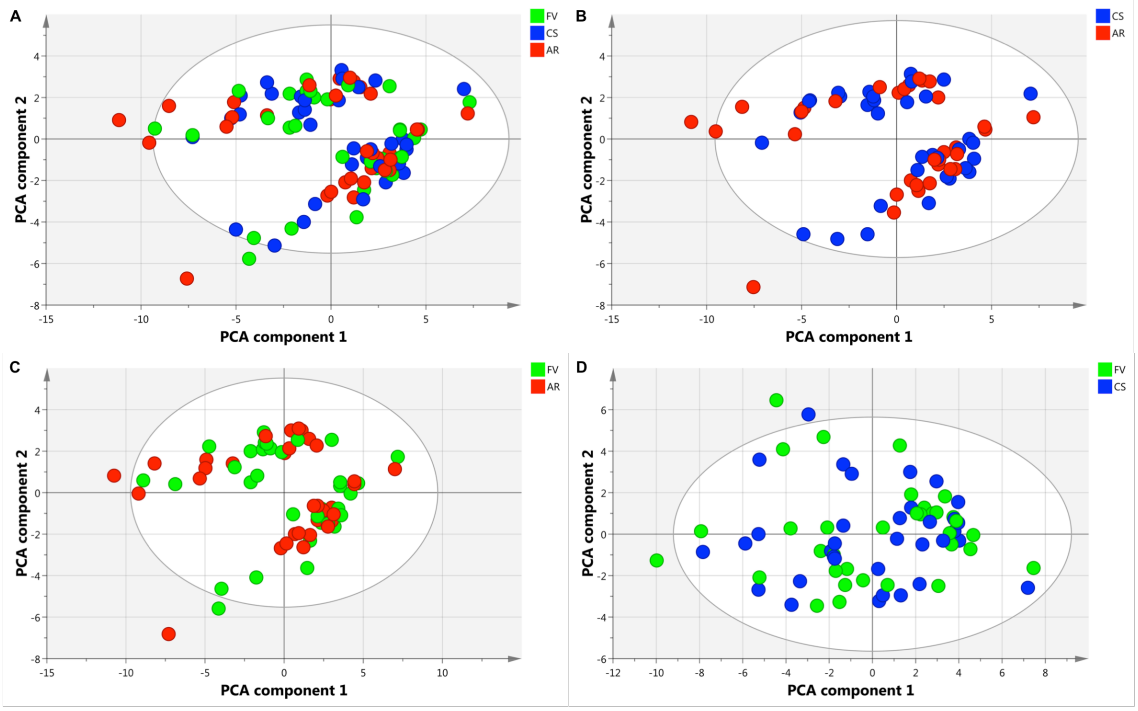

Figure 4.1.1: Principal component analysis (PCA) scores plot of acylcarnitines between all the collection sites combined together (A), AR vs CS (B), AR vs FV (C) and FV vs CS (D); analysis performed in the HCM cohort at baseline. AR: aortic root (red circle); CS: coronary sinus (blue circle); FV: femoral vein (green circle).

Conclusions from the analysis of acylcarnitines at baseline

Similar to the control cohort, the acylcarnitines were unable to discriminate the samples collected from the three-collection sites of the HCM cohort. This indicated no significant difference in acylcarnitine concentration between the three-collection sites. As discussed before in Section 3.3.1 similar findings have been reported in patients with underlying coronary artery and valvular heart disease undergoing coronary artery bypass surgery, but there are no reports of similar findings in patients with HCM.[285]

A higher concentration of acylcarnitines in HCM patients as compared to controls and hypertensives has been previously reported. Acylcarnitine levels in these patients were measured only in the peripheral blood samples, and thus no information regarding the arterial-venous gradient could be provided.[303,304] Also Shah *et al* reported changes in concentration of acylcarnitines post alcohol septal ablation in peripheral and coronary sinus samples, but again no arterial samples were collected during this study. [305] Thus in summary presence of no arterial-venous gradient of acylcarnitines in HCM patients is being reported for the first time. As discussed before in section 3.3.1, this is possible because acylcarnitines are long-lived species.

4.1.1.2 Pacing

a) All three-collection sites combined

Analysis of acylcarnitines between all three-collection sites during pacing was performed in an unbiased manner using the PCA approach. This exhibited no separation between the three-collection sites as seen on the PCA scores plot in figure 4.1.2 (plot A). This was verified with supervised multivariate analysis using the PLS-DA approach, where no model could be built either. Thus samples collected during pacing from the three-collection sites could not be discriminated using acylcarnitines.

b) Aortic root vs coronary sinus

Unsupervised multivariate analysis of acylcarnitines between the aortic root and coronary sinus collection sites was performed using the PCA approach, which demonstrated no separation (figure 4.1.2, plot B). This was verified using the PLS-DA approach, where no model could be built either. Thus aortic root and coronary sinus samples collected during pacing could not be discriminated using acylcarnitines.

c) Aortic root vs femoral vein

PCA analysis of acylcarnitines was performed between the aortic root and femoral vein samples, to provide a general overview of their distribution. This did not exhibit any separation between the two-collection sites as seen on the PCA scores plot in figure 4.1.2 (plot C). The PLS-DA analysis was then performed to verify these results, and using this approach no model could be built either. Thus acylcarnitines could not discriminate between the aortic root and femoral vein samples collected from the HCM cohort during pacing.

d) Femoral vein vs coronary sinus

PCA analysis of acylcarnitines demonstrated no separation between the femoral vein and coronary sinus collection sites as seen on the scores plot in figure 4.1.2 (plot D). On further supervised multivariate testing using the PLS-DA approach a weak model was built (R^2X=0.48, R^2Y=0.20, Q^2=−0.11). Clear separation was not visualised between the two-collection sites on its scores plot. The validity and goodness of fit of the original model were assessed using 100 random permutations. This demonstrated majority of permuted R^2 and Q^2 values on the left to be higher or equal than the original values on the right (intercepts: R^2=[0.0,0.20], Q^2=[0.0,−0.14]). This was indicative of the original model not being valid. A further independent assessment of the most discriminating metabolites (VIP score ≥1) using univariate analysis demonstrated that none of them were present in significantly different concentrations between the two-collection sites (C16-OH, C16:1 and C20:1).

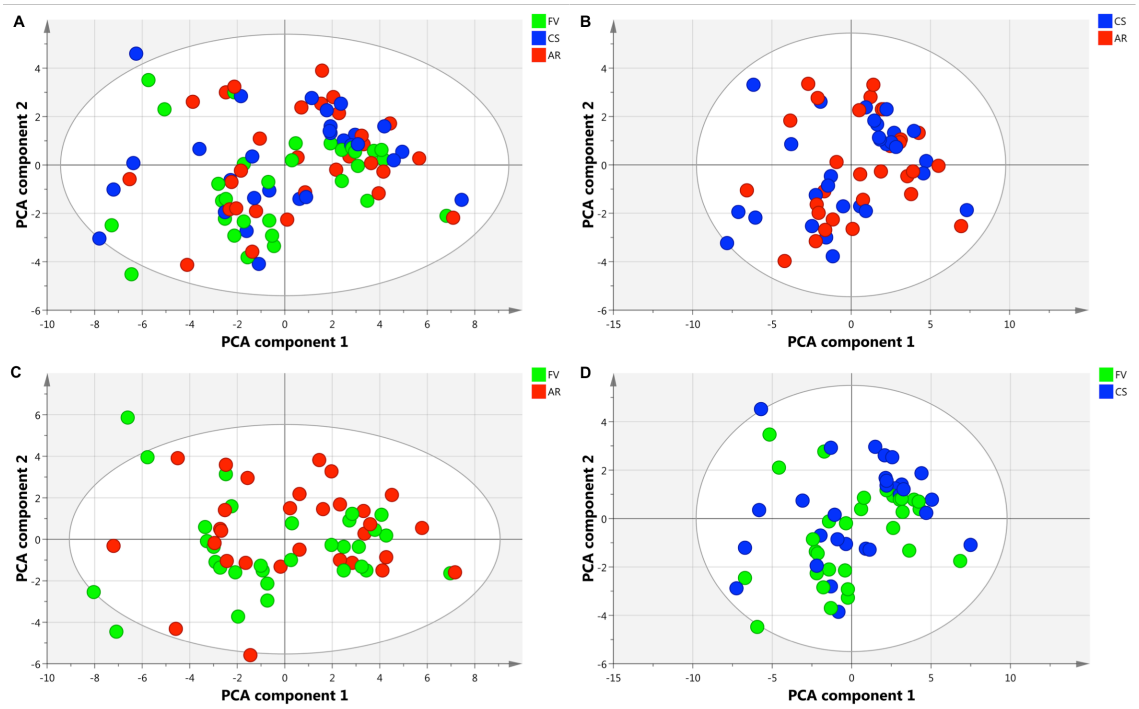

Figure 4.1.2: Principal component analysis (PCA) scores plot of acylcarnitines between all the collection sites combined together (A), AR vs CS (B), AR vs FV (C) and FV vs CS (D); analysis performed in the HCM cohort during pacing. AR: aortic root (red circle); CS: coronary sinus (blue circle); FV: femoral vein (green circle).

Conclusions from the analysis of acylcarnitines during pacing

The analysis of pacing samples from all three-collection sites demonstrated that they could not be discriminated using the acylcarnitines. This was indicative of no difference in their concentration between the three-collection sites. As discussed in Section 3.3.1 and 4.1.1.1, acylcarnitines are long-lived species with no significant difference measured in their concentration between samples collected from different sites in the body within a short interval of time.

4.1.1.3 Baseline vs pacing

a) Femoral vein

Femoral vein samples were analysed using unsupervised multivariate analysis to provide a general overview of acylcarnitine distribution between the baseline and pacing states. Analysis was performed using the PCA method, which exhibited no separation between the two states as seen on the scores plot in figure 4.1.3 (plot A). These findings were verified using the PLS-DA approach, where no model could be built either. Thus baseline and pacing samples collected from the femoral vein could not be discriminated using the acylcarnitines.

b) Coronary sinus

Multivariate analysis (PCA and PLS-DA) of acylcarnitines between baseline and pacing states in the coronary sinus samples demonstrated that they could not discriminate between the two states. This is visualised on the PCA scores plot in figure 4.1.3 (plot B), where no separation was exhibited between samples collected during the two states from the coronary sinus of patients with HCM.

c) Aortic root

Aortic root samples collected during the baseline and pacing states where analysed using multivariate analysis. Initial PCA analysis demonstrated no separation between the two states as exhibited on the scores plot in figure 4.1.3 (plot C). Further conformation of this was obtained using the PLS-DA approach, where no model could be built either. Thus baseline and pacing samples collected from the aortic root could not be discriminated using the acylcarnitines.

d) All three-collection sites combined

PCA analysis was performed to provide an unbiased overview of the acylcarnitine distribution between the baseline and pacing states in samples combined from all three sites. This exhibited no separation between the two states as visualised on the PCA scores plot in figure 4.1.3 (plot D). On further supervised multivariate testing using the PLS-DA approach, a weak model was built (R^2X=0.43, R^2Y=0.08, Q^2=−0.02). The validity and goodness of fit of the original model were assessed by using a 100 random permutations; this demonstrated that the majority of permuted R^2 and Q^2 values on the left were higher or equal than the original values on the right (intercepts: R^2=[0.0,0.07], Q^2=[0.0,−0.09]). This was indicative of the original model not being valid. This was further independently verified using univariate testing, where none of the

most discriminating acylcarnitines (VIP score ≥1) (C8, C10 and C12:1) were present in a significantly different concentration between the two states.

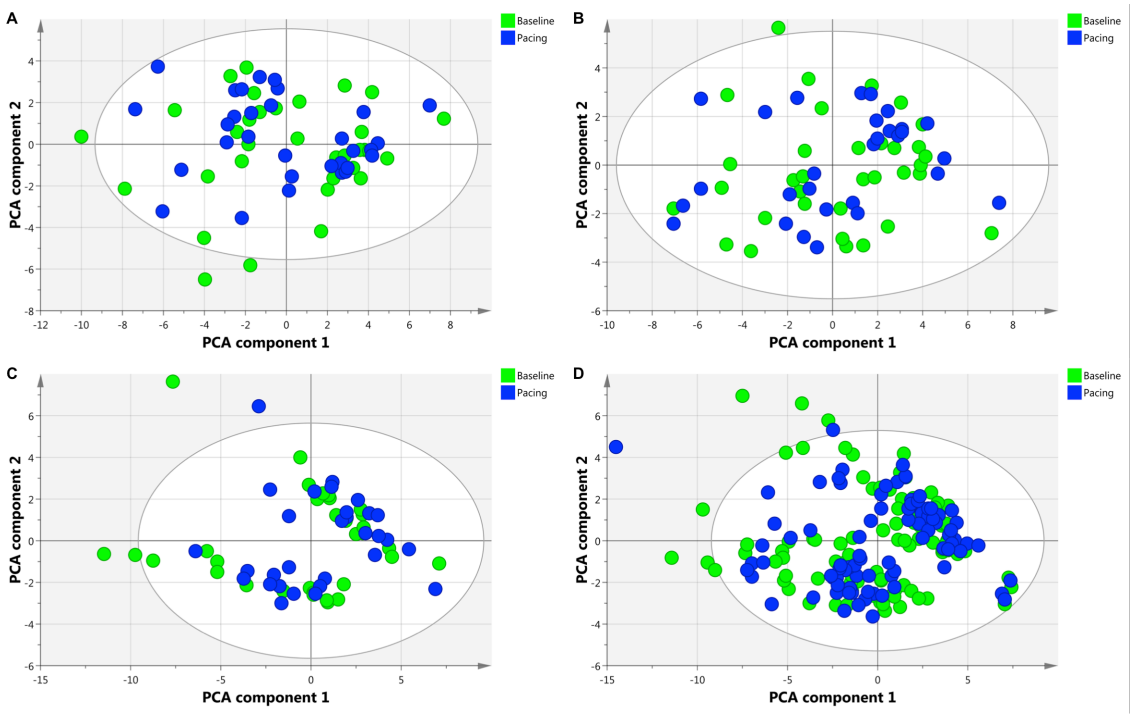

Figure 4.1.3: Principal component analysis (PCA) scores plot of acylcarnitines between baseline (green circles) and pacing (blue circles) states, in the femoral vein (A), coronary sinus (B), aortic root (C) and in all the collection sites combined together (D); analysis performed in the HCM cohort.

Conclusions from the analysis of acylcarnitines between baseline and pacing states

Analysis of acylcarnitines in samples from all three-collection sites in HCM patients demonstrated no difference in their concentration between the baseline and pacing states. In previous work reported by Shah *et al* the concentration of acylcarnitines including C2, C3, C4-OH, C10 and C14:1-OH/C12:1-

DC, changed in the peripheral plasma samples collected from HCM patients post alcohol septal ablation.[305] The lack of such a difference in the concentration of acylcarnitines between baseline and pacing states in our study is possibly explained by the lower intensity of myocardial stress induced by pacing, as compared to alcohol septal ablation.

4.1.2 Aqueous metabolite analysis of the HCM cohort

4.1.2.1 Baseline

a) All three-collection sites combined

PCA analysis was performed on the samples from all three-collection sites to gain a general overview of the aqueous metabolite distribution at baseline in the HCM patients. This unbiased multivariate analytical approach exhibited only small separation between the three-collection sites. To obtain a more reliable statistical analysis, PLS-DA method was used for supervised multivariate testing. A weak model was built, which demonstrated some separation between the three-collection sites as visualised on the PLS-DA scores plot in figure 4.1.4 (plot A) (R^2X=0.27, R^2Y=0.30, Q^2=0.10). To assess the validity and goodness of fit of the original model a 100 random permutations were used, which found the majority of permuted R^2 and Q^2 values on the left to be lower than the original values on the right (intercepts: R^2=[0.0,0.07], Q^2=[0.0,−0.11]). This indicated that the original model was valid. The most discriminating metabolites (VIP score ≥1) were then independently assessed using ANOVA with an appropriate post-test correction (Bonferroni's) for multiple comparisons (table 4.1.1).

The concentrations of alanine, arginine, glycine, malate and pyruvate were significantly higher in the femoral vein, while that of glutamate was higher in the aortic root. The concentration of succinate was highest in the coronary sinus. These differences were then further analysed in pair wise analysis of the collection sites (aortic root vs coronary sinus / aortic root vs femoral vein) to determine the differences between cardiac and peripheral metabolism.

b) Aortic root vs coronary sinus

Aortic root and coronary sinus samples collected at baseline were analysed using the PCA analysis to obtain a general overview of the aqueous metabolite distribution. This demonstrated some separation between the two-collection sites and was further assessed using the PLS-DA approach. This generated a weak model with some separation between the two sites as visualised on its scores plot in figure 4.1.4 (plot B) (R^2X=0.36, R^2Y=0.35, Q^2=−0.11). The validity and goodness of fit of the original model were confirmed by using 100 random permutations (intercepts: R^2=[0.0,0.23], Q^2=[0.0,−0.10]).

The results of multivariate analysis were then independently verified by assessing the most discriminating metabolites (VIP score ≥1) using either the two-tailed Student's t-test or the Mann-Whitney U-test. This demonstrated a significantly higher concentration of glutamate in the aortic root, while malate, 3-hydroxy butyric acid (3OBHA) and succinate were present in a significantly lower concentration (table 4.1.2). Thus it was observed that while there was a net extraction of glutamate, there was a net elution of malate, 3OBHA and succinate by the heart in HCM patients at baseline.

c) Aortic root vs femoral vein

PCA analysis of the aqueous metabolites was performed between the aortic root and femoral vein samples, which showed clear separation between the two-collection sites. This was verified using the PLS-DA approach, where a robust model was built differentiating the samples from the two-collection sites as seen on its scores plot in figure 4.1.4 (plot C) (R^2X=0.36, R^2Y=0.79, Q^2=0.49). The validity and goodness of fit of the original model were confirmed by using 100 random permutations (intercepts: R^2=[0.0,0.38], Q^2=[0.0,−0.36]).

Univariate analysis of the most discriminating metabolites (VIP score ≥1) was then performed using either the two-tailed Student's t-test or the Mann-Whitney U-test. This indicated that while there was an extraction of only glutamate (present in a significantly lower concentration in the femoral vein), there was an elution of a whole series of metabolites including aconitate, alanine, arginine, citrulline, malate, methionine, pyruvate and succinate, (present in a significantly higher concentration in the femoral vein) (table 4.1.2).

d) Femoral vein vs coronary sinus

A clear separation between the femoral vein and coronary sinus collection sites was exhibited on the PCA scores plot built analysing the aqueous metabolites in samples from the two-collection sites. PLS-DA analysis confirmed these findings where a robust model was formed, with clear separation seen between the two sites on its scores plot (figure 4.1.4, plot D) (R^2X=0.47, R^2Y=0.71, Q^2=0.42). The validity and goodness of fit of the original model were confirmed by using 100 random permutations (intercepts: R^2=[0.0,0.29], Q^2=[0.0,−0.28]).

Table 4.1.4 shows the list of metabolites, which were most discriminating on PLS-DA analysis (VIP score ≥1) and were found to be present in significantly different concentrations on independent univariate testing between the two-

collection sites. While there was a notably higher concentration of alanine, arginine, glycine, KVal and pyruvate in the femoral vein, the concentration of fumarate and glutamate was significantly lower.

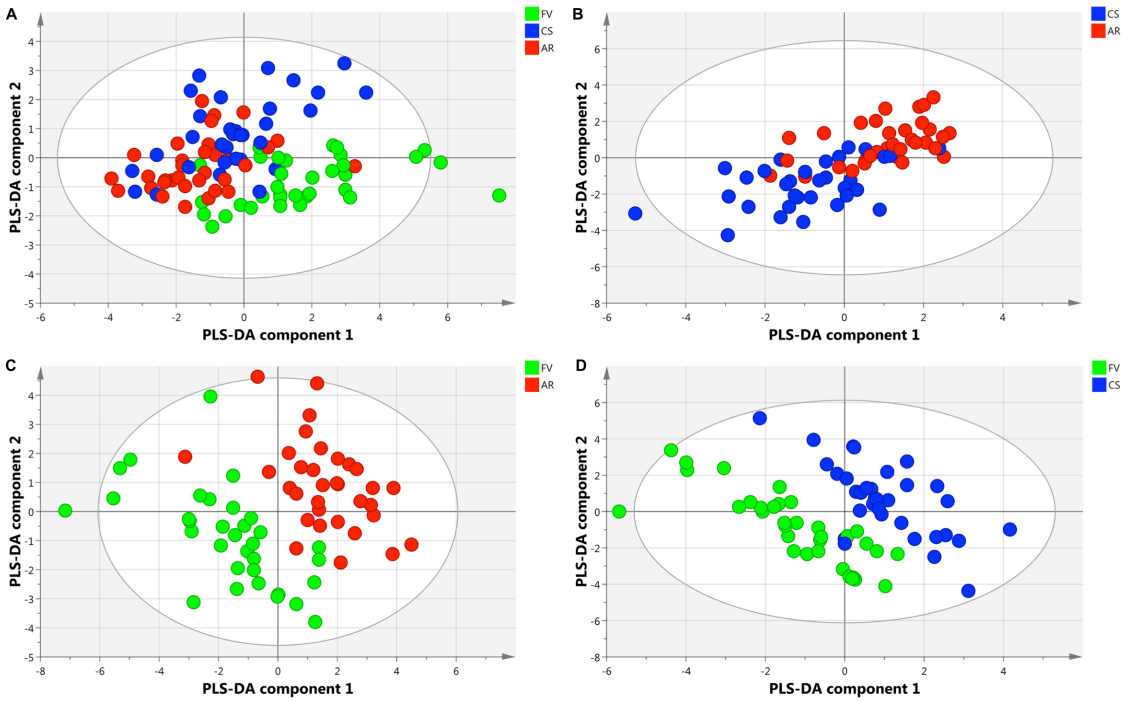

Figure 4.1.4: Partial least squares- discriminant analysis (PLS-DA) scores plot of aqueous metabolites between all the collection sites combined together (A), AR vs CS (B), AR vs FV (C) and FV vs CS (D); analysis performed in the HCM cohort at baseline. AR: aortic root (red circle); CS: coronary sinus (blue circle); FV: femoral vein (green circle).

Table 4.1.1: Concentration of aqueous metabolites which were significantly different on analysis between the femoral vein, coronary sinus and aortic root samples, in the HCM cohort at baseline. Differences between the groups statistically analysed using ANOVA with Bonferroni's post-test for multiple comparisons. In comparing aortic root with coronary sinus: * represents p<0.05, ** p<0.01, *** p<0.001 and **** p<0.0001. In comparing aortic root vs femoral vein: $^{\#}$ represents p<0.05, $^{\#\#}$ p<0.01, $^{\#\#\#}$

p<0.001 and #### p<0.0001. In comparing femoral vein vs coronary sinus: ^ represents p<0.05, ^^ p<0.01, ^^^ p<0.001 and ^^^^ p<0.0001. Metabolites listed in alphabetical order.

Metabolite	Femoral vein	Coronary sinus	Aortic root
Alanine	0.99 (0.79 - 1.11)^^^^	0.73 (0.64 - 0.89)	0.68 (0.59 - 0.82)####
Arginine	2.82 (2.44 - 3.42)^^	2.45 (2.15 - 2.89)	2.42 (2.11 - 2.66)###
Glycine	0.0032 (0.0030 - 0.0040)^^^^	0.0027 (0.0020 - 0.0030)	0.0030 (0.0020 - 0.0035)
Glutamate	0.99 (0.88 - 1.19)^^^^	1.39 (1.07 - 1.88)	2.45 (1.85 - 2.94)****####
Malate	1.86 (1.41 - 2.18)	1.50 (1.12 - 2.07)	1.25 (0.95 - 1.62)*###
Pyruvate	0.32 (0.25 - 0.35)^^	0.23 (0.18 - 0.29)	0.23 (0.19 - 0.29)##
Succinate	0.58 (0.49 - 0.72)	0.63 (0.54 - 0.76)	0.45 (0.39 - 0.54)***####

Values shown are median (quartiles 1 to 3) concentrations of the respective metabolites. Concentrations are presented as area ratio after normalisation to the internal standards.

Table 4.1.2: Concentration of aqueous metabolites which were significantly different on a pair wise analysis between the aortic root and coronary sinus, aortic root and femoral vein, and femoral vein and coronary sinus, in the HCM cohort at baseline. Differences between the groups statistically analysed using either two-tailed Student's t-test or Mann-Whitney U-test. Statistical significance was defined as a p-value<0.05. Metabolites listed in alphabetical order.

Metabolite	Aortic root	Coronary sinus	p value

Glutamate	2.45 (1.85 - 2.94)	1.39 (1.07 - 1.88)	<0.0001
Malate	1.25 (0.95 - 1.62)	1.50 (1.12 - 2.07)	0.03
3OBHA	0.40 (0.34 - 0.52)	0.52 (0.39 - 0.72)	0.01
Succinate	0.45 (0.39 - 0.54)	0.63 (0.54 - 0.76)	0.0002

Metabolite	Aortic root	Femoral vein	p value
Aconitate	0.31 (0.27 - 0.39)	0.39 (0.29 - 0.51)	0.02
Alanine	0.68 (0.59 - 0.82)	0.99 (0.79 - 1.11)	<0.0001
Arginine	2.42 (2.11 - 2.66)	2.82 (2.44 - 3.42)	0.0006
Citrulline	41.7 (31.0 - 50.5)	55.9 (45.1 - 72.1)	0.001
Glutamate	2.45 (1.85 - 2.94)	0.99 (0.88 - 1.19)	<0.0001
Malate	1.25 (0.95 - 1.62)	1.86 (1.41 - 2.18)	0.0001
Methionine	59.9 (47.5 - 76.7)	70.9 (52.8 - 89.8)	0.03
Pyruvate	0.23 (0.19 - 0.29)	0.32 (0.25 - 0.35)	0.002
Succinate	0.45 (0.39 - 0.54)	0.58 (0.49 - 0.72)	<0.0001

Metabolite	Femoral vein	Coronary sinus	p value
Alanine	0.99 (0.79 - 1.11)	0.73 (0.64 - 0.89)	<0.0001
Arginine	2.82 (2.44 - 3.42)	2.45 (2.15 - 2.89)	0.002
Fumarate	0.06 (0.03 - 0.08)	0.07 (0.04 - 0.16)	0.02
Glutamate	0.99 (0.88 - 1.19)	1.39 (1.07 - 1.88)	<0.0001
Glycine	0.0032 (0.0030 - 0.0040)	0.0027 (0.0020 - 0.0030)	<0.0001

KVal	2.56 (2.16 - 3.19)	2.25 (1.82 - 2.66)	0.02
Pyruvate	0.32 (0.25 - 0.35)	0.23 (0.18 - 0.29)	0.002

Values shown are median (quartiles 1 to 3) concentrations of the respective metabolites. Concentrations are presented as area ratio after normalisation to the internal standards.

Conclusions from the analysis of aqueous metabolite at baseline

The cardiac and peripheral metabolism of HCM patients was different at baseline. There were differences observed between the degree of extraction or elution of various metabolite, which are detailed bellow:

1) Alanine, glutamate and succinate: the extraction of glutamate and the elution of succinate was common to both central and peripheral metabolism. There was elution of alanine during peripheral metabolism, with a significantly higher concentration present in the femoral vein as compared to the aortic root. Reports of similar findings in previous human studies and the role of these metabolites in amino acid and carbohydrate metabolism have been discussed in Section 3.3.2. In the work published by Lewis *et al* a relative change in the concentration of alanine and glutamate was reported in the coronary sinus and femoral vein of HCM patients post alcohol septal ablation, but they did not describe net extraction or elution of these metabolites as they had not collected arterial samples.[294]

2) Malate: it was eluted during cardiac and peripheral metabolism, with a significantly higher concentration in the coronary sinus and femoral vein. The

metabolism of malate, which plays a vital role in the citric acid cycle, has been discussed in detail in Chapter 8.[164]

3) Aconitate, arginine citrulline, methionine, and pyruvate: they were all present in a significantly higher concentration in the femoral vein, implying net elution during peripheral metabolism.

4.1.2.2 Pacing

a) All three-collection sites combined

Aqueous metabolites in the pacing samples from all three-collection sites were first assessed using unsupervised multivariate analytical approach. This exhibited some separation between the three collection-sites, and was verified by supervised multivariate testing. The PLS-DA analytical approach was used and a robust model was built which demonstrated clear separation between the three-collection sites as seen on the scores plot in figure 4.1.5 (plot A) (R^2X=0.30, R^2Y=0.38, Q^2=0.22). The validity and goodness of fit of the original model were confirmed by using 100 random permutations, where all the permuted values were lower as compared to original values (intercepts: R^2=[0.0,0.08], Q^2=[0.0,−0.20]).

ANOVA analysis was then performed to independently validate the discriminating ability of the most significant metabolites (VIP score ≥1). As described in table 4.1.3, several metabolites were present in significantly different concentrations between the three-collection sites. The concentration of glutamate was significantly higher in the aortic root, while that of alanine, arginine, citrulline, malate and methionine was significantly higher in the femoral

vein. Following this a detailed pair wise analysis of the individual collection sites was performed to assess for differences between the cardiac and peripheral metabolism.

b) Aortic root vs coronary sinus

Unsupervised multivariate analytical approach using the PCA method was employed to obtain a general overview of the aqueous metabolite profile between the aortic root and coronary sinus samples collected during pacing. This did not show a clear separation between the two-collection sites. Supervised multivariate testing was then performed using the PLS-DA approach. A weak model was built, which did discriminate the two-collection sites as visualised in its scores plot in figure 4.1.5 (plot B) (R^2X=0.31, R^2Y=0.50, Q^2=0.05).

The validity and degree of over fit of the original model were assessed by using 100 random permutations, which demonstrated that the majority of the permuted R^2 and Q^2 values on the left to be lower than the original values on the right (intercepts: R^2=[0.0,0.31], Q^2=[0.0,−0.16]). This was indicative of a valid original model and the most discriminating metabolites (VIP score ≥1) from it were further independently assessed using either the two-tailed Student's t-test or the Mann-Whitney U-test. This demonstrated glutamate, KLeu and succinate were present in significantly different concentrations between the aortic root and coronary sinus (Table 4.1.4). Further assessment indicated that while there was a net extraction of glutamate and KLeu, there was a net elution of succinate in the heart during pacing.

c) Aortic root vs femoral vein

The aortic root and femoral vein samples collected during pacing in HCM patients were then assessed using multivariate and univariate analytical approach. The presence of separation between the two sites as seen on the PCA scores plot, was further assessed using the PLS-DA analysis. This demonstrated a clear separation between the two-collection sites on the scores plot of a robust PLS-DA model (figure 4.1.5, plot C) (R^2X=0.39, R^2Y=0.88, Q^2=0.65). The models validity and goodness of fit were confirmed by using 100 random permutations (intercepts: R^2=[0.0,0.39], Q^2=[0.0,−0.39]).

Further independent validation of the results obtained from multivariate analysis was performed using either the two-tailed Student's t-test or the Mann-Whitney U-test. This demonstrated a lower concentration of glutamate, and a higher concentration of alanine, aconitate, arginine, citrulline, malate, methionine, phenylalanine, pyruvate, succinate and threonine in the femoral vein samples of the HCM cohort during pacing (table 4.1.4). These measurements were indicative of a net extraction of glutamate, and a net elution of alanine, aconitate, arginine, citrulline, malate, methionine, phenylalanine, pyruvate, succinate and threonine.

d) Femoral vein vs coronary sinus

The femoral vein and coronary sinus samples were last to be assessed and were found to discriminate using the aqueous metabolites when analysed in an unbiased fashion employing the PCA analytical method. This was confirmed using the PLS-DA approach where a strong model was generated, with clear separation between the two sites visualised on its scores plot (figure 4.1.5, plot D) (R^2X=0.34, R^2Y=0.77, Q^2=0.56). The validity and goodness of fit of the

original model were confirmed by using 100 random permutations (intercepts: R^2=[0.0,0.27], Q^2=[0.0,−0.21]).

Further assessment of the most discriminating metabolites (VIP score ≥1) using either the two-tailed Student's t-test or the Mann-Whitney U-test demonstrated that alanine, arginine, citrulline, glutamate, glutamine, KLeu, KVal, leucine and phenylalanine were present in significantly different concentrations between the two sites (table 4.1.4).

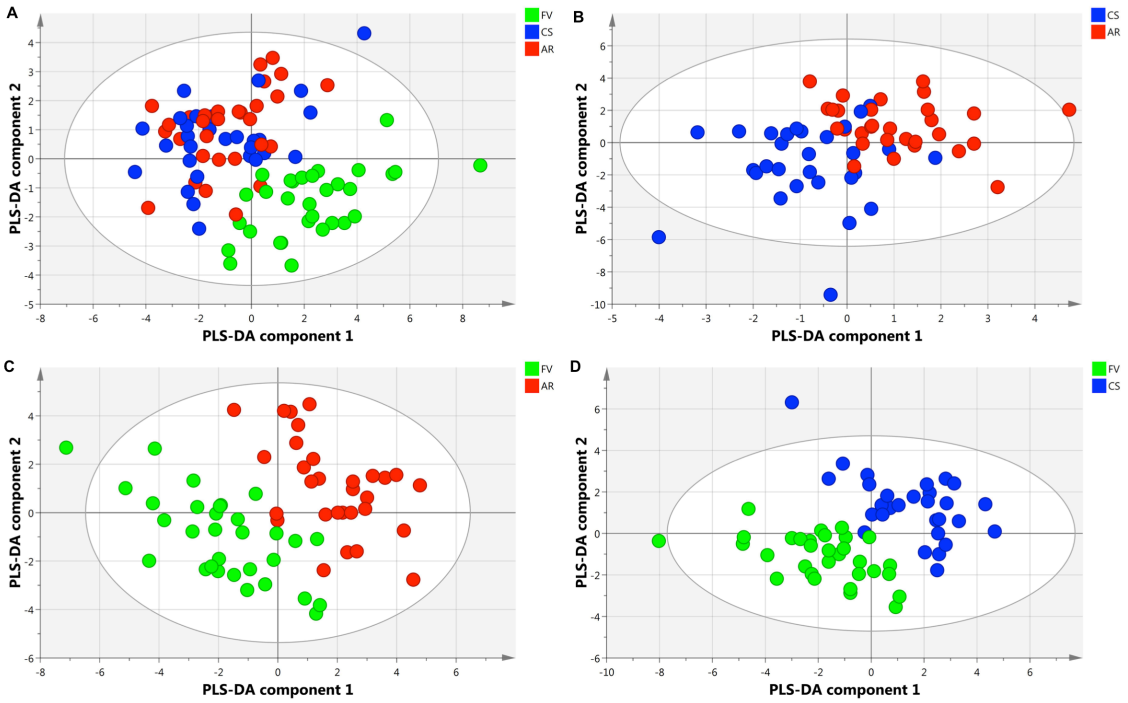

Figure 4.1.5: Partial least squares- discriminant analysis (PLS-DA) scores plot of aqueous metabolites between all the collection sites combined together (A), AR vs CS (B), AR vs FV (C) and FV vs CS (D); analysis performed in the HCM cohort during pacing. AR: aortic root (red circle); CS: coronary sinus (blue circle); FV: femoral vein (green circle).

Table 4.1.3: Concentration of aqueous metabolites which were significantly different on analysis between the femoral vein, coronary

sinus and aortic root samples, in the HCM cohort during pacing. Differences between the groups statistically analysed using ANOVA with Bonferroni's post-test for multiple comparisons. In comparing aortic root with coronary sinus: * represents p<0.05, ** p<0.01, *** p<0.001 and **** p<0.0001. In comparing aortic root vs femoral vein: # represents p<0.05, ## p<0.01, ### p<0.001 and #### p<0.0001. In comparing femoral vein vs coronary sinus: ^ represents p<0.05, ^^ p<0.01, ^^^ p<0.001 and ^^^^ p<0.0001. Metabolites listed in alphabetical order.

Metabolite	Femoral vein	Coronary sinus	Aortic root
Alanine	0.96 (0.85 - 1.09)^^^^	0.69 (0.59 - 0.82)	0.66 (0.59 - 0.82)####
Arginine	2.79 (2.57 - 3.21)^^^	2.43 (2.13 - 2.69)	2.59 (2.24 - 2.89)#
Citrulline	64.82 (41.91 - 79.80)^^^	42.85 (33.89 - 51.45)	40.91 (33.32 - 46.97)####
Glutamate	0.92 (0.80 - 1.05)^^^^	1.99 (1.49 - 2.56)	2.78 (2.16 - 3.10)***####
Malate	1.76 (1.45 - 2.19)	1.34 (1.01 - 1.78)	1.23 (0.92 - 1.64)####
Methionine	71.85 (59.69 - 88.66)	53.87 (46.77 - 70.99)	58.85 (53.73 - 69.17)##

Values shown are median (quartiles 1 to 3) concentrations of the respective metabolites. Concentrations are presented as area ratio after normalisation to the internal standards.

Table 4.1.4: Concentration of aqueous metabolites which were significantly different on a pair wise analysis between the aortic root and coronary sinus, aortic root and femoral vein, and femoral vein and coronary sinus, in the HCM cohort during pacing. Differences between the groups statistically analysed using either two-tailed Student's t-test or

Mann-Whitney U-test. Statistical significance was defined as a p-value<0.05. Metabolites listed in alphabetical order.

Metabolite	Aortic root	Coronary sinus	p value
Glutamate	2.78 (2.16 - 3.10)	1.99 (1.49 - 2.56)	0.0004
KLeu	10.12 (8.01 - 12.70)	8.71 (6.68 - 10.26)	0.04
Succinate	0.47 (0.41 - 0.64)	0.64 (0.51 - 0.87)	0.009

Metabolite	Aortic root	Femoral vein	p value
Aconitate	0.32 (0.27 - 0.39)	0.43 (0.32 - 0.49)	0.003
Alanine	0.66 (0.59 - 0.82)	0.96 (0.85 - 1.09)	<0.0001
Arginine	2.59 (2.24 - 2.89)	2.79 (2.57 - 3.21)	0.02
Citrulline	40.91 (33.32 - 46.97)	64.82 (41.91 - 79.80)	<0.0001
Glutamate	2.78 (2.16 - 3.10)	0.92 (0.80 - 1.05)	<0.0001
Malate	1.23 (0.92 - 1.64)	1.76 (1.45 - 2.19)	<0.0001
Methionine	58.85 (53.73 - 69.17)	71.85 (59.69 - 88.66)	0.003
Phenylalanine	1.63 (1.44 - 1.77)	1.83 (1.59 - 1.99)	0.02
Pyruvate	0.24 (0.18 - 0.33)	0.33 (0.24 - 0.39)	0.009
Succinate	0.47 (0.41 - 0.64)	0.66 (0.53 - 0.79)	0.0004
Threonine	0.29 (0.25 - 0.33)	0.33 (0.29 - 0.38)	0.009

Metabolite	Femoral vein	Coronary sinus	p value

Alanine	0.96 (0.85 - 1.09)	0.69 (0.59 - 0.82)	<0.0001
Arginine	2.79 (2.57 - 3.21)	2.43 (2.13 - 2.69)	0.0007
Citrulline	64.82 (41.91 - 79.80)	42.85 (33.89 - 51.45)	0.0005
Glutamate	0.92 (0.80 - 1.05)	1.99 (1.49 - 2.56)	<0.0001
Glutamine	13.5 (12.9 - 14.1)	12.9 (12.4 - 13.5)	0.02
Leucine	2.79 (2.44 - 3.16)	2.54 (2.08 - 2.82)	0.01
KLeu	11.09 (9.09 - 13.51)	8.71 (6.68 - 10.26)	0.001
KVal	2.68 (2.38 - 3.12)	2.18 (1.59 - 2.39)	0.0004
Phenylalanine	1.83 (1.59 - 1.99)	1.53 (1.32 - 1.72)	0.003

Values shown are median (quartiles 1 to 3) concentrations of the respective metabolites. Concentrations are presented as area ratio after normalisation to the internal standards.

Conclusions from the analysis of aqueous metabolite during pacing

From the analysis and results described above certain differences were noted between the cardiac and peripheral metabolism which are detailed below:

1) Glutamate: it was extracted during cardiac and peripheral metabolism, which was higher peripherally. This is possible as a result of a higher rate of metabolism in the lower limbs, which have a much larger muscle mass than the heart.

   In previous work by Lewis *et al* it was reported that the median percent change in the concentration of glutamate from baseline to post alcohol septal ablation was lower in the femoral vein as compared to the coronary sinus of HCM patients.[294] A similar assessment was performed in our HCM cohort, and the median percent change of glutamate from baseline to pacing

was similarly found to be significantly lower in the femoral vein as compared to the coronary sinus (0.11 vs 44.1, p=0.0002).

2) Alanine: there was a net elution of alanine during peripheral metabolism, which was not observed during cardiac metabolism. Like glutamate, the median percent change in the concentration of alanine between baseline and pacing states in the femoral vein samples was assessed. Similar findings as reported by Lewis *et al* were observed, with a fall in the concentration of alanine in the femoral vein during pacing (median percentage change from baseline: −2.8%, 0.98 vs 0.91).[294]
3) Succinate: it was eluted during cardiac and peripheral metabolism, with no difference between the two.
4) KLeu: it was extracted during cardiac metabolism, this was not observed during peripheral metabolism. This has been discussed further in Chapter 8.
5) Aconitate, arginine, citrulline, malate, methionine, phenylalanine, pyruvate, and threonine: they were all eluted during peripheral metabolism, with a significantly higher concentration in the femoral vein.

4.1.2.3 Baseline vs pacing

a) Femoral vein

The femoral vein samples were assessed using PCA approach to obtain a general overview of any differences in the aqueous metabolites between the baseline and pacing states. This demonstrated no separation between the two states as seen on the PCA scores plot in figure 4.1.6 (plot A). This was validated using the PLS-DA approach, where no model differentiating the two

sites could be built. Thus baseline and pacing samples collected from the femoral vein could not be discriminated using the aqueous metabolites.

b) Coronary sinus

Unsupervised multivariate analysis using the PCA approach was performed on the coronary sinus samples, to view if there was any separation between the baseline and pacing states using the aqueous metabolites. As shown in the scores plot in figure 4.1.6 (plot B), there was no separation between the two states. A very weak model was built using the PLS-DA approach (R^2X=0.38, R^2Y=0.31, Q^2=−0.09), which failed validation using 100 random permutations (intercepts: R^2=[0.0,0.23], Q^2=[0.0,−0.16]). Further independent analysis of the most discriminating metabolites (VIP score ≥1) using either the two-tailed Student's t-test or the Wilcoxon Signed-Rank test found no significant difference in their concentration between the baseline and pacing states. This confirmed that aqueous metabolites could not discriminate between the baseline and pacing states in samples collected from the coronary sinus.

c) Aortic root

Samples from the aortic root collected at baseline and during pacing were analysed to assess for any differences in the concentration of aqueous metabolites between the two states. The initial multivariate testing using the PCA approach exhibited no separation between the two states (figure 4.1.6, plot C). This was confirmed on supervised multivariate testing using the PLS-DA method, where no model discriminating the two states could be built. Thus the samples collected from the aortic root at baseline and during pacing could not be discriminated using the aqueous metabolites.

d) All three-collection sites combined

The final analysis was done combining samples from all three-collection sites, and assessing if there were differences in the concentration of aqueous metabolites between the baseline and pacing states. The PCA analysis exhibited no separation between the two states as seen on the scores plot in figure 4.1.6 (plot D). On further supervised testing using the PLS-DA approach a very weak model was built (R^2X=0.19, R^2Y=0.05, Q^2=−0.001), which failed validation using 100 random permutations (intercepts: R^2=[0.0,0.05], Q^2=[0.0,−0.04]). Further assessment of the most discriminating metabolites was performed using ANOVA, which found no difference in their concentration between the baseline and pacing states.

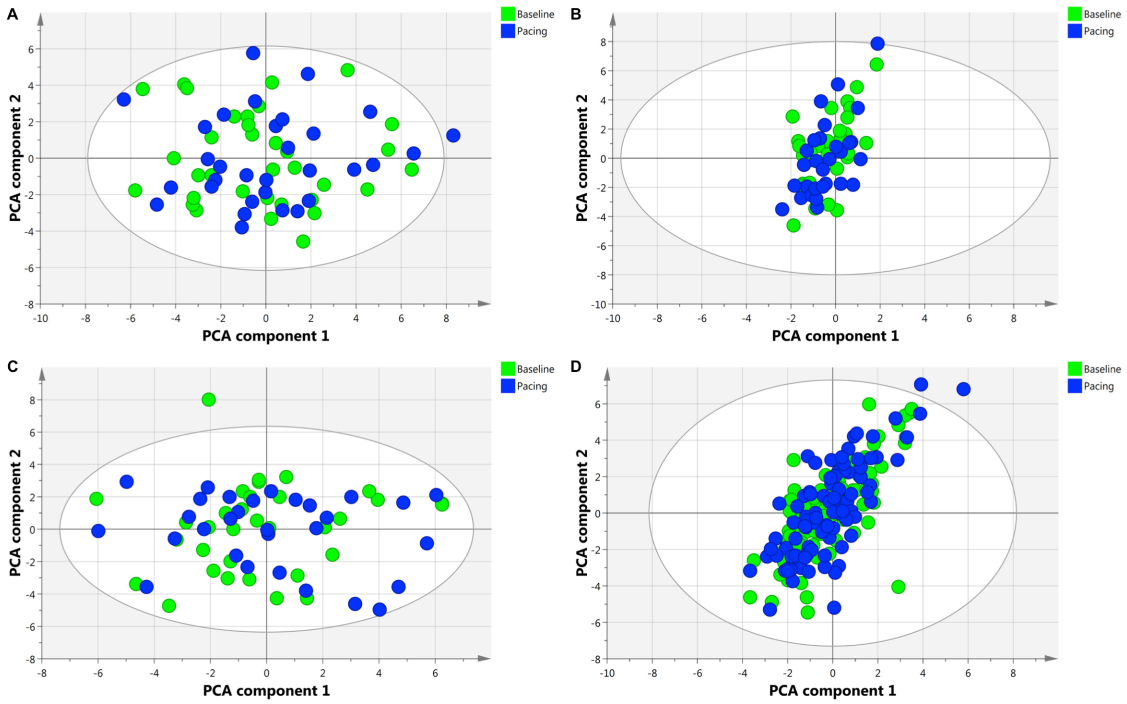

Figure 4.1.6: Principal component analysis (PCA) scores plot of aqueous metabolites between baseline (green circles) and pacing (blue circles) states, in the femoral vein (A), coronary sinus (B), aortic root (C) and in all

the collection sites combined together (D); analysis performed in the HCM cohort.

Conclusions from the analysis of aqueous metabolites between baseline and pacing states

Aqueous metabolites were found to be non-discriminating and present in concentrations which were not-significantly different between the baseline and pacing states when assessed in samples from individual collection sites. In work reported by Lewis *et al*, hypoxanthine, inosine, malic acid and glutamate showed at least a 1.3-fold enrichment in the coronary sinus at 10 minutes post alcohol septal ablation in HCM patients.[294] The lack of such difference in our samples is possibly explained by the lower intensity of myocardial stress induced by pacing, as compared to alcohol septal ablation which was used as a model of planned myocardial infarction by Lewis *et al*.[294]

4.1.2.3.1 Cardiac metabolism (baseline vs pacing)

Table 4.1.5 details the differences in cardiac metabolism between the baseline and pacing states, in the HCM cohort. The most significant differences were as follows:

1) KLeu: it was eluted at baseline, which switched to extraction during pacing.

2) Citrulline and malate: they were both eluted at baseline, which switched to extraction of malate and a fall in the elution of citrulline during pacing.

3) Isocitrate: it was eluted at baseline, which switched to extraction during pacing.

This change in the metabolism of KLeu, citrulline, malate and isocitrate reflects the overall change in the activity of metabolic pathways regulating the energy production in the myocardium, and these changes have been discussed in Chapter 8.

As discussed previously the extraction or elution of the above-described metabolites could be influenced by the increased coronary blood flow during pacing. A tendency towards increased extraction or decreased elution of the metabolites during pacing may occur while the underlying net flux remains unchanged, which is compensated by the increased blood flow. As we do not have previous literature in HCM patients and are limited by the lack of coronary sinus blood flow measurements, the direct interpretation of extraction and elution values as changes in the underlying net flux should be done cautiously.

Table 4.1.5: Trans-cardiac gradient (aortic root – coronary sinus) of selected aqueous metabolites measured within individual patients in the HCM cohort, and compared between baseline and pacing. Differences between the groups statistically analysed using either two-tailed Student's t-test or Wilcoxon Signed-Rank test. Statistical significance was defined as a p-value<0.05. Metabolites listed in alphabetical order.

Metabolite	Baseline	Pacing	p value
Alanine	−0.04 (−0.13 - 0.04)	−0.02 (−0.09 - 0.05)	0.99

BAIBA	0.0 (−0.0004 - 0.0004)	0.0 (−0.0005 - 0.0003)	0.89
Citrulline	−9.63 (−21.63 - −2.49)	−1.64 (−9.99 - 11.45)	0.04
Glutamate	0.89 (0.65 - 1.15)	0.67 (0.35 - 0.80)	0.13
Isocitrate	−0.66 (−2.67 - 0.69)	0.30 (−0.78 - 1.70)	0.02
KLeu	−0.84 (−1.79 - 1.89)	1.19 (−0.09 - 3.56)	0.04
KVal	0.51 (−0.28 - 0.74)	0.69 (−0.08 - 1.22)	0.09
Malate	−0.39 (−0.63 - −0.07)	0.001 (−0.29 - 0.32)	0.04
Succinate	−0.21 (−0.33 - −0.09)	−0.10 (−0.34 - 0.05)	0.57

Values shown are median (quartiles 1 to 3) concentrations of the respective metabolites. Concentrations are presented as area ratio after normalisation to the internal standards.

4.1.2.4 Overall summary

As seen with the metabolism of the control cohort, no differences were found in the concentration of metabolites between the baseline and pacing states when samples collected from individual collection sites were assessed in the HCM cohort too. Similarly there were differences observed in the concentration of certain aqueous metabolites when assessment was performed between any two-collection sites, which possibly resulted from the net extraction or elution of these respective metabolites (table 4.1.6). Differences were also observed in the cardiac metabolism between the baseline and pacing states, which was likely due to the myocardial stress induced by pacing.

Table 4.1.6: Summary of the most significant results from the metabolomic analysis of the HCM cohort during baseline and pacing.

Differences between the groups statistically analysed using either two-tailed Student's t-test, Mann-Whitney U-test or Wilcoxon Signed-Rank test. Statistical significance was defined as a p-value<0.05.

HCM cohort			
Trans-Cardiac gradient (Cardiac metabolism)			
	Aortic root	**Coronary sinus**	**p value**
Baseline			
Glutamate	2.45 (1.85 - 2.94)	1.39 (1.07 - 1.88)	<0.0001
Malate	1.25 (0.95 - 1.62)	1.50 (1.12 - 2.07)	0.03
3OBHA	0.40 (0.34 - 0.52)	0.52 (0.39 - 0.72)	0.01
Succinate	0.45 (0.39 - 0.54)	0.63 (0.54 - 0.76)	0.0002
Pacing			
Glutamate	2.78 (2.16 - 3.10)	1.99 (1.49 - 2.56)	0.0004
KLeu	10.12 (8.01 - 12.70)	8.71 (6.68 - 10.26)	0.04
Succinate	0.47 (0.41 - 0.64)	0.64 (0.51 - 0.87)	0.009
Aorto-Femoral gradient (Peripheral metabolism)			
	Aortic root	**Femoral vein**	
Baseline			
Aconitate	0.31 (0.27 - 0.39)	0.39 (0.29 - 0.51)	0.02
Alanine	0.68 (0.59 - 0.82)	0.99 (0.79 - 1.11)	<0.0001
Arginine	2.42 (2.11 - 2.66)	2.82 (2.44 - 3.42)	0.0006
Citrulline	41.7 (31.0 - 50.5)	55.9 (45.1 - 72.1)	0.001
Glutamate	2.45 (1.85 - 2.94)	0.99 (0.88 - 1.19)	<0.0001
Malate	1.25 (0.95 - 1.62)	1.86 (1.41 - 2.18)	0.0001
Methionine	59.9 (47.5 - 76.7)	70.9 (52.8 - 89.8)	0.03

Pyruvate	0.23 (0.19 - 0.29)	0.32 (0.25 - 0.35)	0.002
Succinate	0.45 (0.39 - 0.54)	0.58 (0.49 - 0.72)	<0.0001
Pacing			
Aconitate	0.32 (0.27 - 0.39)	0.43 (0.32 - 0.49)	0.003
Alanine	0.66 (0.59 - 0.82)	0.96 (0.85 - 1.09)	<0.0001
Arginine	2.59 (2.24 - 2.89)	2.79 (2.57 - 3.21)	0.02
Citrulline	40.91 (33.32 - 46.97)	64.82 (41.91 - 79.80)	<0.0001
Glutamate	2.78 (2.16 - 3.10)	0.92 (0.80 - 1.05)	<0.0001
Malate	1.23 (0.92 - 1.64)	1.76 (1.45 - 2.19)	<0.0001
Methionine	58.85 (53.73 - 69.17)	71.85 (59.69 - 88.66)	0.003
Phenylalanine	1.63 (1.44 - 1.77)	1.83 (1.59 - 1.99)	0.02
Pyruvate	0.24 (0.18 - 0.33)	0.33 (0.24 - 0.39)	0.009
Succinate	0.47 (0.41 - 0.64)	0.66 (0.53 - 0.79)	0.0004
Threonine	0.29 (0.25 - 0.33)	0.33 (0.29 - 0.38)	0.009

Trans-Cardiac gradient (Baseline vs Pacing)

	Baseline	**Pacing**	
Citrulline	−9.63 (−21.63 - −2.49)	−1.64 (−9.99 - 11.45)	0.04
Isocitrate	−0.66 (−2.67 - 0.69)	0.30 (−0.78 - 1.70)	0.02
KLeu	−0.84 (−1.79 - 1.89)	1.19 (−0.09 - 3.56)	0.04
Malate	−0.39 (−0.63 - −0.07)	0.001 (−0.29 - 0.32)	0.04

Values shown are median (quartiles 1 to 3) concentrations of the respective metabolites. Concentrations are presented as area ratio after normalisation to the internal standards.

4.2 Metabolomics in the aortic stenosis cohort

Metabolomic analysis in the aortic stenosis cohort was performed following similar analytical strategy as used for controls and HCM cohorts described in Section 3.3. The acylcarnitines and aqueous metabolites were analysed, separately during the baseline and pacing states and then for any differences between the two states. Clinical characteristics and demographics of the aortic stenosis cohort are described in detail in Chapter 3. A total of 36 aortic stenosis patients from the discovery cohort were included in the final metabolomics analysis.

4.2.1 Acylcarnitine profile of the aortic stenosis cohort

4.2.1.1 Baseline

a) All three-collection sites combined

Following the analytical strategy described above the metabolites in the aortic stenosis cohort were analysed, starting with acylcarnitines. Samples from all three-collection sites were analysed using the PCA method to obtain a general overview of acylcarnitine distribution and assess if there was any separation between them. The PCA scores plot did not show any separation between the three-collection sites (figure 4.2.1, plot A). On further supervised multivariate testing using the PLS-DA approach no model could be built either. Thus it was confirmed that samples from the three-collection sites could not be discriminated using the acylcarnitines.

b) Aortic root vs coronary sinus

Analysis of acylcarnitines between the aortic root and coronary sinus collection sites was performed using unsupervised multivariate testing approach. Unbiased overview of the samples using the PCA approach showed no separation between the two-collection sites as seen on its scores plot in figure 4.2.1 (plot B). This was confirmed using the PLS-DA approach, where using supervised multivariate testing no model able to discriminate the two sites could be built either.

c) Aortic root vs femoral vein

PCA analysis of the acylcarnitines between aortic root and femoral vein samples was performed to assess for any separation between the two-collection sites. The resultant PCA scores plot did not exhibit any separation between the two-collection sites (figure 4.2.1, plot C). Supervised multivariate analysis using the PLS-DA approach was then used, and no model could be built either. This indicated the inability of acylcarnitines to discriminate between the aortic root and femoral vein samples in the aortic stenosis cohort at baseline.

d) Femoral vein vs coronary sinus

Femoral vein and coronary sinus samples were analysed using the multivariate analysis. The initial unbiased overview of the samples using PCA analysis, exhibited no separation between the two-collection sites using the acylcarnitines (figure 4.2.1, plot D). This was further validated using the PLS-DA approach, where no model could be built either. Thus the baseline samples from the femoral vein and coronary sinus could not be discriminated using the acylcarnitines.

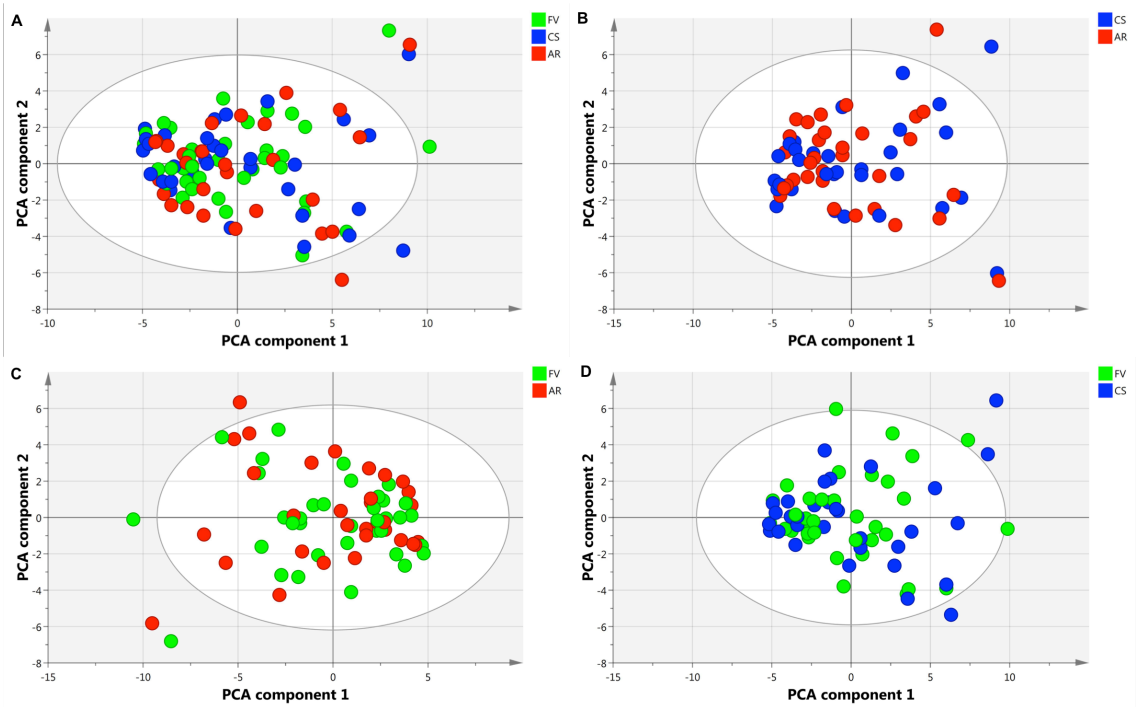

Figure 4.2.1: Principal component analysis (PCA) scores plot of acylcarnitines between all the collection sites combined together (A), AR vs CS (B), AR vs FV (C) and FV vs CS (D); analysis performed in the aortic stenosis cohort at baseline. AR: aortic root (red circle); CS: coronary sinus (blue circle); FV: femoral vein (green circle).

Conclusions from the analysis of acylcarnitines at baseline

As described in the results above, the acylcarnitines could not discriminate between the baseline samples from the three-collection sites. This was indicative of there being no significant difference in their concentration between the three-collection sites. As described for the control and HCM cohorts, these results are explained by the acylcarnitines being long-lived species, which do not get rapidly metabolised. Thus no difference was observed in their concentration if samples were collected from different sites in the body within a short period of time.

Turer *et al* have reported similar findings, where a subset of their study population undergoing coronary artery bypass surgery were patients with aortic stenosis. Though they have not provided data separately for the aortic stenosis subgroup, they reported no difference between the arterial and coronary sinus concentration of acylcarnitines in the entire study cohort at baseline.[285]

4.2.1.2 Pacing

a) All three-collection sites combined

Multivariate analysis of the acylcarnitines was performed between the three-collection sites in the aortic stenosis cohort during pacing. The initial unsupervised multivariate analysis using the PCA approach did not exhibit any separation between the three-collection sites as visualised on its scores plot in figure 4.2.2 (plot A). The samples were further assessed using the PLS-DA analytical method, using this supervised multivariate analytical approach no model could be built which could discriminate between the collection sites. Thus similar to the baseline results, the pacing samples from the three-collection sites could not be discriminated using the acylcarnitines.

b) Aortic root vs coronary sinus

PCA analysis of acylcarnitines was performed between the aortic root and coronary sinus samples to demonstrate if there was any separation between the two-collection sites. The analysis demonstrated no separation between the two-collection sites as seen on the PCA scores plot in figure 4.2.2 (plot B). This was further confirmed using the PLS-DA analytical approach, where no model

could be built either. Thus the samples from the two-collection sites could not be discriminated using the acylcarnitines.

c) Aortic root vs femoral vein

Multivariate analysis of the acylcarnitines was performed between the aortic root and femoral vein samples. The unsupervised PCA analytical approach did not exhibit any separation between the two-collection sites as seen on its scores plot in figure 4.2.2 (plot C). On further supervised multivariate analysis using the PLS-DA method, no model could be built either. Thus the samples from the two-collection sites could not be discriminated using the acylcarnitines.

d) Femoral vein vs coronary sinus

PCA analysis between the femoral vein and coronary sinus samples using the acylcarnitines did not exhibit any separation as seen on its scores plot in figure 4.2.2 (plot D). No model could be built either using the PLS-DA approach, thus indicating that the acylcarnitines could not discriminate between the pacing samples from the two-collection sites.

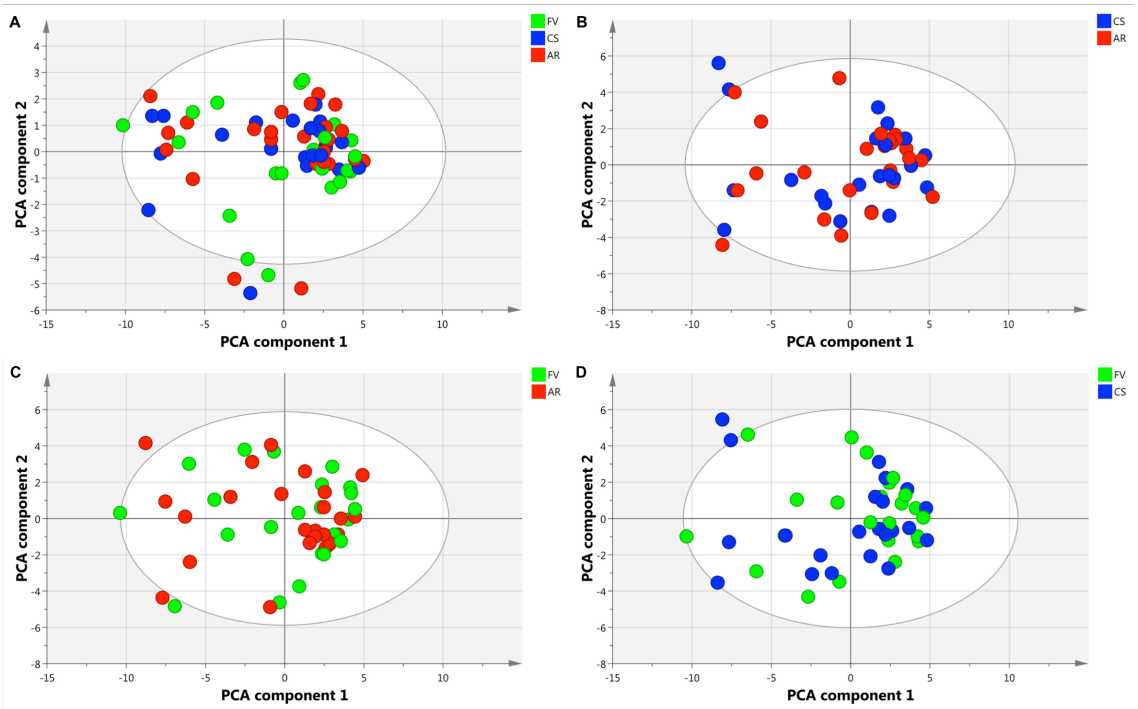

Figure 4.2.2: Principal component analysis (PCA) scores plot of acylcarnitines between all the collection sites combined together (A), AR vs CS (B), AR vs FV (C) and FV vs CS (D); analysis performed in the aortic stenosis cohort during pacing. AR: aortic root (red circle); CS: coronary sinus (blue circle); FV: femoral vein (green circle).

Conclusions from the analysis of acylcarnitines during pacing

The conclusion drawn from the above analysis was the inability of the acylcarnitines to discriminate between the samples obtained during pacing from the three-collection sites. This was suggestive of no significant difference in the concentration of acylcarnitines between the three-collection sites during pacing. A change in the trans-myocardial gradient (net elution) of acetyl-carnitine (C2) and β-hydroxybutyryl-carnitine (C4-OH) was reported by Turer *et al* post I/R in patients undergoing coronary artery bypass surgery.[285] As mentioned before a subset of these patients had aortic stenosis, but no separate results were reported for them. A lack of similar difference in the concentration of

acylcarnitines in our study is possibly explained by the lower intensity of myocardial stress induced by the brief duration of pacing, as compared to I/R in patients undergoing cardiac surgery.

4.2.1.3 Baseline vs pacing

a) Femoral vein

Unsupervised multivariate analysis using the PCA approach was performed on the femoral vein samples to obtain a general overview of the acylcarnitine distribution between the baseline and pacing states. The analysis did not show any separation between the two states as seen on the PCA scores plot in figure 4.2.3 (plot A). On further supervised multivariate testing using the PLS-DA approach no model could be built either. Thus the acylcarnitines could not discriminate between the baseline and pacing samples collected from the femoral vein.

b) Coronary sinus

The coronary sinus samples were assessed using the PCA method to obtain a visual overview of any separation if present between the baseline and pacing states, using the aqueous metabolites. The analysis demonstrated no separation between the two states as seen on the PCA scores plot in figure 4.2.3 (plot B). The samples were then assessed by supervised multivariate approach using the PLS-DA analytical method. The analysis did not result in any model being built, which suggested that the baseline and pacing samples collected from the coronary sinus could not be discriminated using the acylcarnitines.

c) Aortic root

As seen in the analysis of samples from the femoral vein and coronary sinus, no separation was seen between the baseline and pacing samples collected from the aortic root, when using the acylcarnitines to perform a PCA analysis. This is demonstrated on the PCA scores plot in figure 4.2.3 (plot C), where an overlap is visualised between baseline and pacing samples. PLS-DA analysis was then performed to verify these findings, using which no model could be built either. Thus the baseline and pacing samples from the aortic root could not be discriminated using the acylcarnitines.

d) All three-collection sites combined

The final analysis of the acylcarnitines was conducted combining all the samples to assess for any differences between the baseline and pacing states. The initial approach was using the PCA analysis, which demonstrated no separation as visualised on its scores plot in figure 4.2.3 (plot D). Further assessment was performed using the PLS-DA approach, where no model discriminating the two states could be built either. Thus the baseline and pacing samples from the three-collection sites combined together could not be discriminated using the acylcarnitines.

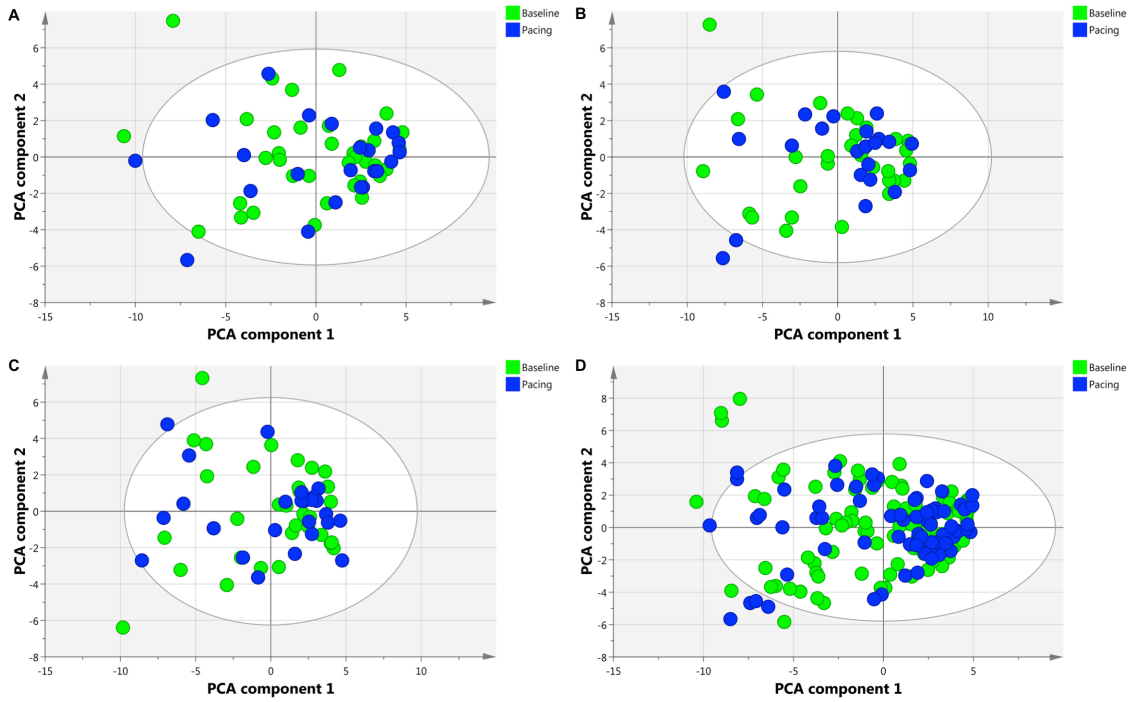

Figure 4.2.3: Principal component analysis (PCA) scores plot of acylcarnitines between baseline (green circles) and pacing (blue circles) states, in the femoral vein (A), coronary sinus (B), aortic root (C) and in all the collection sites combined together (D); analysis performed in the aortic stenosis cohort.

Conclusions from the analysis of acylcarnitines between baseline and pacing states

Thus as seen with the control and HCM cohorts, in the aortic stenosis cohort also there was no significant difference observed in the concentration of acylcarnitines either between the individual collection sites or the two physiological states (rest/stress). As discussed before in Section 4.2.1.2 the lack of difference in the concentration of acylcarnitines between the baseline and pacing states is possibly due to the small degree of myocardial stress induced by pacing, which is insufficient to significantly alter the acylcarnitine metabolism. While changes in acylcarnitine metabolism have been reported in patients (including aortic stenosis) undergoing cardiac surgery, there are no

previous human studies describing the cardiac and peripheral metabolism of acylcarnitines under near normal circumstances (coronary angiography) in patients with aortic stenosis.[285]

4.2.2 Aqueous metabolite analysis of the aortic stenosis cohort

4.2.2.1 Baseline

a) All three-collection sites combined

The samples from all three sites collected at baseline were analysed to determine for any differences in the concentration of aqueous metabolites between them. Initially the PCA analysis was performed to provide a general overview of aqueous metabolites distribution between the three-collection sites. The PCA scores plot did not show any clear separation between the three-collection sites. This was further assessed using the supervised multivariate analytical approach. By using the PLS-DA method a weak model was built, the scores plot from which showed some separation between the three-collection sites (figure 4.2.4, plot A) (R^2X=0.28, R^2Y=0.28, Q^2=0.12). The validity and degree of over fit of the original model were assessed by using 100 random permutations, which demonstrated that all the permuted R^2 and Q^2 values on the left were lower than the original values on the right (intercepts: R^2=[0.0,0.09], Q^2=[0.0,−0.17]). This indicated a valid original model and the most discriminating metabolites (VIP score ≥1) from this model were independently verified using ANOVA.

Analysis using ANOVA with an appropriate post-test correction (Bonferroni's) for multiple comparisons, demonstrated that glutamate and KVal were present

in significantly different concentrations between the three sites. While glutamate was present in a significantly higher concentration in the aortic root, the concentration of KVal was highest in the femoral vein (table 4.2.1). A detailed pair wise analysis of the collection sites was then performed to assess the cardiac and peripheral metabolism in the aortic stenosis cohort at baseline.

b) Aortic root vs coronary sinus

PCA analysis of the aqueous metabolites was performed between the aortic root and coronary sinus samples to assess for any discrimination between the two-collection sites. The resultant scores plot showed some separation and these results were verified using the supervised multivariate approach. The PLS-DA analysis built a model on whose scores plot clear clustering was seen between the two-collection sites as visualised in figure 4.2.4 (plot B) (R^2X=0.26, R^2Y=0.51, Q^2=0.04). The validity and goodness of fit of the original model were confirmed by using 100 random permutations (intercepts: R^2=[0.0,0.26], Q^2=[0.0,−0.18]).

The most discriminating metabolites (VIP score ≥1) on PLS-DA analysis were then further assessed using either the Student's t-test or the Mann-Whitney U-test. The concentrations of glutamate, KIle, KLeu and KVal were found to be significantly lower in the coronary sinus (table 4.2.2). These observations indicated a net extraction of these metabolites by the heart at baseline.

c) Aortic root vs femoral vein

The analyses of aqueous metabolites between the aortic root and femoral vein collection sites was done to assess the peripheral metabolism in the aortic stenosis cohort at baseline. The PCA analysis of the samples showed overlap between the two-collection sites. To further assess these results supervised

multivariate testing was performed using the PLS-DA method. This demonstrated a clear discrimination between the two-collection sites as visualised on the scores plot of the model built (figure 4.2.4, plot C) (R^2X=0.27, R^2Y=0.63, Q^2=0.20). The validity and goodness of fit of the original model were confirmed by using 100 random permutations (intercepts: R^2=[0.0,0.26], Q^2=[0.0,−0.20]). Further univariate analysis of the most discriminating metabolites (VIP score ≥1) demonstrated a significantly lower concentration of glutamate and a significantly higher concentration of alanine in the femoral vein. This was suggestive of net extraction of glutamate and net elution of alanine during the peripheral metabolism in the aortic stenosis cohort (table 4.2.2).

d) Femoral vein vs coronary sinus

PCA analysis of the aqueous metabolites between the femoral vein and coronary sinus collection sites exhibited minor separation between the two. To gain a more reliable statistical analysis further assessment using the PLS-DA approach was performed. The resultant model built demonstrated a clear separation between the two-collection sites as seen on its scores plot in figure 4.2.4 (plot D) (R^2X=0.30, R^2Y=0.52, Q^2=0.13). The validity and goodness of fit of the original model were confirmed using 100 random permutations, which showed that the majority of the permuted R^2 and Q^2 values were lower than the original values (intercepts: R^2=[0.0,0.27], Q^2=[0.0,−0.19]).

Univariate analysis of the most discriminating metabolites (VIP score ≥1) using either the Student's t-test or the Mann-Whitney U-test, found a significantly lower concentration of alanine, glutamate, histidine, KIle, KLeu, KVal, methionine and pyruvate in the coronary sinus (table 4.2.2).

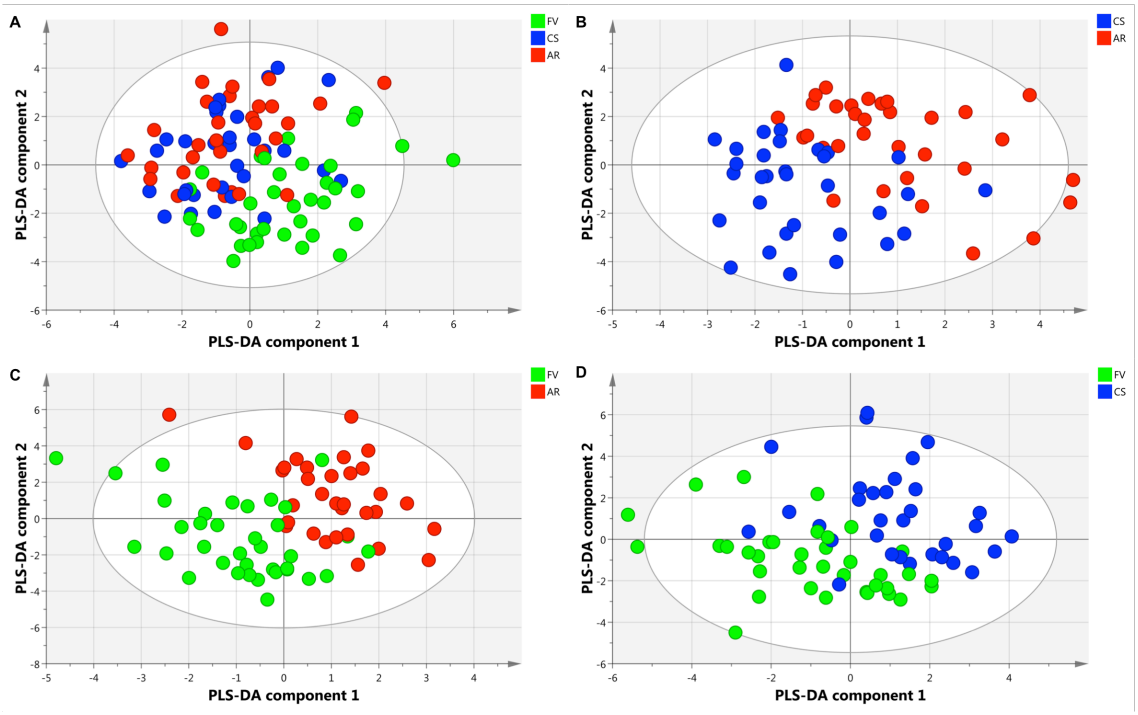

Figure 4.2.4: Partial least squares- discriminant analysis (PLS-DA) scores plot of aqueous metabolites between all the collection sites combined together (A), AR vs CS (B), AR vs FV (C) and FV vs CS (D); analysis performed in the aortic stenosis cohort at baseline. AR: aortic root (red circle); CS: coronary sinus (blue circle); FV: femoral vein (green circle).

Table 4.2.1: Concentration of aqueous metabolites which were significantly different on analysis between the femoral vein, coronary sinus and aortic root samples, in the aortic stenosis cohort at baseline. Differences between the groups statistically analysed using ANOVA with Bonferroni's post-test for multiple comparisons. In comparing aortic root with coronary sinus: * represents p<0.05, ** p<0.01, *** p<0.001 and **** p<0.0001. In comparing aortic root vs femoral vein: $^{\#}$ represents p<0.05, $^{\#\#}$ p<0.01, $^{\#\#\#}$ p<0.001 and $^{\#\#\#\#}$ p<0.0001. In comparing femoral vein vs coronary sinus: ^ represents p<0.05, ^^ p<0.01, ^^^ p<0.001 and ^^^^ p<0.0001. Metabolites listed in alphabetical order.

Metabolite	Femoral vein	Coronary sinus	Aortic root
Glutamate	1.11 (0.85 - 1.42)^^^	1.69 (1.25 - 2.29)	2.36 (1.85 - 2.85)***####
KVal	2.84 (2.24 - 3.79)^^^^	2.04 (1.72 - 2.46)	2.77 (2.29 - 4.01)****

Values shown are median (quartiles 1 to 3) concentrations of the respective metabolites. Concentrations are presented as area ratio after normalisation to the internal standards.

Table 4.2.2: Concentration of aqueous metabolites which were significantly different on a pair wise analysis between the aortic root and coronary sinus, aortic root and femoral vein, and femoral vein and coronary sinus, in the aortic stenosis cohort at baseline. Differences between the groups statistically analysed using either the Student's t-test or Mann-Whitney U-test. Statistical significance was defined as a p-value<0.05. Metabolites listed in alphabetical order.

Metabolite	Aortic root	Coronary sinus	p value
Glutamate	2.36 (1.85 - 2.85)	1.69 (1.25 - 2.29)	0.0002
KIle	6.08 (5.00 - 7.37)	4.85 (3.99 - 6.19)	0.04
KLeu	9.36 (7.08 - 12.68)	7.29 (5.90 - 9.38)	0.004
KVal	2.77 (2.29 - 4.01)	2.04 (1.72 - 2.46)	<0.0001

Metabolite	Aortic root	Femoral vein	p value

Alanine	0.86 (0.68 - 1.07)	0.98 (0.83 - 1.35)	0.04
Glutamate	2.36 (1.85 - 2.85)	1.11 (0.85 - 1.42)	<0.0001

Metabolite	Femoral vein	Coronary sinus	p value
Alanine	0.98 (0.83 - 1.35)	0.79 (0.65 - 1.24)	0.05
Glutamate	1.11 (0.85 - 1.42)	1.69 (1.25 - 2.29)	0.0005
Histidine	1.50 (1.32 - 1.75)	1.38 (1.20 - 1.56)	0.03
KIle	6.16 (4.83 - 7.64)	4.85 (3.99 - 6.19)	0.04
KLeu	9.67 (7.55 - 11.92)	7.29 (5.90 - 9.38)	0.02
KVal	2.84 (2.24 - 3.79)	2.04 (1.72 - 2.46)	<0.0001
Methionine	74.8 (62.7 - 83.9)	67.5 (53.4 - 82.4)	0.04
Pyruvate	0.37 (0.30 - 0.45)	0.27 (0.18 - 0.36)	0.002

Values shown are median (quartiles 1 to 3) concentrations of the respective metabolites. Concentrations are presented as area ratio after normalisation to the internal standards.

Conclusions from the analysis of aqueous metabolites at baseline

As described above there were differences in the cardiac and peripheral metabolism of certain metabolites at baseline. These differences are detailed below:

1) Glutamate: it was extracted during cardiac and peripheral metabolism, with a higher extraction during peripheral metabolism.
2) Alanine: it was eluted during the peripheral metabolism.

3) KIle, KLeu and KLeu: these BCAAs were extracted during the cardiac metabolism only.

The cardiac extraction of glutamate has been reported before in patients undergoing cardiac surgery by Turer *et al*.[285] A subset of their study population was patients with aortic stenosis, for which they did not report the result separately. The role of glutamate and alanine in linking the amino acid and carbohydrate metabolism via the alanine/cahill cycle has been discussed before in Section 3.3.2.3.1. The higher extraction of glutamate in peripheral metabolism is possibly explained by the larger muscle mass of lower limbs as compared to the cardiac muscle, which have a proportionally larger requirement for the metabolic fuels.

The role of BCAAs in cardiac metabolism has been discussed in Chapter 8.

4.2.2.2 Pacing

a) All three-collection sites combined

A detailed multivariate and univariate analysis was done for aqueous metabolites in samples collected from all three-collection sites during pacing. Unsupervised multivariate testing was performed using the PCA approach to gain a general overview of the aqueous metabolites distribution between the three-collection sites. The resultant scores plot showed an overlap between the three-collection sites. Further assessment was performed using the PLS-DA approach, where the scores plot of the generated model exhibited a clear separation between the three-collection sites (figure 4.2.5 [plot A]) (R^2X=0.32, R^2Y=0.31, Q^2=0.11). The validity and goodness of fit of the original model were

confirmed by using 100 random permutations, where all the permuted R^2 and Q^2 values on the left were lower than original values on the right (intercepts: R^2=[0.0,0.10], Q^2=[0.0,−0.17]).

Independent validation of the most discriminating metabolites (VIP score ≥1) on multivariate testing was performed using ANOVA. Only glutamate was present in significantly different concentrations between the three sites (table 4.2.3). The concentration of glutamate was significantly higher in the aortic root. A further pair wise analysis was then performed between the collection sites to assess the cardiac and peripheral metabolism.

b) Aortic root vs coronary sinus

The first pair to be analysed was the aortic root and coronary sinus, which would reflect the cardiac metabolism of aortic stenosis patients during pacing. The initial unsupervised multivariate testing using the PCA approach did not show any separation between the two-collection sites. Further assessment was performed using the PLS-DA approach, where distinct clusters were visualised on the scores plot of the generated model (figure 4.2.5, plot B) (R^2X=0.23, R^2Y=0.55, Q^2=−0.11). The weak original model performed poorly when compared to 100 random permutations (intercepts: R^2=[0.0,0.37], Q^2=[0.0,−0.15]).

On further univariate analysis of the most discriminating metabolites (VIP score ≥1) β-aminoisobutyric acid (BAIBA) and KVal were found to be present in a significantly higher concentration in the aortic root as compared to the coronary sinus. This was suggestive of a possible net extraction of BAIBA and KVal by the heart (table 4.2.4).

c) Aortic root vs femoral vein

Aortic root and femoral vein samples were initially assessed using the PCA analytical method, which demonstrated no separation between the two-collection sites. Further assessment using the PLS-DA analytical approach built a robust model, where a clear separation was exhibited between the two-collection sites as seen on its scores plot (figure 4.2.5, plot C) (R^2X=0.32, R^2Y=0.75, Q^2=0.49). The validity and goodness of fit of the original model were confirmed by using 100 random permutations (intercepts: R^2=[0.0,0.30], Q^2=[0.0,−0.21]).

Univariate analysis of the most discriminating metabolites (VIP score ≥1) using either the two-tailed Student's t-test or the Mann-Whitney U-test, demonstrated alanine and glutamate to be present in significantly different concentrations between the two sites. These results indicated that while glutamate was extracted, alanine was eluted during the peripheral metabolism.

d) Femoral vein vs coronary sinus

The last of the pair wise analysis was between the femoral vein and coronary sinus to understand the difference in concentration of metabolites post cardiac and peripheral metabolism. The scores plot from PCA analysis did not exhibit a clear separation between the two-collection sites. Supervised multivariate testing using the PLS-DA approach built a model, on whose scores plot the two-collection sites formed distinct clusters (figure 4.2.5, plot D) (R^2X=0.36, R^2Y=0.61, Q^2=−0.21). The validity and goodness of fit of the original model were confirmed using 100 random permutations. This demonstrated the majority of the permuted R^2 and Q^2 values on the left to be lower than the original values on the right (intercepts: R^2=[0.0,0.32], Q^2=[0.0,−0.19]). This

indicated a valid original model from which the most discriminating metabolites (VIP score ≥1) were then selected to be independently assessed using univariate testing. The analysis was performed using either the Student's t-test or the Mann-Whitney U-test, and demonstrated a significantly higher concentration of glutamate in the coronary sinus, while KVal and pyruvate were present in a lower concentration.

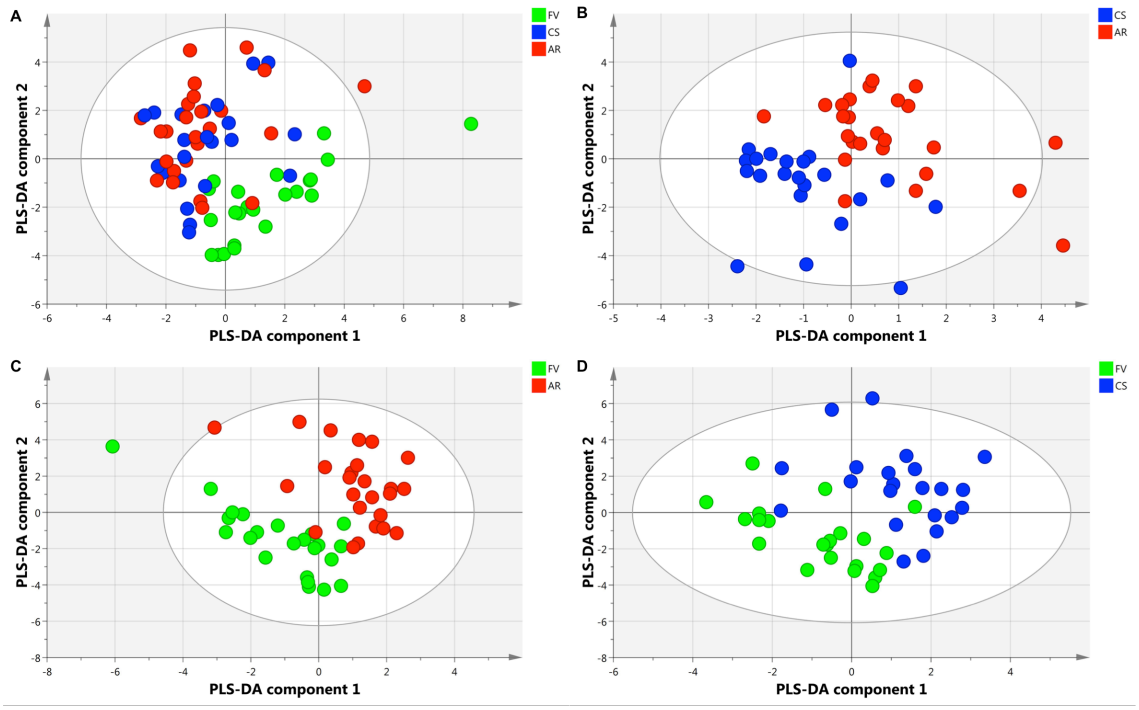

Figure 4.2.5: Partial least squares- discriminant analysis (PLS-DA) scores plot of aqueous metabolites between all the collection sites combined together (A), AR vs CS (B), AR vs FV (C) and FV vs CS (D); analysis performed in the aortic stenosis cohort during pacing. AR: aortic root (red circle); CS: coronary sinus (blue circle); FV: femoral vein (green circle).

Table 4.2.3: Concentration of aqueous metabolites which were significantly different on analysis between the femoral vein, coronary sinus and aortic root samples, in the aortic stenosis cohort during pacing.

Differences between the groups statistically analysed using ANOVA with Bonferroni's post-test for multiple comparisons. In comparing aortic root with coronary sinus: * represents p<0.05, ** p<0.01, *** p<0.001 and **** p<0.0001. In comparing aortic root vs femoral vein: # represents p<0.05, ## p<0.01, ### p<0.001 and #### p<0.0001. In comparing femoral vein vs coronary sinus: ^ represents p<0.05, ^^ p<0.01, ^^^ p<0.001 and ^^^^ p<0.0001. Metabolites listed in alphabetical order. Metabolites listed in alphabetical order.

Metabolite	Femoral vein	Coronary sinus	Aortic root
Glutamate	1.09 (0.93 - 1.55)^^^^	2.14 (1.66 - 3.05)	2.68 (2.12 - 3.04)####

Values shown are median (quartiles 1 to 3) concentrations of the respective metabolites. Concentrations are presented as area ratio after normalisation to the internal standards.

Table 4.2.4: Concentration of aqueous metabolites which were significantly different on a pair wise analysis between the aortic root and coronary sinus, aortic root and femoral vein, and femoral vein and coronary sinus, in the aortic stenosis cohort during pacing. Differences between the groups statistically analysed using either Student's t-test or Mann-Whitney U-test. Statistical significance was defined as a p-value<0.05. Metabolites listed in alphabetical order. Metabolites listed in alphabetical order.

Metabolite	Aortic root	Coronary sinus	p value

BAIBA	0.0044 (0.0032 - 0.0072)	0.0031 (0.0020 - 0.0043)	0.002
KVal	2.72 (2.29 - 3.13)	2.07 (1.76 - 2.75)	0.002

Metabolite	Aortic root	Femoral vein	p value
Alanine	0.83 (0.61 - 1.12)	0.96 (0.79 - 1.34)	0.03
Glutamate	2.68 (2.12 - 3.04)	1.09 (0.93 - 1.55)	<0.0001

Metabolite	Femoral vein	Coronary sinus	p value
Glutamate	1.09 (0.93 - 1.55)	2.14 (1.66 - 3.05)	<0.0001
KVal	2.77 (2.17 - 3.12)	2.07 (1.76 - 2.75)	0.02
Pyruvate	0.37 (0.29 - 0.56)	0.24 (0.21 - 0.41)	0.04

Values shown are median (quartiles 1 to 3) concentrations of the respective metabolites. Concentrations are presented as area ratio after normalisation to the internal standards.

Conclusions from the analysis of aqueous metabolites during pacing

The differences between cardiac and peripheral metabolism during pacing are listed below:

1) Glutamate: it was extracted during peripheral metabolism with a significantly lower concentration in the femoral vein. The extraction of glutamate during

peripheral metabolism has been previously reported as discussed in Section 3.3.2.

Though the trans-cardiac measurements did not demonstrate a significantly lower concentration of glutamate in the coronary sinus, the trend was indicative of extraction (aortic root vs coronary sinus, 2.68 vs 2.14, p=0.11). Similar findings of glutamate extraction post myocardial stress in patients undergoing cardiac surgery (a subset of these patients included aortic stenosis) have previously been reported by Turer *et al*.[285] The difference between the two studies is the intensity of myocardial stress applied. The aortic stenosis patients studied by Turer *et al* underwent cardiac surgery and were subjected to I/R; comparatively our study population underwent pacing to induce myocardial stress.

2) Alanine: it was eluted during peripheral metabolism.
3) BAIBA: it was extracted during cardiac metabolism.
4) KVal: it was extracted during cardiac metabolism.

As reported before in the HCM and control cohorts, BCAAs were extracted during the cardiac metabolism; the significance of this and of BAIBA in cardiac metabolism is discussed in Chapter 8.

4.2.2.3 Baseline vs pacing

a) Femoral vein

Samples from each individual collection site were then analysed to assess for any differences between the baseline and pacing states. The femoral vein samples were first to be analysed and on unsupervised multivariate testing

using the PCA approach no separation was seen between the baseline and pacing states (figure 4.2.6, plot A). No model could be built using the PLS-DA approach either. Thus the baseline and pacing samples from the femoral vein could not be discriminated using the aqueous metabolites.

b) Coronary sinus

Samples from the coronary sinus were analysed next and similar to the femoral vein, no separation was exhibited on the PCA scores plot as seen in figure 4.2.6 (plot B). The results were confirmed by using the PLS-DA analytical approach, where no model could be built either. Thus the baseline and pacing samples collected from the coronary sinus could not be discriminated using the aqueous metabolites.

b) Aortic root

Aortic root samples collected during the baseline and pacing states were assessed using the PCA approach, which demonstrated no separation between the two states (figure 4.2.6, plot C). On further analysis using the PLS-DA approach no model could be built, and thus the baseline and pacing samples from the aortic root could not be discriminated using the aqueous metabolites.

c) All three-collection sites combined

The final analysis was done after combining samples from all three-collection sites. As seen on the PCA scores plot in figure 4.2.6 (plot D) no separation was visualised between the baseline and pacing states. These results were then verified using the PLS-DA approach where no model could be built which could discriminate the baseline and pacing states.

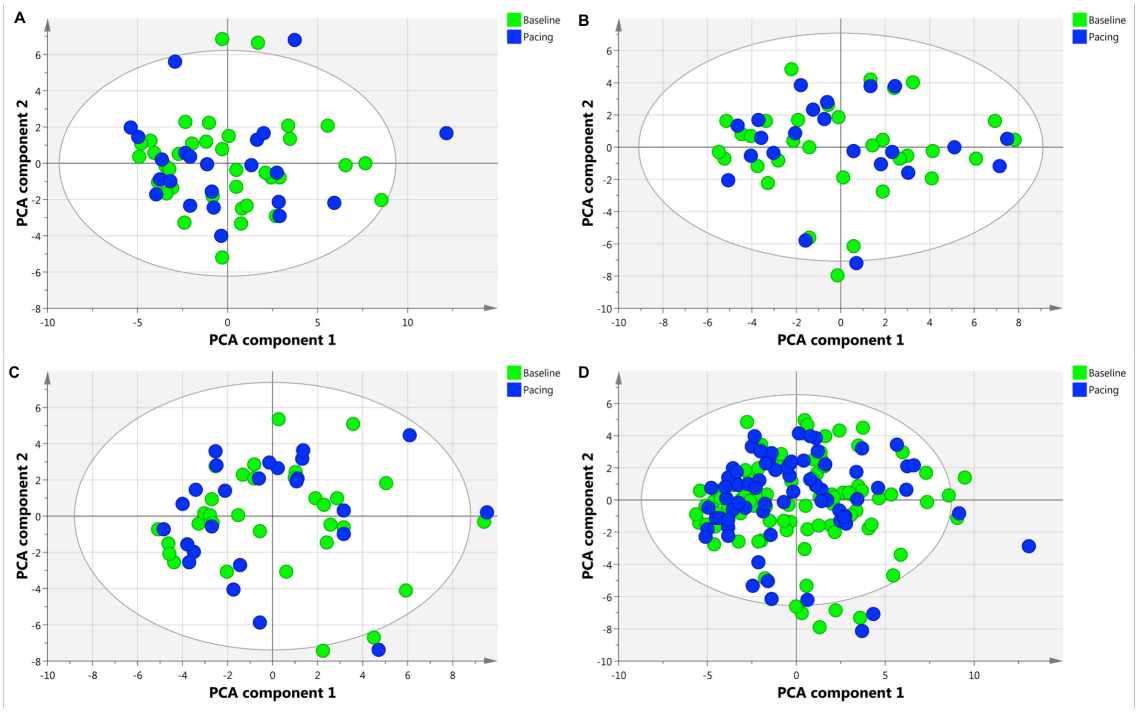

Figure 4.2.6: Principal component analysis (PCA) scores plot of aqueous metabolites between baseline (green circles) and pacing (blue circles) states, in the femoral vein (A), coronary sinus (B), aortic root (C) and in all the collection sites combined together (D); analysis performed in the aortic stenosis cohort.

Conclusions from the analysis of aqueous metabolites between baseline and pacing states

Samples collected during the baseline and pacing states from any of the three-collection sites could not be discriminated using the aqueous metabolites. This was suggestive of no significant difference in the concentration of aqueous metabolites between the baseline and pacing samples.

Thus the intensity of myocardial stress induced by pacing did not significantly alter the concentration of aqueous metabolites within individual collection sites. But when two-collection sites were assessed in a pair wise manner (cardiac/peripheral metabolism), the difference between the two

(extraction/elution) changed significantly from baseline to pacing. This change in the cardiac metabolism between the baseline and pacing states is now described in the following section.

4.2.2.3.1 Cardiac metabolism (baseline vs pacing)

The cardiac metabolism of glutamate and BAIBA altered significantly between the baseline and pacing states and is described bellow (table 4.2.5).

1. Glutamate: it was extracted both during baseline and pacing states, with its net extraction decreasing significantly during pacing.

The fall in glutamate extraction post myocardial stress in aortic stenosis patients has been previously reported by Turer *et al*.[285] This was accompanied with an increase in cardiac elution of alanine; this was similarly seen in our study population, though the change was not significant. These findings were explained possibly from the changes in the citric acid cycle and alanine/cahill cycle activity. Turer *et al* had reported impaired citric acid cycle flux following I/R, and a similar trend was observed following pacing in our aortic stenosis patients, which has been discussed in Chapter 8. Impaired citric acid cycle activity leads to decreased uptake of glutamate, which is transaminated to form α-ketoglutarate an anaplerotic substrate of the citric acid cycle.

Also during pacing there is an accumulation of lactate in the coronary sinus of aortic stenosis patients as reported in section 3.2.2. As reported before during increased myocardial stress and anaerobic metabolism, there is an increased conversion of pyruvate to lactate. The mass action effect of lactate accumulation inhibits its own production and augments the conversion of

pyruvate to alanine (pyruvate transamination).[306] This results in an increased elution of alanine as reported above. Though glutamate acts as the nitrogen donor during pyruvate transamination reaction, its net consumption falls, possibly because less of its pool is being oxidised or used for other transamination reactions.

2. BAIBA: its metabolism switched from elution to extraction between the baseline and pacing states. The significance of this change has been discussed in Chapter 8.

It is important to highlight that the lack of coronary sinus blood flow measurements limits our ability to calculate the net flux of metabolites. Turer *et al* had a similar limitation, but reported that the changes in trans-cardiac gradient post I/R were unlikely to be solely influenced by changes in coronary blood flow, which had previously been reported to be relatively small as compared the magnitude of extraction/elution.[285,307,308] As we observed a similar fall in glutamate extraction post myocardial stress, it could be concluded with reservation that there was a possible fall in the underlying net flux of glutamate.

Table 4.2.5: Trans-cardiac gradient (aortic root – coronary sinus) of selected aqueous metabolites measured within individual patients in the aortic stenosis cohort, and compared between baseline and pacing. Differences between the groups statistically analysed using either two-tailed Student's t-test or Wilcoxon Signed-Rank test. Statistical significance was defined as a p-value<0.05. Metabolites listed in alphabetical order.

Metabolite	Baseline	Pacing	p value
Alanine	−0.01 (−0.07 - 0.08)	−0.03 (−0.17 - 0.05)	0.57
BAIBA	−0.0002 (−0.0009 - 0.0)	6.835e-005 (−0.0002 - 0.001)	0.02
Citrulline	5.70 (−4.66 - 13.42)	0.89 (−6.88 - 7.93)	0.51
Glutamate	0.78 (0.54 - 0.86)	0.45 (0.20 - 0.69)	0.008
Isocitrate	1.07 (−0.39 - 2.21)	0.01 (−0.77 - 1.08)	0.28
KLeu	1.62 (0.69 - 3.34)	1.53 (0.07 - 2.48)	0.50
KVal	0.71 (0.60 - 1.45)	0.69 (−0.07 - 0.99)	0.28
Malate	0.11 (−0.27 - 0.46)	0.09 (−0.18 - 0.36)	0.82
Succinate	−0.06 (−0.23 - 0.02)	−0.12 (−0.35 - −0.05)	0.27

Values shown are median (quartiles 1 to 3) concentrations of the respective metabolites. Concentrations are presented as area ratio after normalisation to the internal standards.

4.2.2.4 Summary & Future Analytical strategy

The analysis of metabolites in the aortic stenosis cohorts found similar results as the HCM and control cohorts. Thus on analysing individual collection sites there was no difference in the concentration of acylcarnitines and aqueous metabolites between the baseline and pacing states. There were differences in the concentration of aqueous metabolites between individual collection sites (extraction / elution), which changed from baseline to pacing (table 4.2.6). Thus further analysis between the individual cohorts was conducted following the **analytical strategy** described bellow:

1) **Baseline and pacing combined:**

   The baseline and pacing samples from individual collection sites were combined, when assessing for acylcarnitine and aqueous metabolite differences between cohorts.

2) **Baseline vs pacing:**

   The trans-cardiac gradient of aqueous metabolites during the baseline and pacing states was also analysed for differences between cohorts.

Table 4.2.6: Summary of the most significant results from the metabolomic analysis of the aortic stenosis cohort during baseline and pacing. Differences between the groups statistically analysed using either two-tailed Student's t-test, Mann-Whitney U-test or Wilcoxon Signed-Rank test. Statistical significance was defined as a p-value<0.05.

Aortic stenosis cohort			
Trans-Cardiac gradient (Cardiac metabolism)			
	Aortic root	**Coronary sinus**	**p value**
Baseline			
Glutamate	2.36 (1.85 - 2.85)	1.69 (1.25 - 2.29)	0.0002
KIle	6.08 (5.00 - 7.37)	4.85 (3.99 - 6.19)	0.04
KLeu	9.36 (7.08 - 12.68)	7.29 (5.90 - 9.38)	0.004
KVal	2.77 (2.29 - 4.01)	2.04 (1.72 - 2.46)	<0.0001
Pacing			
BAIBA	0.0044 (0.0032 - 0.0072)	0.0031 (0.0020 - 0.0043)	0.002

KVal	2.72 (2.29 - 3.13)	2.07 (1.76 - 2.75)	0.002

Aorto-Femoral gradient (Peripheral metabolism)

	Aortic root	**Femoral vein**	
Baseline			
Alanine	0.86 (0.68 - 1.07)	0.98 (0.83 - 1.35)	0.04
Glutamate	2.36 (1.85 - 2.85)	1.11 (0.85 - 1.42)	<0.0001
Pacing			
Alanine	0.83 (0.61 - 1.12)	0.96 (0.79 - 1.34)	0.03
Glutamate	2.68 (2.12 - 3.04)	1.09 (0.93 - 1.55)	<0.0001

Trans-Cardiac gradient (Baseline vs Pacing)

	Baseline	**Pacing**	
BAIBA	−0.0002 (−0.0009 - 0.0)	6.835e-005 (−0.0002 - 0.001)	0.02
Glutamate	0.78 (0.54 - 0.86)	0.45 (0.20 - 0.69)	0.008

Values shown are median (quartiles 1 to 3) concentrations of the respective metabolites. Concentrations are presented as area ratio after normalisation to the internal standards.

5 METABOLOMIC DIFFERENCES BETWEEN COHORTS

Results from the metabolomic analysis between different patient cohorts are reported and discussed in this chapter. Following the metabolomic analysis of individual disease cohorts metabolomic differences between cohorts in a pair wise fashion were analysed. Controls were compared with HCM and aortic stenosis, and HCM were also compared to the aortic stenosis group. Metabolites were investigated distinctly, to allow in depth understanding of (i) acylcarnitines (ii) aqueous metabolites.

Analysis for all the three pairs was divided into 3 parts following the analytical strategy described in Section 4.2.2.4:

1) Acylcarnitines: they were analysed between the cohorts in a pair wise fashion. Baseline and pacing samples from an individual collection site were combined and then assessed between the two cohorts.
2) Aqueous metabolites: they were analysed in a similar manner as the acylcarnitines.
3) Cardiac metabolism (aortic root – coronary sinus): the cardiac metabolism of aqueous metabolites was assessed for differences between the cohorts during the baseline and pacing states.

5.1 Metabolomic differences between the control and HCM cohorts

The first pair wise analysis was performed between the control and HCM cohorts, where 38 control and 35 HCM patients were included in the final analysis. The clinical characteristics of the two cohorts are described in Section 3.1. The results from this comparative analysis are described below.

5.1.1 Analysis of acylcarnitines between the control and HCM cohorts

a) Femoral vein

Femoral vein samples were analysed for differences in concentration of acylcarnitines between the control and HCM cohorts. The baseline and pacing samples were combined as described in the analytical strategy (Section 4.2.2.4).

For an overview of samples, unsupervised multivariate strategy was employed using PCA approach and this showed no separation between the two cohorts. Further analysis was carried out using the supervised PLS-DA approach. The PLS-DA model (R^2X=0.15, R^2Y=0.08, Q^2=0.01) identified several acylcarnitines, which were responsible for separation (figure 5.1.1, plot A). The validity and goodness of fit of the original model were assessed using 100 random permutations. This demonstrated that the majority of the permuted R^2 values were the same as the original model, and the majority of the permuted Q^2 values were equal or lower than the original values (intercepts: R^2=[0.0,0.06], Q^2=[0.0,−0.06]). This indicated a valid original model and the most discriminating metabolites from this model (VIP score ≥1) were selected for further analysis using either the two-tailed Student's t-test or the Mann-Whitney

U-test. This demonstrated that C2, C12:1, C16:1 and C18-OH were all present in a significantly higher concentration in the HCM cohort, while C8-DC was present in a lower concentration (table 5.1.1).

b) Coronary sinus

PCA analysis of acylcarnitines in the coronary sinus samples between the control and HCM cohorts did not exhibit a clear separation. These results were further verified by supervised multivariate testing using the PLS-DA approach. This demonstrated a separation between the two cohorts on the scores plot of a weak PLS-DA model (figure 5.1.1, plot B) (R^2X=0.13, R^2Y=0.17, Q^2=0.05). The validity and goodness of fit of the original model were confirmed using 100 random permutations, where nearly all the permuted R^2 and Q^2 values were lower than the original values (intercepts: R^2=[0.0,0.05], Q^2=[0.0,−0.06]). The most discriminating metabolites (VIP score ≥1) were then independently assessed using either the two-tailed Student's t-test or the Mann-Whitney U-test. This demonstrated a significantly higher concentration of free carnitine, C2, C16:1, C18-OH and C18:2-OH in the HCM cohort, while C8-DC was present in a significantly lower concentration in the HCM cohort (table 5.1.1).

c) Aortic root

Unsupervised univariate analysis of the acylcarnitines between the aortic root samples of the control and HCM cohorts was performed using the PCA approach. This provided a visual over view of the samples, where separation was exhibited between the control and HCM cohorts. Further confirmation was obtained on the scores plot of the PLS-DA model, where the two cohorts separated as distinct clusters (figure 5.1.1, plot C) (R^2X=0.12, R^2Y=0.12, Q^2=0.03). The validity and goodness of fit of the original model were confirmed

using 100 random permutations (intercepts: R^2=[0.0,0.05], Q^2=[0.0,−0.06]). Assessment of the most discriminating metabolites (VIP score ≥1) using either the two-tailed Student's t-test or the Mann-Whitney U-test, demonstrated that several species including free carnitine, C2, C12:1, C16:1 and C18-OH were present in a significantly higher concentration in the HCM cohort, while C8-DC was present in a significantly lower concentration (table 5.1.1).

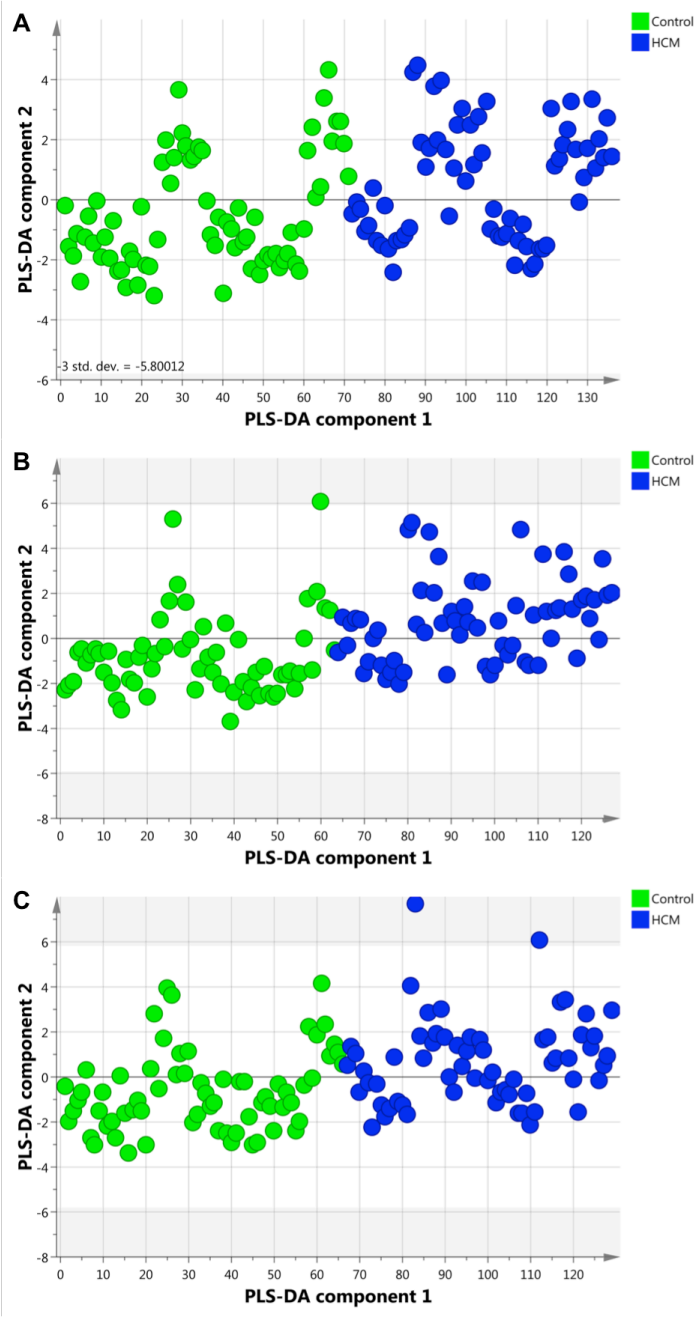

Figure 5.1.1: Partial least squares- discriminant analysis (PLS-DA) scores plot of acylcarnitines between control (green circles) & HCM (blue circles) cohorts in the femoral vein (A), coronary sinus (B) and aortic root (C) collection sites.

Table 5.1.1: Concentration of acylcarnitines which were significantly different between the control and HCM cohorts; measured in femoral vein, coronary sinus and aortic root collection sites. Both baseline and pacing samples were combined for analysis. Differences between the groups statistically analysed using either two-tailed Student's t-test or Mann-Whitney U-test. Statistical significance was defined as a p-value<0.05. Metabolites listed in alphabetical order.

Metabolite	Control	HCM	p value
Femoral vein			
C2	1.45 (1.23 - 3.43)	2.50 (1.27 - 4.39)	0.02
C8-DC	0.011 (0.005 - 0.019)	0.007 (0.004 - 0.013)	0.045
C12:1	0.16 (0.12 - 0.24)	0.20 (0.17 - 0.25)	0.04
C16:1	0.11 (0.08 - 0.16)	0.14 (0.10 - 0.18)	0.04
C18-OH	0.003 (0.002 - 0.006)	0.005 (0.003 - 0.007)	0.008
Coronary sinus			
Carnitine	2.59 (2.38 - 2.95)	3.01 (2.59 - 4.23)	0.002
C2	1.50 (1.20 - 2.62)	2.78 (1.37 - 4.32)	0.002
C8-DC	0.012 (0.005 - 0.025)	0.007 (0.004 - 0.013)	0.02
C16:1	0.11 (0.07 - 0.15)	0.16 (0.12 - 0.19)	<0.0001
C18-OH	0.003 (0.002 - 0.005)	0.006 (0.004 - 0.008)	<0.0001
C18:2-OH	0.004 (0.002 - 0.006)	0.005 (0.004 - 0.008)	0.02

Aortic root			
Carnitine	2.61 (2.51 - 3.12)	3.25 (2.66 - 4.07)	0.001
C2	1.38 (1.20 - 3.33)	3.17 (1.47 - 4.72)	0.0006
C8-DC	0.013 (0.004 - 0.024)	0.007 (0.004 - 0.014)	0.03
C12:1	0.15 (0.11 - 0.24)	0.18 (0.16 - 0.24)	0.03
C16:1	0.13 (0.08 - 0.16)	0.16 (0.12 - 0.19)	0.001
C18-OH	0.004 (0.003 - 0.006)	0.006 (0.004 - 0.008)	0.0003

Values shown are median (quartiles 1 to 3) concentrations of the respective metabolites. Concentrations are presented as area ratio after normalisation to the internal standards.

Conclusions from the analysis of acylcarnitines

Analysis of acylcarnitines between the control and HCM cohorts demonstrated a higher concentration of long chain acylcarnitines such as C16:1 and C18-OH in the HCM cohort across all three-collection sites. C8-DC a medium chain acylcarnitine was present in a significantly lower concentration in the HCM cohort across all three-collection sites. As acylcarnitines are excreted in the urine, subsequent analysis was performed after normalisation of these acylcarnitines to the eGFR. This similarly demonstrated a significantly high concentration of C16:1 and C18-OH, and a trend towards lower concentration of C8-DC in the HCM cohort as compared to controls.[309]

Similar findings with higher concentration of long chain acylcarnitines (these were even chain acylcarnitine species) and a lower concentration of medium chain species have been reported in states of incomplete fatty acid β−

oxidation.[310-312] Higher concentration of free carnitine and lower concentration of acylcarnitine as present in our HCM patients, has been previously described by Nakamuru and colleagues.[303] These findings are suggestive of reduced uptake of free carnitine by the myocytes and impairment in myocardial energetics, which is now considered to be an important mechanism in the pathogenesis of HCM.[313] These findings, especially their comparison to the aortic stenosis cohort are further discussed in Chapter 8.

5.1.2 Analysis of aqueous metabolites between the control and HCM cohorts

a) Femoral vein

PCA analysis of the aqueous metabolites between the control and HCM cohorts in the femoral vein samples exhibited no separation between the two cohorts. Further supervised multivariate assessment was performed using the PLS-DA approach. A robust model was built, which separated the two cohorts as visualised on its scores plot in figure 5.1.2 (plot A) (R^2X=0.35, R^2Y=0.29, Q^2=0.15). The validity and goodness of fit of the original model were confirmed using 100 random permutations (intercepts: R^2=[0.0,0.12], Q^2=[0.0,−0.09]).

The most discriminating metabolites (VIP score ≥1) were then assessed using either the two-tailed Student's t-test or the Mann-Whitney U-test. This demonstrated AAA (amino adipic acid), BAIBA, creatinine, glutamate, methyl-cytosine, proline, SAM (S-adenosyl methyonine), taurine and threonine were most differentiating. AAA, BAIBA, creatinine, proline, SAM and taurine were present in a significantly higher concentration in the HCM cohort, while the

concentration of glutamate, methyl-cytosine and threonine was significantly lower (table 5.1.2).

b) Coronary sinus

Coronary sinus samples from the control and HCM cohorts were assessed using PCA analysis, which demonstrated an overlap between the two cohorts. These samples were then assessed using the PLS-DA approach, which showed a clear separation on the scores plot of the generated model (figure 5.1.2, plot B) (R^2X=0.28, R^2Y=0.31, Q^2=0.09). The validity and goodness of fit of the original model were confirmed using 100 random permutations (intercepts: R^2=[0.0,0.14], Q^2=[0.0,−0.14]).

There was an extensive list of discriminating metabolites (VIP score ≥1), which were further assessed using either the two-tailed Student's t-test or the Mann-Whitney U-test. This demonstrated that AAA, BAIBA, cystine, cytosine, oxaloacetate and SAM were present in a significantly higher concentration in the HCM cohort, while the concentration of carnosine, isoleucine, methyl-cytosine and threonine was significantly lower (table 5.1.2).

c) Aortic root

PCA analysis of the aortic root samples between the control and HCM cohorts showed some separation. This was further assessed using the PLS-DA approach, where a model was built on whose scores plot the two cohorts were clearly discriminated (figure 5.1.2, plot C) (R^2X=0.25, R^2Y=0.28, Q^2=0.08). The validity and goodness of fit of the original model were confirmed using 100 random permutations (intercepts: R^2=[0.0,0.12], Q^2=[0.0,−0.12]). Univariate analysis of the most discriminating metabolites (VIP score ≥1) was performed

using either the two-tailed Student's t-test or the Mann-Whitney U-test. This demonstrated that metabolites such as AAA, BAIBA and SAM were present in a higher concentration in the HCM cohort, while the concentration of betane, carnosine, citrulline, fumarate, isocitrate, KIle, malate, pyruvate and threonine was significantly lower (table 5.1.2).

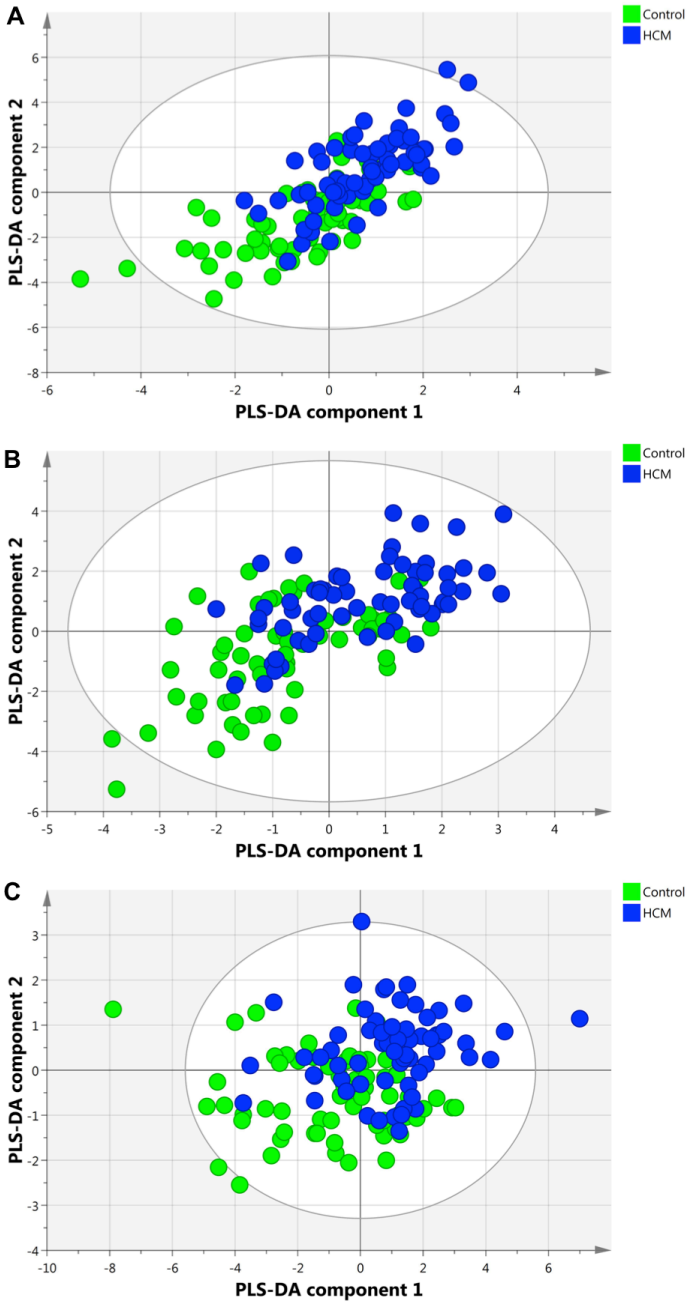

Figure 5.1.2 Partial least squares- discriminant analysis (PLS-DA) scores plot of aqueous metabolites between control (green circles) & HCM (blue circles) cohorts in the femoral vein (A), coronary sinus (B) and aortic root (C) collection sites.

Table 5.1.2: Concentration of aqueous metabolites which were significantly different between the control and HCM cohorts; measured in femoral vein, coronary sinus and aortic root collection sites. Both baseline and pacing samples were combined for analysis. Differences between the groups statistically analysed using either two-tailed Student's t-test or Mann-Whitney U-test. Statistical significance was defined as a p-value<0.05. Metabolites listed in alphabetical order.

Metabolite	Control	HCM	p value
Femoral			
AAA	0.001 (0.001 - 0.003)	0.003 (0.001 - 0.004)	0.002
BAIBA	0.003 (0.002 - 0.004)	0.004 (0.003 - 0.005)	0.0008
Createnine	0.30 (0.27 - 0.34)	0.32 (0.29 - 0.36)	0.02
Glutamate	1.14 (0.85 - 1.38)	0.94 (0.83 - 1.15)	0.006
Methyl-Cytosine	0.001 (0.001 - 0.001)	0.0009 (0.0006 - 0.001)	0.0002
Proline	4.07 (3.15 - 4.83)	4.49 (3.71 - 5.36)	0.03
SAM	0.0 (0.0 - 0.0)	9.101e-005 (0.0 - 0.0002)	<0.0001
Taurine	0.007 (0.006 - 0.008)	0.008 (0.006 - 0.009)	0.005
Threonine	0.34 (0.30 - 0.39)	0.32 (0.28 - 0.38)	0.03
Coronary			
AAA	0.001 (0.001 - 0.003)	0.003 (0.001 - 0.004)	0.001

BAIBA	0.003 (0.002 - 0.004)	0.003 (0.003 - 0.005)	0.02
Carnosine	0.001 (0.001 - 0.001)	0.0009 (0.0005 - 0.001)	<0.0001
Cystine	0.026 (0.021 - 0.032)	0.029 (0.024 - 0.034)	0.008
Cytosine	0.0 (0.0 - 0.0)	4.539e-005 (0.0 - 0.0002)	0.0002
Isoleucine	1.67 (1.37 - 2.27)	1.52 (1.22 - 1.73)	0.005
Methyl-Cytosine	0.001 (0.001 - 0.001)	0.0008 (0.0006 - 0.001)	<0.0001
Oxaloacetate	0.49 (0.44 - 0.57)	0.54 (0.47 - 0.65)	0.01
SAM	0.0 (0.0 - 0.0)	7.739e-005 (0.0 - 0.0002)	<0.0001
Threonine	0.31 (0.28 - 0.37)	0.29 (0.24 - 0.34)	0.04
Aortic root			
AAA	0.001 (0.001 - 0.003)	0.003 (0.001 - 0.004)	0.002
BAIBA	0.0030 (0.0020 - 0.0040)	0.0031 (0.0028 - 0.0044)	0.02
Betane	15.19 (13.19 - 18.00)	13.12 (11.52 - 15.82)	0.001
Carnosine	0.001 (0.001 - 0.001)	0.0008 (0.0004 - 0.001)	0.006
Citrulline	45.97 (34.84 - 59.78)	40.94 (32.56 - 48.68)	0.048
Fumarate	0.09 (0.06 - 0.13)	0.06 (0.04 - 0.08)	0.0004
Isocitrate	7.28 (5.32 - 9.51)	6.00 (4.91 - 7.56)	0.01
KIle	6.59 (5.78 - 8.01)	5.90 (4.94 - 7.34)	0.03
Malate	1.52 (1.09 -1.88)	1.25 (0.93 - 1.61)	0.02
Pyruvate	0.31 (0.25 - 0.39)	0.24 (0.19 - 0.31)	0.0004
SAM	0.0 (0.0 - 0.0)	0.0001 (0.0 - 0.0002)	<0.0001
Threonine	0.31 (0.28 - 0.35)	0.29 (0.25 - 0.33)	0.02

Values shown are median (quartiles 1 to 3) concentrations of the respective metabolites. Concentrations are presented as area ratio after normalisation to the internal standards.

Conclusions from the analysis of aqueous metabolites

Analysis of aqueous metabolites between the control and HCM cohorts found that several metabolites were present in different concentrations between the two cohorts. Common to all three-collection sites there was a significantly higher concentration of AAA, BAIBA and SAM in the HCM cohort, while threonine was present in a significantly lower concentration. Role of these metabolites in human metabolism is discussed below.

AAA was present in a higher concentration in the HCM cohort. It is an intermediate in the metabolism of lysine and was reported by Olszewski *et al* to be present in a higher concentration in post myocardial infarction patients.[314] They also reported a high concentration of homocysteine in these patients, and it was postulated that AAA and homocysteine have a similar metabolic marker role in the etiology of atherosclerosis. The role of AAA as a predictive biomarker in the development of diabetes has also been extensively reported, but there are no studies describing its role in HCM.[315,316]

The role of BAIBA in cardiac and skeletal muscle metabolism is discussed in detail in Chapter 8.

SAM is formed from ATP and methionine in a reaction catalysed by methionine adenosyltransferase. It plays an important role in several anabolic reactions, where it transfers the methyl group to various substrates including lipids, proteins and nucleic acids. It is used as a dietary supplement, antidepressant and in the treatment of osteoarthritis.[317] As with AAA, increased concentration

of SAM has been reported in patients with ischemic heart disease, but there are no previous studies reporting a high concentration of SAM in HCM patients.[318]

Threonine is an essential amino acid, which is not synthesized by humans and has to be absorbed from dietary sources. The major part of its metabolism occurs in a reaction catalysed by threonine dehydrogenase, where threonine is catabolised to acetyl-CoA and glycine. While acetyl-CoA is channeled into the citric acid cycle for energy production, glycine acts as a major neuro-transmitter. The role of threonine in treatment of genetic spastic disorders and multiple sclerosis is well reported.[319,320] In work published by Lewis *et al* threonine levels were reported to decrease peripherally post alcohol septal ablation in HCM patients.[294] They did not compare the baseline levels of threonine between the HCM patients and a control group. A low level of threonine in our HCM population as compared to controls could possibly be explained by its increased channeling into the citric acid cycle via acetyl-CoA for energy production. This could occur to meet the higher energy demand in HCM due to the underlying metabolic dysregulation (discussed in Section 1.3.2).[228]

In a recent study of HCM patients with MYBPC3-Q1061X mutation, a higher concentration of BCAAs was reported in HCM patients with a phenotype of LVH when compared to controls.[321] The controls were family members of HCM patients, who did not have either the phenotype or genotype for HCM. We did not observe similar results and on the contrary the concentration of KIle was lower in the aortic root of HCM patients. This could be explained by the difference in recruitment strategy used for our study. While the recruitment of HCM patients was not constrained by their genotype or phenotype, the

recruitment of controls was done from the general population and they were not family members of the HCM patients.

5.1.3 Cardiac metabolism between the control and HCM cohorts at baseline and during pacing

The next step was to determine the differences in cardiac metabolism between the control and HCM cohorts during baseline and pacing (table 5.1.3), these differences are described bellow:

1) KLeu and KVal: at baseline the metabolism of KLeu and KVal was different between the two cohorts, with a significantly higher extraction in the control cohort. The difference in the extraction of KLeu and KVal was not observed during pacing, which was possibly explained by the higher increase in extraction of these metabolites between the baseline and pacing states in the HCM cohort when compared to controls (KLeu: 1.62 vs 0.43, p=0.27; KVal: 0.36 vs 0.14, p=0.46). The increased extraction of BCAAs during pacing has been further discussed in Chapter 8.
2) Citrulline and malate: the metabolism of citrulline and malate altered significantly between the baseline and pacing states in the HCM cohort. Both citrulline and malate were eluted at baseline, which switched to extraction of malate and decreased elution of citrulline during pacing in the HCM cohort. A similar trend towards increased uptake of these metabolites during pacing though non-significant was observed in the control cohort.
3) Isocitrate: the metabolism of isocitrate, which is a key intermediate of the citric acid cycle also changed significantly between the baseline and pacing

states in the HCM cohort (switched from elution to extraction). These changes reflect an adaptive response in the metabolism during a state of increased energy requirement induced by pacing; these changes have been further discussed in Chapter 8.

It is important to consider that the extraction or elution of these metabolites will be influenced by the increased coronary blood flow during pacing, and these considerations in the control and HCM cohorts have been discussed in Sections 3.3.2 and 4.1.2.

Table 5.1.3: Trans-cardiac gradient (aortic root – coronary sinus) of selected aqueous metabolites measured within each patient, at baseline and during pacing in the control and HCM cohorts. Differences between the groups statistically analysed using either two-tailed Student's t-test or Mann-Whitney U-test. Statistical significance was defined as a p-value<0.05. Metabolites listed in alphabetical order.

Metabolite	Control	HCM	p value
Baseline			
Alanine	−0.02 (-0.07 - 0.06)	−0.04 (−0.13 - 0.04)	0.48
BAIBA	0.0 (−0.0005 - 0.0)	0.0 (−0.0004 - 0.0004)	0.44
Citrulline	0.13 (−10.04 - 9.22)	−9.63 (−21.63 - −2.49)	0.12
Glutamate	1.15 (0.61 - 1.39)	0.89 (0.65 - 1.15)	0.18
Isocitrate	0.25 (−0.71 - 1.66)	−0.66 (−2.67 - 0.69)	0.05
KLeu	2.47 (−0.06 - 3.72)	−0.84 (−1.79 - 1.89)	0.003
KVal	0.70 (0.34 - 1.13)	0.51 (−0.28 - 0.74)	0.04

Malate	−0.04 (−0.26 - 0.21)	−0.39 (−0.63 - −0.07)	0.05
Succinate	−0.14 (−0.28 - −0.03)	−0.21 (−0.33 - −0.09)	0.71
Pacing			
Alanine	0.05 (−0.11 - 0.09)	−0.02 (−0.09 - 0.05)	0.28
BAIBA	0.0 (−0.0006 - 0.0)	0.0 (−0.0005 - 0.0003)	0.36
Citrulline	5.79 (−4.13 - 15.35)	−1.64 (−9.99 - 11.45)	0.46
Glutamate	0.86 (0.39 - 1.09)	0.67 (0.35 - 0.80)	0.36
Isocitrate	0.33 (−0.57 - 2.45)	0.30 (−0.78 - 1.70)	0.67
KLeu	3.00 (0.57 - 4.35)	1.19 (−0.09 - 3.56)	0.38
KVal	0.93 (0.07 - 1.85)	0.69 (−0.08 - 1.22)	0.49
Malate	0.21 (−0.39 - 0.45)	0.001 (−0.29 - 0.32)	0.87
Succinate	−0.11 (−0.34 - 0.02)	−0.10 (−0.34 - 0.05)	0.89

Values shown are median (quartiles 1 to 3) concentrations of the respective metabolites. Concentrations are presented as area ratio after normalisation to the internal standards.

5.1.4 Summary

On a detailed analysis of the metabolism between the control and HCM cohorts the following conclusions were drawn (table 5.1.4):

1) There was a significantly higher concentration of long chain acylcarnitines such as C16:1 and C18-OH in the HCM cohort across all three-collection sites.
2) Metabolites such as AAA, BAIBA and SAM were present in a higher concentration in the HCM cohort across all three-collection sites.

3) Threonine was present in a lower concentration across all three-collection sites in the HCM cohort.
4) KLeu and KVal had a significantly higher extraction during cardiac metabolism in the control cohort at baseline. The extraction of KLeu increased significantly during pacing in the HCM cohort.
5) The metabolism of citrulline and malate was different between baseline and pacing, with a shift towards increased uptake of these metabolites during pacing in the HCM and control cohorts.

Table 5.1.4: Summary of the most significant results on comparing the metabolomic profile between the control and HCM cohorts. Both baseline and pacing samples were combined for analysis. Differences between the groups statistically analysed using either two-tailed Student's t-test or Mann-Whitney U-test. Statistical significance was defined as a p-value<0.05.

Control vs HCM cohorts			
Femoral vein			
	Control	**HCM**	**p value**
C16:1	0.11 (0.08 - 0.16)	0.14 (0.10 - 0.18)	0.04
C18-OH	0.003 (0.002 - 0.006)	0.005 (0.003 - 0.007)	0.008
AAA	0.001 (0.001 - 0.003)	0.003 (0.001 - 0.004)	0.002
BAIBA	0.0030 (0.0020 - 0.0040)	0.0040 (0.0030 - 0.0050)	0.0008
SAM	0.0 (0.0 - 0.0)	9.101e-005 (0.0 - 0.0002)	<0.0001

Threonine	0.34 (0.30 - 0.39)	0.32 (0.28 - 0.38)	0.03

Coronary sinus

	Control	HCM	
C16:1	0.11 (0.07 - 0.15)	0.16 (0.12 - 0.19)	<0.0001
C18-OH	0.003 (0.002 - 0.005)	0.006 (0.004 - 0.008)	<0.0001
AAA	0.001 (0.001 - 0.003)	0.003 (0.001 - 0.004)	0.001
BAIBA	0.0030 (0.0020 - 0.0040)	0.0030 (0.0030 - 0.0050)	0.02
SAM	0.0 (0.0 - 0.0)	7.739e-005 (0.0 - 0.0002)	<0.0001
Threonine	0.31 (0.28 - 0.37)	0.29 (0.24 - 0.34)	0.04

Aortic root

	Control	HCM	
C16:1	0.13 (0.08 - 0.16)	0.16 (0.12 - 0.19)	0.001
C18-OH	0.004 (0.003 - 0.006)	0.006 (0.004 - 0.008)	0.0003
AAA	0.001 (0.001 - 0.003)	0.003 (0.001 - 0.004)	0.002
BAIBA	0.0030 (0.0020 - 0.0040)	0.0031 (0.0028 - 0.0044)	0.02
SAM	0.0 (0.0 - 0.0)	0.0001 (0.0 - 0.0002)	<0.0001
Threonine	0.31 (0.28 - 0.35)	0.29 (0.25 - 0.33)	0.02

Trans-Cardiac gradient

	Control	HCM	
Baseline			
Citrulline	0.13 (−10.04 - 9.22)	−9.63 (−21.63 - −2.49)	0.12
KLeu	2.47 (−0.06 - 3.72)	−0.84 (−1.79 - 1.89)	0.003
KVal	0.70 (0.34 - 1.13)	0.51 (−0.28 - 0.74)	0.04
Malate	−0.04 (−0.26 - 0.21)	−0.39 (−0.63 - −0.07)	0.05

Pacing			
Citrulline	5.79 (−4.13 - 15.35)	−1.64 (−9.99 - 11.45)	0.46
KLeu	3.00 (0.57 - 4.35)	1.19 (−0.09 - 3.56)	0.38
KVal	0.93 (0.07 - 1.85)	0.69 (−0.08 - 1.22)	0.49
Malate	0.21 (−0.39 - 0.45)	0.001 (−0.29 - 0.32)	0.87

Values shown are median (quartiles 1 to 3) concentrations of the respective metabolites. Concentrations are presented as area ratio after normalisation to the internal standards.

5.2 Metabolomic differences between the control and aortic stenosis cohorts

Metabolomic differences between the control and aortic stenosis cohorts were assessed using the analytical strategy described in Section 4.2.2.4. A total of 38 controls and 36 aortic stenosis patients were included in the final analysis. The acylcarnitines were first to be analysed, followed by the aqueous metabolites and finally the cardiac metabolism was assessed between the two cohorts.

5.2.1 Analysis of acylcarnitines between the control and aortic stenosis cohorts

a) Femoral vein

Acylcarnitines were the first to be analysed in the femoral vein samples using the PCA approach. This was to obtain a general overview of the samples, and it demonstrated a clear separation between the two cohorts. To obtain a more reliable statistical analysis these results were verified using the PLS-DA

approach. This resulted in a good PLS-DA model on whose scores plot a clear separation was visualised between the two cohorts (figure 5.2.1, plot A) (R^2X=0.49, R^2Y=0.33, Q^2=0.25). The original model was validated using 100 random permutations, where all permuted R^2 and Q^2 values were much lower than the original values (intercepts: R^2=[0.0,0.09], Q^2=[0.0,−0.12]).

Acylcarnitines with a VIP score of ≥1 were then assessed using either the two-tailed Student's t-test or the Mann-Whitney U-test. This demonstrated a significantly higher concentration of several acylcarnitines in the aortic stenosis cohort, these included free carnitine, C2, C6, C12:1, C14-OH, C16:1, C16-OH, C18-OH and C20:1 (table 5.2.1). C8-DC and C18:2 were present in a significantly lower concentration in the aortic stenosis patients.

b) Coronary sinus

Coronary sinus samples from the two cohorts were first assessed using the PCA approach. This exhibited an overlap between the two cohorts. A further supervised multivariate testing was then performed using the PLS-DA approach. This generated a good PLS-DA model on whose scores plot two cohorts separated as distinct clusters (figure 5.2.1, plot B) (R^2X=0.52, R^2Y=0.33, Q^2=0.23). The validity and goodness of fit of the original model were confirmed using 100 random permutations (intercepts: R^2=[0.0,0.09], Q^2=[0.0,−0.12]).

On further univariate analysis of the most discriminating acylcarnitines (VIP score ≥1), several of them were found to be present in a significantly higher concentration in the coronary sinus of the aortic stenosis patients, these included: free carnitine, C2, C3, C12, C12:1, C14-OH, C16:1, C16-OH, C18-OH

and C20:1 (table 5.2.1). C8-DC was present in a significantly lower concentration in the aortic stenosis patients.

c) Aortic root

Aortic root samples were analysed to assess for any differences in the concentration of acylcarnitines between the two cohorts. Unsupervised multivariate testing of the samples using the PCA approach exhibited little separation between the two cohorts. The PLS-DA analysis of these samples built a model on whose scores plot a better separation was visualised (figure 5.2.1, plot C) (R^2X=0.49, R^2Y=0.31, Q^2=0.23). Using 100 random permutations it was demonstrated that the original model performed much better than the permuted models and this confirmed its validity and goodness of fit (intercepts: R^2=[0.0,0.09], Q^2=[0.0,−0.12]).

Either two-tailed Student's t-test or Mann-Whitney U-test were used to independently verify the discriminating ability of acylcarnitines with a VIP score ≥1. This demonstrated a significantly higher concentration of free carnitine, C12, C12:1, C14-OH, C16:1, C16-OH, C18-OH, and C20:1 in the aortic root samples from the aortic stenosis cohort (table 5.2.1). C8-DC was present in a significantly lower concentration in the aortic stenosis patients.

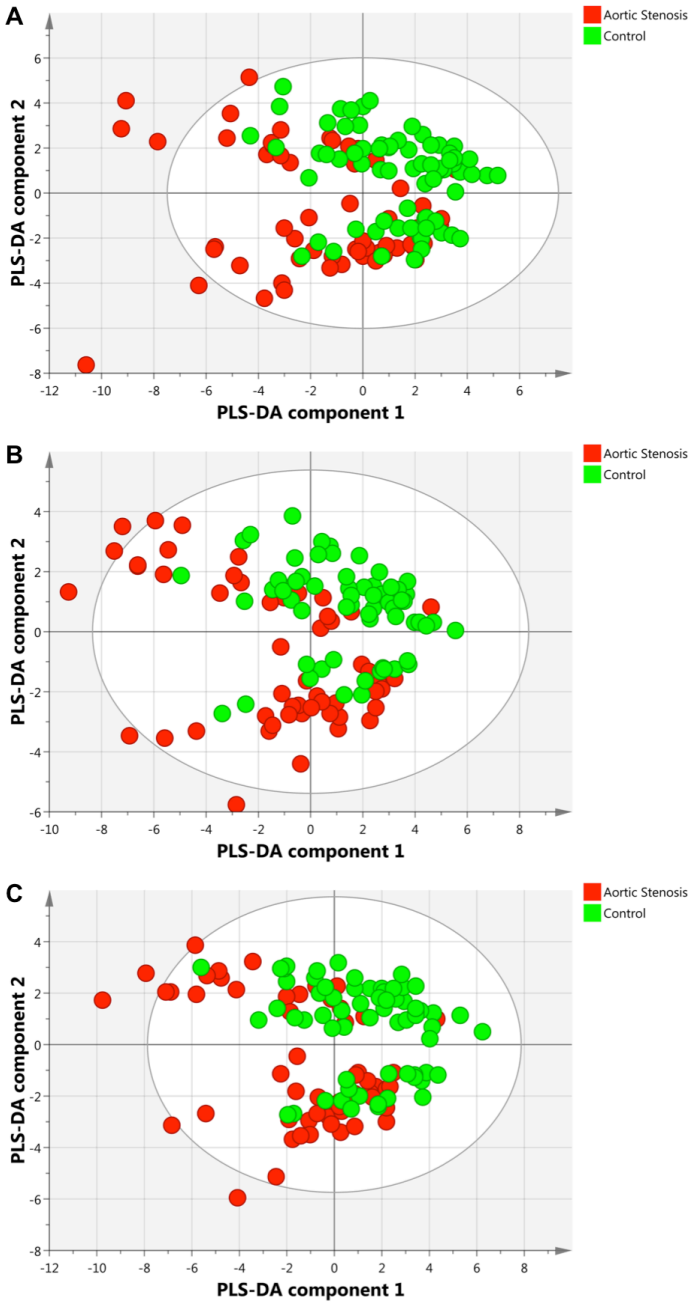

Figure 5.2.1: Partial least squares- discriminant analysis (PLS-DA) scores plot of acylcarnitines between control (green circles) & aortic stenosis (red circles) cohorts in the femoral vein (A), coronary sinus (B) and aortic root (C) collection sites.

Table 5.2.1: Concentration of acylcarnitines which were significantly different between the control and aortic stenosis cohorts; measured in femoral vein, coronary sinus and aortic root collection sites. Both baseline and pacing samples were combined for analysis. Differences

between the groups statistically analysed using either two-tailed Student's t-test or Mann-Whitney U-test. Statistical significance was defined as a p-value<0.05. Metabolites listed in alphabetical order.

Metabolite	Control	Aortic stenosis	p value
Femoral vein			
Carnitine	2.71 (2.53 - 3.49)	3.34 (2.63 - 4.66)	0.005
C2	1.45 (1.23 - 3.43)	3.59 (1.18 - 5.12)	0.004
C6	0.14 (0.10 - 0.21)	0.20 (0.14 - 0.30)	0.0002
C8-DC	0.011 (0.005 - 0.019)	0.006 (0.003 - 0.016)	0.02
C12:1	0.16 (0.12 - 0.24)	0.24 (0.16 - 0.34)	0.0003
C14-OH	0.010 (0.007 - 0.015)	0.015 (0.010 - 0.021)	<0.0001
C16:1	0.11 (0.08 - 0.16)	0.19 (0.14 - 0.28)	<0.0001
C16-OH	0.008 (0.006 - 0.012)	0.013 (0.009 - 0.018)	0.0002
C18-OH	0.003 (0.002 - 0.006)	0.007 (0.005 - 0.009)	<0.0001
C18:2	0.08 (0.05 - 0.10)	0.05 (0.04 - 0.09)	0.049
C20:1	0.006 (0.005 - 0.008)	0.008 (0.006 - 0.010)	0.0001
Coronary sinus			
Carnitine	2.59 (2.38 - 2.95)	3.26 (2.65 - 4.70)	<0.0001
C2	1.50 (1.20 - 2.62)	3.12 (1.19 - 4.67)	0.04
C3	0.72 (0.58 - 0.92)	0.94 (0.64 - 1.19)	0.004
C8-DC	0.012 (0.005 - 0.025)	0.006 (0.004 - 0.015)	0.02
C12	0.14 (0.10 - 0.17)	0.17 (0.12 - 0.32)	0.001
C12:1	0.17 (0.13 - 0.22)	0.22 (0.18 - 0.36)	0.0004
C14-OH	0.011 (0.008 - 0.016)	0.015 (0.011 - 0.023)	0.0006
C16:1	0.11 (0.07 - 0.15)	0.17 (0.13 - 0.27)	<0.0001

C16-OH	0.009 (0.006 - 0.012)	0.013 (0.009 - 0.019)	<0.0001
C18-OH	0.003 (0.002 - 0.005)	0.006 (0.004 - 0.010)	<0.0001
C20:1	0.006 (0.004 - 0.008)	0.008 (0.006 - 0.011)	<0.0001
Aortic root			
Carnitine	2.61 (2.51 - 3.12)	3.36 (2.81 - 4.67)	0.0002
C8-DC	0.013 (0.004 - 0.024)	0.005 (0.004 - 0.018)	0.03
C12	0.12 (0.09 - 0.19)	0.17 (0.13 - 0.31)	0.0002
C12:1	0.15 (0.11 - 0.24)	0.23 (0.16 - 0.32)	0.0004
C14-OH	0.011 (0.008 - 0.015)	0.015 (0.010 - 0.023)	0.0006
C16:1	0.13 (0.08 - 0.16)	0.19 (0.13 - 0.27)	<0.0001
C16-OH	0.009 (0.007 - 0.011)	0.013 (0.009 - 0.017)	0.0001
C18-OH	0.004 (0.003 - 0.006)	0.007 (0.005 - 0.010)	<0.0001
C20:1	0.006 (0.004 - 0.008)	0.008 (0.007 - 0.011)	<0.0001

Values shown are median (quartiles 1 to 3) concentrations of the respective metabolites. Concentrations are presented as area ratio after normalisation to the internal standards.

Conclusions from the analysis of acylcarnitines

The analysis of acylcarnitines between the control and aortic stenosis cohorts found several long chain species to be present in a higher concentration in the aortic stenosis cohort. These included C12:1, C14-OH, C16:1, C16-OH, C18-OH and C20:1, which were present in a significantly higher concentration across all collection sites in the aortic stenosis cohort. C8-DC was present in a significantly lower concentration across all collection sites in the aortic stenosis

cohort. Similar results were observed when analysis was performed after normalisation of these acylcarnitines to the eGFR.

As discussed in Section 5.1.1 higher concentration of long chain acylcarnitines (even chain acylcarnitine species) has been previously reported in states of incomplete fatty acid β-oxidation, and a similar pattern in our aortic stenosis patients indicates metabolic dysregulation in their fatty acid metabolism.[310,312] There are previous reports of impaired fatty acid metabolism in animal models of pressure induced hypertrophy and of metabolic improvements in patients with aortic stenosis post aortic valve replacement assessed non-invasively (cardiac MRI);[322-324] but this is the first time such a detailed assessment of acylcarnitine metabolism in aortic stenosis patients has been performed, and compared to controls and HCM patients. These findings are further discussed in Chapter 8.

5.2.2 Analysis of aqueous metabolites between the control and aortic stenosis cohorts

a) Femoral vein

Aqueous metabolites in the femoral vein samples were first assessed using the PCA approach to obtain a visual overview of the samples. The scores plot of this analysis exhibited some separation between the two cohorts. Further supervised multivariate testing of these samples using the PLS-DA approach, built a model on whose scores plot a clear separation was visualised between the two cohorts (figure 5.2.2, plot A), ((R^2X=0.24, R^2Y=0.46, Q^2=0.29). The

validity and tightness of fit of the original model were confirmed using 100 random permutations (intercepts: R^2=[0.0,0.11], Q^2=[0.0,−0.13]).

Significance of the most discriminating metabolites (VIP score ≥1) on multivariate analysis was independently assessed using either the two-tailed Student's t-test or the Mann-Whitney U-test. The following metabolites were present in a significantly higher concentration in the femoral vein samples of the aortic stenosis cohort: AAA, aconitate, BAIBA, choline, citrate, citrulline, creatinine, cystine, isocitrate, ornithine, proline and SAM. Arginine, asparagine, carnosine, pyruvate and threonine, were present in a significantly lower concentration in the aortic stenosis cohort (table 5.2.2).

b) Coronary sinus

Coronary sinus samples were analysed using a similar analytical strategy as the femoral vein samples. The unsupervised PCA analysis demonstrated a partial separation between the two cohorts. These results were then verified using the supervised multivariate approach of PLS-DA analysis. This generated a robust model, which exhibited a clear separation between the two cohorts on its scores plot (figure 5.2.2, plot B) (R^2X=0.29, R^2Y=0.55, Q^2=0.42). The validity and goodness of fit of the original model were assessed and confirmed using 100 random permutations (intercepts: R^2=[0.0,0.17], Q^2=[0.0,−0.21]).

On further univariate analysis of the most discriminating metabolites (VIP score ≥1) the following were found to be present in a higher concentration in the coronary sinus of aortic stenosis cohort: AAA, aconitate, alanine, asparagine, BAIBA, choline, citrate, citrulline, creatinine, cystine, cytidine, isocitrate, lysine, malate, methionine, ornithine, proline, SAM and tyrosine. The concentration of

asparagine and KLeu was significantly lower in the aortic stenosis cohort (table 5.2.2).

c) Aortic root

Aortic root samples from the two cohorts were assessed using the PCA approach; this exhibited a partial separation between the two cohorts. PLS-DA analysis was then performed, which built a robust model on whose scores plot a clear separation was seen between the control and aortic stenosis cohorts (figure 5.2.2, plot C) (R^2X=0.44, R^2Y=0.58, Q^2=0.46). By using 100 random permutations it was demonstrated that the original model performed far superiorly than the permuted models (intercepts: R^2=[0.0,0.16], Q^2=[0.0,−0.28]). This confirmed the validity and goodness of fit of the original model and the most discriminating metabolites from it were assessed using either the two-tailed Student's t-test or the Mann-Whitney U-test.

A significant difference was found in the concentration of several aqueous metabolites between the two cohorts. While metabolites such as AAA, aconitate, alanine, BAIBA, citrate, citrulline, cystine, hydroxy-proline, isocitrate, lysine, malate, methionine, ornithine, proline, SAM, succinate and tyrosine were present in a significantly higher concentration in the aortic stenosis cohort, others such as fumarate, KIle and KLeu were present in a significantly lower concentration (table 5.2.2).

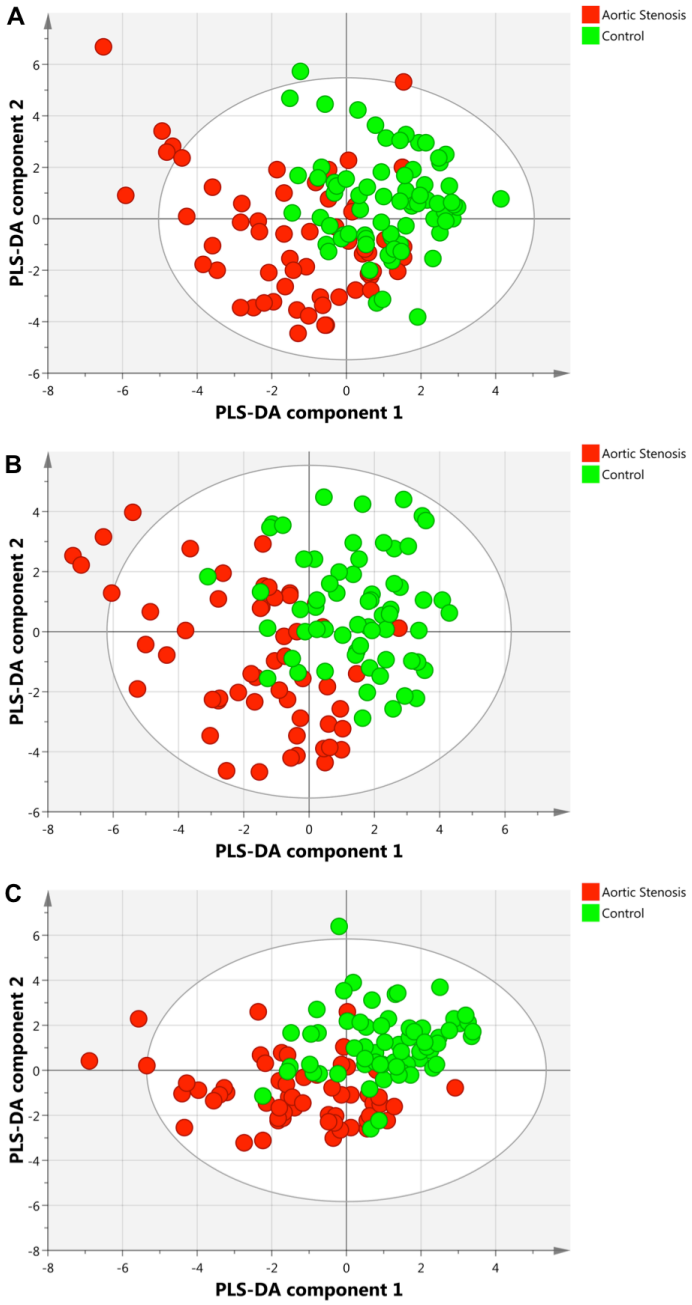

Figure 5.2.2: figure 5.2.1: Partial least squares- discriminant analysis (PLS-DA) scores plot of aqueous metabolites between control (green circles) & aortic stenosis (red circles) cohorts in the femoral vein (A), coronary sinus (B) and aortic root (C) collection sites.

Table 5.2.2: Concentration of aqueous metabolites which were significantly different between the control and aortic stenosis cohorts; measured in femoral vein, coronary sinus and aortic root collection sites. Both baseline and pacing samples were combined for analysis.

Differences between the groups statistically analysed using either two-tailed Student's t-test or Mann-Whitney U-test. Statistical significance was defined as a p-value<0.05. Metabolites listed in alphabetical order.

Metabolite	Control	Aortic stenosis	p value
Femoral vein			
AAA	0.001 (0.001 - 0.003)	0.003 (0.001 - 0.004)	0.0002
Aconitate	0.41 (0.29 - 0.59)	0.53 (0.35 - 0.77)	0.005
Arginine	2.82 (2.38 - 3.18)	2.54 (2.22 - 3.07)	0.03
Asparagine	0.053 (0.042 - 0.280)	0.043 (0.035 - 0.050)	0.0003
BAIBA	0.003 (0.002 - 0.004)	0.005 (0.003 - 0.007)	<0.0001
Carnosine	0.001 (0.001 - 0.001)	0.0009 (0.0006 - 0.0010)	0.002
Choline	0.28 (0.23 - 0.34)	0.31 (0.27 - 0.39)	0.01
Citrate	0.82 (0.70 - 1.03)	1.03 (0.87 - 1.26)	0.0003
Citrulline	60.53 (45.20 - 74.33)	62.33 (52.53 - 91.37)	0.02
Creatinine	0.30 (0.27 - 0.34)	0.34 (0.28 - 0.38)	0.002
Cystine	0.026 (0.021 - 0.031)	0.036 (0.029 - 0.045)	<0.0001
Isocitrate	6.71 (5.15 - 10.48)	8.14 (6.48 - 13.24)	0.03
Ornithine	0.09 (0.07 - 0.12)	0.12 (0.09 - 0.14)	<0.0001
Proline	4.07 (3.15 - 4.83)	4.69 (4.00 - 5.81)	0.002
Pyruvate	0.31 (0.23 - 0.41)	0.37 (0.29 - 0.54)	0.007
SAM	0.0 (0.0 - 0.0)	0.0003 (0.0 - 0.0004)	<0.0001
Threonine	0.34 (0.30 - 0.39)	0.32 (0.28 - 0.38)	0.03
Coronary sinus			
AAA	0.001 (0.001 - 0.003)	0.003 (0.002 - 0.004)	<0.0001
Aconitate	0.36 (0.26 - 0.51)	0.46 (0.35 - 0.65)	0.0007

Alanine	0.76 (0.60 - 1.02)	0.85 (0.67 - 1.19)	0.03
Asparagine	0.044 (0.034 - 0.256)	0.039 (0.032 - 0.044)	0.02
BAIBA	0.003 (0.002 - 0.004)	0.004 (0.003 - 0.007)	<0.0001
Choline	0.27 (0.22 - 0.32)	0.31 (0.25 - 0.39)	0.005
Citrate	0.86 (0.71 - 1.19)	1.06 (0.90 -1.32)	0.004
Citrulline	47.52 (35.04 - 62.16)	58.94 (41.63 - 87.47)	0.005
Creatinine	0.29 (0.27 - 0.32)	0.32 (0.28 - 0.38)	0.0006
Cystine	0.026 (0.020 - 0.033)	0.034 (0.029 - 0.044)	<0.0001
Cytidine	0.002 (0.002 - 0.004)	0.004 (0.003 - 0.006)	0.0002
Isocitrate	7.24 (5.19 - 10.15)	8.15 (6.21 - 12.44)	0.03
KLeu	8.93 (7.09 - 11.01)	7.16 (5.88 - 9.47)	0.0007
Lysine	0.27 (0.24 - 0.32)	0.31 (0.26 - 0.37)	0.0005
Malate	1.64 (1.18 - 2.05)	1.79 (1.25 - 3.16)	0.03
Methionine	60.06 (48.17 - 68.24)	67.05 (55.20 - 79.57)	0.005
Ornithine	0.08 (0.07 - 0.11)	0.12 (0.09 - 0.15)	<0.0001
Proline	3.72 (2.98 - 4.31)	4.46 (3.97 - 5.70)	<0.0001
SAM	0.0 (0.0 - 0.0)	0.0002 (0.0 - 0.003)	<0.0001
Tyrosine	0.50 (0.45 - 0.59)	0.57 (0.46 - 0.68)	0.01
Aortic root			
AAA	0.001 (0.001 - 0.003)	0.003 (0.002 -0.005)	0.0001
Aconitate	0.34 (0.26 - 0.49)	0.44 (0.35 - 0.68)	0.0003
Alanine	0.72 (0.59 - 0.99)	0.83 (0.64 - 1.08)	0.01
BAIBA	0.003 (0.002 - 0.004)	0.005 (0.004 - 0.007)	<0.0001
Citrate	0.87 (0.73 - 1.14)	1.07 (0.94 - 1.36)	0.0009
Citrulline	45.97 (34.84 - 59.78)	55.88 (41.7 - 85.52)	0.001
Cystine	0.026 (0.020 - 0.033)	0.034 (0.029 - 0.043)	<0.0001
Fumarate	0.09 (0.06 - 0.13)	0.06 (0.05 - 0.10)	0.04
Hydroxy-Proline	0.15 (0.13 - 0.21)	0.18 (0.16 - 0.22)	0.004

Isocitrate	7.28 (5.32 - 9.51)	8.32 (6.36 - 11.85)	0.02
KIle	6.59 (5.78 - 8.01)	5.97 (4.78 - 7.31)	0.02
KLeu	10.79 (8.72 - 13.37)	9.23 (6.97 - 11.83)	0.009
Lysine	0.27 (0.23 - 0.31)	0.30 (0.24 - 0.36)	0.004
Malate	1.52 (1.09 -1.88)	1.70 (1.24 - 3.08)	0.02
Methionine	61.05 (52.52 - 73.30)	69.04 (56.35 - 79.47)	0.02
Ornithine	0.08 (0.06 - 0.09)	0.12 (0.09 - 0.14)	<0.0001
Proline	3.66 (2.84 - 4.56)	4.55 (3.93 - 5.73)	<0.0001
SAM	0.0 (0.0 - 0.0)	0.0002 (0.0 - 0.0003)	<0.0001
Succinate	0.55 (0.43 - 0.63)	0.58 (0.48 - 0.78)	0.03
Tyrosine	0.49 (0.44 - 0.56)	0.58 (0.49 - 0.69)	0.002

Values shown are median (quartiles 1 to 3) concentrations of the respective metabolites. Concentrations are presented as area ratio after normalisation to the internal standards.

Conclusions from the analysis of aqueous metabolites

Analysis of the aqueous metabolites between the aortic stenosis and control cohorts demonstrated several of them to be present in significantly different concentrations between the two cohorts. Metabolites such as AAA, aconitate, BAIBA, citrate, citrulline, cystine, isocitrate, ornithine, proline and SAM were all present in a significantly higher concentration across all collection sites in the aortic stenosis cohort. The presence of a higher concentration of AAA, BAIBA and SAM is similar to the HCM cohort, and the role of these metabolites in human metabolism and their limited exploration in cardiac diseases has been discussed in Section 5.1.2 and Chapter 8. The metabolism of citrulline,

isocitrate and ornithine under normal conditions (control cohort) and its alterations during cardiac diseases has been discussed in Chapter 8.

Turer *et al* reported changes in the concentration of certain aqueous metabolites post I/R in patients undergoing cardiac surgery.[285] A subset of these patients had aortic stenosis, but a separate analysis of their results was not provided. As it was patients undergoing cardiac surgery who were recruited for the study, they could not recruit patients with no underlying cardiac disease. Therefore to the best of my knowledge, comparison of aqueous metabolites between patients with no underlying cardiac disease to those with aortic stenosis is being reported for the first time.

5.2.3 Cardiac metabolism between the control and aortic stenosis cohorts at baseline and during pacing

Assessment of the cardiac metabolism between the control and aortic stenosis cohorts at baseline and during pacing was performed. There were several metabolites whose overall trend in the metabolism (extraction or elution) was similar between the two cohorts (table 5.2.3). This included the extraction of glutamate and KLeu, and the elution of succinate at baseline, which remained the same during pacing in both the cohorts. Besides these similarities, there were some notable differences in the cardiac metabolism between the two cohorts. These differences are described below:

1) Glutamate: it was extracted in both the cohorts at baseline, with significantly lower extraction in the aortic stenosis cohort. During pacing the extraction decreased in both cohorts, with no significant difference between the two.

2) BAIBA: during baseline and pacing there was no significant difference in the trans-cardiac gradient between the control and aortic stenosis cohorts. But its metabolism switched from elution to extraction between the baseline and pacing states in the aortic stenosis cohort, and was significantly different between the two states. This net increase in extraction of BAIBA from baseline to pacing was significantly higher in the aortic stenosis cohort as compared to the controls (0.0006 vs 0.0, p=0.02). The significance of this result and the role of BAIBA in cardiac and skeletal muscle metabolism have been discussed further in Chapter 8.
3) KLeu: it was extracted at baseline in both the cohorts with no significant difference between them. During pacing its net extraction increased in the control cohort, while it slightly decreased in the aortic stenosis cohort. The difference in the net increase of extraction in the control cohort versus the net fall of extraction in the aortic stenosis cohort was not significantly different (0.18 vs 0.35, p=0.38). The metabolism of BCAAs is different between various cohorts and it changes from baseline to pacing; these results are comprehensively discussed in Chapter 8.
4) Citrulline: the metabolism of citrulline followed a different trend between the baseline and pacing states in the control and aortic stenosis cohorts. There was an increased extraction of citrulline during pacing in the control cohort, while the extraction decreased in the aortic stenosis cohort. Though the changes between the baseline and pacing states were not significant in both the cohorts, its important to note that an opposite trend was observed. These results are further discussed in Chapter 8, where the role citrulline and the changes in its metabolism in various cohorts has been described.

The influence of increased coronary blood flow on extraction and elution of metabolites in the control and aortic stenosis cohorts has been considered and discussed in Sections 3.3.3 and 4.2.2.

Table 5.2.3: Trans-cardiac gradient (aortic root – coronary sinus) of selected aqueous metabolites measured within each patient, at baseline and during pacing in the control and aortic stenosis cohorts. Differences between the groups statistically analysed using either two-tailed Student's t-test or Mann-Whitney U-test. Statistical significance was defined as a p-value<0.05. Metabolites listed in alphabetical order.

Metabolite	Control	Aortic stenosis	p value
Baseline			
Alanine	−0.02 (-0.07 - 0.06)	−0.01 (−0.07 - 0.08)	0.56
BAIBA	0.0 (−0.0005 - 0.0)	−0.0002 (−0.0009 - 0.0)	0.46
Citrulline	0.13 (−10.04 - 9.22)	5.70 (−4.66 - 13.42)	0.31
Glutamate	1.15 (0.61 - 1.39)	0.78 (0.54 - 0.86)	0.02
Isocitrate	0.25 (−0.71 - 1.66)	1.07 (−0.39 - 2.21)	0.26
KLeu	2.47 (−0.06 - 3.72)	1.62 (0.69 - 3.34)	0.91
KVal	0.70 (0.34 - 1.13)	0.71 (0.60 - 1.45)	0.45
Malate	−0.04 (−0.26 - 0.21)	0.11 (−0.27 - 0.46)	0.38
Succinate	−0.14 (−0.28 - −0.03)	−0.06 (−0.23 - 0.02)	0.38
Pacing			
Alanine	0.05 (−0.11 - 0.09)	−0.03 (−0.17 - 0.05)	0.09

BAIBA	0.0 (−0.0006 - 0.0)	6.835e-005 (−0.0002 - 0.001)	0.11
Citrulline	5.79 (−4.13 - 15.35)	0.89 (−6.88 - 7.93)	0.47
Glutamate	0.86 (0.39 - 1.09)	0.45 (0.20 - 0.69)	0.08
Isocitrate	0.33 (−0.57 - 2.45)	0.01 (−0.77 - 1.08)	0.20
KLeu	3.00 (0.57 - 4.35)	1.53 (0.07 - 2.48)	0.21
KVal	0.93 (0.07 - 1.85)	0.69 (−0.07 - 0.99)	0.46
Malate	0.21 (−0.39 - 0.45)	0.09 (−0.18 - 0.36)	0.74
Succinate	−0.11 (−0.34 - 0.02)	−0.12 (−0.35 - −0.05)	0.65

Values shown are median (quartiles 1 to 3) concentrations of the respective metabolites. Concentrations are presented as area ratio after normalisation to the internal standards.

5.2.4 Summary

Following conclusions were drawn from the metabolomic analysis between the control and aortic stenosis cohorts (table 5.2.4):

1) There was a significantly higher concentration of long chain acylcarnitines species such as C12:1, C14-OH, C16:1, C16-OH, C18-OH and C20:1 across all-three collection sites in the aortic stenosis cohort, while C8-DC was present in a significantly lower concentration.
2) AAA, aconitate, BAIBA, citrate, citrulline, cystine, isocitrate, ornithine, proline and SAM were present in a higher concentration in the aortic stenosis cohort across all-three collection sites, while threonine was present in a significantly lower concentration.

3) The metabolism of BAIBA switched from elution to extraction between the baseline and pacing states in the aortic stenosis cohort, with the net increase in extraction from baseline to pacing being significantly higher as compared to controls.

Table 5.2.4: Summary of the most significant results on comparing the metabolomic profile between the control and aortic stenosis cohorts. Both baseline and pacing samples were combined for analysis. Differences between the groups statistically analysed using either two-tailed Student's t-test or Mann-Whitney U-test. Statistical significance was defined as a p-value<0.05.

Control vs Aortic stenosis cohorts			
Femoral vein			
	Control	**Aortic stenosis**	**p value**
C12:1	0.16 (0.12 - 0.24)	0.24 (0.16 - 0.34)	0.0003
C14-OH	0.010 (0.007 - 0.015)	0.015 (0.010 - 0.021)	<0.0001
C16:1	0.11 (0.08 - 0.16)	0.19 (0.14 - 0.28)	<0.0001
C16-OH	0.008 (0.006 - 0.012)	0.013 (0.009 - 0.018)	0.0002
C18-OH	0.003 (0.002 - 0.006)	0.007 (0.005 - 0.009)	<0.0001
C20:1	0.006 (0.005 - 0.008)	0.008 (0.006 - 0.010)	0.0001
AAA	0.001 (0.001 - 0.003)	0.003 (0.001 - 0.004)	0.0002
Aconitate	0.41 (0.29 - 0.59)	0.53 (0.35 - 0.77)	0.005
BAIBA	0.003 (0.002 - 0.004)	0.005 (0.003 - 0.007)	<0.0001
Citrate	0.82 (0.70 - 1.03)	1.03 (0.87 - 1.26)	0.0003
Citrulline	60.53 (45.20 - 74.33)	62.33 (52.53 - 91.37)	0.02

Cystine	0.026 (0.021 - 0.031)	0.036 (0.029 - 0.045)	<0.0001
Isocitrate	6.71 (5.15 - 10.48)	8.14 (6.48 - 13.24)	0.03
Ornithine	0.09 (0.07 - 0.12)	0.12 (0.09 - 0.14)	<0.0001
Proline	4.07 (3.15 - 4.83)	4.69 (4.00 - 5.81)	0.002
SAM	0.0 (0.0 - 0.0)	0.0003 (0.0 - 0.0004)	<0.0001

Coronary sinus

	Control	**Aortic stenosis**	
C12:1	0.17 (0.13 - 0.22)	0.22 (0.18 - 0.36)	0.0004
C14-OH	0.011 (0.008 - 0.016)	0.015 (0.011 - 0.023)	0.0006
C16:1	0.11 (0.07 - 0.15)	0.17 (0.13 - 0.27)	<0.0001
C16-OH	0.009 (0.006 - 0.012)	0.013 (0.009 - 0.019)	<0.0001
C18-OH	0.003 (0.002 - 0.005)	0.006 (0.004 - 0.010)	<0.0001
C20:1	0.006 (0.004 - 0.008)	0.008 (0.006 - 0.011)	<0.0001
AAA	0.001 (0.001 - 0.003)	0.003 (0.002 - 0.004)	<0.0001
Aconitate	0.36 (0.26 - 0.51)	0.46 (0.35 - 0.65)	0.0007
BAIBA	0.003 (0.002 - 0.004)	0.004 (0.003 - 0.007)	<0.0001
Citrate	0.86 (0.71 - 1.19)	1.06 (0.90 -1.32)	0.004
Citrulline	47.52 (35.04 - 62.16)	58.94 (41.63 - 87.47)	0.005
Cystine	0.026 (0.020 - 0.033)	0.034 (0.029 - 0.044)	<0.0001
Isocitrate	7.24 (5.19 - 10.15)	8.15 (6.21 - 12.44)	0.03
Ornithine	0.08 (0.07 - 0.11)	0.12 (0.09 - 0.15)	<0.0001
Proline	3.72 (2.98 - 4.31)	4.46 (3.97 - 5.70)	<0.0001
SAM	0.0 (0.0 - 0.0)	0.0002 (0.0 - 0.003)	<0.0001

Aortic root

	Control	**Aortic stenosis**	
C12:1	0.15 (0.11 - 0.24)	0.23 (0.16 - 0.32)	0.0004
C14-OH	0.011 (0.008 - 0.015)	0.015 (0.010 - 0.023)	0.0006

C16:1	0.13 (0.08 - 0.16)	0.19 (0.13 - 0.27)	<0.0001
C16-OH	0.009 (0.007 - 0.011)	0.013 (0.009 - 0.017)	0.0001
C18-OH	0.004 (0.003 - 0.006)	0.007 (0.005 - 0.010)	<0.0001
C20:1	0.006 (0.004 - 0.008)	0.008 (0.007 - 0.011)	<0.0001
AAA	0.001 (0.001 - 0.003)	0.003 (0.002 -0.005)	0.0001
Aconitate	0.34 (0.26 - 0.49)	0.44 (0.35 - 0.68)	0.0003
BAIBA	0.003 (0.002 - 0.004)	0.005 (0.004 - 0.007)	<0.0001
Citrate	0.87 (0.73 - 1.14)	1.07 (0.94 - 1.36)	0.0009
Citrulline	45.97 (34.84 - 59.78)	55.88 (41.7 - 85.52)	0.001
Cystine	0.026 (0.020 - 0.033)	0.034 (0.029 - 0.043)	<0.0001
Isocitrate	7.28 (5.32 - 9.51)	8.32 (6.36 - 11.85)	0.02
Ornithine	0.08 (0.06 - 0.09)	0.12 (0.09 - 0.14)	<0.0001
Proline	3.66 (2.84 - 4.56)	4.55 (3.93 - 5.73)	<0.0001
SAM	0.0 (0.0 - 0.0)	0.0002 (0.0 - 0.0003)	<0.0001

Trans-Cardiac gradient

	Control	**Aortic stenosis**	
Baseline			
BAIBA	0.0 (−0.0005 - 0.0)	−0.0002 (−0.0009 - 0.0)	0.46
Pacing			
BAIBA	0.0 (−0.0006 - 0.0)	6.835e-005 (−0.0002 - 0.001)	0.11

Values shown are median (quartiles 1 to 3) concentrations of the respective metabolites. Concentrations are presented as area ratio after normalisation to the internal standards.

5.3 Metabolomic differences between the HCM and aortic stenosis cohorts

The final pair-wise analysis was performed between the HCM and aortic stenosis cohorts. A total of 35 HCM and 36 aortic stenosis patients were included in the final analysis. The clinical characteristics of these patients are described in Section 3.1.

5.3.1 Analysis of acylcarnitines between the HCM and aortic stenosis cohorts

a) Femoral vein

PCA analysis of the acylcarnitines in the femoral vein samples from the HCM and aortic stenosis cohorts was performed. The PCA scores plot exhibited an overlap between the two cohorts. Further assessment of these samples was performed using the PLS-DA method, where better separation was seen on the scores plot of the generated model (figure 5.3.1, plot A) (R^2X=0.48, R^2Y=0.27, Q^2=0.16). The validity and goodness of fit of the original model were confirmed using 100 random permutations, which demonstrated that all the permuted R^2 and Q^2 values on the left were lower than the original values on the right (intercepts: R^2=[0.0,0.09], Q^2=[0.0,−0.12]). This indicated a valid original model, and the most discriminating (VIP score ≥1) metabolites from it were assessed using either the two-tailed Student's t-test or the Mann-Whitney U-test to independently verify their significance. The following acylcarnitines were present in a significantly higher concentration in the femoral vein samples from the aortic stenosis cohort: C6, C8, C10, C12, C12:1, C14, C14-OH, C16:1, C16-OH, C18-OH and C20:1 (table 5.3.1).

b) Coronary sinus

Using both multivariate (unsupervised & supervised) and univariate method's a detailed assessment of the coronary sinus samples from the HCM and aortic stenosis cohorts was performed. The PCA analysis on its scores plot demonstrated an overlap between the two cohorts. Further assessment using the PLS-DA approach built a model, which exhibited clear separation between the two cohorts (figure 5.3.1, plot B) (R^2X=0.52, R^2Y=0.25, Q^2=0.12). The validity and goodness of fit of the original model were confirmed using 100 random permutations (intercepts: R^2=[0.0,0.09], Q^2=[0.0,−0.12]).

Further univariate analysis of the most discriminating (VIP score ≥1) metabolites using either the two-tailed Student's t-test or the Mann-Whitney U-test demonstrated a significantly higher concentration of C8, C10, C12, C14-OH, C16-OH and C20:1 in the coronary sinus samples from the aortic stenosis cohort (table 5.3.1).

c) Aortic root

Analysis of aortic root samples from the HCM and aortic stenosis cohorts was performed using similar analytical strategy as applied during the assessment of femoral vein and coronary sinus samples. Unbiased multivariate testing using the PCA approach demonstrated little separation between the two cohorts. A more reliable statistical assessment of these samples was then performed using the PLS-DA approach. This exhibited a distinct separation between the two cohorts on the scores plot of the generated model (figure 5.3.1, plot C) (R^2X=0.49, R^2Y=0.25, Q^2=0.12). The validity and goodness of fit of the original model were confirmed using 100 random permutations, where all permuted R^2 and Q^2 values were lower than the original values (intercepts: R^2=[0.0,0.09],

Q^2=[0.0,−0.12]). Further assessment of the most discriminating (VIP score ≥1) metabolites using either the two-tailed Student's t-test or the Mann-Whitney U-test demonstrated that the following acylcarnitines were present in a significantly higher concentration in the aortic root samples from the aortic stenosis cohort: C8, C10, C12, C14-OH, C16:1, C16-OH, C18-OH, C20 and C20:1 (table 5.3.1).

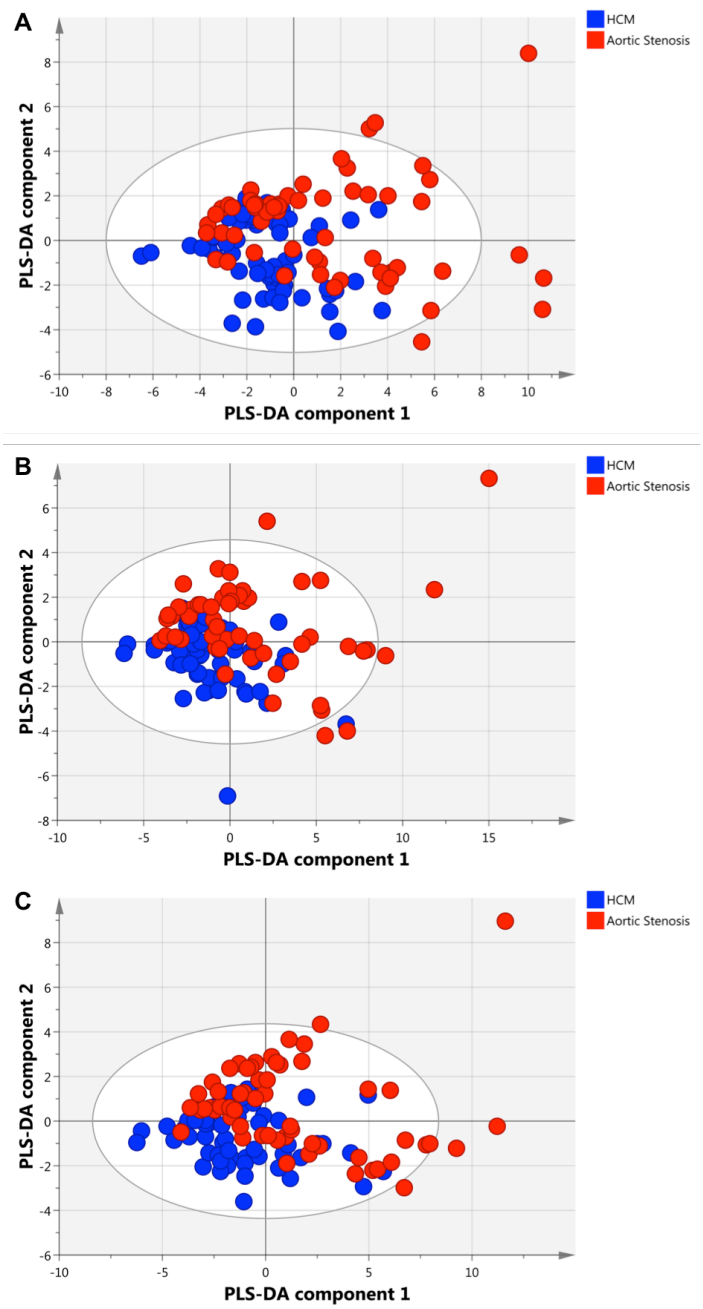

Figure 5.3.1: Partial least squares- discriminant analysis (PLS-DA) scores plot of acylcarnitines between HCM (blue circles) & aortic stenosis (red circles) cohorts in the femoral vein (A), coronary sinus (B) and aortic root (C) collection sites.

Table 5.3.1: Concentration of acylcarnitines which were significantly different between the HCM and aortic stenosis cohorts; measured in femoral vein, coronary sinus and aortic root collection sites. Both baseline and pacing samples were combined for analysis. Differences between the groups statistically analysed using either two-tailed Student's t-test or Mann-Whitney U-test. Statistical significance was defined as a p-value<0.05. Metabolites listed in alphabetical order.

Metabolite	HCM	Aortic stenosis	p value
Femoral vein			
C6	0.17 (0.11 - 0.21)	0.20 (0.14 - 0.30)	0.0009
C8	0.29 (0.22 - 0.39)	0.37 (0.25 - 0.47)	0.006
C10	0.46 (0.37 - 0.61)	0.59 (0.43 - 0.74)	0.008
C12	0.13 (0.12 - 0.19)	0.18 (0.12 - 0.27)	0.014
C12:1	0.20 (0.17 - 0.25)	0.24 (0.16 - 0.34)	0.002
C14	0.09 (0.07 - 0.12)	0.11 (0.08 - 0.15)	0.03
C14-OH	0.011 (0.009 - 0.015)	0.015 (0.010 - 0.021)	<0.0001
C16:1	0.14 (0.10 - 0.18)	0.19 (0.14 - 0.28)	0.007
C16-OH	0.009 (0.007 - 0.012)	0.013 (0.009 - 0.018)	<0.001
C18-OH	0.005 (0.003 - 0.007)	0.007 (0.005 - 0.009)	0.003
C20:1	0.006 (0.005 - 0.008)	0.008 (0.006 - 0.010)	<0.0001
Coronary			

C8	0.29 (0.20 - 0.34)	0.37 (0.28 - 0.48)	0.0002
C10	0.44 (0.32 - 0.56)	0.57 (0.42 - 0.76)	0.0004
C12	0.14 (0.12 - 0.18)	0.17 (0.12 - 0.32)	0.01
C14-OH	0.011 (0.009 - 0.014)	0.015 (0.011 - 0.023)	<0.0001
C16-OH	0.009 (0.008 - 0.014)	0.013 (0.009 - 0.019)	0.004
C20:1	0.006 (0.005 - 0.008)	0.008 (0.006 - 0.011)	0.0008
Aortic root			
C8	0.26 (0.17 - 0.34)	0.36 (0.25 - 0.45)	<0.0001
C10	0.41 (0.28 - 0.54)	0.55 (0.40 - 0.67)	0.001
C12	0.14 (0.12 - 0.17)	0.17 (0.13 - 0.31)	0.003
C14-OH	0.011 (0.009 - 0.014)	0.015 (0.010 - 0.023)	0.003
C16:1	0.16 (0.12 - 0.19)	0.19 (0.13 - 0.27)	0.03
C16-OH	0.009 (0.007 - 0.012)	0.013 (0.009 - 0.017)	0.0009
C18-OH	0.006 (0.004 - 0.008)	0.007 (0.005 - 0.010)	0.048
C20	0.0016 (0.0013 - 0.0022)	0.0020 (0.0017 - 0.0025)	0.006
C20:1	0.007 (0.005 - 0.008)	0.008 (0.007 - 0.011)	<0.0001

Values shown are median (quartiles 1 to 3) concentrations of the respective metabolites. Concentrations are presented as area ratio after normalisation to the internal standards.

Conclusions from the analysis of acylcarnitines

Analysis of acylcarnitines between the HCM and aortic stenosis cohorts demonstrated a significantly higher concentration of the following medium and long chain acylcarnitines in the aortic stenosis cohort across all-three collection sites: C8, C10, C12, C14-OH, C16-OH and C20:1. Subsequent analysis of

these acylcarnitines after normalisation to eGFR yielded similar results. As described before in the analysis of the control versus HCM cohorts (Section 5.1.1) and control vs aortic stenosis (Section 5.2.1) cohorts, the higher concentration of these acylcarnitines is suggestive of dys-regulation in fatty acid β−oxidation. A detailed review of this dysregulation and its validation through correlation with changes in the metabolomic transcriptome are described in Chapters 7 & 8.

5.3.2 Analysis of aqueous metabolites between the HCM and aortic stenosis cohorts

a) Femoral vein

Aqueous metabolites were analysed in the femoral vein samples from the HCM and aortic stenosis cohorts in an unbiased manner using the PCA approach. This demonstrated a clear separation between the two cohorts. Further assessment of these samples was performed using the PLS-DA approach. A distinct separation was visualised between the two cohorts on the scores plot of the generated model (figure 5.3.2, plot A) (R^2X=0.37, R^2Y=0.58, Q^2=0.26). The validity and tightness of fit of the original model were confirmed using 100 random permutations, where all permuted R^2 and Q^2 values were lower than the original values (intercepts: R^2=[0.0,0.22], Q^2=[0.0,−0.28]).

Metabolites with a VIP score of ≥1 were further assessed using either the two-tailed Student's t-test or the Mann-Whitney U-test. This demonstrated a significantly higher concentration of aconitate, BAIBA, citrate, citrulline, cystine, glutamate, hydroxy-proline, isocitrate, methyl-histidine, ornithine, pyruvate and

SAM in the aortic stenosis cohort, and a significantly lower concentration of arginine and histidine (table 5.3.2).

b) Coronary sinus

Coronary sinus samples from the two cohorts were analysed to assess for any differences in the aqueous metabolites between them. PCA analysis of the samples from the two cohorts showed separation on its scores plot. This was further verified using the PLS-DA analysis, where the generated model clearly discriminated the two cohorts as visualised on its scores plot (figure 5.3.2, plot B) (R^2X=0.32, R^2Y=0.38, Q^2=0.24). The validity and goodness of fit of the original model were confirmed using 100 random permutations (intercepts: R^2=[0.0,0.14], Q^2=[0.0,−0.17]).

On subsequent univariate analysis, alanine aconitate, BAIBA, betane, choline citrate, citrulline, isocitrate, malate, methyl-histidine, ornithine, proline and SAM were all present in a significantly higher concentration in the aortic stenosis cohort. Only two metabolites histidine and KLeu were present in a significantly lower concentration in the aortic stenosis cohort (table 5.3.2).

c) Aortic root

Unsupervised univariate analysis of the aortic root samples was performed using the PCA approach, which demonstrated separation between the two cohorts. PLS-DA analysis of the same samples exhibited a better separation on the scores plot of a robust model (figure 5.3.2, plot C) (R^2X=0.34, R^2Y=0.62, Q^2=0.37). Using 100 random permutations it was demonstrated that the permuted values were significantly lower than the original values, indicating a

valid original model with high goodness of fit (intercepts: R^2=[0.0,0.21], Q^2=[0.0,−0.32]).

The most discriminating metabolites (VIP score of ≥1) on the PLS-DA model were further assessed using either the two-tailed Student's t-test or the Mann-Whitney U-test. This demonstrated a significantly high concentration of aconitate, alanine, BAIBA, citrate, citrulline, glutamine, hydroxy-proline isocitrate, lysine, malate, ornithine, phenylalanine, proline, pyruvate, SAM and succinate in the aortic stenosis cohort, while histidine was present in a significantly lower concentration (table 5.3.2).

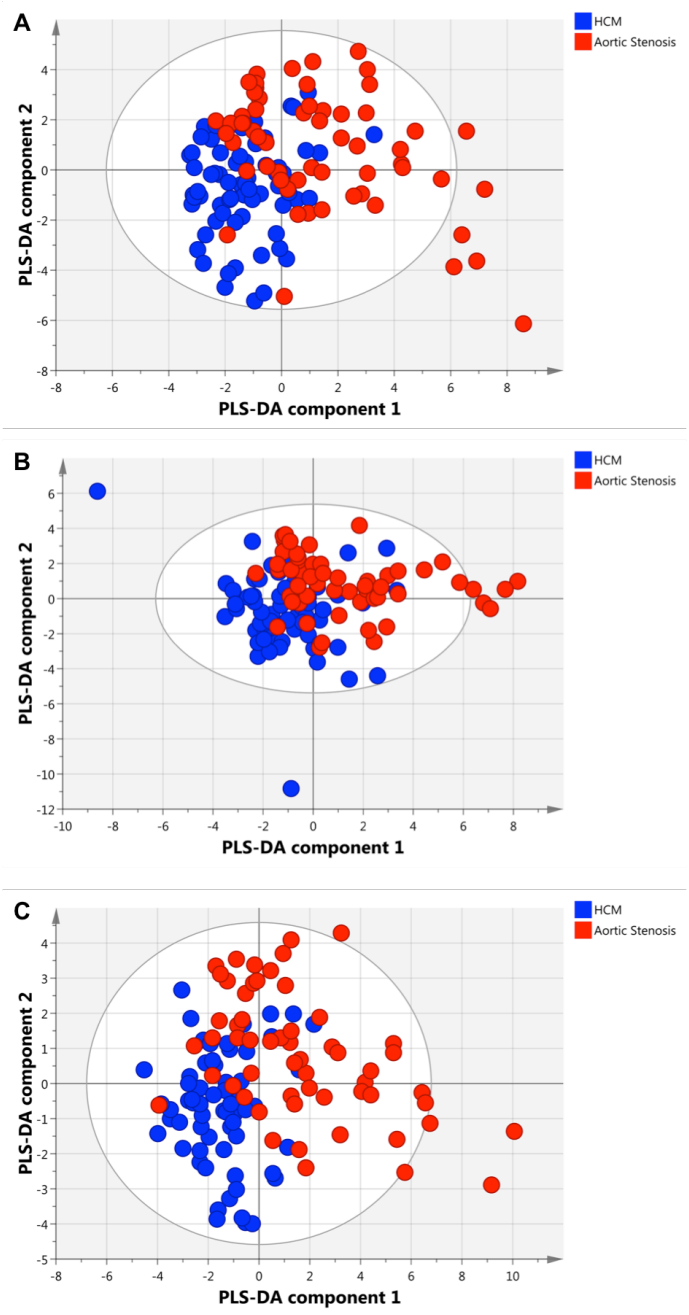

Figure 5.3.2: Partial least squares- discriminant analysis (PLS-DA) scores plot of aqueous metabolites between HCM (blue circles) & aortic stenosis (red circles) cohorts in the femoral vein (A), coronary sinus (B) and aortic root (C) collection sites.

Table 5.3.2: Concentration of aqueous metabolites which were significantly different between the HCM and aortic stenosis cohorts; measured in femoral vein, coronary sinus and aortic root collection sites. Both baseline and pacing samples were combined for analysis.

Differences between the groups statistically analysed using either two-tailed Student's t-test or Mann-Whitney U-test. Statistical significance was defined as a p-value<0.05. Metabolites listed in alphabetical order.

Metabolite	HCM	Aortic stenosis	p value
Femoral vein			
Aconitate	0.41 (0.32 - 0.50)	0.53 (0.35 - 0.77)	0.0007
Arginine	2.79 (2.49 - 3.29)	2.54 (2.22 - 3.07)	0.007
BAIBA	0.004 (0.003 - 0.005)	0.005 (0.003 - 0.007)	0.0004
Citrate	0.86 (0.77 - 1.02)	1.03 (0.87 - 1.26)	0.0008
Citrulline	59.67 (44.60 - 75.04)	62.33 (52.53 - 91.37)	0.03
Cystine	0.027 (0.023 - 0.034)	0.036 (0.029 - 0.045)	<0.0001
Glutamate	0.94 (0.83 - 1.15)	1.09 (0.86 - 1.45)	0.006
Histidine	1.74 (1.54 - 1.96)	1.49 (1.32 - 1.75)	0.0003
Hydroxy-Proline	0.17 (0.13 - 0.23)	0.20 (0.17 - 0.24)	0.02
Isocitrate	6.99 (5.53 - 8.78)	8.14 (6.48 - 13.24)	0.005
Methyl-Histidine	0.20 (0.10 - 0.41)	0.29 (0.18 - 0.57)	0.02
Ornithine	0.10 (0.07 - 0.12)	0.12 (0.09 - 0.14)	0.001
Pyruvate	0.32 (0.25 - 0.38)	0.37 (0.29 - 0.54)	0.002
SAM	9.101e-005 (0.0 - 0.0002)	0.0003 (0.0 - 0.0004)	0.002
Coronary sinus			
Aconitate	0.36 (0.28 - 0.45)	0.46 (0.35 - 0.65)	0.0003
Alanine	0.72 (0.61 - 0.82)	0.85 (0.67 - 1.19)	0.003
BAIBA	0.003 (0.003 - 0.005)	0.004 (0.003 - 0.007)	0.006
Betane	12.95 (11.69 - 15.93)	13.90 (12.73 - 18.39)	0.04

Choline	0.26 (0.22 - 0.33)	0.31 (0.25 - 0.39)	0.009
Citrate	0.89 (0.76 - 1.49)	1.06 (0.90 -1.32)	0.0005
Citrulline	45.45 (35.60 - 57.15)	58.94 (41.63 - 87.47)	0.001
Histidine	1.61 (1.33 - 1.85)	1.37 (1.23 - 1.58)	0.02
Isocitrate	6.43 (5.20 - 8.90)	8.15 (6.21 - 12.44)	0.0006
KLeu	8.99 (7.07 - 11.19)	7.16 (5.88 - 9.47)	0.007
Malate	1.41 (1.11 - 1.88)	1.79 (1.25 - 3.16)	0.003
Methyl-Histidine	0.19 (0.09 - 0.43)	0.26 (0.17 - 0.54)	0.02
Ornithine	0.09 (0.06 - 0.12)	0.12 (0.09 - 0.15)	0.002
Proline	4.13 (3.28 - 4.63)	4.46 (3.97 - 5.70)	0.003
SAM	7.739e-005 (0.0 - 0.0002)	0.0002 (0.0 - 0.003)	0.004
Aortic root			
Aconitate	0.31 (0.27 - 0.39)	0.44 (0.35 - 0.68)	<0.0001
Alanine	0.68 (0.60 - 0.82)	0.83 (0.64 - 1.08)	<0.0001
BAIBA	0.003 (0.003 - 0.004)	0.005 (0.004 - 0.007)	0.0003
Citrate	0.89 (0.82 - 1.08)	1.07 (0.94 - 1.36)	0.0003
Citrulline	40.94 (32.56 - 48.68)	55.88 (41.7 - 85.52)	<0.0001
Glutamine	12.95 (12.20 - 13.54)	13.41 (12.81 - 14.16)	0.006
Histidine	1.63 (1.45 - 1.83)	1.42 (1.24 - 1.68)	0.01
Hydroxy-Proline	0.15 (0.12 - 0.22)	0.18 (0.16 - 0.22)	0.02
Isocitrate	6.00 (4.91 - 7.56)	8.32 (6.36 - 11.85)	<0.0001
Lysine	0.26 (0.24 - 0.31)	0.30 (0.24 - 0.36)	0.02
Malate	1.25 (0.92 - 1.61)	1.70 (1.24 - 3.08)	<0.0001
Ornithine	0.10 (0.06 - 0.12)	0.12 (0.09 - 0.14)	0.004
Phenylalanine	1.63 (1.39 - 1.81)	1.70 (1.58 - 2.02)	0.01
Proline	4.14 (3.32 - 4.79)	4.55 (3.93 - 5.73)	0.01
Pyruvate	0.24 (0.19 - 0.31)	0.31 (0.23 - 0.43)	0.0003

SAM	0.0001 (0.0 - 0.0002)	0.0002 (0.0 - 0.0003)	0.008
Succinate	0.46 (0.39 - 0.56)	0.58 (0.48 - 0.78)	<0.0001

Values shown are median (quartiles 1 to 3) concentrations of the respective metabolites. Concentrations are presented as area ratio after normalisation to the internal standards.

Conclusions from the analysis of aqueous metabolite

Analysis of the aqueous metabolites between the HCM and aortic stenosis cohorts found several metabolites to be present in significantly different concentrations. While there was a higher concentration of aconitate, BAIBA, citrate, citrulline, isocitrate ornithine and SAM in the aortic stenosis cohort across all-three collection sites, the concentration of histidine was significantly lower. As previously mentioned there are no reported studies describing the metabolomic profile of aortic stenosis patients or its comparison with HCM.

The role of BAIBA and SAM in the human metabolism and the alterations in their metabolism during cardiovascular diseases has been discussed in Section 5.1.2 and Chapter 8. Aconitate, citrate and isocitrate play a vital role in the energy homeostasis via the citric acid cycle activity. The changes in the citric acid cycle activity in different cohorts, assessed by the changes in the metabolism of some of its key intermediates has been discussed in Chapter 8. In the same chapter alteration in amino acid metabolism including that of citrulline and ornithine have been discussed.

5.3.3 Cardiac metabolism between the HCM and aortic stenosis cohorts at baseline and during pacing

Cardiac metabolism between the two cohorts was then assessed during the baseline and pacing states (Table5.3.3). The most significant differences observed at baseline were as follows:

1) KLeu and KVal: they were extracted in the aortic stenosis cohort, which was significantly higher than the HCM cohort.
2) Aconitate, citrulline, isocitrate and malate: they were all extracted in the aortic stenosis cohort and eluted in the HCM cohort, with a significant difference between the two.

Metabolism of HCM and aortic stenosis patients altered during pacing and thus the differences present at baseline were not observed during pacing, these changes were as follows:

1) KLeu: there was a significant increase in the extraction of KLeu in the HCM cohort, while the extraction decreased marginally in the aortic stenosis cohort.
2) Citrulline and malate: there was a significant decrease in their elution during pacing in the HCM cohort, while their extraction decreased non-significantly during pacing in the aortic stenosis cohort.
3) Isocitrate: its metabolism switched from elution to extraction in the HCM cohort during pacing; this was significantly higher than baseline. The extraction of isocitrate decreased in the aortic stenosis cohort, this change was not significant.
4) Aconitate: at baseline it was extracted in the aortic stenosis cohort and eluted in the HCM cohort, with a significant difference between the two.

During pacing its metabolism switched to elution in the aortic stenosis cohort and the elution decreased in the HCM cohort.

The changes in the metabolism of BCAAs, malate, citrulline and isocitrate have been discussed in Chapter 8.

The increased coronary blood influences the extraction and elution of metabolites during pacing and the impact of this consideration in the HCM and aortic stenosis cohorts has been discussed in Sections 4.1.2 and 4.2.2.

Table 5.3.3: Trans-cardiac gradient (aortic root – coronary sinus) of selected aqueous metabolites measured within each patient, at baseline and during pacing in the HCM and aortic stenosis cohorts. Differences between the groups statistically analysed using either two-tailed Student's t-test or Mann-Whitney U-test. Statistical significance was defined as a p-value<0.05. Metabolites listed in alphabetical order.

Metabolite	HCM	AS	p value
Baseline			
Aconitate	−0.06	0.05	0.03
Alanine	−0.04 (−0.13 - 0.04)	−0.01 (−0.07 - 0.08)	0.76
BAIBA	0.0 (−0.0004 - 0.0004)	−0.0002 (−0.0009 - 0.0)	0.11
Citrulline	−9.63 (−21.63 - −2.49)	5.70 (−4.66 - 13.42)	0.01
Glutamate	0.89 (0.65 - 1.15)	0.78 (0.54 - 0.86)	0.08
Isocitrate	−0.66 (−2.67 - 0.69)	1.07 (−0.39 - 2.21)	0.01
KLeu	−0.84 (−1.79 - 1.89)	1.62 (0.69 - 3.34)	0.01
KVal	0.51 (−0.28 - 0.74)	0.71 (0.60 - 1.45)	0.01

Malate	−0.39 (−0.63 - −0.07)	0.11 (−0.27 - 0.46)	0.01
Succinate	−0.21 (−0.33 - −0.09)	−0.06 (−0.23 - 0.02)	0.19
Pacing			
Aconitate	−0.02	−0.01	0.55
Alanine	−0.02 (−0.09 - 0.05)	−0.03 (−0.17 - 0.05)	0.74
BAIBA	0.0 (−0.0005 - 0.0003)	6.835e-005 (−0.0002 - 0.001)	0.32
Citrulline	−1.64 (−9.99 - 11.45)	0.89 (−6.88 - 7.93)	0.99
Glutamate	0.67 (0.35 - 0.80)	0.45 (0.20 - 0.69)	0.11
Isocitrate	0.30 (−0.78 - 1.70)	0.01 (−0.77 - 1.08)	0.37
KLeu	1.19 (−0.09 - 3.56)	1.53 (0.07 - 2.48)	0.79
KVal	0.69 (−0.08 - 1.22)	0.69 (−0.07 - 0.99)	0.94
Malate	0.001 (−0.29 - 0.32)	0.09 (−0.18 - 0.36)	0.63
Succinate	−0.10 (−0.34 - 0.05)	−0.12 (−0.35 - −0.05)	0.74

Values shown are median (quartiles 1 to 3) concentrations of the respective metabolites. Concentrations are presented as area ratio after normalisation to the internal standards.

5.3.4 Summary

Following conclusion were drawn from the analysis of HCM and aortic stenosis cohorts (table 5.3.4):

1) Long and medium chain acylcarnitines were present in a higher concentration in the aortic stenosis cohort across all-three collection sites, these included: C8, C10, C12, C14-OH, C16-OH and C20:1.

2) There was higher concentration of aconitate, BAIBA, citrate, citrulline, isocitrate, ornithine and SAM in the aortic stenosis cohort across all-three collection sites. Only histidine was found in a lower concentration consistently across all-three collection sites in the aortic stenosis cohort.
3) There was a significantly higher extraction of KLeu and KVal in the aortic stenosis cohort at baseline when compared to the HCM cohort. This difference was not present during pacing as the net extraction of these metabolites increased in the HCM cohort, while it decreased in the aortic stenosis cohort.
4) There were changes in net extraction or elution of several metabolites including citrulline, isocitrate and malate, between the baseline and pacing states in the two cohorts.

Table 5.3.4: Summary of the most significant results on comparing the metabolomic profile between the HCM and aortic stenosis cohorts. Both baseline and pacing samples were combined for analysis. Differences between the groups statistically analysed using either two-tailed Student's t-test or Mann-Whitney U-test. Statistical significance was defined as a p-value<0.05.

HCM vs Aortic stenosis cohorts			
Femoral vein			
	HCM	**Aortic stenosis**	**p value**
C8	0.29 (0.22 - 0.39)	0.37 (0.25 - 0.47)	0.006
C10	0.46 (0.37 - 0.61)	0.59 (0.43 - 0.74)	0.008

C12	0.13 (0.12 - 0.19)	0.18 (0.12 - 0.27)	0.014
C14-OH	0.011 (0.009 - 0.015)	0.015 (0.010 - 0.021)	<0.0001
C16-OH	0.009 (0.007 - 0.012)	0.013 (0.009 - 0.018)	<0.001
C20:1	0.006 (0.005 - 0.008)	0.008 (0.006 - 0.010)	<0.0001
Aconitate	0.41 (0.32 - 0.50)	0.53 (0.35 - 0.77)	0.0007
BAIBA	0.004 (0.003 - 0.005)	0.005 (0.003 - 0.007)	0.0004
Citrate	0.86 (0.77 - 1.02)	1.03 (0.87 - 1.26)	0.0008
Citrulline	59.67 (44.60 - 75.04)	62.33 (52.53 - 91.37)	0.03
Isocitrate	6.99 (5.53 - 8.78)	8.14 (6.48 - 13.24)	0.005
Ornithine	0.10 (0.07 - 0.12)	0.12 (0.09 - 0.14)	0.001
SAM	9.101e-005 (0.0 - 0.0002)	0.0003 (0.0 - 0.0004)	0.002

Coronary sinus

	HCM	**Aortic stenosis**	
C8	0.29 (0.20 - 0.34)	0.37 (0.28 - 0.48)	0.0002
C10	0.44 (0.32 - 0.56)	0.57 (0.42 - 0.76)	0.0004
C12	0.14 (0.12 - 0.18)	0.17 (0.12 - 0.32)	0.01
C14-OH	0.011 (0.009 - 0.014)	0.015 (0.011 - 0.023)	<0.0001
C16-OH	0.009 (0.008 - 0.014)	0.013 (0.009 - 0.019)	0.004
C20:1	0.006 (0.005 - 0.008)	0.008 (0.006 - 0.011)	0.0008
Aconitate	0.36 (0.28 - 0.45)	0.46 (0.35 - 0.65)	0.0003
BAIBA	0.003 (0.003 - 0.005)	0.004 (0.003 - 0.007)	0.006
Citrate	0.89 (0.76 - 1.49)	1.06 (0.90 -1.32)	0.0005
Citrulline	45.45 (35.60 - 57.15)	58.94 (41.63 - 87.47)	0.001
Isocitrate	6.43 (5.20 - 8.90)	8.15 (6.21 - 12.44)	0.0006
Ornithine	0.09 (0.06 - 0.12)	0.12 (0.09 - 0.15)	0.002

SAM	7.739e-005 (0.0 - 0.0002)	0.0002 (0.0 - 0.003)	0.004

Aortic root

	HCM	Aortic stenosis	
C8	0.26 (0.17 - 0.34)	0.36 (0.25 - 0.45)	<0.0001
C10	0.41 (0.28 - 0.54)	0.55 (0.40 - 0.67)	0.001
C12	0.14 (0.12 - 0.17)	0.17 (0.13 - 0.31)	0.003
C14-OH	0.011 (0.009 - 0.014)	0.015 (0.010 - 0.023)	0.003
C16-OH	0.009 (0.007 - 0.012)	0.013 (0.009 - 0.017)	0.0009
C20:1	0.007 (0.005 - 0.008)	0.008 (0.007 - 0.011)	<0.0001
Aconitate	0.31 (0.27 - 0.39)	0.44 (0.35 - 0.68)	<0.0001
BAIBA	0.003 (0.003 - 0.004)	0.005 (0.004 - 0.007)	0.0003
Citrate	0.89 (0.82 - 1.08)	1.07 (0.94 - 1.36)	0.0003
Citrulline	40.94 (32.56 - 48.68)	55.88 (41.7 - 85.52)	<0.0001
Isocitrate	6.00 (4.91 - 7.56)	8.32 (6.36 - 11.85)	<0.0001
Ornithine	0.10 (0.06 - 0.12)	0.12 (0.09 - 0.14)	0.004
SAM	0.0001 (0.0 - 0.0002)	0.0002 (0.0 - 0.0003)	0.008

Trans-Cardiac gradient

	HCM	Aortic stenosis	
Baseline			
Citrulline	−9.63 (−21.63 - −2.49)	5.70 (−4.66 - 13.42)	0.01
Isocitrate	−0.66 (−2.67 - 0.69)	1.07 (−0.39 - 2.21)	0.01
KLeu	−0.84 (−1.79 - 1.89)	1.62 (0.69 - 3.34)	0.01
KVal	0.51 (−0.28 - 0.74)	0.71 (0.60 - 1.45)	0.01
Malate	−0.39 (−0.63 - −0.07)	0.11 (−0.27 - 0.46)	0.01
Pacing			

Citrulline	−1.64 (−9.99 - 11.45)	0.89 (−6.88 - 7.93)	0.99
Glutamate	0.67 (0.35 - 0.80)	0.45 (0.20 - 0.69)	0.11
Isocitrate	0.30 (−0.78 - 1.70)	0.01 (−0.77 - 1.08)	0.37
KLeu	1.19 (−0.09 - 3.56)	1.53 (0.07 - 2.48)	0.79
KVal	0.69 (−0.08 - 1.22)	0.69 (−0.07 - 0.99)	0.94
Malate	0.001 (−0.29 - 0.32)	0.09 (−0.18 - 0.36)	0.63

Values shown are median (quartiles 1 to 3) concentrations of the respective metabolites. Concentrations are presented as area ratio after normalisation to the internal standards.

6 METABOLOMICS IN VALIDATION COHORT

The metabolomic analysis of the discovery cohort identified several metabolites present at significantly different concentrations in the disease cohorts. As planned we then proceeded to validate these results in a separate cohort of patients (validation cohort) and the results of this validation analysis are presented in this chapter.

This analysis was important not only to validate the methodology and results from the discovery analysis, but also to validate the effect size in a separate study population. A successful validation of these metabolomic differences using selected metabolites would open up avenues for them to be explored as potential biomarkers for disease identification, prognosis and stratification. As peripheral samples from the validation cohort were used for this analysis, the role of these metabolites could possibly be extended to every-day clinical practice, where such samples are routinely collected as a part of patients care.

6.1 Methods

To minimise bias, the recruitment of subjects for the validation cohort and their metabolomic analysis were performed separately from the discovery cohort. Peripheral blood samples (from a vein in the arm) from fasting patients were collected in the validation cohort and processed similarly to the discovery cohort (Chapter 2). The metabolites most significantly differentiating the cohorts from discovery analysis were selected and their ability to differentiate similar cohorts from the validation group was assessed using ROC analysis (Section 2.6.3.7).[299]

The ROC analysis was performed between cohorts in a pair-wise manner (control vs aortic stenosis, control vs HCM and HCM vs aortic stenosis), comparing the results from discovery (***blue line***) and validation (***pink line***) groups. The closeness of the two ROC curves generated (discovery / validation) for each pair-wise analysis was indicative of the similarity in the area under the curve (AUC) values. AUC is a metric, which is indicative of the probability with which a classifier/metabolite will rank a randomly chosen positive instance higher than the randomly chosen negative one. Thus the quality of a given classifier (in this study it's a set of metabolites) in differentiating the conditions being assessed can be roughly classified as follows based on the AUC values (AUC classification):[299]

a) 0.90 – 1 = excellent
b) 0.80 – 0.90 = good
c) 0.70 – 0.80 = fair
d) 0.60 – 0.70 = poor
e) 0.50 – 0.60 = fail

The metabolites from the discovery analysis, which were most significantly differentiating between a pair of cohorts across all three-collection sites (femoral vein, coronary sinus and aortic root), were selected for analysis and compared to the peripheral samples from the validation cohort. These selected acylcarnitines and aqueous metabolites were analysed separately and in combination to generate ROC curves yielding the following results:

1) The predictive ability of the selected metabolites in differentiating the two cohorts during the discovery analysis (***blue line***).

2) The predictive ability of the selected metabolites in differentiating similar cohorts during the validation analysis (***pink line***).

6.2 Results

6.2.1 Clinical characteristics

A total of 80 patients were included in the final analysis of the validation cohort. These included 23 controls, 27 aortic stenosis and 30 HCM patients. The clinical characteristics of the validation cohort are described in table 6.1.1 and were assessed for differences between cohorts using ANOVA and Chi-square tests. Patients in the HCM cohort were significantly younger as compared to the aortic stenosis cohort. All patients had a normal left ventricular (LV) ejection fraction (>50%) and the majority of them were men.

As compared with the discovery cohort, aortic stenosis (81 vs 71, p=<0.0001, Student's t-test) and HCM (61 vs 53, p=0.0002, Student's t-test) patients in the validation cohort were significantly younger.

Table 6.1.1: Clinical and demographic characteristics of the controls, aortic stenosis and HCM Cohorts in the validation group. Differences between the groups statistically analysed using ANOVA with Bonferroni's post-test for multiple comparisons and Chi-square test. Statistical significance was defined as a p-value<0.05.

	Controls (n=23)	Aortic Stenosis (n=27)	HCM (n = 30)	p value

Age (years)	61 (41- 65)	71 (65 - 76)	53 (41 - 58)	<0.0001
Men, n (%)	61	76	67	0.52
LVEF (%)	69 ± 11	74 ± 6	77 ± 8	0.003

Values are mean ± SD, percentages or median (quartiles 1 to 3). LVEF = left ventricular (LV) ejection fraction.

6.2.2 Validation using selected acylcarnitines

Acylcarnitines selected from the discovery analysis were assessed for their discriminating ability in the validation cohort using ROC analysis; the results from this analysis are presented below.

a) Control vs aortic stenosis cohorts:

Free carnitine, C14-OH, C16:1 and C18-OH were selected for the ROC analysis between the control and aortic stenosis cohorts. This generated AUC values of 0.81 and 0.85 from the analysis of discovery and validation cohorts respectively (figure 6.2.1), which was suggestive of:

1) A good predictive ability (refer to AUC classification) of these acylcarnitines in differentiating the control and aortic stenosis cohorts during the discovery stage.
2) A successful validation of these acylcarnitines in there ability to differentiate the same cohorts in the validation stage with a good predictive ability.

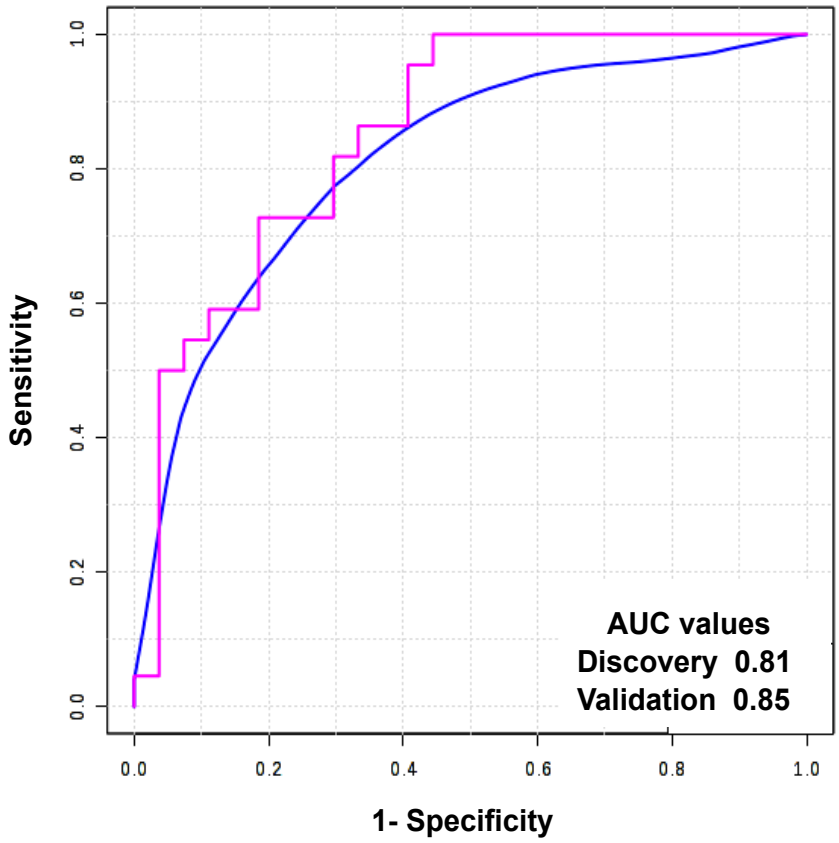

Figure 6.2.1: Receiver operating characteristic (ROC) analysis of the selected acylcarnitines for differentiating the control and aortic stenosis cohorts, during discovery (blue) and validation (pink) stages.

b) Control vs HCM cohorts:

C2, C16:1 and C18-OH were selected for the ROC analysis between the control and HCM cohorts. The AUC values generated from the analysis of discovery and validation cohorts were 0.67 and 0.67 respectively (figure 6.2.2), which was suggestive of:

1) Poor predictive ability (refer to AUC classification) of these acylcarnitines in differentiating the control and HCM cohorts during the discovery stage.

2) Poor predictive ability of these acylcarnitines in differentiating the same cohorts in the validation stage, which was similar to the observations from discovery stage.

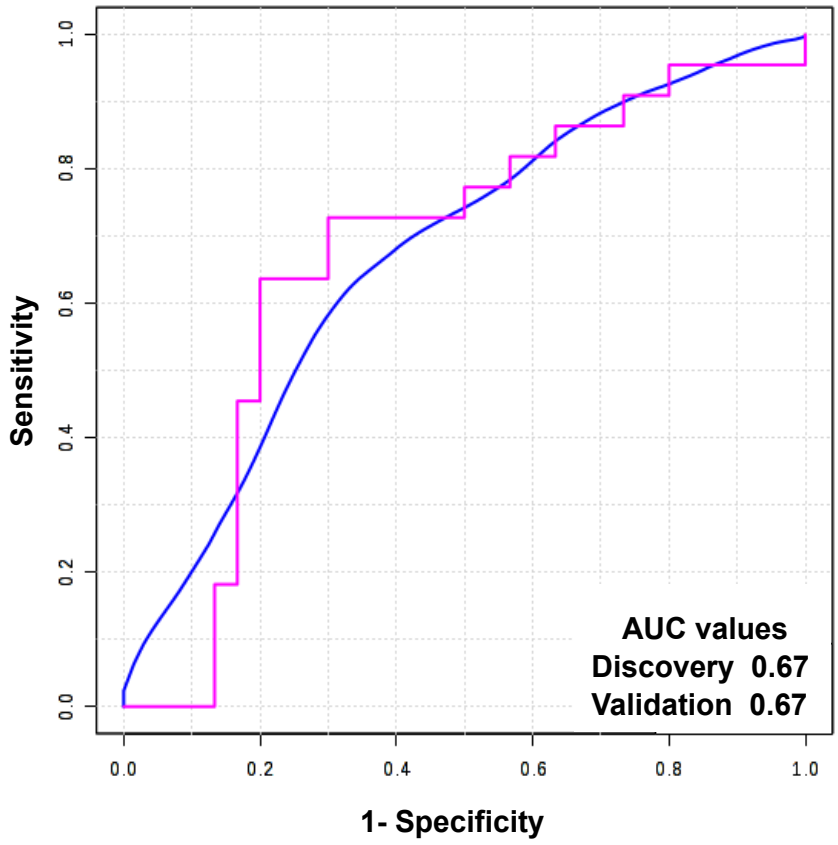

Figure 6.2.2: Receiver operating characteristic (ROC) analysis of the selected acylcarnitines for differentiating the control and HCM cohorts, during discovery (blue) and validation (pink) stages.

c) HCM vs aortic stenosis cohorts:

C8, C14-OH, C16-OH and C20:1 were selected for ROC analysis between the HCM and aortic stenosis cohorts. The ROC analysis generated AUC values of 0.75 and 0.74 for the discovery and validation cohorts respectively (figure 6.2.3), this suggested:

1) Fair predictive ability (refer to AUC classification) of these acylcarnitines in differentiating the HCM and aortic stenosis cohorts during the discovery stage.
2) The predictive ability of these metabolites remains similar to the discovery stage when analysing the same cohorts in the validation stage.

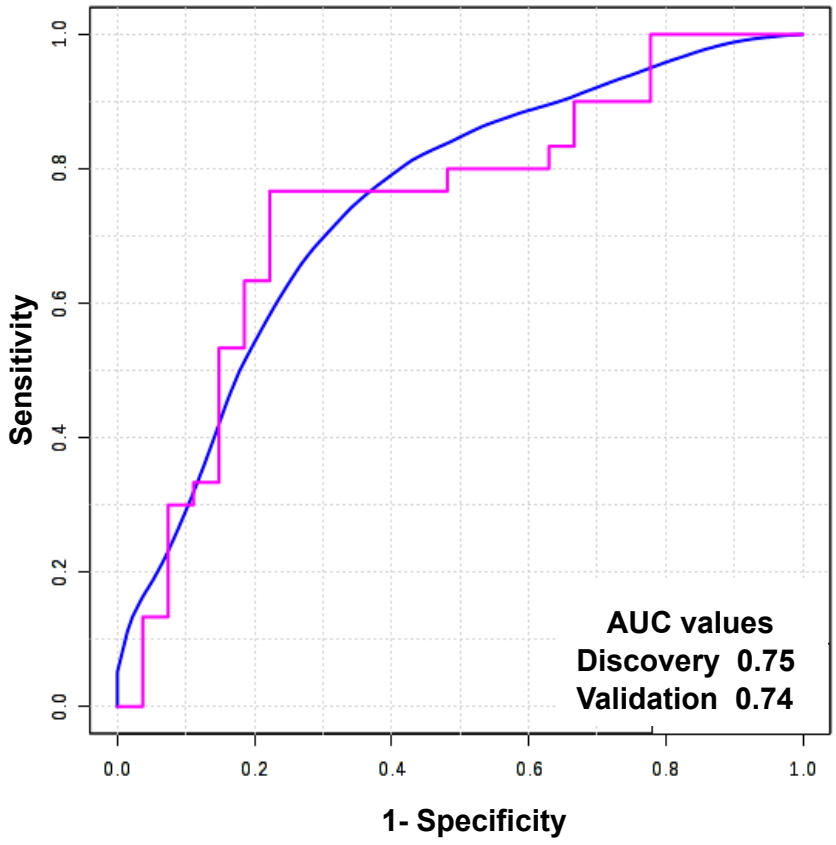

Figure 6.2.3: Receiver operating characteristic (ROC) analysis of the selected acylcarnitines for differentiating the HCM and aortic stenosis cohorts, during discovery (blue) and validation (pink) stages.

6.2.3 Validation using selected aqueous metabolites

The most discriminating aqueous metabolites from discovery analysis were then assessed for their discriminating ability in the validation cohort; the results from this analysis are presented below.

a) Control vs aortic stenosis cohorts:

The aqueous metabolites selected for ROC analysis between control and aortic stenosis cohorts were cystine, ornithine, citrate and aconitate. The AUC values of 0.78 and 0.73 were generated from the analysis of discovery and validation cohorts respectively (figure 6.2.4), these results were suggestive of:

1) A fair predictive ability (refer to AUC classification) of these metabolites in differentiating the control and aortic stenosis cohorts during the discovery stage.
2) The selected metabolites had a fair predictive ability to differentiate the same cohorts in the validation stage too.

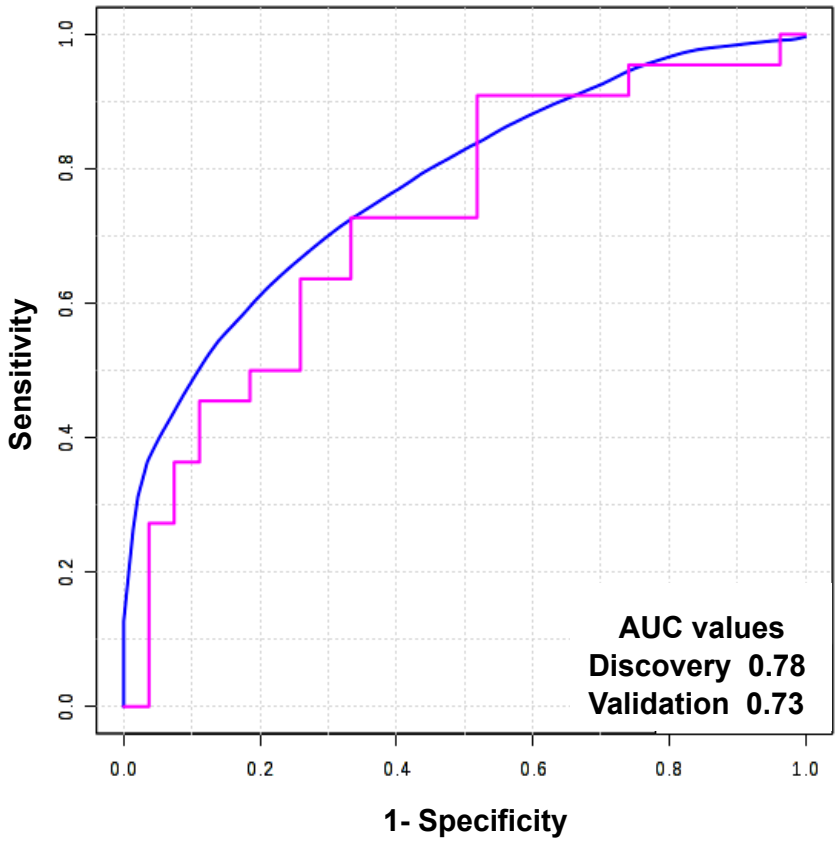

Figure 6.2.4: Receiver operating characteristic (ROC) analysis of the selected aqueous metabolites for differentiating the control and aortic stenosis cohorts, during discovery (blue) and validation (pink) stages.

b) Control vs HCM cohorts:

AAA and BAIBA were selected for ROC analysis between the control and HCM cohorts. The analysis of discovery and validation cohorts generated AUC values of 0.52 and 0.65 respectively (figure 6.2.5), these results suggested:

1) These metabolites were not able to differentiate between the control and HCM cohorts in the discovery stage (refer to AUC classification).
2) The metabolites had poor predictive ability in differentiating the two cohorts during the validation stage.

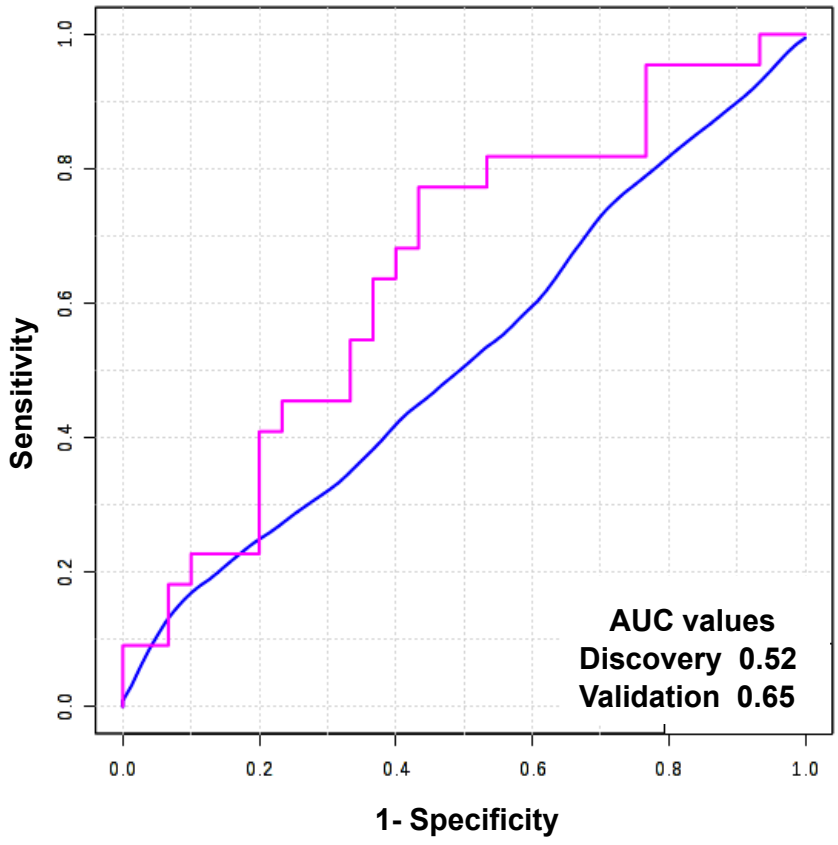

Figure 6.2.5: Receiver operating characteristic (ROC) analysis of the selected aqueous metabolites for differentiating the control and HCM cohorts, during discovery (blue) and validation (pink) stages.

c) HCM vs aortic stenosis cohorts:

Aconitate, isocitrate, citrate and citrulline were selected for ROC analysis between the HCM and aortic stenosis cohorts. The analysis generated AUC values of 0.77 and 0.78 for the discovery and validation cohorts respectively (figure 6.2.6), this suggested:

1) A fair predictive ability (refer to AUC classification) of these metabolites in differentiating the two cohorts during the discovery stage.
2) The predictive ability of these metabolites in differentiating the same cohorts remains the same during the validation stage too.

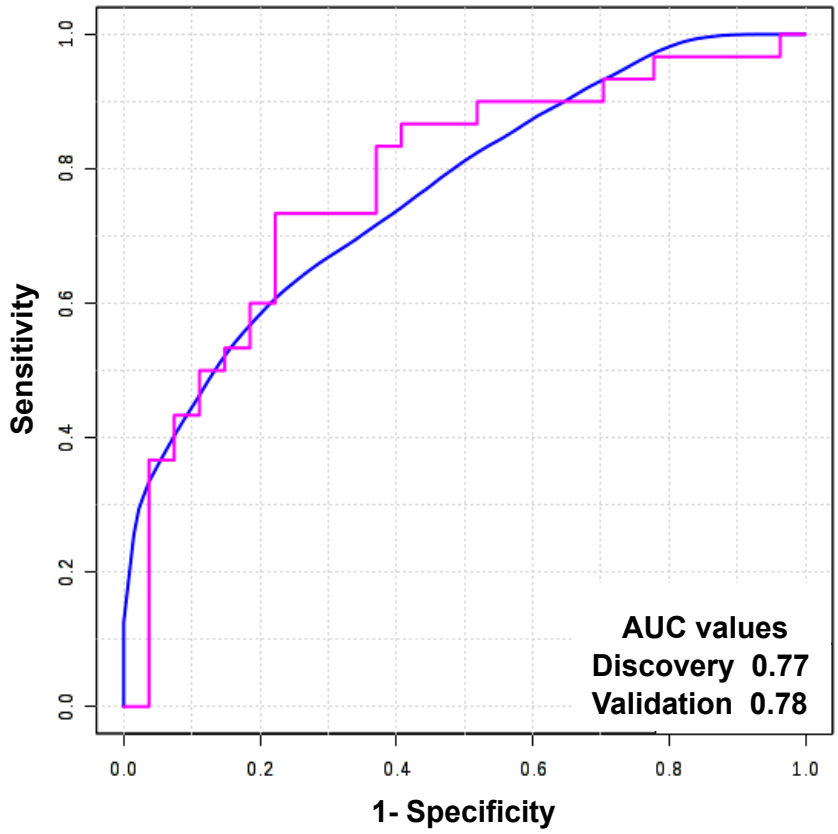

Figure 6.2.6: Receiver operating characteristic (ROC) analysis of the selected aqueous metabolites for differentiating the HCM and aortic stenosis cohorts, during discovery (blue) and validation (pink) stages.

6.2.4 Validation using selected acylcarnitines and aqueous metabolites

The validation was then performed combining the selected acylcarnitines and aqueous metabolites from discovery analysis.

a) Control vs aortic stenosis cohorts:

The following acylcarnitines and aqueous metabolites were selected for the combined ROC analysis between the control and aortic stenosis cohorts: carnitine, C14-OH, C16:1, C18-OH, citrate, aconitate, cystine and ornithine. The

AUC value generated following ROC analysis were 0.86 and 0.85 for the discovery and validation cohorts (figure 6.2.7), this suggested:

1) During the discovery stage, combination of acylcarnitines and aqueous metabolites provided a better predictive ability in differentiating the two cohorts as compared to their analysis separately.
2) The predictive ability of these selected metabolites in differentiating the same cohorts remained good (refer to AUC classification) during the validation stage too.

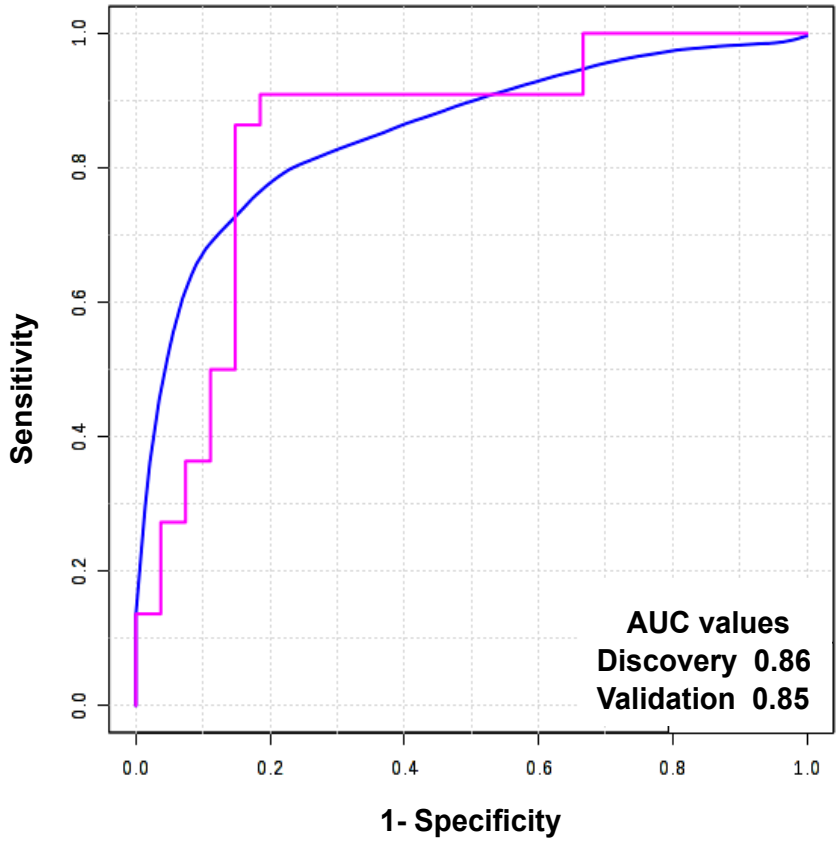

Figure 6.2.7: Receiver operating characteristic (ROC) analysis of the selected acylcarnitines and aqueous metabolites, for differentiating the control and aortic stenosis cohorts, during discovery (blue) and validation (pink) stages.

b) Control vs HCM cohorts:

The following metabolites were selected for ROC analysis between the HCM and control cohorts: C2, C16:1, C18-OH, AAA and BAIBA. The AUC values generated following ROC analysis were 0.65 and 0.70 for the discovery and validation cohorts respectively (figure 6.2.8), these results suggested:

1) Poor predictive ability (refer to AUC classification) of these metabolites in differentiating the control and HCM cohorts during the discovery stage.

2) The predictive ability of these metabolites was fair in differentiating the same cohorts during the validation stage.

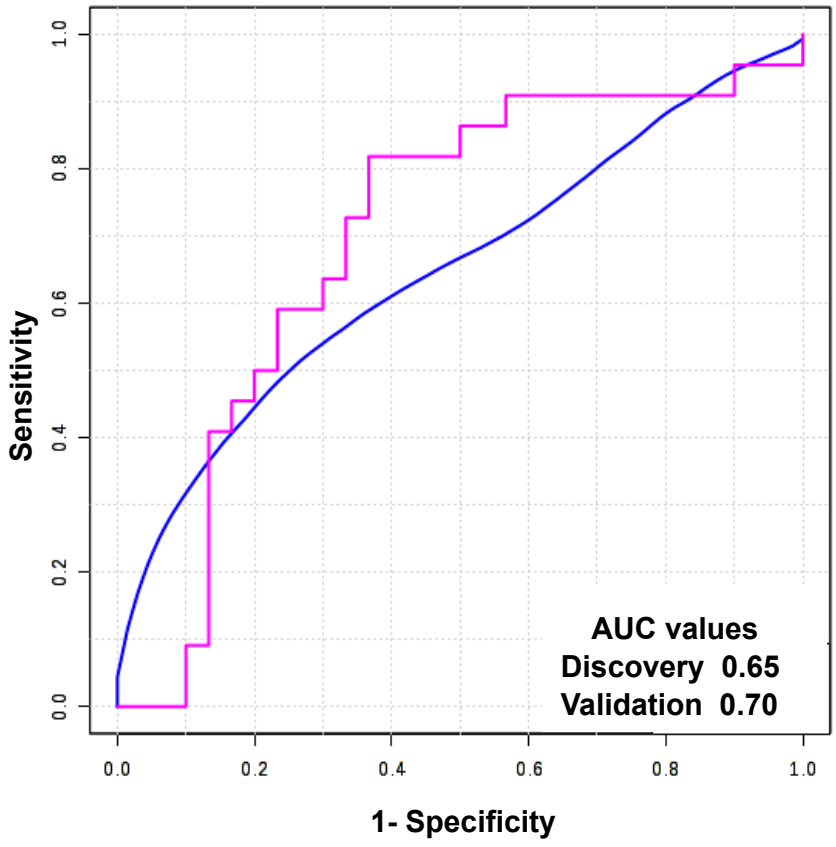

Figure 6.2.8: Receiver operating characteristic (ROC) analysis of the selected acylcarnitines and aqueous metabolites, for differentiating the control and HCM cohorts, during discovery (blue) and validation (pink) stages.

c) HCM vs aortic stenosis cohorts:

C8, C14-OH, C16-OH, C20:1, aconitate, citrate, citrulline and isocitrate were selected for ROC analysis between the HCM and aortic stenosis cohorts. The AUC values generated were 0.83 and 0.77 from the analysis of discovery and validation cohorts respectively (figure 6.2.9), these results suggested:

1) A good predictive ability (refer to AUC classification) of these metabolites in differentiating the two cohorts during the discovery stage.
2) A fair predictive ability in differentiating the two cohorts during the validation stage.

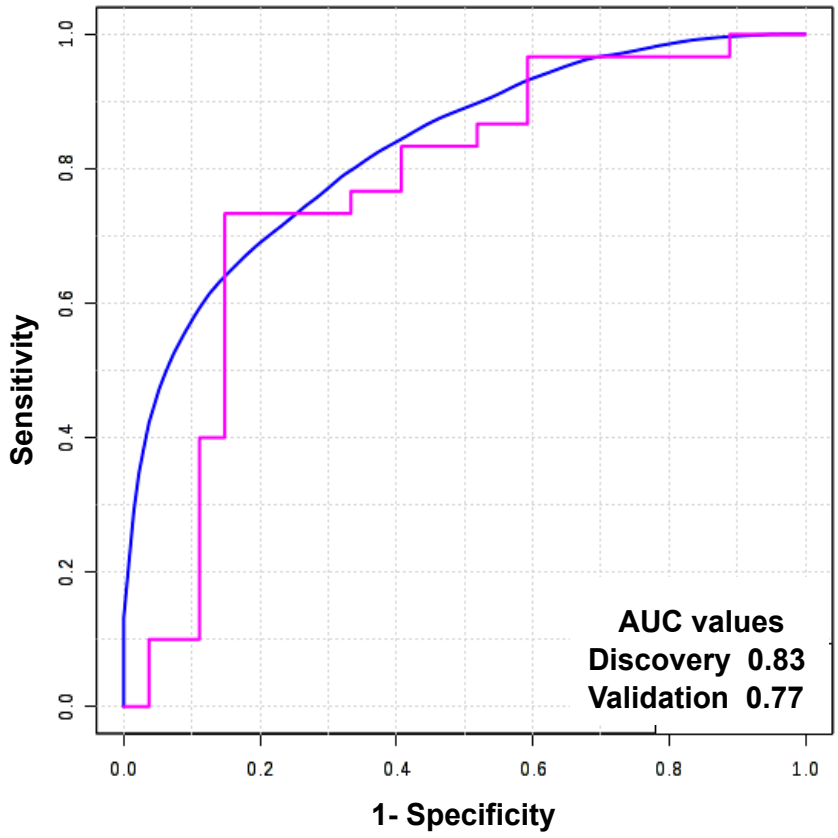

Figure 6.2.9: Receiver operating characteristic (ROC) analysis of the selected acylcarnitines and aqueous metabolites, for differentiating the HCM and aortic stenosis cohorts, during discovery (blue) and validation (pink) stages.

6.2.5 Conclusions

The ROC analysis between the discovery and validation cohorts found the predictive ability of metabolites to be similar between the two cohorts. Thus selected acylcarnitines and aqueous metabolites differentiating cohorts in the discovery stage, differentiated with almost similar predictive ability during the validation stage too.

It was the combination of selected acylcarnitines and aqueous metabolites differentiating control vs aortic stenosis and HCM vs aortic stenosis cohorts that had the greatest predictive ability with AUC values of 0.86 and 0.83 respectively. It's also important to highlight that despite a difference in the age of aortic stenosis and HCM patients between the discovery and validation cohorts, their metabolomic patterns were similar.

Thus in summary this analysis validates our metabolomic findings and methodology from the discovery cohort. The set of metabolites which included long chain acylcarnitines (C14-OH, C16-OH and C20:1) and aqueous metabolites such as aconitate and citrate, were able to differentiate aortic stenosis from HCM and controls with a high predictive ability in both discovery and validation cohorts. These metabolites should be explored for potential future use as biomarkers.

Table 6.2.2: Summary of the ROC analysis using acylcarnitines and aqueous metabolites separately and in combination between the different disease cohorts, during the discovery and validation stages.

	Discovery	Validation
Control vs Aortic stenosis		
Carnitine, C14-OH, C16:1, C18-OH	0.81	0.85
Cystine, ornithine, citrate, aconitate	0.78	0.73
Acylcarnitines and aqueous metabolites combined	0.86	0.85
Control vs HCM		
C2, C16:1, C18-OH	0.67	0.67
AAA, BAIBA	0.52	0.65
Acylcarnitines and aqueous metabolites combined	0.65	0.70
HCM vs Aortic stenosis		
C8, C14-OH, C16-OH, C20:1	0.75	0.74
Aconitate, isocitrate, citrate, citrulline	0.77	0.78
Acylcarnitines and aqueous metabolites combined	0.83	0.77

Values shown are area under the curve (AUC) values

7 Biological validation – Transcriptomic analysis

The metabolomic genome encompasses a large number of genes, which regulate many metabolic pathways directly by encoding metabolic enzymes or indirectly via signalling and epigenetic, transcriptional, and posttranslational regulation.[107,129,271] An altered expression of these genes produces changes in the corresponding metabolic pathways and their respective metabolites. In this chapter I analysed the results from a detailed microarray analysis done on LV biopsy samples from aortic stenosis patients. Several genes were selected from the metabolomic genome, which were relevant to fatty acid β-oxidation, amino acid and glucose metabolism. The results from this analysis were then compared to the respective metabolic changes described in the previous chapters.

7.1 Methods

An extensive microarray analysis on left ventricular (LV) biopsy samples was performed. Mr. Neil Howell collected LV biopsy samples from patients with aortic stenosis (patients with critical aortic stenosis) and controls (patients with ischaemic heart disease and normal LV systolic function undergoing coronary artery bypass grafting) undergoing cardiac surgery. The data from this analysis was utilised by me to study the expression of genes regulating fatty acid, glucose and amino acid metabolism, and place the metabolomic data in the previous chapters in context.

Gene expression arrays*:* using the RNeasy Mini Kit (Qiagen, UK) total RNA was extracted from snap-frozen and pulverized heart tissue following the

manufacturers recommendations. Subsequent steps of RNA conversion, hybridisation, quality control, dataset normalisation and microarray analysis were undertaken by the Genomics and Bioinformatics Core Facilities at the Wellcome Trust Centre for Human Genetics.

Microarray data analysis: RNA was prepared and hybridised to Illumina BeadChip microarrays following manufacturers' protocols. Raw data were imported into the R statistical software (http://www.R-project.org) for further processing and analysis using BioConductor packages.[325] Raw signal intensities were background corrected, prior to being transformed and normalised using the 'vsn' package.[326] A range of quality control checks were made. The dataset was then filtered to remove genes not detected above background levels (detection score <0.95) in any of the samples, resulting in a final dataset of 19210 genes.

Statistical analysis to identify differential gene expression was performed with the Linear Models for Microarray Analysis (limma) package.[327] Raw p-values were corrected for multiple testing using the false discovery rate (FDR) controlling procedurere of Benjamini and Hochberg.[328] At 5% FDR, 2132 genes showed significant changes ($p<0.05$) in their expression level between experimental groups. Results were annotated with gene information using the relevant BioConductor annotation package (Illumina HumanHT12v4 annotation data) from the Illumina website (http://www.illumina.com).

7.2 Results

7.2.1 Clinical characteristics (aortic stenosis vs controls)

A total of 50 patients were included in the final transcriptomic analysis, which included 36 patients with aortic stenosis and 14 controls. Their clinical characteristics are described in table 7.2.1 and were assessed for differences using either two-tailed Student's t-test, Mann-Whitney U-test or Chi-square test. The majority of patients in both cohorts were men, with aortic stenosis subjects being significantly younger than controls (68 vs 73, p=0.04). Patients in both cohorts had a preserved left ventricular ejection fraction.

Aortic stenosis patients recruited for microarray analysis were much younger as compared to those recruited in discovery cohort (68 vs 81, p=<0.0001), but there was no difference when compared to those in the validation cohort (68 vs 71, p=0.48). Controls recruited for microarray analysis were much older as compared to those recruited in discovery (73 vs 62, p=0.002) or validation (73 vs 61, p=<0.0001) cohorts. There were no differences in gender distribution between all the cohorts.

Table 7.2.1: Demographic characteristics of the controls and aortic stenosis patients selected for transcriptomic analysis. Differences between the groups statistically analysed using either two-tailed Students t-test, Mann-Whitney U-test or Chi-square test. p-value<0.05 was considered significant.

	Controls (n=14)	Aortic Stenosis (n=36)	p value
Age (years)	73 (67- 78)	68 (64 - 73)	0.04
Men, n (%)	9 (64)	27 (75)	1.0

Values are mean ± SD, percentages or median (quartiles 1 to 3).

7.2.2 Transcriptomic analysis

After curating an extensive database of 2132 significantly different genes, 61 genes were selected which exhibited differential expression between the two cohorts. These genes were selected as they encode proteins, which directly (enzymes) or indirectly (transcriptomic regulators) regulate fatty acid, glucose and amino acid metabolism (Table 7.2.2). The function and expression of these selected genes in patients with aortic stenosis is now described in detail.

7.2.3 Genes encoding AMPK

1) *PRKAG1*

The expression of protein kinase, AMP-activated, gamma 1 non-catalytic subunit *(PRKAG1)* gene was significantly downregulated in patients with aortic stenosis (log fold change of −1.78, p=0.0003). *PRKAG1* encodes the γ1 regulatory subunit of the AMP-activated protein kinase (AMPK). AMPK plays an important role in regulating β-oxidation by inhibiting acetyl-CoA carboxylase (ACC) and 3-hydroxy-3-methyl-glutaryl-CoA reductase (HMGCR) (described in

Section 1.3.2.2 and discussed further in the conclusion section of this chapter). The γ regulatory subunit has nucleotide binding modules, which bind to adenosine monophosphate (AMP), adenosine diphosphate (ADP) or ATP, resulting in activation or inhibition of AMPK.

2) *PRKAG2*

The expression of protein kinase, AMP-activated, gamma 2 non-catalytic subunit *(PRKAG2)* gene was slightly upregulated in patients with aortic stenosis (log fold change of 0.10, p=0.42). *PRKAG2* encodes the γ2 regulatory subunit of AMPK.

3) *PRKAB1*

The expression of protein kinase, AMP-activated, beta 1 non-catalytic subunit *(PRKAB1)* gene was downregulated in patients with aortic stenosis (log fold change of −0.07, p=0.51). *PRKAB1* encodes the β1 regulatory subunit of AMPK.

4) *PRKAA1*

The expression of protein kinase, AMP-activated, alpha 1 catalytic subunit *(PRKAA1)* gene was downregulated in patients with aortic stenosis (log fold change of −0.17, p=0.15). *PRKAA1* encodes the α1 catalytic subunit of AMPK. The α catalytic subunit has two isoforms α1 and α2, both of which have a cardiac expression.

5) *PRKAA2*

The expression of protein kinase, AMP-activated, alpha 2 catalytic subunit *(PRKAA2)* gene was significantly downregulated in patients with aortic stenosis

(log fold change of −0.57, p=4.02E-05). *PRKAA2* encodes the α2 catalytic subunit of AMPK.

7.2.4 Genes encoding transcriptomic factors

1) *PPARA*

The expression of peroxisome proliferator-activated receptor alpha *(PPARA)* gene was significantly upregulated in patients with aortic stenosis (log fold change of 0.38, p=0.003). *PPARA* encodes peroxisomal proliferator activated receptor (PPAR) α, which plays an important role in metabolic regulation as described in Section 1.3.2.4 and discussed further in the conclusion section of this chapter.[329]

2) *PPARGC1A*

The expression of peroxisome proliferator-activated receptor gamma, coactivator 1 alpha *(PPARGC1A)* gene was slightly upregulated in patients with aortic stenosis (log fold change of 0.10, p=0.46). *PPARGC1A* encodes peroxisomal proliferator-activated receptor γ coactivator-1 (PGC-1) α, which as described in Section 1.3.2.4 is a transcription factor that plays an important role in metabolic regulation.

7.2.5 Genes regulating transportation of fatty acids for β-oxidation

1) *SLC27A5 / FATP5*

The expression of solute carrier family 27 (fatty acid transporter), member 5 *(SLC27A5),* which is also known as fatty acid transporter protein-5 *(FATP-5)*, was downregulated in patients with aortic stenosis (log fold change of −0.07, p=0.58). This gene encodes isozyme of very long-chain acyl-CoA synthetase

(VLCS), which activated very long chain fatty acids, facilitating their transport across the sacrolemmal membrane.

2) *FABP6*

The expression of fatty acid binding protein 6, ileal (*FABP6)* gene was downregulated in patients with aortic stenosis (log fold change of −0.22, p=0.36). *FABP6* encodes fatty acid binding proteins, which play a vital role in fatty acid transport across the sacrolemmal membrane.

3) *CD36*

The expression of CD36 molecule (thrombospondin receptor) *(CD36)* gene was downregulated in patients with aortic stenosis (log fold change of −0.21, p=0.19). *CD36* encodes the enzyme FAT/CD36, which facilitates the transport of free fatty acids across the sacrolemmal membrane.

4) *SLC25A11*

The expression of solute carrier family 25 (mitochondrial carrier; oxoglutarate carrier), member 11 *(SLC25A11)* gene was downregulated in patients with aortic stenosis (log fold change of −0.02, p=0.89). This gene encodes for the oxoglutarate/malate carrier, which transports 2-oxoglutrarate across the inner mitochondrial membrane in exchange for malate.

5) *SLC25A10*

The expression of solute carrier family 25 (mitochondrial carrier; dicarboxylate transporter), member 10 *(SLC25A10)* gene was upregulated in patients with aortic stenosis (log fold change of 0.12, p=0.36). This gene encodes for proteins which translocates small metabolites (malate, succinate etc.) across the

mitochondrial membrane, which act as substrates in the citric acid cycle or fatty acid synthesis.

6) *ABCD3*

The expression of ATP binding cassette subfamily D member 3 *(ABCD3)* gene was significantly downregulated in patients with aortic stenosis (log fold change of −0.44, p=0.008). This gene encodes proteins, which are involved in peroxisomal import of fatty acids and/or fatty acyl-CoAs in the organelle.

7.2.6 Genes regulating fatty acid β-oxidation

1) *ACSL3*

The expression of acyl-CoA synthetase long-chain family member 3 *(ACSL3)* gene was downregulated in patients with aortic stenosis (log fold change of -0.23, p=0.24). This gene encodes the isozyme of the long-chain fatty-acid-coenzyme A ligase family, which converts long-chain fatty acids to their acyl-CoA derivatives via thio-esterification. This is a vital step in directing fatty acids toward various metabolic pathways (lipid biosynthesis or β-oxidation).

2) *ACOT1*, *ACOT4*, *ACOT7* & *ACOT8*

The expression of acyl-CoA thioesterase 1 *(ACOT1)* and acyl-CoA thioesterase 4 *(ACOT4)* genes was decreased (log fold changes of -0.27 and -0.02 respectively), while that of acyl-CoA thioesterase 7 *(ACOT7)* and acyl-CoA thioesterase 8 *(ACOT8)* genes was marginally increased in aortic stenosis patients (log fold changes of 0.0002 and 0.04 respectively). These genes encode proteins, which hydrolyse the CoA thioester of fatty acids. This is an important step allowing formation of fatty acids, which can then be transported out of the peroxisomes into the mitochondria for further oxidation.

3) *CROT*

The expression of carnitine O-octanoyltransferase *(CROT)* gene was upregulated in patients with aortic stenosis (log fold change of 0.18, p=0.24). *CROT* encodes protein which catalyses the conversion of acyl-CoA to acylcarnitine, a vital step allowing transfer of the fatty acids from peroxisome to mitochondria.

4) *CRAT*

The expression of carnitine O-acetyltransferase *(CRAT)* gene was upregulated in patients with aortic stenosis (log fold change of 0.03, p=0.79). *CRAT* encodes protein (carnitine O-acetyltransferase) which catalyses the conversion of acetyl-CoA to acetyl-carnitine.

5) *CPT1A*, *CPT1B* & *CPT1C*

The expression of carnitine palmitoyltransferase 1A (liver) *(CPT1A)*, carnitine palmitoyltransferase 1B *(CPT1B)* and carnitine palmitoyltransferase 1C *(CPT1C)* genes was upregulated in patients with aortic stenosis; with log fold changes of 0.03, 0.29 and 0.01 respectively. These genes encode various isoforms of carnitine palmitoyl transferase 1, a key enzyme required for the formation of long-chain fatty acyl-CoAs.

6) *CPT2*

The expression of carnitine palmitoyltransferase 2 *(CPT2)* gene was down regulated in patients with aortic stenosis (log fold change of −0.02, p=0.89). *CPT2* encodes protein (carnitine palmitoyltransferase 2) which catalyses the conversion of acylcarnitine into acyl-CoA, which can then be used for β-oxidation.

7) *ACOX1*

The expression of acyl-CoA oxidase 1, palmitoyl (*ACOX1)* gene was slightly upregulated in patients with aortic stenosis (log fold change of 0.14, p=0.22). The protein encoded by the gene catalyzses the first step in β-oxidation pathway (desaturation of acyl-CoAs to 2-trans-enoyl-CoAs).

8) *ACAD8*, *ACADM*, *ACADSB*, *ACAD11*

The expression of acyl-CoA dehydrogenase family member 8 *(ACAD8)* gene was significantly downregulated (log fold change of −0.54, p=0.004), while that of acyl-CoA dehydrogenase, C-4 to C-12 straight chain *(ACADM)*, acyl-CoA dehydrogenase, short/branched chain *(ACADSB)* and acyl-CoA dehydrogenase family member 11 *(ACAD11)* genes was either downregulated or slightly upregulated (log fold changes of −0.005, −0.06 and 0.05 respectively). These *ACAD* genes encode proteins, which form acyl CoA dehydrogenases that catalyses the dehydrogenation of acyl-CoAs of various chain lengths (short, medium and long chain).

9) *EHHADH*

The expression of enoyl-CoA, hydratase/3-hydroxyacyl CoA dehydrogenase *(EHHADH)* gene was significantly downregulated in patients with aortic stenosis (log fold change of −0.46, p=0.001). The protein encoded by this gene forms a functional enzyme (enoyl-CoA hydratase & 3-hydroxyacyl CoA dehydrogenase), which plays a crucial role in the β-oxidation pathway.

10) *HSD17B4*

The expression of hydroxysteroid (17-beta) dehydrogenase 4 *(HSD17B4)* gene was downregulated in patients with aortic stenosis (log fold change of −0.19,

p=0.11). *HSD17B4* encodes the bifunctional enzyme, which plays a critical role in peroxisomal fatty acid β-oxidation.

11) *DECR2*

The expression of 2,4-dienoyl-CoA reductase 2, peroxisomal *(DECR2)* gene was upregulated in patients with aortic stenosis (log fold change of 0.19, p=0.11). *DECR2* encodes 2,4-dienoyl CoA reductase 2, that plays a critical role in the metabolism of mono- and poly unsaturated fatty acids.

12) *ETFDH*

The expression of electron-transferring-flavoprotein dehydrogenase *(ETFDH)* gene was downregulated in patients with aortic stenosis (log fold change of −0.12, p=0.46). This gene encodes protein (electron-transferring-flavoprotein dehydrogenase), which shuttles electrons from acyl-CoA dehydrogenase to the electron transport chain.[330]

7.2.7 Genes regulating microsomal fatty acid oxidation

1) *CYP4B1*

The expression of cytochrome P450, family 4, subfamily B, polypeptide 1 *(CYP4B1)* gene was downregulated in patients with aortic stenosis (log fold change of −0.48, p=0.27). This gene encodes a protein, which is a member of cytochrome P450 superfamily of enzymes. The cytochrome P450 proteins are monooxygenases that catalyze many reactions involved in drug metabolism and synthesis of cholesterol, steroids and other lipids

2) *CYP27A1*

The expression of cytochrome P450, family 27, subfamily A, polypeptide 1 *(CYP27A1)* gene was downregulated in aortic stenosis patients (log fold change of −0.12, p=0.46). *CYP27A1* encodes a member of cytochrome P450 superfamily.

7.2.8 Genes regulating lipid storage and biosynthesis

1) *ELOVL1*

The expression of ELOVL fatty acid elongase 1 *(ELOVL1)* gene was downregulated in patients with aortic stenosis (log fold change −0.02, p=0.80). This gene encodes member of the ELO family (fatty acid elongase 1).

2) *ELOVL2*

The expression of ELOVL fatty acid elongase 2 *(ELOVL2)* gene was downregulated in patients with aortic stenosis (log fold change of −0.36, p=0.03). This gene encodes member of the ELO family (fatty acid elongase 2), which plays a role in the fatty acid elongation.

3) *ELOVL6*

The expression of ELOVL fatty acid elongase 6 *(ELOVL6)* gene was slightly upregulated in patients with aortic stenosis (log fold change 0.07, p=0.69). This gene encodes member of the ELO family (fatty acid elongase 6).

4) *GPAM*

The expression of glycerol-3-phosphate acyltransferase, mitochondrial *(GPAM)* gene was downregulated in patients with aortic stenosis (log fold change of −0.18, p=0.31). *GPAM* encodes glycerol-3-phosphate acyltransferase, which catalyses the first step in glycerolipid biosynthesis.

5) *LPIN2*

The expression of lipin 2 *(LPIN2)* gene was downregulated in patients with aortic stenosis (log fold change of −0.21, p=0.12). The protein encoded by this gene play a role in triglyceride metabolism.

6) *DGAT1* & *DGAT2*

The expression of diacylglycerol O-acyltransferase 1 *(DGAT1)* gene was slightly increased, while that of diacylglycerol O-acyltransferase 2 *(DGAT2)* gene was significantly decreased in patients with aortic stenosis, with respective log fold changes of 0.09 and −0.46. *DGAT1* encodes the protein which catalyses the conversion of diacylglycerol and fatty acyl CoA to triacylglycerol. *DGAT2* encodes the enzyme which catalyses the binding of diacylglycerol to long chain fatty acyl-CoAs, the final reaction in triglyceride synthesis.

7) *PNPLA2*

The expression of patatin like phospholipase domain containing 2 *(PNPLA2)* gene was downregulated in patients with aortic stenosis (log fold change of −0.09, p= 0.51). This gene encodes the enzyme patatin-like phospholipase domain containing protein 2 which catalyses the hydrolysis of triglycerides.

8) *AGPAT5* & *AGPAT7*

The expression of both 1-acylglycerol-3-phosphate O-acyltransferase 5 *(AGPAT5)* & 1-acylglycerol-3-phosphate O-acyltransferase 7 *(AGPAT7)* genes was significantly decreased in patients with aortic stenosis, with respective log fold changes of −0.62 and −0.43 (p=0.006 and 0.005 respectively). They encode proteins, which are members of the 1-acylglycerol-3-phosphate O-

acyltransferase family, which catalyses lysophosphatidic acid (LPA) conversion to phosphatidic acid (PA), a precursor in the biosynthesis of all glycerolipids.

7.2.9 Genes regulating glucose metabolism

1) *SLC2A4*

The expression of solute carrier family 2 (facilitated glucose transporter), member 4 (*SLC2A4*), also known as *GLUT4* was upregulated in patients with aortic stenosis (log fold change of 0.06, p=0.62). This gene encodes proteins which function as insulin-regulated facilitative glucose transporter.

2) *PCK2*

The expression of phosphoenolpyruvate carboxykinase 2 *(PCK2)* gene was significantly downregulated in patients with aortic stenosis (log fold change of −0.57, p=0.0001). This gene encodes phosphoenolpyruvate carboxykinase 2, which catalyses the conversion of pyruvate to oxaloacetate, which is a vital step in gluconeogenesis.

3) *G6PC3*

The expression of glucose 6 phosphatase, catalytic, 3 *(G6PC3)* gene was upregulated in patients with aortic stenosis (log fold change of 0.03, p=0.77). This gene encodes the catalytic subunit of glucose-6-phosphatase, which catalyses the conversion of glucose-6-phospahte to glucose in final step of gluconeogenesis.

4) *PDK1*, *PDK2* & *PDK4*

The expression of pyruvate dehydrogenase kinase, isozyme 1 *(PDK1)*, pyruvate dehydrogenase kinase, isozyme 2 *(PDK2)* & pyruvate dehydrogenase kinase,

isozyme 4 *(PDK4)* genes was downregulated in patients with aortic stenosis with respective log fold change of −0.50, −0.02 and −0.64 respectively (p=0.001, 0.91 and 0.11 respectively). *PDK1* encodes the enzyme pyruvate dehydrogenase which catalyses the conversion of pyruvate to acetyl-CoA. *PDK2* encodes a protein, which phosphorylates pyruvate dehydrogenase, thus down regulating the activity of pyruvate dehydrogenase complex. *PDK4* encodes proteins, which phosphorylates one of the subunits of pyruvate dehydrogenase complex thus inhibiting its function.

5) *HK2*

The expression of hexokinase 2 *(HK2)* gene was upregulated in patients with aortic stenosis (log fold change of 0.43, p=0.08). *HK2* encodes the enzyme hexokinase which catalyses the conversion of glucose to glucose-6-phoshate, the first step in most glucose metabolism pathways.

6) *PFKFB2*

The expression of 6-phosphofructo-2-kinase/fructose-2,6-biphosphatase 2 *(PFKFB2)* gene was significantly upregulated in patients with aortic stenosis (log fold change of 0.35, p=0.04). This gene encodes two enzymes 6-phosphofructo-2-kinase and fructose-2,6-biphosphatase, which play a vital role in regulating glycolysis.

7.2.10 Genes regulating amino acid metabolism & urea cycle

1) *OAZ3*

The expression of ornithine decarboxylase antizyme 3 *(OAZ3)* gene was downregulated in patients with aortic stenosis (log fold change of −0.37,

p=0.07). *OAZ3* encodes ornithine decarboxylase antizyme 3, which inhibits ornithine decarboxylase a key enzyme in polyamine synthesis.

2) *ASS1*

The expression of argininosuccinate synthase 1 *(ASS1)* gene was downregulated in patients with aortic stenosis (log fold change of −0.06, p=0.67). It encodes argininosuccinate synthetase, which catalyses the conversion of citrulline to argininosuccinate in the urea cycle.

3) *ARG2*

The expression of arginase 2 (*ARG2)* gene was downregulated in patients with aortic stenosis (log fold change of −0.05, p=0.77). *ARG2* encodes arginase which catalyses the conversion of arginine to ornithine and urea in the urea cycle. The *ARG2* isoform of the gene has higher expression in the mitochondria of extra-hepatic tissues.

4) *VNN1*

The expression of vanin 1 (*VNN1)* gene was downregulated in patients with aortic stenosis (log fold change of −0.15, p=0.51). *VNN1* encodes for pantetheinase, which catalyses the hydrolysis of pantetheine into pantothenic acid (vitamin B5) and cysteamine. Serum levels of *VNN1* are highly correlated to PPARα activity in the liver.[331]

7.2.11 Genes regulating retinoid metabolism

1) *DHRS3*

The expression of dehydrogenase/reductase (SDR family) member 3 *(DHRS3)* gene was downregulated in patients with aortic stenosis (log fold change of

−0.04, p=0.67). This gene encodes the formation of Short-chain dehydrogenases/reductases (SDRs), which catalyse the oxidation/reduction of retinoids and steroids.

2) *ADH1B* & *ADH1C*

The expression of both alcohol dehydrogenase 1B (class I), beta polypeptide *(ADH1B)* & alcohol dehydrogenase 1C (class I), gamma polypeptide *(ADH1C)* genes was significantly downregulated in patients with aortic stenosis, with respective log fold change of −0.73 and −0.80 (p=0.003 and 0.001). These genes encode proteins, which are member of the alcohol dehydrogenase family, which metabolises several compounds including retinols.

7.2.12 Genes regulating the citric acid cycle

1) *ACO2*

The expression of aconitase 2 *(ACO2)* gene was significantly downregulated in patients with aortic stenosis (log fold change of −0.29, p=0.02). This gene encodes enzyme aconitase which catalyses the conversion of citrate to isocitrate in the citric acid cycle.

Table 7.2.2: Table details the differential expression of selected genes, which regulate the metabolomic pathways, between the control and aortic stenosis cohorts. Differences between the groups statistically analysed using either two-tailed Student's t-test or Mann-Whitney U-test. Statistical significance was defined as a p-value<0.05.

Gene	Log fold change	p value
PRKAG1	−1.78	0.0003
PRKAG2	0.10	0.42
PRKAB1	−0.07	0.51
PRKAA1	−0.17	0.15
PRKAA2	−0.57	4.02E-05
PPARA	0.38	0.003
PPARGC1A	0.10	0.46
SLC27A5/FATP5	−0.07	0.58
FABP6	−0.22	0.36
CD36	−0.21	0.19
SLC25A11	−0.02	0.89
SLC25A10	0.12	0.36
ABCD3	−0.44	0.008
ACSL3	−0.23	0.24
ACOT1	−0.27	0.10
ACOT4	−0.02	0.91
ACOT7	0.0002	0.99
ACOT8	0.04	0.79
CROT	0.18	0.24
CRAT	0.03	0.79
CPT1A	0.03	0.78
CPT1B	0.29	0.12
CPT1C	0.01	0.95
CPT2	−0.02	0.89
ACOX1	0.14	0.22
ACAD8	−0.54	0.004
ACADM	−0.005	0.98
ACADSB	−0.06	0.76
ACAD11	0.05	0.72
EHHADH	−0.46	0.001
HSD17B4	−0.19	0.11
DECR2	0.19	0.11
ETFDH	−0.12	0.46
CYP4B1	−0.48	0.27

CYP27A1	**−0.12**	**0.46**
ELOVL1	**−0.02**	**0.81**
ELOVL2	**−0.36**	**0.03**
ELOVL6	**0.07**	**0.69**
GPAM	**−0.18**	**0.31**
LPIN2	**−0.21**	**0.12**
DGAT1	**0.09**	**0.47**
DGAT2	**−0.46**	**0.002**
PNPLA2	**−0.09**	**0.51**
AGPAT5	**−0.62**	**0.006**
AGPAT7	**−0.43**	**0.005**
SLC2A4	**0.06**	**0.62**
PCK2	**−0.57**	**0.0001**
G6PC3	**0.03**	**0.77**
PDK1	**−0.50**	**0.001**
PDK2	**−0.02**	**0.91**
PDK4	**−0.64**	**0.11**
HK2	**0.43**	**0.08**
PFKFB2	**0.35**	**0.04**
OAZ3	**−0.37**	**0.07**
ASS1	**−0.06**	**0.67**
ARG2	**−0.05**	**0.77**
VNN1	**−0.15**	**0.51**
DHRS3	**−0.04**	**0.67**
ADH1B	**−0.73**	**0.003**
ADH1C	**−0.80**	**0.001**
ACO2	**−0.29**	**0.02**

7.3 Conclusions from transcriptomic analysis

The detailed transcriptomic analysis revealed expression of several genes to be significantly up or downregulated in patients with aortic stenosis. These included *PPARA* and *PFKFB2*, whose expression was significantly upregulated, while the expression of *PRKAG1*, *PRKAA2*, *ABCD3*, *EHHADH*, *DGAT2*,

AGPAT5, *AGPAT7*, *PCK2*, *PDK1*, *ADH1B*, *ADH1C* and *ACO2* was significantly downregulated. Besides the above-mentioned genes several others regulating fatty acid, glucose and amino acid metabolism were found to have an altered expression. *PRKAG1* and *PRKAA2* encode proteins which form the regulatory and catalytic subunits of AMPK, while *PPARA* encodes the protein which constitutes PPARα. AMPK and PPARα play a vital role in the regulation of metabolism by directly affecting the activity of many of the enzymes involved. The roles of AMPK and PPARαare discussed first and followed by the description of genes and proteins regulated by them, including the majority of the genes (or their protein products) listed above.

7.3.1 AMPK regulation

The expression of *PPRKAG1* and *PRKAA2* was a significantly downregulated in the aortic stenosis cohort (Section 7.2.1). These genes encode for the γ1 regulatory and the α2 catalytic subunit of AMPK. There was also a trend to decreased expression (non statistically significant) of *PRKAB1* and *PRKAA1*; these genes encode the β1 regulatory and the α1 catalytic subunit of AMPK. These changes are suggestive of an overall downregulation in the activity of AMPK in patients with aortic stenosis. AMPK is a hetrodimeric enzyme conserved across species, which plays a vital role in regulating the pathways responsible for fuel supply and energy generation.[332-337] Thus it has also been defined as the 'fuel gauge of the mammalian cell', as in response to the energy requirement of the tissues (cardiac muscle, skeletal muscle, central nervous system, liver) it regulates and produces necessary alterations in various metabolic pathways.[338] It is now well known that during a state of normal

cardiac function AMPK is abundant and inactive, but during a state of increased energy demand (increased AMP/ATP ratio) the enzyme gets activated.[337,339]

AMPK has 3 subunit's α, β and γ, their interaction with one another and with external regulating factors, determines the overall AMPK activity. Each of these subunits have different isoforms, with 2 isoforms for α (α1 & α2) and β (β1 & β2) subunit's and three for the γ (γ1, γ2 and γ3) subunit.[340] The human heart has an equal activity of α1 and α2 subunits, while in mice α2 subunit is more dominant.[340] While the α subunit is catalytic in function, the β and γ subunits are regulatory. The α subunit has a protein kinase domain and a phosphorylation site (threonine 172), which is phosphorylated by the upstream kinases. The β subunit has phosphorylation, myristoylation and glycogen binding sites.[341,342] The γ subunit has 4 CBS sequences (cystathionine β-synthase); each pair of these forms a nucleotide-binding domain (Bateman domain) that binds to the adenosyl compounds (AMP/ATP).[343,344] While high concentrations of ATP inhibit AMPK by binding to the γ subunit, the AMP binding results in AMPK activation. The AMP induced activation is produced by allosteric activation of AMPK and by changes in the phosphorylation site of α subunit (conformational changes resulting in increased phosphorylation and by inhibiting its dephosphorylation).[345,346]

AMPK activity is also regulated by two upstream kinases LKB1 and C2+/ calmodulin dependent kinase.[347,348] LKB1 acts by phosphorylating the α catalytic subunit, preferentially during ischaemia.[349] The activated AMPK acts by phosphorylating acetyl-CoA carboxylase (ACC) at serine residues (Ser 79 isoform in the liver and Ser 221 isoform in the muscle). ACC is the key enzyme required in the formation of malonyl CoA, which is an inhibitor of carnitine

palmitoyl transferase (CPT) 1. Thus the upregulation of CPT1 promotes fatty acid metabolism via oxidation in the heart.[129] AMPK also acts by increasing the protein expression and plasmalemma content of FAT/CD36 and FABP, GLUT 1 and GLUT 4, which increases the transfer of vital metabolic fuels into the cells.[130,350-352] AMPK also regulates the glucose metabolism, which is independent of the insulin-signaling pathway.[353,354] It promotes glycolysis by upregulating enzymes such as phosphofructokinases (PFK 1&2) and hexokinase II. While it directly activates PFK 2, the activation of hexokinase II is mediated by the upregulation of transcription factors such PPARα.[355,356] In keeping with the decreased AMPK activity in our study population, there was a decreased expression of *FAT/CD36*, *FABP* and *GLUT4*. The increased expression of *HK2* in our patients is possibly explained by the upregulation in PPARα activity.

The role of AMPK has been extensively studied in murine models, even though there are conflicting reports of AMPK activation from animal and cellular models of cardiac hypertrophy. While Tian *et al*. reported upregulation of AMPK activity (specifically the α1 and α2) in murine model of pressure overload induced hypertrophy, similar changes were not reported by Dolinsky *et al*. either in other forms of murine LVH (genetically mutated mice with spontaneous hypertension) or in hypertrophied cardiac myocytes using pharmacological agonist.[357-359] Increased cardiac hypertrophy in response to pressure overload was reported in alpha-2 null and adiponectin deficient mice, where AMPK activity was downregulated similar to our patients.[360-362]

Aortic stenosis patients with left ventricular hypertrophy experience increased wall stress and local oxygen demand, leading to a state of energy deficiency,

contractile dysfunction and finally heart failure.[112,184,363-365] It is now well established that the degree of left ventricular hypertrophy in humans is proportional to the decrease in phosphorylation ability of the heart and this can be used as a predictor of mortality.[364] Recently Lu *et al.* reported a downregulation in AMPK activity and Sirt1 expression in cardiomyocytes from patients with severe heart failure due to dilated cardiomyopathy.[366] These results are similar to ours where besides downregulation of genes encoding AMPK we also found a significant downregulation in *SIRT1* expression (log fold change of −0.58, p=2.47E-07).

Such a downregulation in AMPK activity appears to be a maladaptive response to a state of increased energy requirement, which requires the metabolism to switch from a state of anabolic ATP consumption to catabolic ATP production. AMPK activation achieves this by decreasing gluconeogenesis, glycogen synthesis, lipogenesis, cholesterol synthesis and protein synthesis; and by increasing fatty acid oxidation, glucose oxidation, glycolysis and mitochondrial biogenesis (via activation of PGC-1α).[367,368] This was validated in our patients too, where the decreased AMPK activity was accompanied with a decreased expression of several genes, which encode enzymes vital to metabolic pathways such as fatty acid β-oxidation and critic acid cycle (Section 7.2).

7.3.2 PPARα regulation

PPARA expression was significantly upregulated in aortic stenosis patients. It encodes PPARα, which is one of the most important transcriptional regulators of metabolism and was the first member of the PPAR family to be cloned.[369] There are 2 other isoforms of PPAR β/δ and γ, and together this subfamily is a member of a larger family of nuclear receptors.[370] The structure and function of

PPAR is described in detail in Section 1.3.2.4. The metabolic effects of PPARα have been studied in detail in cardiac and liver tissue using murine models and its now been firmly established as the master regulator of metabolism during fastng.[371-375] During fasting PPARα up regulates the enzymes involved in hepatic fatty acid β-oxidation, ketogenesis and glucose metabolism. The regulation of these enzymes by PPARα was clearly elucidated in PPARα -/- mice subjected to fasting.[375-377] During fasting in these mice a blunted response of several genes involved in fatty acid β-oxidation and ketogenesis (e.g. *Cpt1a*, *Cpt2*, *Acadvl*, *Hadha*, *Hmgcs2*, *Hmgcl*, *Acat1*) was observed, while the genes regulating the urea cycle and amino acid metabolism were up regulated (*Got1*, *Prodh*, *Gls2*, *Pah*, *Sds*, *Asl*, *Ass1*, *Cps1*).[330,378] This resulted in increased levels of long chain acylcarnitines, triglycerides, free fatty acids and urea cycle intermediates; while there were decreased levels of short chain acylcarnitines, free carnitine and ketone bodies.[310,373] There were several genes from glucose metabolism, which were up regulated (e.g. *Pcx*, *Pck1*, *G6pc*, *Gpd1*, *Gyk*), resulting in severe fasting induced hypoglycemia and reduced hepatic glucose levels.

In these fasted mice there was an increase in the concentration of C16, C18:1 and C18:2 (long chain acylcarnitine esters), and a fall in the levels of short to medium chain species. This was a result of a metabolic block distal to carnitine palmitoyl transferase 1, the key enzyme required in formation of long chain acylcarnitines (the first committed step in fatty acid β-oxidation). Increased levels of long chain acylcarnitine species then resulted in inhibition carnitine palmitoyl transferase 1 itself. The plasma, hepatic and skeletal muscle levels of free carnitine were also reduced and there was a decreased expression of

several genes involved in carnitine biosynthesis (e.g. gamma-butyrobetaine hydroxylase 1 (*Bbox1*) and carnitine /organic cation transporter (*OCTN2* or *SLC22A5*)).

This downregulation of fatty acid β-oxidation results in increased amino acid catabolism. There was an increased skeletal muscle level of C5, which is formed from the catabolism of leucine (decreased levels) by enzymes isovaleryl-CoA dehydrogenase (IVD) (up regulated) and HMG-CoA lyase (HMGCL). With this compensatory switch in metabolism there was decrease in hepatic levels of gluconeogenic (alanine) and ketogenic (tyrosine) amino acids. There was also an upregulation of the urea cycle resulting in increased levels of aspartate, arginine and citrulline. Levels of malate and fumarate were increased as they were formed as intermediates in the up regulated urea cycle. This also resulted in decreased α-ketoglutarate levels, which acts as an amine group acceptor in various transamination reactions. In the skeletal muscle there was a decrease in levels of most of the amino acids and intermediates of the citric acid cycle, which was further worsened by fasting.

Thus PPARα affects a wide range of metabolic pathways regulating several genes, but the specificity of the genes regulated is dependent on how PPARα is activated. PPARα activation can be physiological, nutritional (includes natural ligands such as dietary fatty acids and fatty acid derived compounds) and pharmacological.[330,379,380] There are various drugs used in treatment of dyslipidemia (fibrates) and diabetes **(**thiazolidinedione's), which act as PPAR agonist.[381,382] The hypolipidemic fibrate drugs include finofibrate, clofibrate, gemfibrozil and Wy14643, which are PPARα agonists. These drugs lower the plasma triglyceride levels and increase HDL by acting on various target genes.

Thus different genes are regulated by PPARα based on the stimuli, which can be divided into three categories based on several studies done in murine models: a) under physiological regulation only b) common to pharmacological and physiological regulation c) significantly more sensitive to pharmacologically upregulation (figure 7.3.1).[383] This difference in regulation of PPARα activity by fibrates and natural fatty acids occurs potentially because of the following reasons: a) PPARα in kupffer cells is activated by fibrates and is not activated during fasting b) fibrates bind more avidly to PPARα and produce different conformational change as compared to fatty acids c) the elevated free fatty acid levels during fasting could activate PPARδ, not activated by fibrates.[384,385]

The genes from bile synthesis/secretion and retinol metabolism are exclusively regulated during fasting; whereas genes regulating expression of proteins catalyzing triglyceride synthesis (*Gpam*, *Lpin2*, *Dgat1*) and those encoding lipid droplet associated proteins (*Plin2*, *Plin4*, *Plin5*, *Fitm1*, *Cidea* and *Cidec*) are significantly up regulated by pharmacological agonist.[330,386,387] This categorisation is also valid in humans, as several studies have reported a similar expression of PPARα in mice and humans and the genes regulating the lipid pathways are well conserved between the two species.[380,388]

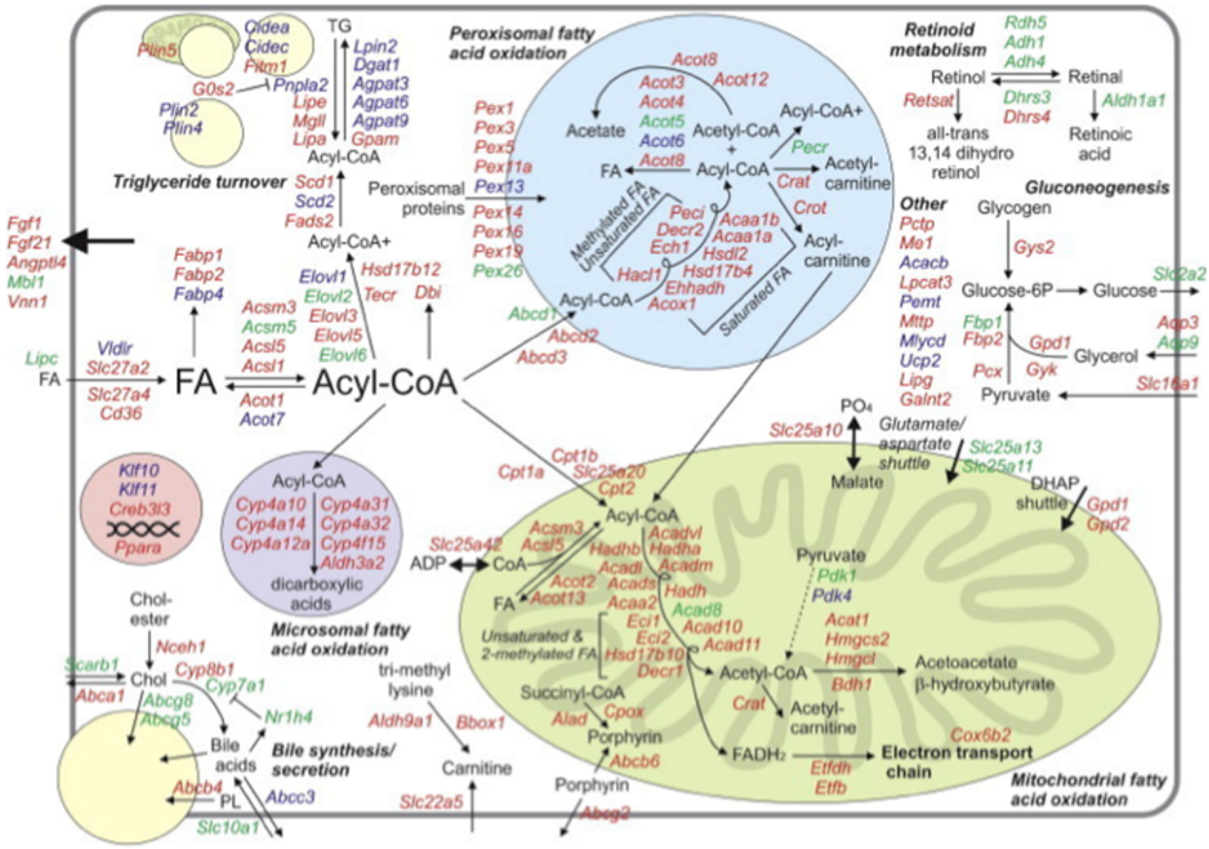

Figure 7.3.1: Illustrates various genes regulated by PPARα in response to different stimuli; the genes are color coded according to the stimuli activating PPARα, green: activated in response to physiological stimulation of PPARα, blue: activated in response to pharmacological stimulation of PPARα and red: activated in response to both physiological and pharmacological activation of PPARα. Figure reproduced by author with permission from: Sander Kersten. Integrated physiology and systems biology of PPARα. Molecular Metabolism. 2014 Mar 6;3(4):354-71.

Guided by the existing literature, PPARα regulated genes from various metabolic pathways (described in Section 7.2.2) can be categorised based on their response to different stimuli: physiological, pharmacological or common to both.

a) Physiological activation

The expression of the following genes was downregulated in patients with aortic stenosis:

1) Transporters: *SLC25A11*

2) β-oxidation: *ACAD8*

3) Lipid storage and biosynthesis: *ELVOL2*

4) Glucose utilization: *PDK1*

5) Retinol metabolism: *DHRS3*, *ADH1B*, *ADH1C*

The expression of the following genes was upregulated in patients with aortic stenosis:

1) Lipid storage and biosynthesis: *ELVOL6*

b) Pharmacological activation

The expression of the following genes was downregulated in patients with aortic stenosis:

1) β-oxidation: *ACSL3*

2) Lipid storage and biosynthesis: *LPIN2*, *PNPLA2*

The expression of the following genes was upregulated in patients with aortic stenosis:

3) β-oxidation: *ACOT7*

4) Lipid storage and biosynthesis *DGAT1*

c) Common to physiological and pharmacological activation

The expression of following genes was downregulated in patients with aortic stenosis:

1) Transporters: *CD36*, *ABCD3*
2) β-oxidation: *ACOT1*, *CPT2*, *ACADM*, *EHHADH*, *HSD17B4*, *ETFDH*
3) Lipid storage and biosynthesis: *GPAM*
4) Vanin: *VNN1*

The expression of following genes was upregulated in patients with aortic stenosis:

1) Transporters: *SLC25A10*
2) β-oxidation: *ACOX1*, *CP1A*, *CPT1B*, *CPT1C*, *CROT*, *CRAT*, *ACAD11*, *DECR2*

The detailed transcriptomic analysis of aortic stenosis patients was consequently suggestive of only a partial upregulation in PPARα activity, which was associated with an impaired expression of several genes regulating fatty acid β-oxidation. It can thus be postulated that upregulating PPARα activity using a suitable pharmacological agonist will augment expression of the downregulated genes and improve the cardiac metabolism in these patients. This therapeutic target holds promise, as several of the downregulated genes are sensitive to pharmacological stimulation using PPARα agonist such as fibrates. As discussed above this PPARα mediated genetic dysregulation results in downstream changes in the activity of several metabolic pathways and thus alter the levels of related metabolites. These metabolic changes in different patient cohorts are discussed in detail in Chapter 8.

8 Discussion & Future work

Combining invasive access to HCM patients undergoing physiological stimuli, coupled with advances in platforms permitting detailed metabolomic studies, created an opportunity to undertake this project with an aim to better understand the underlying metabolic defects contributing to the pathophysiology of cardiac diseases characterised by left ventricular hypertrophy. The primary focus was on hypertrophic cardiomyopathy and severe aortic stenosis, both of which can have a phenotype of left ventricular hypertrophy, albeit secondary to different mechanisms (genetic/pressure-overload). A targeted metabolomic analysis profiling the acylcarnitines and aqueous metabolites was performed, which provided insights into the fatty acid metabolism, amino acid metabolism and the citric acid cycle activity. These findings were then validated using metabolomic and transcriptomic analysis in separate cohorts of patients. The overall changes in the metabolites, the metabolic pathways subtended and their regulatory processes are now summarised.

8.1 Acylcarnitines

L-carnitine (beta-hydroxy-gamma-trimethylammonium butyrate) is a water-soluble quaternary amine obtained either from dietary source or from endogenous synthesis.[389] Carnitine is synthesized from trimethylated lysine residues derived from protein degradation in the liver, where proteins encoded by the *BBOX1* gene catalyse the rate-limiting step. Acylcarnitine esters are generated from their respective acetyl CoA intermediates by a reaction catalysed by CPT1. Following translocation into the mitochondria CPT2

catalyses the release of acetyl CoA from acylcarnitine, which is a vital metabolic substrate for the fatty acid β-oxidation pathway and the citric acid cycle.

As described in Chapter 7, the expression of *CPT2* was decreased, albeit not significantly, in patients with aortic stenosis, which would likely result in an accumulation of un-utilised acylcarnitines. In our metabolomic analysis, we found an increased concentration of long chain acylcarnitine species in patients with aortic stenosis and hypertrophic cardiomyopathy. C14-OH, C16-OH and C20:1 were all present in a significantly higher concentration in patients with aortic stenosis when compared to HCM and controls across all-three collection sites. Similar results were observed when analysis was performed after normalisation of these acylcarnitines to the estimated glomerular filtration rate (eGFR). On a three way analysis between cohorts, long chain acylcarnitines C16:1 and C18-OH were present in an incrementally higher concentration (significantly different between the pairs) between the control, HCM and aortic stenosis cohorts in the femoral vein and aortic root collection sites (controls < HCM < aortic stenosis).

Increased concentration of long chain acylcarnitines reflects incomplete fatty acid β-oxidation, which appeared to be explained by a decreased expression of several genes regulating fatty acid metabolism in aortic stenosis (Section 7.2). There have been previous studies which have reported similar findings in animals and humans with different cardiac disorders (e.g. compensated left ventricular hypertrophy (mechanical pressure-overload/hypertension), dilated/ischemic cardiomyopathy, mitral valve disease and HCM); but to the best of our knowledge, this is the first time such an extensive analysis of fatty

acid metabolism (transcript and extensive acylcarnitine profiling) in patients with aortic stenosis and its comparison to HCM has been reported.[303,304,322,323,390-398]

Similar states of metabolic dysregulation with impaired PPARα activity, reduced hepatic β-oxidation, depleted carnitine stores, impaired switching of metabolism during stress and increased amino acid catabolism are seen in conditions such as obesity and type-2 diabetes.[399,400]

8.2 Aqueous metabolites

In this section the changes in metabolism of aqueous metabolites that play a vital role in the citric acid cycle and the changes in metabolism of selected amino acids have been described. The metabolism of glutamate, alanine, glucose and lactate has been already been discussed in chapters 3, 4 and 5.

1) Isocitrate and malate (citric acid cycle intermediates)

Isocitrate and malate are key intermediates of the citric acid cycle.[164] Their metabolism at baseline and during pacing is now described in each cohort, and an attempt is made to generate a comprehensive picture of changes in the citric acid cycle activity.

In patients with HCM there was a net elution of isocitrate and malate at baseline, which switched to extraction during pacing. These changes between the baseline and pacing states were significantly different and possibly reflect an increased uptake of these metabolites during pacing for increased energy production via the citric acid cycle.

There was a significantly higher extraction of isocitrate and malate at baseline in patients with aortic stenosis as compared to HCM. During pacing the net extraction of these metabolites decreased in aortic stenosis but significantly increased in HCM.

In the control cohort isocitrate was extracted while malate was eluted at baseline. The elution of these metabolites was significantly higher in the HCM cohort at baseline. During pacing these metabolites were extracted similar to the HCM cohort.

Thus extraction of isocitrate and malate increased significantly during pacing in the HCM cohort with a similar non-significant trend in the controls, but an opposite observation in aortic stenosis. These changes are now described in combination with the metabolism of citrulline, and an attempt made to postulate, how the myocardial metabolism adapts during a state of increased stress (induced by pacing).

2) Citrulline

Citrulline was eluted during cardiac metabolism at baseline in the HCM cohort, which decreased significantly during pacing. In controls similar to the HCM cohort a trend towards increased extraction of citrulline was observed during pacing. The observations were entirely opposite in aortic stenosis, where citrulline was extracted at baseline which was significantly different from the elution observed in HCM. During pacing the extraction decreased in aortic stenosis, which was an opposite trend to HCM and controls. The above-described observations were possibly suggestive of an increased uptake of citrulline, isocitrate and malate during pacing in the HCM cohort, with a similar trend in controls but opposite in aortic stenosis.

Citrulline and malate play a critical role in the urea and citric acid cycle respectively. While citrulline allows detoxification of ammonia, malate is dehydrogenated to oxaloacetate in the citric acid cycle. It has now been extensively studied that an increase in the citric acid cycle intermediates (malate) or the anaplerotic enzymes leads to increase carbon flux through the cycle, which increases energy production and thus improves performance during times of increased energy demand (exercise).[401,402] Several studies have reported similar findings, where citrulline/malate (CM) used in combination as an asthenic treatment improved aerobic energy production, stamina and recovery.[402,403] This was achieved by individual actions of citrulline and malate.

Citrulline increases hepatic ureogenesis, ammonia detoxification and the renal reabsorption of bicarbonates.[404] This provides protection against acidosis and ammonia toxicity, both of which are key in decreasing muscle fatigue and improving performance. Malate through its anaplerotic effects increases the ATP production by increasing flux through the citric acid cycle. It is now known that of all the citric acid cycle intermediates, during exercise the pool of malate has the largest relative and absolute increase.[405,406] The higher concentration of malate upregulates other near equilibrium reactions, such as the activity of malate dehydrogenase, which increases carbon flux through the citric acid cycle.[407]

As detailed above there was possibly an increased uptake of citrulline, malate and isocitrate in HCM and controls during pacing. This indicated an appropriate ‘switch’ in metabolism during a state of increased energy demand. This switch would lead to increased energy production via the citric acid cycle and increased ammonia clearance, thus resulting in greater energy production and

improved muscle performance. This in-vivo upregulation of citric acid cycle activity in HCM patients during increased myocardial stress has not been previously reported.

In contrast, this metabolic 'switch' was possibly active at rest in aortic stenosis, but deactivated during pacing. This was suggestive of an increased myocardial energy demand at baseline, which was met by an adequate citric acid cycle activity. On further increase in energy requirements during pacing, the myocardium was unable to upregulate its energy production, as indicated by the decreased uptake of citric acid cycle intermediates. Previous studies have reported similar compensatory increase in anaplerosis and impaired fatty acid oxidation in hypertrophied mice heart and increased myocardial oxidative metabolism in aortic stenosis patients at baseline (measured using 11 C-acetate positron emission tomography); but this is for the first time such a detailed metabolomic assessment (at baseline and during increased myocardial stress) is being reported in aortic stenosis patients[408,409]

3) Ornithine & citrulline

In patients with aortic stenosis there was a downregulation of both *ASS1* and *ARG2* genes, which encode enzymes that play a vital role in the urea cycle. This possibly results in downregulation in the activity of urea cycle, which leads to an accumulation of urea cycle intermediates such as citrulline and ornithine. These were present in a significantly higher concentration in aortic stenosis patients as compared to controls and HCM, across all collection sites. Similar findings with decreased expression of *ASS* gene accompanied with increased plasma levels of citrulline and ornithine were reported by Sheikh *et al* in mice

treated with Wy14643 (PPARα agonist).[410] To the best of our knowledge, these findings are being reported for the first time in humans with aortic stenosis.

Ornithine can also be produced in cardiac tissue from arginine via arginase, which is the first step in polyamine synthesis.[411,412] An upregulation of the polyamine pathways has been reported before in conditions of cardiac hypertrophy.[413-416] As reported in Chapter 7, aortic stenosis patients had a decreased expression of *OAZ3* gene that encodes ornithine decarboxylase antizyme 3, which inhibits ornithine decarboxylase a key enzyme in polyamine synthesis.[417,418] Such a downregulation will induce polyamine pathway activity, which will result in increased ornithine levels and cardiac hypertrophy; these changes were observed in our aortic stenosis patients and are being reported for the first time.

4) BAIBA (β-aminoisobutyric acid)

BAIBA was eluted during cardiac metabolism at baseline in patients with aortic stenosis. This switched to extraction during pacing, which was significantly different from baseline. BAIBA was also present in a significantly higher concentration in patients with aortic stenosis as compared to controls and HCM across all collection sites.

BAIBA is a small molecule myokine formed from the catabolism of valine in myocytes, which express PGC-1α. Several enzymes of valine degradation pathway are shared with β-oxidation; these include *ACADSB*, *ACAD*, *HADHA* and *HADH*.[419] There is an increased release of BAIBA in exercising muscle (both animals and humans), which is directly related to increased β-oxidation and amino acid catabolism.[279,419] BAIBA acts via PPARα mediated mechanisms increasing hepatic fatty acid β-oxidation, glucose metabolism and upregulating

the expression of brown adipocyte specific genes in white adipocytes.[279,420] These mechanisms explain the exercise-induced protection from cardiometabolic risks in humans, where BAIBA levels are elvated.[279]

Higher levels of BAIBA in aortic stenosis were possibly suggestive of an adaptive mechanism to a state of increased energy demand. This could be in direct response to increased expression of *PPARGC1A* gene in aortic stenosis, which encodes proteins constituting PGC-1α. Increased uptake of BAIBA during pacing could be counter-adaptive in maintaining energy homeostasis. Thus another gateway to future studies is opened, where the affect of BAIBA supplementation (improving energy demand-supply balance) in murine models of pressure-overload induced hypertrophy and in humans with aortic stenosis will be explored.

5) BCAAs (Branched chain amino acids)

The BCAAs, KLeu and KVal were extracted during cardiac metabolism at baseline in controls and aortic stenosis. A similar trend in the extraction of KVal was observed in patients with HCM, but the level of extraction was significantly lower than the controls and aortic stenosis. KLeu was eluted in patients with HCM at baseline, but switched to extraction during pacing. This was significantly different from baseline and a similar trend towards increased extraction was observed for KVal during pacing. There was a similar non-significant trend towards increased extraction of these BCAAs in controls, but an opposite trend was observed in aortic stenosis (decreased extraction).

Amino acids are mostly metabolised in the liver, but a subgroup of essential amino acids, the BCAAs (leucine, isoleucine and valine) are catabolised in extra-hepatic tissues, mostly the myocardium, neurons and kidney.[421] BCAAs

play a key role in peptide synthesis and in the bio synthesis of sterol, keto bodies and glucose.[422] Leucine also has a vital role of nutrient signaling activity in the cell, promoting protein synthesis, metabolism and growth, via the mTOR pathway.[423,424]

The catabolism of BCAAs produces acetyl-CoA and succinyl CoA, which are substrates in the citric acid cycle generating intracellular energy. Experimental evidence has suggested increased oxidation of BCAAs and thereby decreased levels, during protein catabolic states such as sepsis, cancer, trauma and burns.[425,426] Also there is direct evidence of BCAAs being used as a source of fuel in post absorptive patients with coronary artery disease.[427] Thus the increased uptake of BCAAs in HCM and controls during pacing could be possibly explained by their primary anabolic effect on cardiac metabolism. The decreased uptake of BCAAs in aortic stenosis again confirms the underlying dysregulation in cardiac metabolism.

8.3 Transcriptomic regulation

Detailed analysis of the metabolomic transcriptome in aortic stenosis revealed a significant change in the expression of several genes regulating the fatty acid metabolism, citric acid cycle and amino acid metabolism. These findings are described in detail in chapter 7 and only a brief overview is provided here. The expression of *PRKAG1* and *PRKAA2* genes was significantly downregulated; this was suggestive of a possible downregulation in AMPK activity. As discussed before AMPK plays a vital role in regulating the metabolism and such

a change could lead to impaired metabolic upregulation required in response to an existing state of increased energy demand.

The expression of *PPARA* was significantly increased, which encodes PPARα. PPARα is an important transcriptomic regulator of metabolism, which regulates the activity of several genes related to metabolism. However, several of these genes regulating the fatty acid metabolism had a decreased expression despite an increased expression of *PPARA*, these included: *CD36*, *ABCD3*, *ACSL3*, *ACOT1*, *CPT2*, *ACADM*, *EHHADH*, *HSD17B4*, *ETFDH*, *GPAM*, *LPIN2* and *PNPLA2*. This would be predicted result in impaired fatty acid β-oxidation, which was validated by the accumulation of long chain acyl-carnitines in these patients. These changes are indicative of a partial and ineffective compensatory increase in PPARα activity, which could be augmented and corrected by using pharmacological agonist (e.g. hypolipidemic fibrate drugs).

8.4 Conclusions: an emerging paradigm - aortic stenosis is characterized by PPARα/long chain fatty acid metabolic defects

It would appear that in aortic stenosis, the myocardium is unable to efficiently regulate and match the energy demand-supply balance, as indicated by incomplete fatty acid β-oxidation, and failed upregulation of citric acid cycle activity and BCAA metabolism during pacing. Similar findings of transcriptomic downregulation, alteration in fatty acid β-oxidation and citric acid cycle activity have been reported in both animals and humans with different cardiac etiologies (compensated LVH, heart failure, dilated cardiomyopathy and

ischemia).[311,393,394,428-434] Our study is the first correspondingly extensive investigation in humans with aortic stenosis and HCM.

Two previous studies had reported the effects of metabolic modulations using glucose-insulin-potassium (GIK) and glutamate in aortic stenosis patients undergoing valve replacement.[435,436] They had focused on measuring the activity of metabolic regulators [GIK study: AMPK and Akt phosphorylation) and the metabolism of specific amino acids (glutamate study: glutamate, alanine, tyrosine and BCAAs) pre and post modulation, but neither attempted a systematic assessment of myocardial metabolism. A state of impaired energetics at baseline and its improvement post valve replacement in critical aortic stenosis has previously been reported, but this was using non-invasive technologies.[324,437-440] Thus in aortic stenosis a comprehensive assessment of underlying transcriptomic and metabolic mechanisms during steady state and the metabolic adaptions during stress (pacing) is being presented for the first time in this study.

The detailed metabolomic assessment in HCM and aortic stenosis has enhanced our understanding of their pathophysiology and also provided new therapeutic targets, such as upregulation of PPARα with pharmacological agonist (e.g. hypolipidemic fibrate drugs and β-aminoisobutyric acid) in aortic stenosis.

8.5 Limitations

The limitation of lack of coronary sinus blood flow measurement should be acknowledged. This limitation has been considered and discussed before in

Chapters 3, 4 and 5, when describing the change in trans-gradient of metabolites in the individual cohorts. The underlying flux of metabolites during cardiac metabolism is measured as a product of aorto-coronary sinus gradient times the coronary sinus blood flow. The lack of coronary sinus blood measurements thus makes the interpretation of trans-cardiac gradient of metabolites in relation to their underlying flux challenging. But as discussed before in several studies where coronary blood flow measurements were undertaken, the trans-cardiac gradient of metabolites was reported to follow a similar trend as their respective underlying flux (increase or decrease) during pacing.[300,301] It is also important to highlight that during pacing we observed trans-cardiac elution of lactate in the HCM cohort and that elution of succinate continued with no significant difference from baseline in the control and HCM cohorts. These observations accompanied with increased coronary blood flow during pacing cannot be explained if the underlying flux of these metabolites is considered to remain unchanged. Such careful considerations have been applied when interpreting the results.

References

1. Maron BJ, Gardin JM, Flack JM, Gidding SS, Kurosaki TT, Bild DE. Prevalence of Hypertrophic Cardiomyopathy in a General Population of Young Adults: Echocardiographic Analysis of 4111 Subjects in the CARDIA Study. Circulation 1995;92:785-9.

2. Teare D. ASYMMETRICAL HYPERTROPHY OF THE HEART IN YOUNG ADULTS. British Heart Journal 1958;20:1-8.

3. Watkins H, Ashrafian H, Redwood C. Inherited Cardiomyopathies. New England Journal of Medicine 2011;364:1643-56.

4. Konno T, Chang S, Seidman JG, Seidman CE. Genetics of hypertrophic cardiomyopathy. Curr Opin Cardiol 2010;25:205-9.

5. Spoladore R, Maron MS, D'Amato R, Camici PG, Olivotto I. Pharmacological treatment options for hypertrophic cardiomyopathy: high time for evidence. Eur Heart J 2012;33:1724-33.

6. Maron BJ, Casey SA, Poliac LC, Gohman TE, Almquist AK, Aeppli DM. Clinical course of hypertrophic cardiomyopathy in a regional United States cohort. Jama-Journal of the American Medical Association 1999;281:650-5.

7. Kitaoka H, Doi Y, Casey SA, Hitomi N, Furuno T, Maron BJ. Comparison of prevalence of apical hypertrophic cardiomyopathy in Japan and the United States. Am J Cardiol 2003;92:1183-6.

8. Maron BJ, Gardin JM, Flack JM, Gidding SS, Kurosaki TT, Bild DE. PREVALENCE OF HYPERTROPHIC CARDIOMYOPATHY IN A GENERAL-POPULATION OF YOUNG-ADULTS - ECHOCARDIOGRAPHIC ANALYSIS OF 4111 SUBJECTS IN THE CARDIA STUDY. Circulation 1995;92:785-9.

9. Semsarian C, Ingles J, Maron MS, Maron BJ. New Perspectives on the Prevalence of Hypertrophic Cardiomyopathy. J Am Coll Cardiol 2015;65:1249-54.

10. Maron BJ, Carney KP, Lever HM, et al. Relationship of race to sudden cardiac death in competitive athletes with hypertrophic cardiomyopathy. J Am Coll Cardiol 2003;41:974-80.

11. Olivotto I, Maron MS, Adabag AS, et al. Gender-related differences in the clinical presentation and outcome of hypertrophic cardiomyopathy. J Am Coll Cardiol 2005;46:480-7.

12. Marian AJ, Roberts R. RECENT ADVANCES IN THE MOLECULAR-GENETICS OF HYPERTROPHIC CARDIOMYOPATHY. Circulation 1995;92:1336-47.

13. Schwartz K, Carrier L, Guicheney P, Komajda M. MOLECULAR-BASIS OF FAMILIAL CARDIOMYOPATHIES. Circulation 1995;91:532-40.

14. Niimura H, Bachinski LL, Sangwatanaroj S, et al. Mutations in the Gene for Cardiac Myosin-Binding Protein C and Late-Onset Familial Hypertrophic Cardiomyopathy. New England Journal of Medicine 1998;338:1248-57.

15. Alcalai R, Seidman JG, Seidman CE. Genetic basis of hypertrophic cardiomyopathy: From bench to the clinics. Journal of Cardiovascular Electrophysiology 2008;19:104-10.

16. Ackerman MJ, VanDriest SL, Ommen SR, et al. Prevalence and age-dependence of malignant mutations in the beta-myosin heavy chain and troponin T genes in hypertrophic cardiomyopathy - A comprehensive outpatient perspective. J Am Coll Cardiol 2002;39:2042-8.

17. Van Driest SL, Ackerman MJ, Ommen SR, et al. Prevalence and severity of "Benign" mutations in the beta-myosin heavy chain, cardiac troponin T, and alpha-tropomyosin genes in hypertrophic cardiomyopathy. Circulation 2002;106:3085-90.

18. Richard P, Charron P, Carrier L, et al. Hypertrophic Cardiomyopathy: Distribution of Disease Genes, Spectrum of Mutations, and Implications for a Molecular Diagnosis Strategy. Circulation 2003;107:2227-32.

19. Landstrom AP, Ackerman MJ, Ho CY. Mutation Type Is Not Clinically Useful in Predicting Prognosis in Hypertrophic Cardiomyopathy. Circulation 2010;122:2441-50.

20. Maron BJ, Maron MS, Semsarian C. Genetics of Hypertrophic Cardiomyopathy After 20 Years Clinical Perspectives. J Am Coll Cardiol 2012;60:705-15.

21. Gersh BJ, Maron BJ, Bonow RO, et al. 2011 ACCF/AHA guideline for the diagnosis and treatment of hypertrophic cardiomyopathy: executive summary: a report of the American College of Cardiology Foundation/American Heart Association Task Force on Practice Guidelines. The Journal of thoracic and cardiovascular surgery 2011;142:1303-38.

22. Ferrans VJ, Roberts WC, Morrow AG. MYOCARDIAL ULTRASTRUCTURE IN IDIOPATHIC HYPERTROPHIC SUBAORTIC STENOSIS - STUDY OF OPERATIVELY EXCISED LEFT VENTRICULAR OUTFLOW TRACT MUSCLE IN 14 PATIENTS. Circulation 1972;45:769-&.

23. Maron BJ, Roberts WC. QUANTITATIVE-ANALYSIS OF CARDIAC-MUSCLE CELL DISORGANIZATION IN THE VENTRICULAR SEPTUM OF PATIENTS WITH HYPERTROPHIC CARDIOMYOPATHY. Circulation 1979;59:689-706.

24. Maron BJ, Wolfson JK, Epstein SE, Roberts WC. INTRAMURAL (SMALL VESSEL) CORONARY-ARTERY DISEASE IN HYPERTROPHIC CARDIOMYOPATHY. J Am Coll Cardiol 1986;8:545-57.

25. Tanaka M, Fujiwara H, Onodera T, et al. Quantitative analysis of narrowings of intramyocardial small arteries in

normal hearts, hypertensive hearts, and hearts with hypertrophic cardiomyopathy. Circulation 1987;75:1130-9.

26. Varnava AM, Elliott PM, Mahon N, Davies MJ, McKenna WJ. Relation between myocyte disarray and outcome in hypertrophic cardiomyopathy. Am J Cardiol 2001;88:275-9.

27. Maron BJ, Anan TJ, Roberts WC. QUANTITATIVE-ANALYSIS OF THE DISTRIBUTION OF CARDIAC-MUSCLE CELL DISORGANIZATION IN THE LEFT-VENTRICULAR WALL OF PATIENTS WITH HYPERTROPHIC CARDIOMYOPATHY. Circulation 1981;63:882-94.

28. Cannon RO, III, Rosing DR, Maron BJ, et al. MYOCARDIAL ISCHEMIA IN PATIENTS WITH HYPERTROPHIC CARDIOMYOPATHY CONTRIBUTION OF INADEQUATE VASODILATOR RESERVE AND ELEVATED LEFT VENTRICULAR FILLING PRESSURES. Circulation 1985;71:234-43.

29. Krams R, Kofflard MJM, Duncker DJ, et al. Decreased coronary flow reserve in hypertrophic cardiomyopathy is related to remodeling of the coronary microcirculation. Circulation 1998;97:230-3.

30. Factor SM, Butany J, Sole MJ, Wigle ED, Williams WC, Rojkind M. PATHOLOGICAL FIBROSIS AND MATRIX CONNECTIVE-TISSUE IN THE SUBAORTIC MYOCARDIUM OF PATIENTS WITH HYPERTROPHIC CARDIOMYOPATHY. J Am Coll Cardiol 1991;17:1343-51.

31. Tanaka M, Fujiwara H, Onodera T, Wu DJ, Hamashima Y, Kawai C. QUANTITATIVE-ANALYSIS OF MYOCARDIAL FIBROSIS IN NORMALS, HYPERTENSIVE HEARTS, AND HYPERTROPHIC CARDIOMYOPATHY. British Heart Journal 1986;55:575-81.

32. Maron BJ, Epstein SE, Roberts WC. HYPERTROPHIC CARDIOMYOPATHY AND TRANSMURAL MYOCARDIAL-INFARCTION WITHOUT SIGNIFICANT

ATHEROSCLEROSIS OF THE EXTRAMURAL CORONARY-ARTERIES. Am J Cardiol 1979;43:1086-102.

33. Shirani J, Pick R, Roberts WC, Maron BJ. Morphology and significance of the left ventricular collagen network in young patients with hypertrophic cardiomyopathy and sudden cardiac death. J Am Coll Cardiol 2000;35:36-44.

34. Nicod P, Polikar R, Peterson KL. Hypertrophic Cardiomyopathy and Sudden Death. New England Journal of Medicine 1988;318:1255-7.

35. Maron BJ, Shen WK, Link MS, et al. Efficacy of implantable cardioverter-defibrillators for the prevention of sudden death in patients with hypertrophic cardiomyopathy. New England Journal of Medicine 2000;342:365-73.

36. Chung M-W, Tsoutsman T, Semsarian C. Hypertrophic cardiomyopathy: from gene defect to clinical disease. Cell Res 2003;13:9-20.

37. Wigle ED, Rakowski H, Kimball BP, Williams WG. HYPERTROPHIC CARDIOMYOPATHY - CLINICAL SPECTRUM AND TREATMENT. Circulation 1995;92:1680-92.

38. Maron BJ, Casey SA, Hauser RG, Aeppli DM. Clinical course of hypertrophic cardiomyopathy with survival to advanced age. J Am Coll Cardiol 2003;42:882-8.

39. Maron BJ, Casey SA, Haas TS, Kitner CL, Garberich RF, Lesser JR. Hypertrophic Cardiomyopathy With Longevity to 90 Years or Older. Am J Cardiol;109:1341-7.

40. Maron BJ, Spirito P, Shen W-K, et al. Implantable cardioverter-defibrillators and prevention of sudden cardiac death in hypertrophic cardiomyopathy. Jama-Journal of the American Medical Association 2007;298:405-12.

41. Maron BJ, Spirito P, Wesley Y, Arce J. DEVELOPMENT AND PROGRESSION OF LEFT-VENTRICULAR HYPERTROPHY IN CHILDREN WITH HYPERTROPHIC CARDIOMYOPATHY. New England Journal of Medicine 1986;315:610-4.

42. Maron BJ, Haas TS, Kitner C, Lesser JR. Onset of Apical Hypertrophic Cardiomyopathy in Adulthood. Am J Cardiol 2011;108:1783-7.

43. Klues HG, Schiffers A, Maron BJ. PHENOTYPIC SPECTRUM AND PATTERNS OF LEFT-VENTRICULAR HYPERTROPHY IN HYPERTROPHIC CARDIOMYOPATHY - MORPHOLOGIC OBSERVATIONS AND SIGNIFICANCE AS ASSESSED BY 2-DIMENSIONAL ECHOCARDIOGRAPHY IN 600 PATIENTS. J Am Coll Cardiol 1995;26:1699-708.

44. Harris KM, Spirito P, Maron MS, et al. Prevalence, clinical profile, and significance of left ventricular remodeling in the end-stage phase of hypertrophic cardiomyopathy. Circulation 2006;114:216-25.

45. Elliott PM, Poloniecki J, Dickie S, et al. Sudden death in hypertrophic cardiomyopathy: Identification of high risk patients. J Am Coll Cardiol 2000;36:2212-8.

46. Maron BJ, Doerer JJ, Haas TS, Tierney DM, Mueller FO. Sudden Deaths in Young Competitive Athletes Analysis of 1866 Deaths in the United States, 1980-2006. Circulation 2009;119:1085-92.

47. McKenna WJ, Deanfield JE. HYPERTROPHIC CARDIOMYOPATHY - AN IMPORTANT CAUSE OF SUDDEN-DEATH. Archives of Disease in Childhood 1984;59:971-5.

48. Spirito P, Chiarella F, Carratino L, Berisso MZ, Bellotti P, Vecchio C. CLINICAL COURSE AND PROGNOSIS OF HYPERTROPHIC CARDIOMYOPATHY IN AN OUTPATIENT POPULATION. New England Journal of Medicine 1989;320:749-55.

49. Shapiro LM, Zezulka A. HYPERTROPHIC CARDIOMYOPATHY - A COMMON DISEASE WITH A GOOD PROGNOSIS - 5 YEAR EXPERIENCE OF A DISTRICT GENERAL-HOSPITAL. British Heart Journal 1983;50:530-3.

50. Cannan CR, Reeder GS, Bailey KR, Melton LJ, Gersh BJ. Natural History of Hypertrophic Cardiomyopathy: A Population-Based Study, 1976 Through 1990. Circulation 1995;92:2488-95.

51. Maron BJ, Semsarian C, Shen W-K, et al. Circadian patterns in the occurrence of malignant ventricular tachyarrhythmias triggering defibrillator interventions in patients with hypertrophic cardiomyopathy. Heart Rhythm 2009;6:599-602.

52. Maron BJ, Haas TS, Shannon KM, Almquist AK, Hodges JS. Long-term survival after cardiac arrest in hypertrophic cardiomyopathy. Heart Rhythm 2009;6:993-7.

53. Maron BJ, Olivotto I, Spirito P, et al. Epidemiology of hypertrophic cardiomyopathy-related death - Revisited in a large non-referral-based patient population. Circulation 2000;102:858-64.

54. Elliott PM, Anastasakis A, Borger MA, et al. 2014 ESC Guidelines on diagnosis and management of hypertrophic cardiomyopathy. The Task Force for the Diagnosis and Management of Hypertrophic Cardiomyopathy of the European Society of Cardiology (ESC) 2014;35:2733-79.

55. Melacini P, Maron BJ, Bobbo F, et al. Evidence that pharmacological strategies lack efficacy for the prevention of sudden death in hypertrophic cardiomyopathy. Heart 2007;93:708-10.

56. Maron BJ, Spirito P, Green KJ, Wesley YE, Bonow RO, Arce J. NONINVASIVE ASSESSMENT OF LEFT-VENTRICULAR DIASTOLIC FUNCTION BY PULSED DOPPLER ECHOCARDIOGRAPHY IN PATIENTS WITH HYPERTROPHIC CARDIOMYOPATHY. J Am Coll Cardiol 1987;10:733-42.

57. Sharma S, Elliott P, Whyte G, et al. Utility of cardiopulmonary exercise in the assessment of clinical determinants of functional capacity in hypertrophic cardiomyopathy. Am J Cardiol 2000;86:162-8.

58. Frenneaux MP, Porter A, Caforio ALP, Odawara H, Counihan PJ, McKenna WJ. DETERMINANTS OF EXERCISE CAPACITY IN HYPERTROPHIC CARDIOMYOPATHY. J Am Coll Cardiol 1989;13:1521-6.

59. Briguori C, Betocchi S, Romano M, et al. Exercise capacity in hypertrophic cardiomyopathy depends on left ventricular diastolic function. Am J Cardiol 1999;84:309-15.

60. Maron BJ, Maron MS. Hypertrophic cardiomyopathy. The Lancet;381:242-55.

61. Melacini P, Basso C, Angelini A, et al. Clinicopathological profiles of progressive heart failure in hypertrophic cardiomyopathy. European Heart Journal 2010;31:2111-23.

62. Autore C, Bernabo P, Barilla CS, Bruzzi P, Spirito P. The prognostic importance of left ventricular outflow obstruction in hypertrophic cardiomyopathy varies in relation to the severity of symptoms. J Am Coll Cardiol 2005;45:1076-80.

63. Olivotto I, Cecchi F, Casey SA, Dolara A, Traverse JH, Maron BJ. Impact of atrial fibrillation on the clinical course of hypertrophic cardiomyopathy. Circulation 2001;104:2517-24.

64. Maron BJ, Olivotto I, Bellone P, et al. Clinical profile of stroke in 900 patients with hypertrophic cardiomyopathy. J Am Coll Cardiol 2002;39:301-7.

65. Gruner C, Care M, Siminovitch K, et al. Sarcomere Protein Gene Mutations in Patients With Apical Hypertrophic Cardiomyopathy. Circulation-Cardiovascular Genetics 2011;4:288-95.

66. Maron MS, Maron BJ, Harrigan C, et al. Hypertrophic Cardiomyopathy Phenotype Revisited After 50 Years With Cardiovascular Magnetic Resonance. J Am Coll Cardiol 2009;54:220-8.

67. Moon JCC, Fisher NG, McKenna WJ, Pennell DJ. Detection of apical hypertrophic cardiomyopathy by

cardiovascular magnetic resonance in patients with non-diagnostic echocardiography. Heart 2004;90:645-9.

68. Rickers C, Wilke NM, Jerosch-Herold M, et al. Utility of cardiac magnetic resonance imaging in the diagnosis of hypertrophic cardiomyopathy. Circulation 2005;112:855-61.

69. Maron BJ, Yeates L, Semsarian C. Clinical Challenges of Genotype Positive (+)–Phenotype Negative (−) Family Members in Hypertrophic Cardiomyopathy. Am J Cardiol;107:604-8.

70. Rowin EJ, Maron MS, Lesser JR, Maron BJ. CMR With Late Gadolinium Enhancement in Genotype Positive-Phenotype Negative Hypertrophic Cardiomyopathy. Jacc-Cardiovascular Imaging 2012;5:119-22.

71. Ho CY, Lopez B, Coelho-Filho OR, et al. Myocardial Fibrosis as an Early Manifestation of Hypertrophic Cardiomyopathy. New England Journal of Medicine 2010;363:552-63.

72. Germans T, Wilde AAM, Dijkmans PA, et al. Structural abnormalities of the inferoseptal left ventricular wall detected by cardiac magnetic resonance imaging in carriers of hypertrophic cardiomyopathy mutations. J Am Coll Cardiol 2006;48:2518-23.

73. Maron M, Harrigan C, Olivotto I, et al. Mitral Valve Abnormalities Identified by Cardiovascular Magnetic Resonance Represent a Primary Phenotypic Expression of Hypertrophic Cardiomyopathy. Circulation 2009;120:S795-S.

74. Gilligan DM, Chan WL, Joshi J, et al. A DOUBLE-BLIND, PLACEBO-CONTROLLED CROSSOVER TRIAL OF NADOLOL AND VERAPAMIL IN MILD AND MODERATELY SYMPTOMATIC HYPERTROPHIC CARDIOMYOPATHY. J Am Coll Cardiol 1993;21:1672-4.

75. Sherrid MV, Pearle G, Gunsburg DZ. Mechanism of benefit of negative inotropes in obstructive hypertrophic

cardiomyopathy (vol 97, pg 41, 1998). Circulation 1998;97:1026-.

76. Nistri S, Olivotto I, Maron MS, et al. β Blockers for Prevention of Exercise-Induced Left Ventricular Outflow Tract Obstruction in Patients With Hypertrophic Cardiomyopathy. Am J Cardiol;110:715-9.

77. Epstein SE, Rosing DR. VERAPAMIL - ITS POTENTIAL FOR CAUSING SERIOUS COMPLICATIONS IN PATIENTS WITH HYPERTROPHIC CARDIOMYOPATHY. Circulation 1981;64:437-41.

78. Sherrid M, Delia E, Dwyer E. ORAL DISOPYRAMIDE THERAPY FOR OBSTRUCTIVE HYPERTROPHIC CARDIOMYOPATHY. Am J Cardiol 1988;62:1085-8.

79. Sherrid MV, Barac I, McKenna WJ, et al. Multicenter study of the efficacy and safety of disopyramide in obstructive hypertrophic cardiomyopathy. J Am Coll Cardiol 2005;45:1251-8.

80. Camm AJ, Lip GYH, De Caterina R, et al. 2012 focused update of the ESC Guidelines for the management of atrial fibrillation. An update of the 2010 ESC Guidelines for the management of atrial fibrillationDeveloped with the special contribution of the European Heart Rhythm Association 2012;33:2719-47.

81. Morrow AG, Brockenbrough EC. SURGICAL TREATMENT OF IDIOPATHIC HYPERTROPHIC SUBAORTIC STENOSIS - TECHNIC AND HEMODYNAMIC RESULTS OF SUBAORTIC VENTRICULOMYOTOMY. Annals of Surgery 1961;154:181-&.

82. Maron BJ, Yacoub M, Dearani JA. Controversies in cardiovascular medicine Benefits of surgery in obstructive hypertrophic cardiomyopathy: bring septal myectomy back for European patients. European Heart Journal 2011;32:1055-U36.

83. Ommen SR, Maron BJ, Olivotto I, et al. Long-term effects of surgical septal myectomy on survival in patients with obstructive hypertrophic cardiomyopathy. J Am Coll Cardiol 2005;46:470-6.

84. Firoozi S, Elliott PM, Sharma S, et al. Septal myotomy-myectomy and transcoronary septal alcohol ablation in hypertrophic obstructive cardiomyopathy - A comparison of clinical, haemodynamic and exercise outcomes. European Heart Journal 2002;23:1617-24.

85. Nagueh SF, Groves BM, Schwartz L, et al. Alcohol Septal Ablation for the Treatment of Hypertrophic Obstructive Cardiomyopathy A Multicenter North American Registry. J Am Coll Cardiol 2011;58:2322-8.

86. Maron MS, Kalsmith BM, Udelson JE, Li W, DeNofrio D. Survival After Cardiac Transplantation in Patients With Hypertrophic Cardiomyopathy. Circulation-Heart Failure 2010;3:574-9.

87. Eveborn GW, Schirmer H, Heggelund G, Lunde P, Rasmussen K. The evolving epidemiology of valvular aortic stenosis. The Tromso Study. Heart 2013;99:396-400.

88. Stewart BF, Siscovick D, Lind BK, et al. Clinical factors associated with calcific aortic valve disease. J Am Coll Cardiol 1997;29:630-4.

89. Nkomo VT, Gardin JM, Skelton TN, Gottdiener JS, Scott CG, Enriquez-Sarano M. Burden of valvular heart diseases: a population-based study. Lancet 2006;368:1005-11.

90. Garg V, Muth AN, Ransom JF, et al. Mutations in NOTCH1 cause aortic valve disease. Nature 2005;437:270-4.

91. Otto CM, Kuusisto J, Reichenbach DD, Gown AM, O'Brien KD. Characterization of the early lesion of 'degenerative' valvular aortic stenosis. Histological and immunohistochemical studies. Circulation 1994;90:844-53.

92. O'Brien KD, Reichenbach DD, Marcovina SM, Kuusisto J, Alpers CE, Otto CM. Apolipoproteins B, (a), and E Accumulate in the Morphologically Early Lesion of 'Degenerative' Valvular Aortic Stenosis. Arteriosclerosis, Thrombosis, and Vascular Biology 1996;16:523-32.

93. Ghaisas NK, Foley JB, O'Briain DS, Crean P, Kelleher D, Walsh M. Adhesion molecules in nonrheumatic aortic valve disease: endothelial expression, serum levels and effects of valve replacement. J Am Coll Cardiol 2000;36:2257-62.

94. Olsson M, Thyberg J, Nilsson J. Presence of Oxidized Low Density Lipoprotein in Nonrheumatic Stenotic Aortic Valves. Arteriosclerosis, Thrombosis, and Vascular Biology 1999;19:1218-22.

95. Caira FC, Stock SR, Gleason TG, et al. Human Degenerative Valve Disease Is Associated With Up-Regulation of Low-Density Lipoprotein Receptor-Related Protein 5 Receptor-Mediated Bone Formation. J Am Coll Cardiol 2006;47:1707-12.

96. Hein S, Arnon E, Kostin S, et al. Progression From Compensated Hypertrophy to Failure in the Pressure-Overloaded Human Heart: Structural Deterioration and Compensatory Mechanisms. Circulation 2003;107:984-91.

97. Owens DS, Katz R, Takasu J, Kronmal R, Budoff MJ, O'Brien KD. Incidence and Progression of Aortic Valve Calcium in the Multi-Ethnic Study of Atherosclerosis (MESA). Am J Cardiol 2010;105:701-8.

98. Novaro GM, Katz R, Aviles RJ, et al. Clinical factors, but not C-reactive protein, predict progression of calcific aortic-valve disease: The cardiovascular health study. J Am Coll Cardiol 2007;50:1992-8.

99. Otto CM, Lind BK, Kitzman DW, Gersh BJ, Siscovick DS, Cardiovascular Hlth S. Association of aortic-valve sclerosis with cardiovascular mortality and morbidity in the elderly. New England Journal of Medicine 1999;341:142-7.

100. Kodali SK, Williams MR, Smith CR, et al. Two-Year Outcomes after Transcatheter or Surgical Aortic-Valve Replacement. New England Journal of Medicine 2012;366:1686-95.

101. Sarantitis I, Papanastasopoulos P, Manousi M, Baikoussis NG, Apostolakis E. The Cytoskeleton of the Cardiac Muscle Cell. Hellenic Journal of Cardiology 2012;53:367-79.

102. Nerbonne JM, Kass RS. Molecular Physiology of Cardiac Repolarization. Physiological Reviews 2005;85:1205-53.

103. Giordano FJ. Oxygen, oxidative stress, hypoxia, and heart failure. J Clin Invest 2005;115:500-8.

104. Ashrafian H, McKenna WJ, Watkins H. Disease Pathways and Novel Therapeutic Targets in Hypertrophic Cardiomyopathy. CircRes 2011;109:86-96.

105. Bing RJ, Siegel A, Ungar I, Gilbert M. METABOLISM OF THE HUMAN HEART .2. STUDIES ON FAT, KETONE AND AMINO ACID METABOLISM. American Journal of Medicine 1954;16:504-15.

106. Neely JR, Morgan HE. RELATIONSHIP BETWEEN CARBOHYDRATE AND LIPID-METABOLISM AND ENERGY-BALANCE OF HEART-MUSCLE. Annual Review of Physiology 1974;36:413-59.

107. Lopaschuk GD, Belke DD, Gamble J, Itoi T, Schonekess BO. REGULATION OF FATTY-ACID OXIDATION IN THE MAMMALIAN HEART IN HEALTH AND DISEASE. Biochimica Et Biophysica Acta-Lipids and Lipid Metabolism 1994;1213:263-76.

108. Opie LH. THE HEART PHYSIOLOGY AND METABOLISM SECOND EDITION1991.

109. Dyck JRB, Berthiaume LG, Thomas PD, et al. Characterization of rat liver malonyl-CoA decarboxylase and the study of its role in regulating fatty acid metabolism. Biochemical Journal 2000;350:599-608.

110. Kudo N, Gillespie JG, Kung L, et al. Characterization of 5'AMP-activated protein kinase activity in the heart and its role in inhibiting acetyl-CoA carboxylase during reperfusion following ischemia. Biochimica Et Biophysica Acta-Lipids and Lipid Metabolism 1996;1301:67-75.

111. Stanley WC, Lopaschuk GD, Hall JL, McCormack JG. Regulation of myocardial carbohydrate metabolism under normal and ischaemic conditions - Potential for pharmacological interventions. Cardiovascular Research 1997;33:243-57.

112. Stanley WC, Recchia FA, Lopaschuk GD. Myocardial Substrate Metabolism in the Normal and Failing Heart. Physiological Reviews 2005;85:1093-129.

113. van der Vusse GJ, van Bilsen M, Glatz JFC. Cardiac fatty acid uptake and transport in health and disease. Cardiovascular Research 2000;45:279-93.

114. Kurien VA, Yates PA, Oliver MF. FREE FATTY ACIDS, HEPARIN, AND ARRHYTHMIAS DURING EXPERIMENTAL MYOCARDIAL INFARCTION. Lancet 1969;2:185-&.

115. Kurien VA, Oliver MF. FREE FATTY-ACIDS DURING ACUTE MYO CARDIAL INFARCTION. Progress in Cardiovascular Diseases 1971;13:361-73.

116. Hauton D, Bennett MJ, Evans RD. Utilisation of triacylglycerol and non-esterified fatty acid by the working rat heart: myocardial lipid substrate preference. Biochimica Et Biophysica Acta-Molecular and Cell Biology of Lipids 2001;1533:99-109.

117. Niu YG, Hauton D, Evans RD. Utilization of triacylglycerol-rich lipoproteins by the working rat heart: routes of uptake and metabolic fates. Journal of Physiology-London 2004;558:225-37.

118. Pulinilkunnil T, Rodrigues B. Cardiac lipoprotein lipase: Metabolic basis for diabetic heart disease. Cardiovascular Research 2006;69:329-40.

119. Goldberg IJ, Eckel RH, Abumrad NA. Regulation of fatty acid uptake into tissues: lipoprotein lipase- and CD36-mediated pathways. Journal of Lipid Research 2009;50:S86-S90.

120. Schwenk RW, Luiken JJFP, Bonen A, Glatz JFC. Regulation of sarcolemmal glucose and fatty acid transporters in cardiac disease. Cardiovascular Research 2008;79:249-58.

121. Luiken J, Coort SLM, Koonen DPY, et al. Regulation of cardiac long-chain fatty acid and glucose uptake by translocation of substrate transporters. Pflugers Archiv-European Journal of Physiology 2004;448:1-15.

122. Muoio DM, Newgard CB. Molecular and metabolic mechanisms of insulin resistance and beta-cell failure in type 2 diabetes. Nature Reviews Molecular Cell Biology 2008;9:193-205.

123. Petersen KF, Shulman GI. Etiology of insulin resistance. American Journal of Medicine 2006;119:10S-6S.

124. Summers SA. Ceramides in insulin resistance and lipotoxicity. Progress in Lipid Research 2006;45:42-72.

125. Lee Y, Naseem RH, Duplomb L, et al. Hyperleptinemia prevents lipotoxic cardiomyopathy in acyl CoA synthase transgenic mice. Proceedings of the National Academy of Sciences of the United States of America 2004;101:13624-9.

126. Chiu HC, Kovacs A, Blanton RM, et al. Transgenic expression of fatty acid transport protein 1 in the heart causes lipotoxic cardiomyopathy. Circulation Research 2005;96:225-33.

127. McGarry JD, Brown NF. The mitochondrial carnitine palmitoyltransferase system - From concept to molecular analysis. European Journal of Biochemistry 1997;244:1-14.

128. AbuElheiga L, AlmarzaOrtega DB, Baldini A, Wakil SJ. Human acetyl-CoA carboxylase 2 - Molecular cloning,

characterization, chromosomal mapping, and evidence for two isoforms. Journal of Biological Chemistry 1997;272:10669-77.

129. Dyck JRB, Lopaschuk GD. AMPK alterations in cardiac physiology and pathology: enemy or ally? The Journal of Physiology 2006;574:95-112.

130. Russell RR, Li J, Coven DL, et al. AMP-activated protein kinase mediates ischemic glucose uptake and prevents postischemic cardiac dysfunction, apoptosis, and injury. Journal of Clinical Investigation 2004;114:495-503.

131. Schulz H. Oxidation of fatty acids in eukaryotes. In: Vance DE, Vance JE, eds. Biochemistry of Lipids, Lipoproteins and Membranes, 5th Edition2008:131-54.

132. Longo N, Filippo CAD, Pasquali M. Disorders of carnitine transport and the carnitine cycle. American Journal of Medical Genetics Part C-Seminars in Medical Genetics 2006;142C:77-85.

133. Weis BC, Cowan AT, Brown N, Foster DW, McGarry JD. USE OF A SELECTIVE INHIBITOR OF LIVER CARNITINE PALMITOYLTRANSFERASE-I (CPT-I) ALLOWS QUANTIFICATION IF ITS CONTRIBUTION TO TOTAL CPT-I ACTIVITY IN RAT-HEART - EVIDENCE THAT THE DOMINANT CARDIAC CPT-I ISOFORM IS IDENTICAL TO THE SKELETAL-MUSCLE ENZYME. Journal of Biological Chemistry 1994;269:26443-8.

134. Neely JR, Morgan HE. RELATIONSHIP BETWEEN CARBOHYDRATE AND LIPID METABOLISM AND THE ENERGY BALANCE OF HEART MUSCLE1974.

135. Desvergne B, Michalik L, Wahli W. Transcriptional Regulation of Metabolism. Physiological Reviews 2006;86:465-514.

136. Finck BN, Kelly DP. PGC-1 coactivators: inducible regulators of energy metabolism in health and disease. Journal of Clinical Investigation 2006;116:615-22.

137. Madrazo JA, Kelly DP. The PPAR trio: Regulators of myocardial energy metabolism in health and disease. Journal of Molecular and Cellular Cardiology 2008;44:968-75.

138. Yang Q, Li Y. Roles of PPARs on regulating myocardial energy and lipid homeostasis. Journal of Molecular Medicine-Jmm 2007;85:697-706.

139. Finck BN, Lehman JJ, Leone TC, et al. The cardiac phenotype induced by PPAR alpha overexpression mimics that caused by diabetes mellitus. Journal of Clinical Investigation 2002;109:121-30.

140. Campbell FM, Kozak R, Wagner A, et al. A role for peroxisome proliferator-activated receptor alpha (PPAR alpha) in the control of cardiac malonyl-CoA levels - Reduced fatty acid oxidation rates and increased glucose oxidation rates in the hearts of mice lacking PPAR alpha are associated with higher concentrations of maloncyl-CoA and reduced expression of malonyl-CoA decarboxlase. Journal of Biological Chemistry 2002;277:4098-103.

141. Burkart EM, Sambandam N, Han X, et al. Nuclear receptors PPAR beta/delta and PPAR alpha direct distinct metabolic regulatory programs in the mouse heart. Journal of Clinical Investigation 2007;117:3930-9.

142. Cheng LH, Ding GL, Qin QH, et al. Peroxisome proliferator-activated receptor delta activates fatty acid oxidation in cultured neonatal and adult cardiomyocytes. Biochemical and Biophysical Research Communications 2004;313:277-86.

143. Son N-H, Park T-S, Yamashita H, et al. Cardiomyocyte expression of PPAR gamma leads to cardiac dysfunction in mice. Journal of Clinical Investigation 2007;117:2791-801.

144. Puigserver P, Wu ZD, Park CW, Graves R, Wright M, Spiegelman BM. A cold-inducible coactivator of nuclear receptors linked to adaptive thermogenesis. Cell 1998;92:829-39.

145. Bing RJ, Michal G. MYOCARDIAL EFFICIENCY. Annals of the New York Academy of Sciences 1959;72:555-8.

146. Simonsen S, Kjekshus JK. EFFECT OF FREE FATTY-ACIDS ON MYOCARDIAL OXYGEN-CONSUMPTION DURING ATRIAL-PACING AND CATECHOLAMINE INFUSION IN MAN. Circulation 1978;58:484-91.

147. Korvald C, Elvenes OP, Myrmel T. Myocardial substrate metabolism influences left ventricular energetics in vivo. American Journal of Physiology-Heart and Circulatory Physiology 2000;278:H1345-H51.

148. Mjos OD, Kjekshus J. INCREASED LOCAL METABOLIC RATE BY FREE FATTY ACIDS IN INTACT DOG HEART. Scandinavian Journal of Clinical & Laboratory Investigation 1971;28:389-&.

149. Hutter JF, Schweickhardt C, Piper HM, Spieckermann PG. INHIBITION OF FATTY-ACID OXIDATION AND DECREASE OF OXYGEN-CONSUMPTION OF WORKING RAT-HEART BY 4-BROMOCROTONIC ACID. Journal of Molecular and Cellular Cardiology 1984;16:105-8.

150. Hinkle PC. P/O ratios of mitochondrial oxidative phosphorylation. Biochimica Et Biophysica Acta-Bioenergetics 2005;1706:1-11.

151. Kadenbach B. Intrinsic and extrinsic uncoupling of oxidative phosphorylation. Biochimica Et Biophysica Acta-Bioenergetics 2003;1604:77-94.

152. Rousset S, Alves-Guerra MC, Mozo J, et al. The biology of mitochondrial uncoupling proteins. Diabetes 2004;53:S130-S5.

153. Schrauwen P, Hoeks J, Schaart G, et al. Uncoupling protein 3 as a mitochondrial fatty acid anion exporter. Faseb Journal 2003;17:2272-+.

154. Hunt MC, Alexson SEH. The role acyl-CoA thioesterases play in mediating intracellular lipid metabolism. Progress in Lipid Research 2002;41:99-130.

155. Jezek P, Modriansky M, Garlid KD. Inactive fatty acids are unable to flip-flop across the lipid bilayer. Febs Letters 1997;408:161-5.

156. Saddik M, Lopaschuk GD. MYOCARDIAL TRIGLYCERIDE TURNOVER DURING REPERFUSION OF ISOLATED RAT HEARTS SUBJECTED TO A TRANSIENT PERIOD OF GLOBAL-ISCHEMIA. Journal of Biological Chemistry 1992;267:3825-31.

157. Huang JMC, Xian H, Bacaner M. LONG-CHAIN FATTY-ACIDS ACTIVATE CALCIUM CHANNELS IN VENTRICULAR MYOCYTES. Proceedings of the National Academy of Sciences of the United States of America 1992;89:6452-6.

158. Shrago E. Long-chain acyl-CoA as a multi-effector ligand in cellular metabolism. Journal of Nutrition 2000;130:290S-3S.

159. Lanoue KF, Watts JA, Koch CD. ADENINE-NUCLEOTIDE TRANSPORT DURING CARDIAC ISCHEMIA. American Journal of Physiology 1981;241:H663-H71.

160. Gertz EW, Wisneski JA, Stanley WC, Neese RA. MYOCARDIAL SUBSTRATE UTILIZATION DURING EXERCISE IN HUMANS - DUAL CARBON-LABELED CARBOHYDRATE ISOTOPE EXPERIMENTS. Journal of Clinical Investigation 1988;82:2017-25.

161. Wisneski JA, Gertz EW, Neese RA, Gruenke LD, Morris DL, Craig JC. METABOLIC-FATE OF EXTRACTED GLUCOSE IN NORMAL HUMAN MYOCARDIUM. Journal of Clinical Investigation 1985;76:1819-27.

162. Patel MS, Korotchkina LG. Regulation of the pyruvate dehydrogenase complex. Biochemical Society Transactions 2006;34:217-22.

163. Randle PJ, Garland PB, Newsholme EA, Hales CN. GLUCOSE FATTY-ACID CYCLE - ITS ROLE IN INSULIN

SENSITIVITY AND METABOLIC DISTURBANCES OF DIABETES MELLITUS. Lancet 1963;1:785-&.

164. Krebs HA. HISTORY OF TRICARBOXYLIC ACID CYCLE. Perspectives in Biology and Medicine 1970;14:154-&.

165. van Hellemond JJ, Opperdoes FR, Tielens AGM. The extraordinary mitochondrion and unusual citric acid cycle in Trypanosoma brucei. Biochemical Society Transactions 2005;33:967-71.

166. MelendezHevia E, Waddell TG, Cascante M. The puzzle of the Krebs citric acid cycle: Assembling the pieces of chemically feasible reactions, and opportunism in the design of metabolic pathways during evolution. Journal of Molecular Evolution 1996;43:293-303.

167. Wan B, Lanoue KF, Cheung JY, Scaduto RC. REGULATION OF CITRIC-ACID CYCLE BY CALCIUM. Journal of Biological Chemistry 1989;264:13430-9.

168. Lommi J, Kupari M, Yki-Jarvinen H. Free fatty acid kinetics and oxidation in congestive heart failure. American Journal of Cardiology 1998;81:45-50.

169. Paolisso G, Gambardella A, Galzerano D, et al. TOTAL-BODY AND MYOCARDIAL SUBSTRATE OXIDATION IN CONGESTIVE-HEART-FAILURE. Metabolism-Clinical and Experimental 1994;43:174-9.

170. Neglia D, De Caterina A, Marraccini P, et al. Impaired myocardial metabolic reserve and substrate selection flexibility during stress in patients with idiopathic dilated cardiomyopathy. American Journal of Physiology-Heart and Circulatory Physiology 2007;293:H3270-H8.

171. Taylor M, Wallhaus TR, DeGrado TR, et al. An evaluation of myocardial fatty acid and glucose uptake using PET with F-18 fluoro-6-thia-heptadecanoic acid and F-18 FDG in patients with congestive heart failure. Journal of Nuclear Medicine 2001;42:55-62.

172. Davila-Roman VG, Vedala G, Herrero P, et al. Altered myocardial fatty acid and glucose metabolism in idiopathic dilated cardiomyopathy. Journal of the American College of Cardiology 2002;40:271-7.

173. Sack MN, Rader TA, Park SH, Bastin J, McCune SA, Kelly DP. Fatty acid oxidation enzyme gene expression is downregulated in the failing heart. Circulation 1996;94:2837-42.

174. Martin MA, Gomez MA, Guillen F, et al. Myocardial carnitine and carnitine palmitoyltransferase deficiencies in patients with severe heart failure. Biochimica Et Biophysica Acta-Molecular Basis of Disease 2000;1502:330-6.

175. Morgan EE, Chandler MP, Young ME, et al. Dissociation between gene and protein expression of metabolic enzymes in a rodent model of heart failure. European Journal of Heart Failure 2006;8:687-93.

176. Remondino A, Rosenblatt-Velin N, Montessuit C, et al. Altered expression of proteins of metabolic regulation during remodeling of the left ventricle after myocardial infarction. Journal of Molecular and Cellular Cardiology 2000;32:2025-34.

177. Barger PM, Brandt JM, Leone TC, Weinheimer CJ, Kelly DP. Deactivation of peroxisome proliferator-activated receptor-alpha during cardiac hypertrophic growth. Journal of Clinical Investigation 2000;105:1723-30.

178. Barger PM, Kelly DP. Fatty acid utilization in the hypertrophied and failing heart: Molecular regulatory mechanisms. American Journal of the Medical Sciences 1999;318:36-42.

179. Labinskyy V, Bellomo M, Chandler MP, et al. Chronic activation of peroxisome proliferator-activated receptor-alpha with fenofibrate prevents alterations in cardiac metabolic phenotype without changing the onset of decompensation in pacing-induced heart failure. Journal of

Pharmacology and Experimental Therapeutics 2007;321:165-71.

180. Pellieux C, Aasum E, Larsen TS, et al. Overexpression of angiotensinogen in the myocardium induces downregulation of the fatty acid oxidation pathway. Journal of Molecular and Cellular Cardiology 2006;41:459-66.

181. Karbowska J, Kochan Z, Smolenski RT. Peroxisome proliferator-activated receptor alpha is downregulated in the failing human heart. Cellular & Molecular Biology Letters 2003;8:49-53.

182. Young ME, Laws FA, Goodwin GW, Taegtmeyer H. Reactivation of peroxisome proliferator-activated receptor alpha is associated with contractile dysfunction in hypertrophied rat heart. Journal of Biological Chemistry 2001;276:44390-5.

183. Morgan EE, Rennison JH, Young ME, et al. Effects of chronic activation of peroxisome proliferator-activated receptor-alpha or high-fat feeding in a rat infarct model of heart failure. American Journal of Physiology-Heart and Circulatory Physiology 2006;290:H1899-H904.

184. Neubauer S. Mechanisms of disease - The failing heart - An engine out of fuel. New England Journal of Medicine 2007;356:1140-51.

185. Rosca MG, Vazquez EJ, Kerner J, et al. Cardiac mitochondria in heart failure: decrease in respirasomes and oxidative phosphorylation. Cardiovascular Research 2008;80:30-9.

186. Lee L, Campbell R, Scheuermann-Freestone M, et al. Metabolic modulation with perhexiline in chronic heart failure - A randomized, controlled trial of short-term use of a novel treatment. Circulation 2005;112:3280-8.

187. Turcani M, Rupp H. Modification of left ventricular hypertrophy by chronic etomoxir treatment. British Journal of Pharmacology 1999;126:501-7.

188. Lionetti V, Linke A, Chandler MP, et al. Carnitine palmitoyl transferase-I inhibition prevents ventricular remodeling and delays decompensation in pacing-induced heart failure. Cardiovascular Research 2005;66:454-61.

189. Fragasso G, Perseghin G, De Cobelli F, et al. Effects of metabolic modulation by trimetazidine on left ventricular function and phosphocreatine/adenosine triphosphate ratio in patients with heart failure. European Heart Journal 2006;27:942-8.

190. Tuunanen H, Engblom E, Naum A, et al. Trimetazidine, a metabolic modulator, has cardiac and extracardiac benefits in idiopathic dilated cardiomyopathy. Circulation 2008;118:1250-8.

191. Christen.Nj, Videbaek J. PLASMA CATECHOLAMINES AND CARBOHYDRATE-METABOLISM IN PATIENTS WITH ACUTE MYOCARDIAL-INFARCTION. Journal of Clinical Investigation 1974;54:278-86.

192. Lloyd SG, Wang PP, Zeng HD, Chatham JC. Impact of low-flow ischemia on substrate oxidation and glycolysis in the isolated perfused rat heart. American Journal of Physiology-Heart and Circulatory Physiology 2004;287:H351-H62.

193. Panchal AR, Comte B, Huang H, et al. Acute hibernation decreases myocardial pyruvate carboxylation and citrate release. American Journal of Physiology-Heart and Circulatory Physiology 2001;281:H1613-H20.

194. Dennis SC, Gevers W, Opie LH. PROTONS IN ISCHEMIA - WHERE DO THEY COME FROM - WHERE DO THEY GO TO. Journal of Molecular and Cellular Cardiology 1991;23:1077-86.

195. Robergs RA, Ghiasvand F, Parker D. Biochemistry of exercise-induced metabolic acidosis. American Journal of Physiology-Regulatory Integrative and Comparative Physiology 2004;287:R502-R16.

196. Liu Q, Docherty JC, Rendell JCT, Clanachan AS, Lopaschuk GD. High levels of fatty acids delay the recovery of intracellular pH and cardiac efficiency in post-ischemic hearts by inhibiting glucose oxidation. Journal of the American College of Cardiology 2002;39:718-25.

197. Kudo N, Barr AJ, Barr RL, Desai S, Lopaschuk GD. HIGH-RATES OF FATTY-ACID OXIDATION DURING REPERFUSION OF ISCHEMIC HEARTS ARE ASSOCIATED WITH A DECREASE IN MALONYL-COA LEVELS DUE TO AN INCREASE IN 5'-AMP-ACTIVATED PROTEIN-KINASE INHIBITION OF ACETYL-COA CARBOXYLASE. Journal of Biological Chemistry 1995;270:17513-20.

198. Ussher JR, Lopaschuk GD. The malonyl CoA axis as a potential target for treating ischaemic heart disease. Cardiovascular Research 2008;79:259-68.

199. Bolli R, Marban E. Molecular and cellular mechanisms of myocardial stunning. Physiological Reviews 1999;79:609-34.

200. Baartscheer A, Schumacher CA, van Borren M, Belterman CN, Coronel R, Fiolet JWT. Increased Na+/H+-exchange activity is the cause of increased Na+ (i) and underlies disturbed calcium handling in the rabbit pressure and volume overload heart failure model. Cardiovascular Research 2003;57:1015-24.

201. Jennings RB, Reimer KA. THE CELL BIOLOGY OF ACUTE MYOCARDIAL-ISCHEMIA. Annual Review of Medicine 1991;42:225-46.

202. Neely JR, Feuvray D. METABOLIC PRODUCTS AND MYOCARDIAL ISCHEMIA. American Journal of Pathology 1981;102:282-91.

203. Thierfelder L, Watkins H, MacRae C, et al. α-tropomyosin and cardiac troponin T mutations cause familial hypertrophic cardiomyopathy: A disease of the sarcomere. Cell;77:701-12.

204. Watkins H, McKenna WJ, Thierfelder L, et al. Mutations in the Genes for Cardiac Troponin T and α-Tropomyosin in Hypertrophic Cardiomyopathy. New England Journal of Medicine 1995;332:1058-65.

205. Marian AJ. Pathogenesis of diverse clinical and pathological phenotypes in hypertrophic cardiomyopathy. Lancet 2000;355:58-60.

206. Watkins H, Seidman CE, Seidman JG, Feng HS, Sweeney HL. Expression and functional assessment of a truncated cardiac troponin T that causes hypertrophic cardiomyopathy - Evidence for a dominant negative action. Journal of Clinical Investigation 1996;98:2456-61.

207. Sata M, Ikebe M. Functional analysis of the mutations in the human cardiac beta-myosin that are responsible for familial hypertrophic cardiomyopathy. Implication for the clinical outcome. The Journal of Clinical Investigation 1996;98:2866-73.

208. Lowey S. Functional consequences of mutations in the myosin heavy chain at sites implicated in familial hypertrophic cardiomyopathy. Trends in Cardiovascular Medicine 2002;12:348-54.

209. Michele DE, Albayya FP, Metzger JM. Direct, convergent hypersensitivity of calcium-activated force generation produced by hypertrophic cardiomyopathy mutant [alpha]-tropomyosins in adult cardiac myocytes. Nat Med 1999;5:1413-7.

210. Ho CY, Sweitzer NK, McDonough B, et al. Assessment of diastolic function with Doppler tissue imaging to predict genotype in preclinical hypertrophic cardiomyopathy. Circulation 2002;105:2992-7.

211. Niimura H, Bachinski LL, Sangwatanaroj S, et al. Mutations in the gene for cardiac myosin-binding protein C and late-onset familial hypertrophic cardiomyopathy. New England Journal of Medicine 1998;338:1248-57.

212. Sweeney HL, Feng HSS, Yang ZH, Watkins H. Functional analyses of troponin T mutations that cause hypertrophic cardiomyopathy: Insights into disease pathogenesis and troponin function. Proceedings of the National Academy of Sciences of the United States of America 1998;95:14406-10.

213. Merante F, Tein I, Benson L, Robinson BH. MATERNALLY INHERITED HYPERTROPHIC CARDIOMYOPATHY DUE TO A NOVEL T-TO-C TRANSITION AT NUCLEOTIDE-9997 IN THE MITOCHONDRIAL TRNA(GLYCINE) GENE. American Journal of Human Genetics 1994;55:437-46.

214. Lodi R, Cooper JM, Bradley JL, et al. Deficit of in vivo mitochondrial ATP production in patients with Friedreich ataxia. Proceedings of the National Academy of Sciences of the United States of America 1999;96:11492-5.

215. Tanaka T, Sohmiya K, Kawamura K. Is CD36 deficiency an etiology of hereditary hypertrophic cardiomyopathy? Journal of Molecular and Cellular Cardiology 1997;29:121-7.

216. Aoyama T, Souri M, Ushikubo S, et al. PURIFICATION OF HUMAN VERY-LONG-CHAIN ACYL-COENZYME-A DEHYDROGENASE AND CHARACTERIZATION OF ITS DEFICIENCY IN 7 PATIENTS. Journal of Clinical Investigation 1995;95:2465-73.

217. Graham BH, Waymire KG, Cottrell B, Trounce IA, MacGregor GR, Wallace DC. A mouse model for mitochondrial myopathy and cardiomyopathy resulting from a deficiency in the heart/muscle isoform of the adenine nucleotide translocator. Nature Genetics 1997;16:226-34.

218. Blair E, Redwood C, Ashrafian H, et al. Mutations in the γ2 subunit of AMP-activated protein kinase cause familial hypertrophic cardiomyopathy: evidence for the central role of energy compromise in disease pathogenesis. Human Molecular Genetics 2001;10:1215-20.

219. Arad M, Benson DW, Perez-Atayde AR, et al. Constitutively active AMP kinase mutations cause glycogen storage disease mimicking hypertrophic cardiomyopathy. Journal of Clinical Investigation 2002;109:357-62.

220. Jung WI, Sieverding L, Breuer J, et al. P-31 NMR spectroscopy detects metabolic abnormalities in asymptomatic patients with hypertrophic cardiomyopathy. Circulation 1998;97:2536-42.

221. Crilley JG, Boehm EA, Blair E, et al. Hypertrophic cardiomyopathy due to sarcomeric gene mutations is characterized by impaired energy metabolism irrespective of the degree of hypertrophy. Journal of the American College of Cardiology 2003;41:1776-82.

222. Arbustini E, Fasani R, Morbini P, et al. Coexistence of mitochondrial DNA and β myosin heavy chain mutations in hypertrophic cardiomyopathy with late congestive heart failure. Heart 1998;80:548-58.

223. Spindler M, Saupe KW, Christe ME, et al. Diastolic dysfunction and altered energetics in the alphaMHC403/+ mouse model of familial hypertrophic cardiomyopathy. The Journal of Clinical Investigation 1998;101:1775-83.

224. Lucas DT, Aryal P, Szweda LI, Koch WJ, Leinwand LA. Alterations in mitochondrial function in a mouse model of hypertrophic cardiomyopathy. American Journal of Physiology-Heart and Circulatory Physiology 2003;284:H575-H83.

225. Wallace DC. Mitochondrial diseases in man and mouse. Science 1999;283:1482-8.

226. D JeAMK, Moon MR, Green GR, et al. Estimation of regional left ventricular wall stresses in intact canine hearts. American Journal of Physiology 1998;275:H1879-H85.

227. Dunn RB. HIGH-ENERGY PHOSPHATE-DEPLETION AND LACTATE ACCUMULATION IN THE INTERVENTRICULAR SEPTUM AND LEFT-VENTRICULAR FREE WALL OF THE DOG AFTER

TOTAL CORONARY-OCCLUSION. Circulation Research 1984;54:405-13.

228. Ashrafian H, Redwood C, Blair E, Watkins H. Hypertrophic cardiomyopathy:a paradigm for myocardial energy depletion. Trends Genet 2003;19:263-8.

229. Abozguia K, Elliott P, McKenna W, et al. Metabolic Modulator Perhexiline Corrects Energy Deficiency and Improves Exercise Capacity in Symptomatic Hypertrophic Cardiomyopathy. Circulation 2010;122:1562-U56.

230. Wishart DS, Jewison T, Guo AC, et al. HMDB 3.0-The Human Metabolome Database in 2013. Nucleic Acids Research 2013;41:D801-D7.

231. Dalgliesh CE, Horning EC, Horning MG, Knox KL, Yarger K. A gas–liquid-chromatographic procedure for separating a wide range of metabolites occuring in urine or tissue extracts. Biochemical Journal 1966;101:792-810.

232. Horning EC, Horning MG. METABOLIC PROFILES - GAS-PHASE METHODS FOR ANALYSIS OF METABOLITES. Clinical Chemistry 1971;17:802-&.

233. Pauling L, Robinson AB, Teranish.R, Cary P. QUANTITATIVE ANALYSIS OF URINE VAPOR AND BREATH BY GAS-LIQUID PARTITION CHROMATOGRAPHY. Proceedings of the National Academy of Sciences of the United States of America 1971;68:2374-&.

234. Nicholson JK, Oflynn MP, Sadler PJ, Macleod AF, Juul SM, Sonksen PH. PROTON-NUCLEAR-MAGNETIC-RESONANCE STUDIES OF SERUM, PLASMA AND URINE FROM FASTING NORMAL AND DIABETIC SUBJECTS. Biochemical Journal 1984;217:365-75.

235. Fossel ET, Carr JM, McDonagh J. DETECTION OF MALIGNANT-TUMORS - WATER-SUPPRESSED PROTON NUCLEAR-MAGNETIC-RESONANCE SPECTROSCOPY OF PLASMA. New England Journal of Medicine 1986;315:1369-76.

236. Nicholson JK, Lindon JC, Holmes E. 'Metabonomics': understanding the metabolic responses of living systems to pathophysiological stimuli via multivariate statistical analysis of biological NMR spectroscopic data. Xenobiotica 1999;29:1181-9.

237. Fiehn O, Kopka J, Dormann P, Altmann T, Trethewey RN, Willmitzer L. Metabolite profiling for plant functional genomics. Nature Biotechnology 2000;18:1157-61.

238. Raamsdonk LM, Teusink B, Broadhurst D, et al. A functional genomics strategy that uses metabolome data to reveal the phenotype of silent mutations. Nature Biotechnology 2001;19:45-50.

239. Oliver SG, Winson MK, Kell DB, Baganz F. Systematic functional analysis of the yeast genome. Trends in Biotechnology 1998;16:373-8.

240. Lewis GD, Asnani A, Gerszten RE. Application of metabolomics to cardiovascular biomarker and pathway discovery. J Am Coll Cardiol 2008;52:117-23.

241. Lusis AJ. A thematic review series: systems biology approaches to metabolic and cardiovascular disorders. Journal of Lipid Research 2006;47:1887-90.

242. Dettmer K, Hammock BD. Metabolomics - A new exciting field within the "omics" sciences. Environmental Health Perspectives 2004;112:A396-A7.

243. Deo RC, Hunter L, Lewis GD, et al. Interpreting Metabolomic Profiles using Unbiased Pathway Models. Plos Computational Biology 2010;6.

244. Pope GA, MacKenzie DA, Defemez M, et al. Metabolic footprinting as a tool for discriminating between brewing yeasts. Yeast 2007;24:667-79.

245. Loscalzo J, Kohane I, Barabasi A-L. Human disease classification in the postgenomic era: A complex systems approach to human pathobiology. Molecular Systems Biology 2007;3.

246. Lenz EM, Bright J, Wilson ID, et al. Metabonomics, dietary influences and cultural differences: a H-1 NMR-based study of urine samples obtained from healthy British and Swedish subjects. Journal of Pharmaceutical and Biomedical Analysis 2004;36:841-9.

247. Walsh MC, Brennan L, Malthouse JPG, Roche HM, Gibney MJ. Effect of acute dietary standardization on the urinary, plasma, and salivary metabolomic profiles of healthy humans. American Journal of Clinical Nutrition 2006;84:531-9.

248. Want EJ, O'Maille G, Smith CA, et al. Solvent-Dependent Metabolite Distribution, Clustering, and Protein Extraction for Serum Profiling with Mass Spectrometry. Analytical Chemistry 2006;78:743-52.

249. Gullberg J, Jonsson P, Nordström A, Sjöström M, Moritz T. Design of experiments: an efficient strategy to identify factors influencing extraction and derivatization of Arabidopsis thaliana samples in metabolomic studies with gas chromatography/mass spectrometry. Analytical Biochemistry 2004;331:283-95.

250. Shortreed MR, Lamos SM, Frey BL, et al. Ionizable Isotopic Labeling Reagent for Relative Quantification of Amine Metabolites by Mass Spectrometry. Analytical Chemistry 2006;78:6398-403.

251. Dunn WB, Bailey NJC, Johnson HE. Measuring the metabolome: current analytical technologies. Analyst 2005;130:606-25.

252. Lindon JC, Holmes E, Nicholson JK. Metabonomics techniques and applications to pharmaceutical research & development. Pharmaceutical Research 2006;23:1075-88.

253. Lenz EM, Bright J, Wilson ID, Morgan SR, Nash AFP. A H-1 NMR-based metabonomic study of urine and plasma samples obtained from healthy human subjects. Journal of Pharmaceutical and Biomedical Analysis 2003;33:1103-15.

254. Nicholson JK, Wilson ID. Understanding 'global' systems biology: Metabonomics and the continuum of metabolism. Nature Reviews Drug Discovery 2003;2:668-76.

255. Mayr M. Metabolomics: Ready for the Prime Time? Circulation: Cardiovascular Genetics 2008;1:58-65.

256. Pendyala G, Want EJ, Webb W, Siuzdak G, Fox HS. Biomarkers for neuroAIDS: The widening scope of metabolomics. Journal of Neuroimmune Pharmacology 2007;2:72-80.

257. Nordström A, Lewensohn R. Metabolomics: Moving to the Clinic. J Neuroimmune Pharmacol 2010;5:4-17.

258. Backstrom T, Goiny M, Lockowandt U, Liska J, Franco-Cereceda A. Cardiac outflow of amino acids and purines during myocardial ischemia and reperfusion. Journal of Applied Physiology 2003;94:1122-8.

259. Denkert C, Budczies J, Weichert W, et al. Metabolite profiling of human colon carcinoma - deregulation of TCA cycle and amino acid turnover. Molecular Cancer 2008;7.

260. Nordstrom A, Want E, Northen T, Lehtioe J, Siuzdak G. Multiple ionization mass spectrometry strategy used to reveal the complexity of metabolomics. Analytical Chemistry 2008;80:421-9.

261. Wang J-N, Zhou Y, Zhu T-Y, Wang X, Guo Y-L. Prediction of acute cellular renal allograft rejection by urinary metabolomics using MALDI-FTMS. Journal of Proteome Research 2008;7:3597-601.

262. Nordström A, O'Maille G, Qin C, Siuzdak G. Nonlinear Data Alignment for UPLC−MS and HPLC−MS Based Metabolomics: Quantitative Analysis of Endogenous and Exogenous Metabolites in Human Serum. Analytical Chemistry 2006;78:3289-95.

263. Fiehn O, Kopka J, Dormann P, Altmann T, Trethewey RN, Willmitzer L. Metabolite profiling for plant functional genomics. Nat Biotech 2000;18:1157-61.

264. Tolstikov VV, Fiehn O. Analysis of Highly Polar Compounds of Plant Origin: Combination of Hydrophilic Interaction Chromatography and Electrospray Ion Trap Mass Spectrometry. Analytical Biochemistry 2002;301:298-307.

265. Appelblad P, Jonsson T, Jiang W, Irgum K. Fast hydrophilic interaction liquid chromatographic separations on bonded zwitterionic stationary phase. Journal of Separation Science 2008;31:1529-36.

266. Novakova L, Solichova D, Solich P. Advantages of ultra performance liquid chromatography over high-performance liquid chromatography: Comparison of different analytical 2 approaches during analysis of diclofenac gel. Journal of Separation Science 2006;29:2433-43.

267. Chen J, Swamidass SJ, Dou Y, Bruand J, Baldi P. ChemDB: a public database of small molecules and related chemoinformatics resources. Bioinformatics 2005;21:4133-9.

268. van der Greef J, Stroobant P, van der Heijden R. The role of analytical sciences medical systems biology. Current Opinion in Chemical Biology 2004;8:559-65.

269. B M. Multivariable Statistical Methods: A Primer: London: Chapman & Hall; 1994.

270. Munger J, Bennett BD, Parikh A, et al. Systems-level metabolic flux profiling identifies fatty acid synthesis as a target for antiviral therapy. Nature Biotechnology 2008;26:1179-86.

271. Lopaschuk GD, Ussher JR, Folmes CDL, Jaswal JS, Stanley WC. Myocardial Fatty Acid Metabolism in Health and Disease. Physiological Reviews 2010;90:207-58.

272. Ingelsson E, Sundstrom J, Arnlov J, Zethelius B, Lind L. Insulin resistance and risk of congestive heart failure. JAMA-J Am Med Assoc 2005;294:334-41.

273. Sharov VG, Todor AV, Silverman N, Goldstein S, Sabbah HN. Abnormal mitochondrial respiration in failed human myocardium. J Mol Cell Cardiol 2000;32:2361-7.

274. Marin-Garcia J, Goldenthal MJ, Moe GW. Abnormal cardiac and skeletal muscle mitochondrial function in pacing-induced cardiac failure. Cardiovasc Res 2001;52:103-10.

275. Chokshi A, Drosatos K, Cheema FH, et al. Ventricular Assist Device Implantation Corrects Myocardial Lipotoxicity, Reverses Insulin Resistance and Normalizes Cardiac Metabolism in Patients with Advanced Heart Failure. Circulation 2012.

276. Opitz CA, Litzenburger UM, Sahm F, et al. An endogenous tumour-promoting ligand of the human aryl hydrocarbon receptor. Nature 2011;478:197-203.

277. Alexander D, Lombardi R, Rodriguez G, Mitchell MM, Marian AJ. Metabolomic distinction and insights into the pathogenesis of human primary dilated cardiomyopathy. European Journal of Clinical Investigation 2011;41:527-38.

278. Solem E, Agarwal DP, Goedde HW. The determination of β-aminoisobutyric acid in human serum by ion-exchange chromatography. Clinica Chimica Acta 1975;59:203-7.

279. Roberts Lee D, Boström P, O'Sullivan John F, et al. β-Aminoisobutyric Acid Induces Browning of White Fat and Hepatic β-Oxidation and Is Inversely Correlated with Cardiometabolic Risk Factors. Cell Metabolism;19:96-108.

280. Sabatine MS, Liu E, Morrow DA, et al. Metabolomic identification of novel biomarkers of myocardial ischemia. Circulation 2005;112:3868-75.

281. Lewis GD, Wei R, Liu E, et al. Metabolite profiling of blood from individuals undergoing planned myocardial infarction reveals early markers of myocardial injury. The Journal of clinical investigation 2008;118:3503-12.

282. Bodi V, Sanchis J, Morales JM, et al. Metabolomic Profile of Human Myocardial Ischemia by Nuclear Magnetic

Resonance Spectroscopy of Peripheral Blood Serum A Translational Study Based on Transient Coronary Occlusion Models. Journal of the American College of Cardiology 2012;59:1629-41.

283. Lamke GT, Allen RD, Edwards WD, Tazelaar HD, Danielson GK. Surgical pathology of subaortic septal myectomy associated with hypertrophic cardiomyopathy: A study of 204 cases (1996-2000). Cardiovasc Pathol 2003;12:149-58.

284. Neglia D, De Caterina A, Marraccini P, et al. Impaired myocardial metabolic reserve and substrate selection flexibility during stress in patients with idiopathic dilated cardiomyopathy. American Journal of Physiology - Heart and Circulatory Physiology 2007;293:H3270-H8.

285. Turer AT, Stevens RD, Bain JR, et al. Metabolomic profiling reveals distinct patterns of myocardial substrate utilization in humans with coronary artery disease or left ventricular dysfunction during surgical ischemia-reperfusion. Circulation 2009;119:1736-46.

286. Lewis GD, Farrell L, Wood MJ, et al. Metabolic Signatures of Exercise in Human Plasma. Sci Transl Med 2010;2.

287. Turer AT, Stevens RD, Bain JR, et al. Metabolomic profiling reveals distinct patterns of myocardial substrate use in humans with coronary artery disease or left ventricular dysfunction during surgical ischemia/reperfusion. Circulation 2009;119:1736-46.

288. Obrzut S, Tiongson J, Jamshidi N, Phan HM, Hoh C, Birgersdotter-Green U. Assessment of Metabolic Phenotypes in Patients with Non-ischemic Dilated Cardiomyopathy Undergoing Cardiac Resynchronization Therapy. J Cardiovasc Transl Res 2010;3:643-51.

289. Nagueh SF, Appleton CP, Gillebert TC, et al. Recommendations for the evaluation of left ventricular diastolic function by echocardiography. Journal of the

American Society of Echocardiography : official publication of the American Society of Echocardiography 2009;22:107-33.

290. Evangelista A, Flachskampf F, Lancellotti P, et al. European Association of Echocardiography recommendations for standardization of performance, digital storage and reporting of echocardiographic studies. European journal of echocardiography : the journal of the Working Group on Echocardiography of the European Society of Cardiology 2008;9:438-48.

291. Devereux RB, Alonso DR, Lutas EM, et al. Echocardiographic assessment of left ventricular hypertrophy: Comparison to necropsy findings. Am J Cardiol;57:450-8.

292. ATS/ACCP Statement on Cardiopulmonary Exercise Testing. American Journal of Respiratory and Critical Care Medicine 2003;167:211-77.

293. Roberts LD, West JA, Vidal-Puig A, Griffin JL. Methods for Performing Lipidomics in White Adipose Tissue. Methods in Enzymology 2014;538:211-31.

294. Lewis GD, Wei R, Liu E, et al. Metabolite profiling of blood from individuals undergoing planned myocardial infarction reveals early markers of myocardial injury. The Journal of Clinical Investigation 2008;118:3503-12.

295. Nyamundanda G, Gormley IC, Fan Y, Gallagher WM, Brennan L. MetSizeR: selecting the optimal sample size for metabolomic studies using an analysis based approach. BMC bioinformatics 2013;14:338.

296. Steuer R, Morgenthal K, Weckwerth W, Selbig J. A Gentle Guide to the Analysis of Metabolomic Data. In: Weckwerth W, ed. Metabolomics: Humana Press; 2007:105-26.

297. Sugimoto M, Kawakami M, Robert M, Soga T, Tomita M. Bioinformatics Tools for Mass Spectroscopy-Based

Metabolomic Data Processing and Analysis. Current Bioinformatics 2012;7:96-108.

298. Fan J, Upadhye S, Worster A. Understanding receiver operating characteristic (ROC) curves. Cjem 2006;8:19-20.

299. Xia J, Broadhurst DI, Wilson M, Wishart DS. Translational biomarker discovery in clinical metabolomics: an introductory tutorial. Metabolomics 2013;9:280-99.

300. Mudge GH, Mills RM, Taegtmeyer H, Gorlin R, Lesch M. Alterations of myocardial amino acid metabolism in chronic ischemic heart disease. Journal of Clinical Investigation 1976;58:1185-92.

301. Thomassen A, Bagger JP, Nielsen TT, Henningsen P. ALTERED GLOBAL MYOCARDIAL SUBSTRATE PREFERENCE AT REST AND DURING PACING IN CORONARY-ARTERY DISEASE WITH STABLE ANGINA-PECTORIS. Am J Cardiol 1988;62:686-93.

302. London DR, Foley TH, Webb CG. Evidence for the Release of Individual Amino-acids from the Resting Human Forearm. Nature 1965;208:588-9.

303. NAKAMURA T, SUGIHARA H, KINOSHITA N, et al. Serum carnitine concentrations in patients with idiopathic hypertrophic cardiomyopathy: relationship with impaired myocardial fatty acid metabolism. Clinical Science 1999;97:493-501.

304. Nakamura T, Sugihara H, Kinoshita N, Yoneyama S, Azuma A, Nakagawa M. Can Serum Carnitine Levels Distinguish Hypertrophic Cardiomyopathy From Hypertensive Hearts? Hypertension 2000;36:215-9.

305. Svati H Shah WEK, Olga Ilkayeva, Robert Stevens, Carol Haynes, Gregory D Lewis, Christopher B Newgard, Robert E Gerszten. Abstract 16632: Metabolomic Profiling in a Human Model of Myocardial Infarction Identifies Novel Early Biomarkers of Cellular Damage. Circulation 2013.

306. Opie LH. Substrate Utilization and Glycolysis in the Heart. Cardiology 1971;56:2-21.

307. Alamanni F, Parolari A, Repossini A, et al. Coronary blood flow, metabolism, and function in dysfunctional viable myocardium before and early after surgical revascularisation. Heart 2004;90:1291-8.

308. Pietersen HG, Langenberg CJM, Geskes G, et al. Myocardial substrate uptake and oxidation during and after routine cardiac surgery. The Journal of Thoracic and Cardiovascular Surgery;118:71-80.

309. Chalmers RA, Roe CR, Stacey TE, Hoppel CL. URINARY-EXCRETION OF L-CARNITINE AND ACYLCARNITINES BY PATIENTS WITH DISORDERS OF ORGANIC-ACID METABOLISM - EVIDENCE FOR SECONDARY INSUFFICIENCY OF L-CARNITINE. Pediatric Research 1984;18:1325-8.

310. Makowski L, Noland RC, Koves TR, et al. Metabolic profiling of PPARα−/− mice reveals defects in carnitine and amino acid homeostasis that are partially reversed by oral carnitine supplementation. The FASEB Journal 2009;23:586-604.

311. SHARMA S, ADROGUE JV, GOLFMAN L, et al. Intramyocardial lipid accumulation in the failing human heart resembles the lipotoxic rat heart. The FASEB Journal 2004;18:1692-700.

312. Adams SH, Hoppel CL, Lok KH, et al. Plasma Acylcarnitine Profiles Suggest Incomplete Long-Chain Fatty Acid β-Oxidation and Altered Tricarboxylic Acid Cycle Activity in Type 2 Diabetic African-American Women. The Journal of Nutrition 2009;139:1073-81.

313. Ashrafian H, Redwood C, Blair E, Watkins H. Hypertrophic cardiomyopathy:a paradigm for myocardial energy depletion. Trends in Genetics;19:263-8.

314. Olszewski AJ, Szostak WB. Homocysteine content of plasma proteins in ischemic heart disease. Atherosclerosis;69:109-13.

315. Wijekoon EP, Skinner C, Brosnan ME, Brosnan JT. Amino acid metabolism in the Zucker diabetic fatty rat: effects of insulin resistance and of type 2 diabetes. Canadian Journal of Physiology and Pharmacology 2004;82:506-14.

316. Wang TJ, Ngo D, Psychogios N, et al. 2-Aminoadipic acid is a biomarker for diabetes risk. The Journal of Clinical Investigation 2013;123:4309-17.

317. Mary Hardy M, Principal Investigator, Ian Coulter, PhD, Sally C Morton, PhD, Joya Favreau, MD, Swamy Venuturupalli, MD, Francesco Chiappelli, PhD, Frederico Rossi, MD, Greg Orshansky, MD, Lara K Jungvig, BA, Elizabeth A Roth, MA, Marika J Suttorp, MS, Paul Shekelle, MD, PhD. S-Adenosyl-L-Methionine for Treatment of Depression, Osteoarthritis, and Liver Disease: Rockville (MD): Agency for Healthcare Research and Quality (US); 2002.

318. Kerins DM, Koury MJ, Capdevila A, Rana S, Wagner C. Plasma S-adenosylhomocysteine is a more sensitive indicator of cardiovascular disease than plasma homocysteine. The American Journal of Clinical Nutrition 2001;74:723-9.

319. Hauser SL, Doolittle TH, Lopez-Bresnahan M, et al. AN antispasticity effect of threonine in multiple sclerosis. Archives of Neurology 1992;49:923-6.

320. Lee A, Patterson V. A double-blind study of L-threonine in patients with spinal spasticity. Acta Neurologica Scandinavica 1993;88:334-8.

321. Jørgenrud B, Jalanko M, Heliö T, et al. The Metabolome in Finnish Carriers of the <italic>MYBPC3</italic>-Q1061X Mutation for Hypertrophic Cardiomyopathy. PLoS ONE 2015;10:e0134184.

322. Reibel DK, Uboh CE, Kent RL. ALTERED COENZYME-A AND CARNITINE METABOLISM IN

PRESSURE-OVERLOAD HYPERTROPHIED HEARTS. American Journal of Physiology 1983;244:H839-H43.

323. Elalaouitalibi Z, Moravec J. DECREASED L-CARNITINE TRANSPORT IN MECHANICALLY OVERLOADED RAT HEARTS. Basic Research in Cardiology 1987;82:223-31.

324. Beyerbacht HP, Lamb HJ, Laarse Avd, et al. Aortic Valve Replacement in Patients with Aortic Valve Stenosis Improves Myocardial Metabolism and Diastolic Function. Radiology 2001;219:637-43.

325. Gentleman RC, Carey VJ, Bates DM, et al. Bioconductor: open software development for computational biology and bioinformatics. Genome Biology 2004;5.

326. Huber W, von Heydebreck A, Sultmann H, Poustka A, Vingron M. Variance stabilization applied to microarray data calibration and to the quantification of differential expression. Bioinformatics (Oxford, England) 2002;18 Suppl 1:S96-104.

327. Gentleman RC, V.; Huber, W.; Irizarry, R.; Dudoit, S; . Bioinformatics and Computational Biology Solutions Using R and Bioconductor: Springer-Verlag, New York 2005.

328. Benjamini Y, Hochberg Y. CONTROLLING THE FALSE DISCOVERY RATE - A PRACTICAL AND POWERFUL APPROACH TO MULTIPLE TESTING. Journal of the Royal Statistical Society Series B-Methodological 1995;57:289-300.

329. Loor JJ. Genomics of metabolic adaptations in the peripartal cow. Animal 2010;4:1110-39.

330. Rakhshandehroo M, Sanderson LM, Matilainen M, et al. Comprehensive Analysis of PPARα-Dependent Regulation of Hepatic Lipid Metabolism by Expression Profiling. PPAR Research 2007;2007:13.

331. Rommelaere S, Millet V, Gensollen T, et al. PPARalpha regulates the production of serum Vanin-1 by liver. FEBS Letters;587:3742-8.

332. Carlson M, Osmond BC, Botstein D. MUTANTS OF YEAST DEFECTIVE IN SUCROSE UTILIZATION. Genetics 1981;98:25-40.

333. Carlson M, Botstein D. 2 DIFFERENTIALLY REGULATED MESSENGER-RNAS WITH DIFFERENT 5' ENDS ENCODE SECRETED AND INTRACELLULAR FORMS OF YEAST INVERTASE. Cell 1982;28:145-54.

334. Weekes J, Ball KL, Caudwell FB, Hardie DG. SPECIFICITY DETERMINANTS FOR THE AMP-ACTIVATED PROTEIN-KINASE AND ITS PLANT HOMOLOG ANALYZED USING SYNTHETIC PEPTIDES. Febs Letters 1993;334:335-9.

335. Kahn BB, Alquier T, Carling D, Hardie DG. AMP-activated protein kinase: Ancient energy gauge provides clues to modern understanding of metabolism. Cell Metabolism 2005;1:15-25.

336. Hardie DG, Hawley SA, Scott J. AMP-activated protein kinase - development of the energy sensor concept. Journal of Physiology-London 2006;574:7-15.

337. Beauloye C, Bertrand L, Horman S, Hue L. AMPK activation, a preventive therapeutic target in the transition from cardiac injury to heart failure. Cardiovascular Research 2011;90:224-33.

338. Hardie DG, Carling D. The AMP-activated protein kinase - Fuel gauge of the mammalian cell? European Journal of Biochemistry 1997;246:259-73.

339. Arad M, Seidman CE, Seidman JG. AMP-activated protein kinase in the heart - Role during health and disease. Circulation Research 2007;100:474-88.

340. Cheung PCF, Salt IP, Davies SP, Hardie DG, Carling D. Characterization of AMP-activated protein kinase

gamma-subunit isoforms and their role in AMP binding. Biochemical Journal 2000;346:659-69.

341. Warden SM, Richardson C, O'Donnell J, Stepleton D, Kemp BE, Witters LA. Post-translational modifications of the beta-1 subunit of AMP-activated protein kinase affect enzyme activity and cellular localization. Biochemical Journal 2001;354:275-83.

342. Hudson ER, Pan DA, James J, et al. A novel domain in AMP-activated protein kinase causes glycogen storage bodies similar to those seen in hereditary cardiac arrhythmias. Current Biology 2003;13:861-6.

343. Kemp BE. Bateman domains and adenosine derivatives form a binding contract. Journal of Clinical Investigation 2004;113:182-4.

344. Scott JW, Hawley SA, Green KA, et al. CBS domains form energy-sensing modules whose binding of adenosine ligands is disrupted by disease mutations. Journal of Clinical Investigation 2004;113:274-84.

345. Frederich M, Balschi JA. The relationship between AMP-activated protein kinase activity and AMP concentration in the isolated perfused rat heart. Journal of Biological Chemistry 2002;277:1928-32.

346. Hardie DG. Minireview: The AMP-activated protein kinase cascade: The key sensor of cellular energy status. Endocrinology 2003;144:5179-83.

347. Hawley SA, Boudeau J, Reid JL, et al. Complexes between the LKB1 tumor suppressor, STRAD alpha/beta and MO25 alpha/beta are upstream kinases in the AMP-activated protein kinase cascade. Journal of biology 2003;2:28-.

348. Hawley SA, Pan DA, Mustard KJ, et al. Calmodulin-dependent protein kinase kinase-β is an alternative upstream kinase for AMP-activated protein kinase. Cell Metabolism;2:9-19.

349. Sakamoto K, Zarrinpashneh E, Budas GR, et al. Deficiency of LKB1 in heart prevents ischemia-mediated activation of AMPKα2 but not AMPKα1. American journal of physiology Endocrinology and metabolism 2006;290:E780-E8.

350. Chabowski A, Momken I, Coort SLM, et al. Prolonged AMPK activation increases the expression of fatty acid transporters in cardiac myocytes and perfused hearts. Molecular and Cellular Biochemistry 2006;288:201-12.

351. Holmes BF, Kurth-Kraczek EJ, Winder WW. Chronic activation of 5 '-AMP-activated protein kinase increases GLUT-4, hexokinase, and glycogen in muscle. Journal of Applied Physiology 1999;87:1990-5.

352. Fryer LGD, Foufelle F, Barnes K, Baldwin SA, Woods A, Carling D. Characterization of the role of the AMP-activated protein kinase in the stimulation of glucose transport in skeletal muscle cells. Biochemical Journal 2002;363:167-74.

353. Kovacic S, Soltys CLM, Barr AJ, Shiojima I, Walsh K, Dyck JRB. Akt activity negatively regulates phosphorylation of AMP-activated protein kinase in the heart. Journal of Biological Chemistry 2003;278:39422-7.

354. Longnus SL, Segalen C, Giudicelli J, Sajan MP, Farese RV, Van Obberghen E. Insulin signalling downstream of protein kinase B is potentiated by 5 ' AMP-activated protein kinase in rat hearts in vivo. Diabetologia 2005;48:2591-601.

355. Marsin AS, Bertrand L, Rider MH, et al. Phosphorylation and activation of heart PFK-2 by AMPK has a role in the stimulation of glycolysis during ischaemia. Current Biology 2000;10:1247-55.

356. Long YC, Barnes BR, Mahlapuu M, et al. Role of AMP-activated protein kinase in the coordinated expression of genes controlling glucose and lipid metabolism in mouse white skeletal muscle. Diabetologia 2005;48:2354-64.

357. Tian R, Musi N, D'Agostino J, Hirshman MF, Goodyear LJ. Increased adenosine monophosphate-activated protein kinase activity in rat hearts with pressure-overload hypertrophy. Circulation 2001;104:1664-9.

358. Dolinsky VW, Chan AYM, Robillard Frayne I, Light PE, Des Rosiers C, Dyck JRB. Resveratrol Prevents the Prohypertrophic Effects of Oxidative Stress on LKB1. Circulation 2009;119:1643-52.

359. Chan AYM, Soltys C-LM, Young ME, Proud CG, Dyck JRB. Activation of AMP-activated Protein Kinase Inhibits Protein Synthesis Associated with Hypertrophy in the Cardiac Myocyte. Journal of Biological Chemistry 2004;279:32771-9.

360. Zarrinpashneh E, Beauloye C, Ginion A, et al. AMPK alpha 2 counteracts the development of cardiac hypertrophy induced by isoproterenol. Biochemical and Biophysical Research Communications 2008;376:677-81.

361. Zhang P, Hu X, Xu X, et al. AMP Activated Protein Kinase-alpha 2 Deficiency Exacerbates Pressure-Overload-Induced Left Ventricular Hypertrophy and Dysfunction in Mice. Hypertension 2008;52:918-24.

362. Shibata R, Ouchi N, Ito M, et al. Adiponectin-mediated modulation of hypertrophic signals in the heart. Nature Medicine 2004;10:1384-9.

363. Nickel A, Loeffler J, Maack C. Myocardial energetics in heart failure. Basic Research in Cardiology 2013;108.

364. Jameel MN, Zhang J. Myocardial energetics in left ventricular hypertrophy. Current cardiology reviews 2009;5:243-50.

365. Ashrafian H, Frenneaux MP, Opie LH. Metabolic mechanisms in heart failure. Circulation 2007;116:434-48.

366. Lu T-M, Tsai J-Y, Chen Y-C, et al. Downregulation of Sirt1 as aging change in advanced heart failure. Journal of Biomedical Science 2014;21:57.

367. Jaeger S, Handschin C, St.-Pierre J, Spiegelman BM. AMP-activated protein kinase (AMPK) action in skeletal muscle via direct phosphorylation of PGC-1 alpha. Proceedings of the National Academy of Sciences of the United States of America 2007;104:12017-22.

368. Hue L, Rider MH. The AMP-activated protein kinase: more than an energy sensor. Essays In Biochemistry 2007;43:121-38.

369. Issemann I, Green S. Activation of a member of the steroid hormone receptor superfamily by peroxisome proliferators. Nature 1990;347:645-50.

370. Chawla A, Repa JJ, Evans RM, Mangelsdorf DJ. Nuclear Receptors and Lipid Physiology: Opening the X-Files. Science 2001;294:1866-70.

371. Georgiadi A, Boekschoten MV, Müller M, Kersten S. Detailed transcriptomics analysis of the effect of dietary fatty acids on gene expression in the heart. Physiological Genomics 2012;44:352-61.

372. Madrazo JA, Kelly DP. The PPAR trio: Regulators of myocardial energy metabolism in health and disease. Journal of Molecular and Cellular Cardiology;44:968-75.

373. Hashimoto T, Cook WS, Qi C, Yeldandi AV, Reddy JK, Rao MS. Defect in peroxisome proliferator-activated receptor alpha-inducible fatty acid oxidation determines the severity of hepatic steatosis in response to fasting. Journal of Biological Chemistry 2000;275:28918-28.

374. Kersten S, Seydoux J, Peters JM, et al. Peroxisome proliferator–activated receptor α mediates the adaptive response to fasting. The Journal of Clinical Investigation 1999;103:1489-98.

375. Leone TC, Weinheimer CJ, Kelly DP. A critical role for the peroxisome proliferator-activated receptor α (PPARα) in the cellular fasting response: The PPARα-null mouse as a model of fatty acid oxidation disorders. Proceedings of the National Academy of Sciences 1999;96:7473-8.

376. SUGDEN MC, BULMER K, GIBBONS GF, KNIGHT BL, HOLNESS MJ. Peroxisome-proliferator-activated receptor-α (PPARα) deficiency leads to dysregulation of hepatic lipid and carbohydrate metabolism by fatty acids and insulin. Biochemical Journal 2002;364:361-8.

377. Sanderson LM, Boekschoten MV, Desvergne B, Müller M, Kersten S. Transcriptional profiling reveals divergent roles of PPARα and PPARβ/δ in regulation of gene expression in mouse liver. Physiological Genomics 2010;41:42-52.

378. KERSTEN S, MANDARD S, ESCHER P, et al. The peroxisome proliferator-activated receptor α regulates amino acid metabolism. The FASEB Journal 2001;15:1971-8.

379. Sanderson LM, de Groot PJ, Hooiveld GJEJ, et al. Effect of Synthetic Dietary Triglycerides: A Novel Research Paradigm for Nutrigenomics. Plos One 2008;3.

380. Muller M, Rakhshandehroo M, Kersten S, Hooiveld G. Comparative Analysis of Gene Regulation by the Transcription Factor PPARa between Mouse and Human. Figshare 2009;1.

381. Georgiadi A, Kersten S. Mechanisms of Gene Regulation by Fatty Acids. Advances in Nutrition: An International Review Journal 2012;3:127-34.

382. Forman BM, Chen J, Evans RM. Hypolipidemic drugs, polyunsaturated fatty acids, and eicosanoids are ligands for peroxisome proliferator-activated receptors α and δ. Proceedings of the National Academy of Sciences 1997;94:4312-7.

383. Kersten S. Integrated physiology and systems biology of PPARα. Molecular Metabolism 2014;3:354-71.

384. Hoekstra M, Kruijt JK, Van Eck M, van Berkel TJC. Specific Gene Expression of ATP-binding Cassette Transporters and Nuclear Hormone Receptors in Rat Liver

Parenchymal, Endothelial, and Kupffer Cells. Journal of Biological Chemistry 2003;278:25448-53.

385. Sanderson LM, Degenhardt T, Koppen A, et al. Peroxisome Proliferator-Activated Receptor β/δ (PPARβ/δ) but Not PPARα Serves as a Plasma Free Fatty Acid Sensor in Liver. Molecular and Cellular Biology 2009;29:6257-67.

386. Targett-Adams P, McElwee MJ, Ehrenborg E, Gustafsson MC, Palmer CN, McLauchlan J. A PPAR response element regulates transcription of the gene for human adipose differentiation-related protein. Biochimica et Biophysica Acta (BBA) - Gene Structure and Expression 2005;1728:95-104.

387. Kadereit B, Kumar P, Wang W-J, et al. Evolutionarily conserved gene family important for fat storage. Proceedings of the National Academy of Sciences 2008;105:94-9.

388. McMullen PD, Bhattacharya S, Woods CG, et al. A map of the PPAR alpha transcription regulatory network for primary human hepatocytes. Chemico-Biological Interactions 2014;209:14-24.

389. Ramsay RR, Gandour RD, van der Leij FR. Molecular enzymology of carnitine transfer and transport. Biochimica Et Biophysica Acta-Protein Structure and Molecular Enzymology 2001;1546:21-43.

390. Arsenian MA. Carnitine and its derivatives in cardiovascular disease. Progress in Cardiovascular Diseases 1997;40:265-86.

391. Regitz V, Shug AL, Fleck E. Defective myocardial carnitine metabolism in congestive heart failure secondary to dilated cardiomyopathy and to coronary, hypertensive and valvular heart diseases. Am J Cardiol;65:755-60.

392. Akki A, Smith K, Seymour A-M. Compensated cardiac hypertrophy is characterised by a decline in palmitate oxidation. Molecular and Cellular Biochemistry 2008;311:215-24.

393. Sack MN, Rader TA, Park S, Bastin J, McCune SA, Kelly DP. Fatty Acid Oxidation Enzyme Gene Expression Is Downregulated in the Failing Heart. Circulation 1996;94:2837-42.

394. Lamb HJ, Beyerbacht HP, van der Laarse A, et al. Diastolic Dysfunction in Hypertensive Heart Disease Is Associated With Altered Myocardial Metabolism. Circulation 1999;99:2261-7.

395. Tateno M, Tamaki N, Yukihiro M, et al. Assessment of Fatty Acid Uptake in Ischemic Heart Disease without Myocardial Infarction. Journal of Nuclear Medicine 1996;37:1981-5.

396. Shug AL, Thomsen JH, Folts JD, et al. Changes in tissue levels of carnitine and other metabolites during myocardial ischemia and anoxia. Archives of Biochemistry and Biophysics 1978;187:25-33.

397. Nakagawa T, Sunamori M, Suzuki A. THE MYOCARDIAL DISTRIBUTION AND PLASMA-CONCENTRATION OF CARNITINE IN PATIENTS WITH MITRAL-VALVE DISEASE. Surgery Today-the Japanese Journal of Surgery 1994;24:313-7.

398. Masumura Y, Kobayashi A, Yamazaki N. MYOCARDIAL FREE CARNITINE AND FATTY ACYLCARNITINE LEVELS IN PATIENTS WITH CHRONIC HEART-FAILURE. Japanese Circulation Journal-English Edition 1990;54:1471-6.

399. Park SW, Goodpaster BH, Strotmeyer ES, et al. Accelerated loss of skeletal muscle strength in older adults with type 2 diabetes - The Health, Aging, and Body Composition Study. Diabetes Care 2007;30:1507-12.

400. Steiber AL, Weatherspoon LJ, Spry L, Davis AT. Serum carnitine concentrations correlated to clinical outcome parameters in chronic hemodialysis patients. Clinical Nutrition 2004;23:27-34.

401. Gibala MJ, Young ME, Taegtmeyer H. Anaplerosis of the citric acid cycle: role in energy metabolism of heart and skeletal muscle. Acta Physiologica Scandinavica 2000;168:657-65.

402. Bendahan D, Mattei JP, Ghattas B, Confort-Gouny S, Le Guern ME, Cozzone PJ. Citrulline/malate promotes aerobic energy production in human exercising muscle. British Journal of Sports Medicine 2002;36:282-9.

403. Creff AF. CONTROLLED DOUBLE-BLIND CLINICAL-STUDY AGAINST STIMOL PLACEBO IN THE TREATMENT OF ASTHENIA. Gazette Medicale De France 1982;89:1926-9.

404. Callis A, Debornier BM, Serrano JJ, Bellet H, Saumade R. ACTIVITY OF CITRULLINE MALATE ON ACID-BASE-BALANCE AND BLOOD AMMONIA AND AMINO-ACID LEVELS - STUDY IN THE ANIMAL AND IN MAN. Arzneimittel-Forschung/Drug Research 1991;41-1:660-3.

405. Sahlin K, Katz A, Broberg S. TRICARBOXYLIC-ACID CYCLE INTERMEDIATES IN HUMAN MUSCLE DURING PROLONGED EXERCISE. American Journal of Physiology 1990;259:C834-C41.

406. Gibala MJ, MacLean DA, Graham TE, Saltin B. Tricarboxylic acid cycle intermediate pool size and estimated cycle flux in human muscle during exercise. American Journal of Physiology - Endocrinology and Metabolism 1998;275:E235-E42.

407. Mullinax TR, Mock JN, McEvily AJ, Harrison JH. REGULATION OF MITOCHONDRIAL MALATE-DEHYDROGENASE - EVIDENCE FOR AN ALLOSTERIC CITRATE-BINDING SITE. Journal of Biological Chemistry 1982;257:13233-9.

408. Pound KM, Sorokina N, Ballal K, et al. Substrate–Enzyme Competition Attenuates Upregulated Anaplerotic Flux Through Malic Enzyme in Hypertrophied Rat Heart and

Restores Triacylglyceride Content: Attenuating Upregulated Anaplerosis in Hypertrophy. Circulation Research 2009;104:805-12.

409. Naya M, Chiba S, Iwano H, et al. Myocardial oxidative metabolism is increased due to haemodynamic overload in patients with aortic valve stenosis: assessment using 11C-acetate positron emission tomography. Eur J Nucl Med Mol Imaging 2010;37:2242-8.

410. Sheikh K, Camejo G, Lanne B, Halvarsson T, Landergren MR, Oakes ND. Beyond lipids, pharmacological PPARα activation has important effects on amino acid metabolism as studied in the rat. American Journal of Physiology - Endocrinology and Metabolism 2007;292:E1157-E65.

411. Smirnov VN, Asafov GB, Cherpach.Nm, et al. AMMONIA NEUTRALIZATION AND UREA SYNTHESIS IN CARDIAC-MUSCLE. Circulation Research 1974;35:58-73.

412. Baranczykkuzma A, Skrzypekosiecka I, Zalejska M, Porembska Z. PURIFICATION AND SOME PROPERTIES OF HUMAN-HEART ARGINASE. Acta Biochimica Polonica 1980;27:181-9.

413. Lipke DW, Newman PS, Tofiq S, et al. Multiple polyamine regulatory pathways control compensatory cardiovascular hypertrophy in coarctation hypertension. Clinical and Experimental Hypertension 1997;19:269-95.

414. Soltis EE, Newman PS, Olson JW. POLYAMINES, VASCULAR SMOOTH-MUSCLE, AND DEOXYCORTICOSTERONE ACETATE-SALT HYPERTENSION. Hypertension 1991;18:85-92.

415. Ibrahim J, Schachter M, Hughes AD, Sever PS. ROLE OF POLYAMINES IN HYPERTENSION INDUCED BY ANGIOTENSIN-II. Cardiovascular Research 1995;29:50-6.

416. Tipnis UR, Frasierscott K, Skiera C. ISOPRENALINE INDUCED CHANGES IN ORNITHINE DECARBOXYLASE ACTIVITY AND POLYAMINE CONTENT IN REGIONS OF

THE RAT-HEART. Cardiovascular Research 1989;23:611-9.

417. Flamigni F, Rossoni C, Stefanelli C, Caldarera CM. POLYAMINE METABOLISM AND FUNCTION IN THE HEART. Journal of Molecular and Cellular Cardiology 1986;18:3-11.

418. Heller JS, Canellakis ES. CELLULAR CONTROL OF ORNITHINE DECARBOXYLASE ACTIVITY BY ITS ANTIZYME. Journal of Cellular Physiology 1981;107:209-17.

419. Leskinen T, Rinnankoski-Tuikka R, Rintala M, et al. Differences in muscle and adipose tissue gene expression and cardio-metabolic risk factors in the members of physical activity discordant twin pairs. PloS one 2010;5.

420. Michael LF, Wu ZD, Cheatham RB, et al. Restoration of insulin-sensitive glucose transporter (GLUT4) gene expression in muscle cells by the transcriptional coactivator PGC-1. Proceedings of the National Academy of Sciences of the United States of America 2001;98:3820-5.

421. A E Harper, R H Miller a, Block KP. Branched-Chain Amino Acid Metabolism. Annual Review of Nutrition 1984;4:409-54.

422. Baquet A, Lavoinne A, Hue L. Comparison of the effects of various amino acids on glycogen synthesis, lipogenesis and ketogenesis in isolated rat hepatocytes. Biochemical Journal 1991;273:57-62.

423. Chotechuang N, Azzout-Marniche D, Bos C, et al. mTOR, AMPK, and GCN2 coordinate the adaptation of hepatic energy metabolic pathways in response to protein intake in the rat. American Journal of Physiology - Endocrinology and Metabolism 2009;297:E1313-E23.

424. Newgard CB, An J, Bain JR, et al. A Branched-Chain Amino Acid-Related Metabolic Signature that Differentiates Obese and Lean Humans and Contributes to Insulin Resistance. Cell Metabolism;9:311-26.

425. Flores EA, Bistrian BR, Pomposelli JJ, Dinarello CA, Blackburn GL, Istfan NW. Infusion of tumor necrosis factor/cachectin promotes muscle catabolism in the rat. A synergistic effect with interleukin 1. The Journal of Clinical Investigation 1989;83:1614-22.

426. Nawabi MD, Block KP, Chakrabarti MC, Buse MG. Administration of endotoxin, tumor necrosis factor, or interleukin 1 to rats activates skeletal muscle branched-chain alpha-keto acid dehydrogenase. The Journal of Clinical Investigation 1990;85:256-63.

427. Young LH, McNulty PH, Morgan C, Deckelbaum LI, Zaret BL, Barrett EJ. MYOCARDIAL PROTEIN-TURNOVER IN PATIENTS WITH CORONARY-ARTERY DISEASE - EFFECT OF BRANCHED-CHAIN AMINO-ACID INFUSION. Journal of Clinical Investigation 1991;87:554-60.

428. Doenst T, Nguyen TD, Abel ED. Cardiac Metabolism in Heart Failure: Implications Beyond ATP Production. Circulation Research 2013;113:709-24.

429. Akki A, Smith K, Seymour A-ML. Compensated cardiac hypertrophy is characterised by a decline in palmitate oxidation. Molecular and Cellular Biochemistry 2008;311:215-24.

430. Christe ME, Rodgers RL. Altered Glucose and Fatty Acid Oxidation in Hearts of the Spontaneously Hypertensive Rat. Journal of Molecular and Cellular Cardiology;26:1371-5.

431. Kato T, Niizuma S, Inuzuka Y, et al. Analysis of Metabolic Remodeling in Compensated Left Ventricular Hypertrophy and Heart Failure. Circulation: Heart Failure 2010;3:420-30.

432. Dávila-Román VG, Vedala G, Herrero P, et al. Altered myocardial fatty acid and glucose metabolism in idiopathic dilated cardiomyopathy. J Am Coll Cardiol 2002;40:271-7.

433. Heather LC, Cole MA, Lygate CA, et al. Fatty acid transporter levels and palmitate oxidation rate correlate with ejection fraction in the infarcted rat heart. Cardiovascular Research 2006;72:430-7.

434. Amorim PA, Nguyen TD, Shingu Y, et al. Myocardial infarction in rats causes partial impairment in insulin response associated with reduced fatty acid oxidation and mitochondrial gene expression. The Journal of Thoracic and Cardiovascular Surgery;140:1160-7.

435. Howell NJ, Ashrafian H, Drury NE, et al. Glucose-Insulin-Potassium Reduces the Incidence of Low Cardiac Output Episodes After Aortic Valve Replacement for Aortic Stenosis in Patients With Left Ventricular Hypertrophy: Results From the Hypertrophy, Insulin, Glucose, and Electrolytes (HINGE) Trial. Circulation 2011;123:170-7.

436. Vánky FB, Håkanson E, Jorfeldt L, Svedjeholm R. Does glutamate influence myocardial and peripheral tissue metabolism after aortic valve replacement for aortic stenosis? Clinical Nutrition 2006;25:913-22.

437. Vanky FB, Hakanson E, Szabo Z, Jorfeldt L, Svedjeholm R. Myocardial metabolism before and after valve replacement for aortic stenosis. Journal of Cardiovascular Surgery 2006;47:305-13.

438. Naya M, Chiba S, Iwano H, et al. Myocardial oxidative metabolism is increased due to haemodynamic overload in patients with aortic valve stenosis: assessment using C-11-acetate positron emission tomography. European Journal of Nuclear Medicine and Molecular Imaging 2010;37:2242-8.

439. Mannacio V, Di Tommaso L, Stassano P, De Amicis V, Vosa C. Myocardial metabolism and diastolic function after aortic valve replacement for aortic stenosis: influence of patient–prosthesis mismatch. European Journal of Cardio-Thoracic Surgery 2012;41:316-21.

440. Mahmod M, Francis JM, Pal N, et al. Myocardial perfusion and oxygenation are impaired during stress in

severe aortic stenosis and correlate with impaired energetics and subclinical left ventricular dysfunction. Journal of Cardiovascular Magnetic Resonance 2014;16:29-.